# Seasons of change: The influence of seasonality on arsenic biogeochemical cycling and ecotoxicity to plankton communities in mining-impacted lakes near Yellowknife (Northwest Territories, Canada).

AMANDA JOAN LITTLE

A dissertation submitted to the Faculty of Graduate Studies in partial fulfilment of the requirements of the Degree of Doctor of Philosophy

Graduate Program in Geography

York University

Toronto, Ontario

April 2026

## Abstract

Relatively little is known about the biogeochemical cycling and bio-uptake of arsenic by freshwater organisms outside of the summer season, despite concerns related to its toxicity and persistence in contaminated aquatic systems. This is particularly true for subarctic lakes that remain ice-covered for the majority of the year. Recent research in shallow, subarctic lakes near Yellowknife (Northwest Territories, Canada) has found that arsenic concentrations undergo significant increases during the winter and changes in chemical form (i.e., speciation), due to cryoconcentration (solute exclusion during lake-ice formation) and sediment efflux under anoxic conditions. This has important implications for its toxicity to under-ice plankton communities, as well as the bio-uptake and transfer of arsenic through lake food webs. This dissertation integrated a field-based study of arsenic biogeochemistry and plankton ecology in five Yellowknife-area lakes that spanned a gradient of legacy arsenic contamination (1.1 – 455 μg $L^{-1}$), incorporating seasonal dynamics. Over a period of 2.5 years (April 2022 – June 2024), the lakes were sampled multiple times during both the open-water and under-ice seasons for water chemistry, plankton community data, and bulk plankton tissue samples for the analysis of arsenic bioaccumulation in phytoplankton and zooplankton. Two key, novel findings emerged from this research: (1) The winter and seasonal transitional periods may be more relevant for arsenic bioavailability and ecotoxicity; and (2) Total arsenic concentrations in lake water did not strongly correlate with arsenic bioaccumulation in plankton, which suggests that other lake-specific factors (particularly dissolved organic carbon (DOC)) influenced the overall bioavailability of arsenic across the five study lakes. As well, this dissertation provides new data on associations between arsenic and individual zooplankton and phytoplankton taxa, including data on specific forms of arsenic (e.g., As(V), As(III)) that are not routinely measured in field-based arsenic toxicity studies. Overall,

this dissertation highlights the importance of sampling across limnological gradients and seasons when assessing arsenic impacts on freshwater ecosystems, particularly in subarctic lakes which remain ice-covered for the majority of the year.

## Acknowledgements

I'd like to thank the Tłı̨cho and Wıılıìdeh Yellowknives Dene First Nations, and the Northwest Territory Métis Nation for inviting me to do research on their traditional lands through my collaboration with the Aurora Research Institute.

My deepest thanks and gratitude to my supervisor, Dr. Jennifer Korosi, for her incredible support, guidance, and patience with me throughout my PhD journey. It's been such an inspiration to learn from another young woman in science, and I hope that I am half the mentor to any future students or staff members that you've been to me. Thank you to the members of my supervisory committee, Dr. Lewis Molot and Dr. Raymond Kwong, as well as to my co-authors and research collaborators, Dr. Mike Palmer, Dr. Marc Amyot, and Dr. John Chételat. You have all been so kind and supportive throughout this experience, and I know that I'm a much better researcher because of the time and effort you've poured into my dissertation. Thank you to the members of Dr. Marc Amyot's lab for their input and support – Dr. Dominic Ponton, Dr. Dominic Bélanger, and Maria Alaoui. Thank you also to Dr. Derek Gray, Dr. Ann St. Amond, Nicole Andreola, and Madeline Patenall for taking the time to make me a better plankton taxonomist.

This research would not have been possible without the support from numerous people who were excited and willing to help me conduct fieldwork. I'd like to thank the staff at the Aurora Research Institute, particularly Dr. Mike Palmer, Seamus Daly, Angela Hamilton, and Nigel Roussouw. I'd also like to thank all of the members of the Limnology and Paleoenvironmental Research Group for both helping me with fieldwork, but also supporting me more generally. Thank you in particular to Charlie West, Sorin-Alexandru Gruia, Rachael Abulu, Rebecca Gasman, Randelle Cheyanna Adano, Thomas Wu, Victoria Carroll, and Altrisha

Rodrigues. Thank you to all of the other wonderful members of the lab who may not have done fieldwork with me, but made me smile while doing lab and coursework. This is such an incredible group of people, and I'm so excited to see where everyone ends up. A special thank you to Dr. Kristen Coleman who helped keep me grounded and (mostly) sane, and to Dr. Joshua Thienpont for his never ending kindness and tech support.

I'd like to thank one last group – the wonderful people I get to call my friends and family who have continued to support me despite not knowing what words like "paleolimnology" and "ecotoxicology" mean. Thank you in particular to my mom, Gwen Little, for always picking up the phone and helping me to keep perspective. To my dad, John Little, for always providing such a calming and peaceful foundation, and to my little brother, Christopher Little, for always being able to make me laugh and feel seen. To my grandparents, Ginger Sage, Roger Sage, and Marilyn Little, for making more sacrifices than I'll ever be able to comprehend, and for installing in me (and my parents) a love for learning. Finally, I'd like to thank Scott Hutchinson for his never ending support, and for putting up with all of my late night ramblings related to arsenic and plankton. I couldn't have done it without you.

Thank you so much to everyone. You all make me a better a researcher, and more importantly, a better person.

# Table of Contents

Abstract ..... ii

Acknowledgements ..... iv

Table of Contents ..... vi

List of Tables ..... ix

List of Tables (Supplementary Information) ..... x

List of Figures ..... xiii

List of Figures (Supplementary Information) ..... xv

Acronyms ..... xvii

Chapter 1: General Introduction ..... 1

1.1 Introduction ..... 1

1.2 Arsenic Biogeochemical Cycling in Freshwater Lakes ..... 1

1.3 Plankton Arsenic Ecotoxicology and Bioaccumulation ..... 3

1.4 The Influence of Seasonality on Arsenic in Subarctic Lakes ..... 6

1.5 Legacy Arsenic Pollution in Yellowknife (Northwest Territories, Canada) ..... 7

1.6 Dissertation Goals & Objectives ..... 8

Chapter 2: Seasonal arsenic cycling and its potential impacts to plankton communities in subarctic lakes ..... 10

2.1 Abstract ..... 11

2.2 Introduction ..... 12

2.3 Materials & Methods ..... 15

2.3.1 Study Site Description ..... 15

2.3.2 Sample Collection ..... 18

2.3.3 Lab Analyses ..... 19

2.3.4 Statistical Analyses ..... 21

2.4 Results ..... 23

2.4.1 Lake Characteristics and Environmental Variables ..... 23

2.4.2 Phytoplankton ..... 26

2.4.3 Rotifers ..... 28

2.4.4 Zooplankton ..... 30

2.5 Discussion ..... 33

2.5.1 Phytoplankton ..... 34

2.5.2 Rotifers ..... 36
2.5.3 Zooplankton ..... 36
2.5.4 Under-Ice Ecology ..... 38
2.6 Conclusions ..... 42
2.7 Supplementary Information ..... 44

Chapter 3: Under-ice ecological and biogeochemical dynamics at the onset of spring thaw in four arsenic-contaminated subarctic lakes ..... 65
3.1 Abstract ..... 66
3.2 Introduction ..... 67
3.3 Materials and Methods ..... 70
3.3.1 Study Lakes ..... 70
3.3.2 Sample Collection ..... 72
3.3.3 Lab Analyses ..... 74
3.3.4 Statistical Analyses ..... 76
3.4 Results ..... 77
3.4.1 Lakewater Arsenic ..... 78
3.4.2 Plankton Communities ..... 81
3.5 Discussion ..... 89
3.5.1 Influence of spring thaw on arsenic biogeochemistry ..... 89
3.5.2 Changes in plankton communities at spring thaw ..... 92
3.5.3 Comparison of a warmer and a colder winter ..... 93
3.6 Conclusions ..... 94
3.7 Supplementary Information ..... 96

Chapter 4: Drivers of arsenic bioaccumulation in plankton from subarctic lakes impacted by legacy mining contamination ..... 109
4.1 Abstract ..... 110
4.2 Introduction ..... 111
4.3 Materials and Methods ..... 114
4.3.1 Study Lakes ..... 114
4.3.2 Field Sample Collection ..... 117
4.3.3 Lab Analyses ..... 119
4.3.4 Statistical Analyses ..... 121
4.4 Results ..... 122
4.4.1 QA/QC ..... 122
4.4.2 Plankton Arsenic Bioaccumulation and Seasonal Cycling ..... 123
4.4.3 Lake Water Arsenic as a Driver of Plankton Arsenic Bioaccumulation ..... 124
4.4.4 Other Potential Drivers of Plankton Arsenic Uptake ..... 127
4.5 Discussion ..... 134

4.6 Supplementary Information ..... 139

Chapter 5: Conclusions & Future Directions ..... 153

5.1 Conclusions ..... 153

5.2 Future Directions ..... 156

References ..... 159

# List of Tables

Table 2.1. The minimum (MN), maximum (MX), and average (AV) values of environmental variables used to determine study lake trophic status and total dissolved arsenic. Method detection limits (DL) for each parameter are as follows: chlorophyll-a (0.1 μg $L^{-1}$), dissolved organic carbon (0.5 mg $L^{-1}$), dissolved phosphorus (10 μg $L^{-1}$), dissolved nitrogen (60 μg $L^{-1}$), and dissolved arsenic (0.2 μg $L^{-1}$). There was no method detection limit for phytoplankton density as these values were counted and calculated manually..... 24

Table 3.1. Arsenic concentrations in the surface (1 m) layer of the four study lakes during pre- and post-snowmelt of the 2022 and 2023 spring thaw periods. Method detection limits (DL) of 0.2, 0.05, 0.01, 0.02, 0.02, and 0.02 μg $L^{-1}$ for dissolved As, As(V), As(III), and the organic arsenic species monomethylarsonate (MMA), dimethylarsonate (DMA), and arsenobetaine (AsB), respectively. The unknown arsenic species was calculated by subtracting the known speciations of arsenic as measured via HPLC-ICP-QQQ from the dissolved arsenic value measured by ICP-MS..... 81

# List of Tables (Supplementary Information)

Table S 2-1. Location and physical characteristics of the five study lakes. ..... 44

Table S 2-2. Field blank (FB) data from the five study lakes collected from 2022-2024 (N = 19). Measurements of total dissolved arsenic (Total As) below the method detection limit of 0.2 μg $L^{-1}$ are indicated by < DL. ..... 44

Table S 2-3. Field replicate data from Handle and Jackfish Lakes collected in November 2020 and January 2021 using the same sampling methods as described in the paper (N = 4). ..... 45

Table S 2-4. Optimization parameters for separation and determination of arsenic species using HPLC-ICP-MS. ... 45

Table S 2-5. Methods and detection limits (DL) for measured water chemistry variables. ICP-MS stands for inductively coupled plasma-mass spectrometry and ICP-QQQ refers to triple quadrupole ICP-MS. ..... 46

Table S 2-6. Reference guides for zooplankton, rotifer, and phytoplankton identification. ..... 47

Table S 2-7. List of environmental variables included in each of the CCA models. Total arsenic (TAs), As(V), As(III), temperature, and DO were included in every model in order to specifically examine plankton community structure along these gradients. Variables indicated by (*) were chosen by the forward selection process (ordistep) in R. DO was not included in the open-water phytoplankton CCA since the model became overfitted when all variables were included. Preference was given to the forward selected variables. ..... 48

Table S 2-8. Minimum, maximum, and average concentrations (□g L-1) of total dissolved arsenic (DAs), As(V), and As(III) during the early open-water (EO; May, June 2022, May 2023), late open-water (LO; September 2022), early ice-on (EI; November 2022), and late ice-on (LI; April 2022, February, April 2023) seasons in each of the five study lakes. Method detection limits were as follows: Total DAs (0.2 μg $L^{-1}$), As(V) (0.05 μg $L^{-1}$), and As(III) (0.01 μg $L^{-1}$). ..... 48

Table S 2-9. List of the phytoplankton genera identified and counted across the five study lakes and which season they were present in. The open-water season was from May – October, and the ice-on season was from November – April. All samples collected from April 2022 – May 2023. ..... 49

Table S 2-10. Phytoplankton genera found to have statistically significant ($p < 0.05$) relationships with an arsenic variable (T = total dissolved arsenic, III = As(III), V = As(V)) according to individual GAMs. Seasons were denoted by A = all sampling dates, I = ice-on, and O = open-water, and brief descriptions of relationships were given (N = negative, P = positive). ..... 50

Table S 2-11. List of the rotifer species identified and counted across the five study lakes and which season they were present in. The open-water season was from May – October, and the ice-on season was from November – April. All samples collected from April 2022 –May 2023. ..... 51

Table S 2-12. Rotifer species found to have statistically significant ($p < 0.05$) relationships with an arsenic variable (T = total dissolved arsenic, III = As(III), V = As(V)) according to individual GAMs. Seasons were denoted by A = all sampling dates, I = ice, and O = open-water, and brief descriptions of relationships were given (N = negative, P = positive). ..... 51

Table S 2-13. List of the zooplankton species identified and counted across the five study lakes and which season they were present in. The open-water season was from May – October, and the ice-on season was from November – April. All samples collected from April 2022 – May 2023. ..... 52

Table S 2-14. Zooplankton species found to have statistically significant ($p < 0.05$) relationships with an arsenic variable (T = total dissolved arsenic, III = As(III), V = As(V)) according to individual GAMs. Seasons were denoted by A = all sampling dates, I = ice-on, and O = open-water, and brief descriptions of relationships were given (N = negative, P = positive). ..... 53

Table S 3-1. Location and physical characteristics of the four study lakes. ..... 96

Table S 3-2. Environmental and meteorological data from our spring thaw sampling dates at our four study lakes. Air temperature data was recorded during sampling from the Environment Canada mobile application. ..... 96

Table S 3-3. Collection size and depth of each sample type taken from our four study lakes. Plankton sampled collected for IDing purposes were integrated from the entire water column, starting from 1 m above the lake bed. ..... 97

Table S 3-4. Field blank (FB) data from the four study lakes collected from 2022-2024 (N = 19). Measurements of DAs below the method detection limit of 0.2 μg $L^{-1}$ are indicated by < MDL. ..... 98

Table S 3-5. Field replicate data from Handle and Jackfish Lakes collected in November 2020 and January 2021 using the same sampling methods as described in the paper (N = 4). ..... 98

Table S 3-6. Total dissolved arsenic (As) concentrations in terrestrial snowmelt water samples collected from runoff sites directly next to three of the study lakes. Meltwater samples were collected during the post-snowmelt 2023 season. Surface lake water total dissolved arsenic concentrations collected during the pre-snowmelt 2023 period included for easier comparison. ..... 99

Table S 3-7. Optimization parameters for separation and determination of arsenic species using HPLC-ICP-MS. Samples were separated by HPLC-ICP-MS/MS (Agilent) and quantified using Agilent software (MassHunter 4.6). ..... 100

Table S 3-8. Environmental variables analyzed via t-tests and Wilcoxon tests and their associated p-values and power test results (where applicable). ..... 101

Table S 3-9. Surface water layer (top 1 m) physical and chemical parameters of the four study lakes during the pre- and post-snowmelt periods and across both study years (2022, 2023). Method detection limit (DL) of 10 μg $L^{-1}$ for dissolved phosphorus. ..... 103

Table S 3-10. The oxidation reduction potential (ORP) and sulphide ($S^{2-}$) concentrations of Frame and Handle Lakes during the ice-on season from 2020-2022. Measurements of dissolved $S^{2-}$ exceeding the maximum DL (MDL) of 800 μg $L^{-1}$ are indicated by > MDL. N/A represents no measurements taken on the indicated sampling date. Data collected and provided via ARI. Oxidation reduction potential measurements were collected via YSI while $S^{2-}$ samples were collected using the peristaltic pump as described in the methods section of this study. Samples were analyzed by Taiga Laboratories (M. Palmer, ARI, unpublished data). ..... 104

Table S 3-11. The environmental variables selected by RDA with forward selection for each plankton type, the amount variance (%) explained by the selected variables, p-values, and $R^2$ values for each model. All samples collected between April 2022 and May 2023. ..... 105

Table S 3-12. Plankton density values for each of the four study lakes across all four sampling periods. Samples collected from April 2022 – May 2023. PR = pre-snowmelt, PO = post-snowmelt. ..... 105

Table S 4-1. Sampling coordinate locations, physical characteristics, average total arsenic concentration, and justification for inclusion in study design for the five study lakes. ..... 139

Table S 4-2. Sampling dates for arsenic analysis in lake water and bulk plankton, and plankton for identification purposes. Samples collected indicated with an “X”. No sample collected indicated with a “/”. ..... 140

Table S 4-3. Field blank (FB) data from the four study lakes collected from 2022-2024 (N = 19). Measurements of dissolved arsenic below the method detection limit of 0.2 μg $L^{-1}$ are indicated by < DL. ..... 141

Table S 4-4. Field replicate data from Handle and Jackfish Lakes collected in November 2020 and January 2021 using the same sampling methods as described in the paper (N = 4). ..... 141

Table S 4-5. Optimization parameters for separation and determination of arsenic species using HPLC-ICP-MS. Samples were separated by HPLC-ICP-MS/MS (Agilent) and quantified using Agilent software (MassHunter 4.6). ..... 142

Table S 4-6. Matrix spike and certified material recovery data (% or □g g-1) for each batch of lake water arsenic speciation samples collected from April 2022 to June 2024. As(III) = arsenite, As(V) = arsenate, and ND refers to “no data”. Certified reference material acronyms: TORT-3 = lobster hepatopancreas, DORM-4 = dogfish tissue. Control sample acronyms: OPR-2 = ongoing precision and recovery, and PTC = Proficiency Testing Canada. *PTC-1-2025 was fortified with the standard As(III) (second source). ..... 143

Table S 4-7. Methods and detection limits (DL) for measured water chemistry variables. ICP-MS stands for inductively coupled plasma-mass spectrometry and ICP-QQQ refers to triple quadrupole ICP-MS. ..... 145

Table S 4-8. Blank and certified material recovery data for each batch of plankton total arsenic bioaccumulation samples collected from April 2022 to June 2024. ND refers to “no data”. Certified reference material acronyms: TORT-3 = lobster hepatopancreas, DORM-4/5 = dogfish tissue. The method detection limit for total arsenic in plankton was 0.002 μg $g^{-1}$. ..... 145

Table S 4-9. Reference guides for zooplankton and phytoplankton identification. ..... 146

Table S 4-10. Plankton arsenic bioaccumulation sample duplicate data. Y = Yes to a duplicate available for a specific sample, while N = No. / = no sample available for that date. Samples found to be lacking a duplicate or thought to have potential QA/QC concerns are flagged with an asterisk (*). More information on all flagged samples is found below in Table S 4-11. ..... 147

Table S 4-11. Plankton arsenic bioaccumulation samples flagged for potential QA/QC issues with a statement about why they were found to be acceptable. ..... 148

Table S 4-12. Results of the final models run for each plankton category based off of the environmental drivers found to be significant predictors of arsenic bioaccumulation. Models were compared in an AIC framework and found to have smaller values than their null model counterparts. *Value after Sammy’s Lake was removed (AIC beforehand = 44.3). ..... 150

# List of Figures

Figure 2.1. Map of the five study lakes in the Yellowknife region, including important historical mine sites. Map created by Seamus Daly. ..... 17

Figure 2.2. CCA plots of phytoplankton communities and statistically correlated environmental gradients for the: a) entire sampling period (April 2022 – May 2023), b) ice-on season (November – April), and c) open-water season (May – October). ..... 27

Figure 2.3. GAM plots of phytoplankton relative abundance data from across all sampling dates (April 2022 – May 2023) with statistically significant correlations between specific genera and: a) total dissolved arsenic, b) As(V), and c) As(III). ..... 28

Figure 2.4. The correlations between total dissolved arsenic and the rotifer species K. longispina, K. species complex, and P. remata as assessed using GAMs across all sampling dates and study lakes. ..... 30

Figure 2.5. CCA plots of zooplankton communities and statistically correlated environmental gradients for the: a) entire sampling period (April 2022 – May 2023), and b) ice-on season (November – April). No environmental gradients were identified for the open-water season. ..... 31

Figure 2.6. Negative correlations between total dissolved arsenic and zooplankton Cladocera species B. longirostris and D. longiremus as assessed using GAMs across all sampling dates and study lakes. ..... 33

Figure 3.1. Map showing the locations of the four study lakes in relation to the historical gold mine property lease boundaries in the Yellowknife (Northwest Territories, Canada) region. Most arsenic emissions are associated with Giant Mine. Coordinates are in decimal degrees. Inset shows the location of Yellowknife within Canada. Map created by Seamus Daly. ..... 71

Figure 3.2. Lake-depth profiles of the four study lakes showing the change in total dissolved arsenic concentration, proportion of different arsenic species, DO, and specific conductivity between the pre- and post-snowmelt periods in both 2022 and 2023. Pre-snowmelt lake arsenic data could not be collected from Handle Lake in 2022. ..... 79

Figure 3.3. a) Combined relative abundance plot of zooplankton (including nauplii and immature copepodites) encountered across all lakes and sampling events; b) RDA ordination plot with explanatory environmental variables highlighted by forward selection for zooplankton community composition across all lakes and sampling events. ..... 83

Figure 3.4. Mean plankton density during the pre-snowmelt and post-snowmelt periods across both study years and all four study lakes. More information related to plankton densities in each study lake from each sampling period can be found in Table S 3-12. ..... 84

Figure 3.5. a) Combined relative abundance plot of rotifers across all lakes and sampling events; and b) RDA ordination plot with explanatory environmental variables highlighted by forward selection for rotifer community composition across all lakes and sampling events. ..... 86

Figure 3.6. a) Combined relative abundance plot for phytoplankton genera, and b) RDA ordination plot with explanatory environmental variables highlighted by forward selection for phytoplankton community composition across all four lakes and study period. ..... 88

Figure 4.1. Site map of the five study lakes and historical mine site boundaries from the Yellowknife, Northwest Territories, Canada region. Map created by Seamus Daly. ..... 116

Figure 4.2. Measurements of arsenic bioaccumulation in plankton (μg $g^{-1}$) from the five study lakes across multiple sampling events from April 2022 to June 2024, including under-ice (circles) and open-water (triangles) sampling: a) small plankton (≥ 20 – 62 μm), b) large plankton (≥ 63 μm), and c) combined plankton (≥ 20 μm; Jackfish Lake only). Samples collected from April 2022 – June 2024. ..... 124

Figure 4.3. The results of statistically significant LR and GAM models highlighting the relationships between: (a) lake water total arsenic and plankton arsenic bioaccumulation for small plankton (≥ 20 – 62 μm); b) lake water total arsenic and plankton arsenic bioaccumulation for large plankton (≥ 63 μm); c) lake water As(V) and plankton arsenic bioaccumulation for small plankton; and d) lake water As(V) and plankton arsenic bioaccumulation for large plankton. All four plots compare the difference between the correlations with (solid line) and without (dashed line) the data from Sammy's Lake. ..... 126

Figure 4.4. A PCA highlighting environmental gradients across the five study lakes. ..... 128

Figure 4.5. Environmental variables found to have a statistically significant relationship with small plankton arsenic concentration: a) DOC and b) season*. *Ice-on data was only available for small plankton samples collected from Handle Lake and Frame Lake due to issues related to low biomass. ..... 130

Figure 4.6. Environmental variables found to have a statistically significant relationship with large plankton arsenic concentration: a) small plankton arsenic concentration, b) DOC, c) iron, d) sulfate, and e) season. ..... 132

# List of Figures (Supplementary Information)

Figure S 2-1. Correlation matrix of all environmental variables in the original dataset created in R (package corrplot). Variables were removed if they were highly correlated (r > 0.7) with another important variable (i.e., arsenic). Variables included in the final model were: plankton densities, arsenic variables (total, As(III), As(V)) temperature, aluminum (Al), DO, chlorophyll-a, nickel (Ni), iron (Fe), total nitrogen (TN), copper (Cu), zinc (Zn), phosphorus (P), and specific conductivity. ..... 54

Figure S 2-2. NMDS plot for the full year phytoplankton dataset collected between April 2022 and May 2023. ..... 55

Figure S 2-3. NMDS plot for the full year rotifer dataset collected between April 2022 and May 2023. ..... 55

Figure S 2-4. NMDS plot for the full year zooplankton dataset collected between April 2022 and May 2023. ..... 56

Figure S 2-5. Lake-depth profiles of the five study lakes showing the change in DO and temperature between the middle of the open-water season (June 2022) and ice-on season (February 2023). ..... 56

Figure S 2-6. Total dissolved arsenic concentrations and proportions of As(III) and As(V) in the top and bottom layers of the five study lakes across all sampling dates (April 2022 – May 2023). Inorganic arsenic samples were not collected from Handle Lake in April 2022 due to equipment malfunction, and no samples were collected from Stuart Lake in May 2023 due to unsafe lake ice conditions. ..... 57

Figure S 2-7. a) Phytoplankton absolute density for the five study lakes, followed by phytoplankton relative abundances and diversity for b) Handle Lake, c) Frame Lake, d) Jackfish Lake, e) Sammy's Lake, and f) Stuart Lake. Phytoplankton ID samples were collected from April 2022 – May 2023 except for in Stuart Lake, which could only be sampled until April 2023. Diversity (Hill's N2) was calculated using the vegan package in RStudio (Oksanen et al., 2019). ..... 58

Figure S 2-8. Combined and averaged phytoplankton relative abundances and diversity values for all five study lakes except for May 2023 when Stuart Lake could not be sampled. Diversity (Hill's N2) was calculated using the vegan package in RStudio (Oksanen et al., 2019). ..... 59

Figure S 2-9. a) The relative abundance of each major phytoplankton group during each sampling date averaged across the five study lakes, and b) the difference in cyanobacteria relative abundance in the four arsenic-contaminated lakes compared to the one reference lake. ..... 59

Figure S 2-10. a) Rotifer absolute density for the five study lakes, followed by rotifer relative abundances and diversity for: b) Handle Lake, c) Frame Lake, d) Jackfish Lake, e) Sammy's Lake, and f) Stuart Lake. Rotifer ID samples were collected from April 2022 – May 2023 except for in Stuart Lake, which could only be sampled until April 2023. Diversity (Hill's N2) was calculated using the vegan package in RStudio (Oksanen et al., 2019). ..... 60

Figure S 2-11. Combined and averaged rotifer relative abundances and diversity values for all five study lakes except for May 2023 when Stuart Lake could not be sampled. Diversity (Hill's N2) was calculated using the vegan package in RStudio (Oksanen et al., 2019). ..... 61

Figure S 2-12. CCA plots of rotifer communities and statistically correlated environmental gradients for the: a) entire sampling period (April 2022 – May 2023), b) ice-on season (November – April), and c) open-water season (May – October). ..... 62

Figure S 2-13. a) Adult zooplankton absolute density for the five study lakes, followed by adult zooplankton relative abundances and diversity for: b) Handle Lake, c) Frame Lake, d) Jackfish Lake, e) Sammy's Lake, and f) Stuart Lake. Zooplankton ID samples were collected from April 2022 – May 2023 except for in Stuart Lake, which could only be sampled until April 2023. Diversity (Hill's N2) was calculated using the vegan package in RStudio (Oksanen et al., 2019). ..... 63

Figure S 2-14. Combined and averaged adult zooplankton relative abundances and diversity values for all five study lakes except for May 2023 when Stuart Lake could not be sampled. Diversity (Hill's N2) was calculated using the vegan package in RStudio (Oksanen et al., 2019). ..... 64

Figure S 3-1. Mean daily air temperatures of: a) 2022 ice-on months, b) 2023 ice-on months, and c) average 2022 versus 2023 ice-on periods. Air temperature data collected by and retrieved from ECCC (2025). ..... 106

Figure S 3-2. Lake-depth profiles of the four study lakes showing the change in chlorophyll-a, total organic arsenic, and PAR between the pre- and post-snowmelt periods during spring thaw in both 2022 and 2023. ..... 107

Figure S 3-3. ORP measurements in each study lake compared to: a) total dissolved arsenic, b) As(III), and c) As(V) concentrations. Lines of best fit were calculated for each lake via linear regression. ..... 108

Figure S 4-1. Results of regression tree analyses identifying which environmental variables best explain total arsenic concentrations in each of the three plankton size categories: a) small plankton, b) large plankton, and c) combined plankton (Jackfish Lake only). ..... 150

Figure S 4-2. Boxplots indicating the range of important environmental variables in the five study lakes with emphasis on the differences in concentration during the ice-on and open-water season and scatterplots indicating plankton density. ..... 151

Figure S 4-3. The seasonal cycling of total dissolved arsenic (black line) and its two major inorganic forms – As(V) (blue) and As(III) (red) in the five study lakes: a) Handle, b) Frame, c) Jackfish, d) Sammy's, and e) Stuart. Samples were collected from April 2022 - June 2024. In certain situations samples could not be taken, such as: April 2022 from Handle Lake (equipment malfunction) and May 2023 from Stuart Lake (unsafe ice conditions). ..... 152

## Acronyms

AIC: Akaike Information Criterion

ARI: Aurora Research Institute

*Ars*: Arsenic Resistance Operon

As: Arsenic

As(V): Arsenate

As(III): Arsenite

$As_2O_3$: Arsenic Trioxide

AsB: Arsenobetaine

AC: Arsenocholine

CALA: Canadian Association for Laboratory Accreditation

CCA: Canonical Correspondence Analysis

CCME: Canadian Council of Ministers of the Environment

CRM: Certified Reference Material

DAs: Dissolved Arsenic

DCA: Detrended Correspondence Analysis

DL: Detection Limit

DMA: Dimethylarsinic Acid

DO: Dissolved Oxygen

DOC: Dissolved Organic Carbon

DOM: Dissolved Organic Matter

DORM-4/5: Fish Protein

$EC_{50}$: Half Maximal Effective Concentration

ECCC: Environment and Climate Change Canada

EDTA: Ethylenediaminetetraacetic Acid

EPA: Environmental Protection Agency

FB: Field Blank

GAM: Generalized Additive Models

HCl: Hydrochloric Acid

HPLC: High-Performance Liquid Chromatography

$IC_{50}$: Half Maximal Inhibitory Concentration

ICP-MS: Inductively Coupled Plasma-Mass Spectrometry

ICP-QQQ: Triple Quadrupole Inductively Coupled Plasma-Mass Spectrometry

$LC_{50}$: Lethal Concentration 50

LR: Linear Regression

MDL: Method Detection Limit

MMA: Monomethylarsonic Acid

MLR: Multiple Linear Regression

$N_2$: Nitrogen

N:P: Nitrogen:Phosphorus Ratio

NMDS: Nonmetric Multidimensional Scaling

NRC: National Research Council

NWT: Northwest Territories

OPR2: Ongoing Precision and Recovery

ORP: Oxidative-Reduction Potential

PAR: Photosynthetically Active Radiation

PERMANOVA: Permutational Multivariate Analysis of Variance

PES: Polyethersulfone

PICT: Pollution-Induced Community Tolerance

$PO_4^{3-}$: Phosphate

PTC: Profiency Testing Canada

QA/QC: Quality Assurance/Quality Control

RDA: Redundancy Analysis

SIMPER: Similarity Percentage Analysis

SLACC: Subarctic Lakes in a Changing Climate

SM: Standard Method

SWI: Sediment-Water Interface

TMAO: Trimethylarsenic Oxide

TORT-3: Lobster Hepatopancreas

US EPA: United States Environmental Protection Agency

UV: Ultra-violet

VIF: Variance Inflation Factor

VNIRS: Visible Near-Infrared Reflectance Spectroscopy

YKDFN: Yellowknives Dene First Nation

YSI: Yellow Springs Instruments

WHO: World Health Organization

# Chapter 1: General Introduction

## 1.1 Introduction

Due to its widespread distribution, high toxicity, and ability to migrate, the contamination of freshwater ecosystems by mining-related arsenic is becoming a global issue of increasing concern (Wagemann, 1978; Wang & Mulligan, 2006). Typically found at concentrations of < 2 $\mu g\ L^{-1}$ in freshwater lakes, natural sources of arsenic to aquatic systems include the erosion of arsenic-bearing rocks, minerals and soils, hydrothermal ore deposits, and other geothermal processes (Korte & Fernando, 1991; Smedley & Kinniburgh, 2002; Wang & Mulligan, 2006). However, recent anthropogenic activities, such as mining, smelting, and the production of fossil fuels, have increased the amount of arsenic found in freshwater systems, with one contaminated lake reported to have had 47,000 $\mu g\ L^{-1}$ of total arsenic during peak industrial activities (Wang & Mulligan, 2006; Palmer et al., 2025). Mining represents the largest anthropogenic source of arsenic to the environment (Barral-Fraga et al., 2020; Faria et al., 2023), with most associated with tailings and roaster emissions from gold and silver mines (Kwong et al., 2006; Jasiak et al., 2021).

## 1.2 Arsenic Biogeochemical Cycling in Freshwater Lakes

Arsenic is found in a variety of different chemical forms (speciation) in freshwater systems, including both inorganic and organic species, and has four main oxidative states (-III, 0, +III, +V) (Wang & Mulligan, 2006). The two most common forms of arsenic in freshwater are arsenate (As(V)) and arsenite (As(III)), both of which are inorganic. As(V) is more stable under oxic conditions, and therefore tends to dominate during most times of the year, compared to As(III) which is more thermodynamically stable under anaerobic conditions (Cullen & Reimer,

1989). Although less common than their inorganic counterparts, monomethylarsonic acid (MMA(V)) and dimethylarsinic acid (DMA(V)) are the most frequently reported forms of organic arsenic detected in freshwater systems (Cullen & Reimer, 1989; Caumette et al., 2012b). Other forms of organic arsenic that have been found to be important in aquatic organisms include arsenosugars, arsenolipids and arsenocholine (AC) (Cullen & Reimer, 1989). Arsenobetaine (AsB) appears to be a common form of organic arsenic in both freshwater and biota, but more research is required before this can be confirmed conclusively (Blais et al., 2025).

Arsenic is a redox-sensitive element which means that it changes chemical form depending on the redox conditions present (e.g., dissolved oxygen (DO) concentration, position of the redoxcline (transition depth between high to low redox potential), availability of electron acceptors/donors, rates of microbial activity, organic matter deposition) (Rodie et al., 1995). The majority of redox-based transformations occur in either the surface waters of lakes or near the sediment-water interface (SWI; thin layer separating bottom sediment from overlying water column), in large part due to changes associated with DO availability. While DO is plentiful in surface waters, it can be quite scarce in the bottom waters of deep lakes in particular. The presence of oxidants and oxyhydroxides in surface sediments establish and maintain a thin oxic layer at the surface of the SWI, which is responsible for controlling the redox conditions and processes immediately above and below it (Nikolaidisa et al., 2004; Couture et al., 2010). With the onset of anoxia, the oxic layer thins and oxidants are reduced over time, releasing redox-sensitive molecules that are bound to oxyhydroxides back into the water column (Hupfer & Lewandowski, 2008). This process is an important control of arsenic mobility, as As(V) coprecipitates with and/or adsorbs onto the surfaces of oxyhydroxides (largely iron and manganese) (Wang & Mulligan, 2006). Under anaerobic conditions, these same oxides are

reduced and subsequently release arsenic back into the hypolimnion, largely as As(III) (Sposito, 1984; Stumm, 1992).

Under aerobic conditions, the transformation and oxidation of As(III) (and also MMA and DMA), into the more thermodynamically stable As(V) occurs relatively quickly, via either microbial or photooxidation processes (Hellweger et al., 2003; Pothier et al., 2020). The oxidation of As(III) into As(V) via abiotic processes is expected to be a function of light intensity and is proportionally quite low compared to microbially-mediated oxidation (Johnson & Pilson, 1975; Hellweger et al., 2003). The reaction sequence is assumed to be: DMA → MMA → As(III) → As(V). AsB has been found to be chemically stable once excreted into the water column, and tends to not be degraded into smaller arsenicals (Zhang et al., 2022). Hence, As(V) is often the most dominant form of inorganic arsenic, while AsB is the most common form of organic arsenic in lakes, although its study in freshwater systems is limited (Blais et al., 2025).

### 1.3 Plankton Arsenic Ecotoxicology and Bioaccumulation

In addition to mobility, the toxicity of arsenic is also dependent on its chemical form. The generally accepted range of arsenic toxicity to freshwater organisms, from most to least toxic, is: DMA(III) = MMA(III) > As(III) > As(V) > MMA(V) = DMA(V) > trimethylarsenic oxide (TMAO(V)) = AsB, with trivalent species generally considered to be more toxic than pentavalent forms (Akter et al., 2005; Rahman & Hassler, 2014). Although the trivalent organic forms DMA(III) and MMA(III) have been found to be extremely toxic, they are highly unstable and tend to be produced in very small quantities compared to other forms of arsenic (Rahman & Hassler, 2014). As a result, inorganic arsenic (As(V), As(III)) is often considered to be more toxic than organic arsenic. For example, some studies have reported decreases in toxicity ranging

from 100 to 1,000 times less for DMA(V) and TMAO(V) compared to As(III) (Hirano et al., 2004). AsB is considered to be virtually non-toxic, which is significant as it's been found to make up over 80% of the arsenic found in the edible portions of marine fish and shellfish (Phillips, 1990; Caumette et al., 2012b). However, despite the clear differences in toxicity between arsenic forms, current guidelines for the protection of both human (e.g., drinking water = 10 $\mu g\ L^{-1}$; WHO, 1993) and environmental (e.g., aquatic life = 5 $\mu g\ L^{-1}$; CCME, 2003) health have remained focused on the impacts of total arsenic, and do not account for specific chemical forms.

Due to structural similarities with phosphate ($PO_4^{3-}$), As(V) has been found to be significantly more toxic to phytoplankton and other aquatic microorganisms compared to As(III) (Cullen & Reimer, 1989). This is because As(V) and $PO_4^{3-}$ compete for uptake into phytoplankton via the $PO_4^{3-}$-transporters located in their cell walls (Hellweger et al., 2003). As(V) has been shown to replace $PO_4^{3-}$ in important glycolytic and respiration pathways that are critical for cellular signalling (Hughes, 2002). However, the structural similarities between the two chemicals means that the toxicity of As(V) is largely influenced by the $PO_4^{3-}$:As(V), since higher concentrations of $PO_4^{3-}$ end up competing with As(V), decreasing its overall toxicity (Levy et al., 2005). This has been well established in the literature, with one study finding a 20-fold difference in the toxicity of As(V) to the green algae *Monoraphidium arcuatum* when phosphorus was included in the experimental set up (Levy et al., 2005). In contrast, As(III) is more toxic to higher trophic organisms, such as zooplankton and fish, and has been found to have a higher affinity for sulfhydryl groups in proteins, which subsequently impairs their function (NRC, 1999). The main entry points for arsenic into exposed zooplankton are through

the ingestion of contaminated food sources and through external structures such as gills (Rahman et al., 2012).

Since phytoplankton are an important food source for many zooplankton, the uptake and bioaccumulation of arsenic by phytoplankton represents an important link in the transfer of arsenic through aquatic food webs. Multiple studies have confirmed that biota collected from lakes with higher arsenic concentrations tend to also have higher levels of total arsenic bioaccumulation (Jia et al., 2018; Lepage et al., 2024; Blais et al., 2025). The bioaccumulation of arsenic in zooplankton has been found to be correlated with the amount of arsenic in phytoplankton (Barrett et al., 2018; Hull et al., 2023), although zooplankton tend to exhibit lower total arsenic concentrations than phytoplankton, which suggests a bio-diminution (decrease) of arsenic with increasing trophic level instead of bio-magnification (increase; Chen & Folt, 2000; Caumette et al., 2012a; Blais et al., 2025).

In addition to bio-diminution, plankton are also able to decrease the overall toxicity of total arsenic through a process known as bio-methylation. Bio-methylation specifically occurs in phytoplankton and other aquatic microorganisms through the uptake of arsenic as As(V) via the $PO_4^{3-}$-transporters discussed earlier (Hellweger et al., 2003). Once inside the cell, As(V) is rapidly transformed into As(III) before undergoing enzymatic methylation via *S*-adensylmethionine in order to form MMA(V) (Edmonds & Francesconi, 1987). MMA(V) then undergoes further reduction and methylation steps in order to yield penta- and trivalent forms of both MMA and DMA, with DMA(III) being an important building block for more complex organic arsenic compounds, including arsenosugars and AsB (Caumette et al., 2012b). AsB is considered to be the endpoint of the bio-detoxification pathway of inorganic arsenic into organic compounds due to its non-toxicity (Caumette et al., 2012b). Although the exact

biotransformation pathway for the production of AsB remains unresolved, it is generally accepted that AC (a precursor to AsB) and AsB are specifically formed after the trophic transfer of less complex forms of organic arsenic, specifically DMA and arsenosugars, by metabolic transformations in higher trophic organisms (Caumette et al., 2012b; 2014; Popowich et al., 2016). Since total arsenic does not bio-magnify in freshwater organisms, higher trophic organisms, such as zooplankton, tend to have lower total arsenic concentrations, but higher concentrations (and/or proportions) of organic arsenic (Caumette et al., 2011; 2012b; 2014; Blais et al., 2025).

### 1.4 The Influence of Seasonality on Arsenic in Subarctic Lakes

The biogeochemical cycling and ecotoxicity of arsenic are all influenced by seasonality, yet very few studies include more than one sampling effort from more than one season, particularly in the subarctic region where lakes are ice covered for approximately half of the year. The majority of limnology-based fieldwork tends to occur during the open-water season (spring to fall), due in large part to the more comfortable sampling conditions (e.g., warm temperatures, no issues with freezing equipment, more daylight hours), but also because winter was once thought to be a period of biological dormancy, and therefore not worth studying from an ecological perspective (Block et al., 2019). However, recent research has revealed that arsenic concentration and chemical form in subarctic lakes can vary substantially between seasons, including documented increases in arsenic from a minimum of 172 $\mu g\ L^{-1}$ in early spring to 846 $\mu g\ L^{-1}$ by mid-winter in a shallow, contaminated lake, with a higher proportion occurring as the more toxic As(III) (Palmer et al., 2019). This differs from what has been reported in shallow, arsenic contaminated temperate lakes, where arsenic concentrations tend to be lower in winter

compared to summer (e.g., Barrett et al., 2018; 2019). Under-ice plankton dynamics are also known to be much more active than originally hypothesized, and often have a significant influence on resource availability for subsequent seasons (Hampton et al., 2015; 2017). Winter therefore represents a unique but understudied period with respect to arsenic biogeochemical cycling and ecotoxicity.

### 1.5 Legacy Arsenic Pollution in Yellowknife (Northwest Territories, Canada)

One of the best known examples of long-term arsenic contamination in Canada is found in and around the City of Yellowknife (Northwest Territories). Previously host to three gold mines within its city limits, the greater Yellowknife area is currently the epicenter of a radius of elevated arsenic (and other mining-related) contamination approximately 80 km wide (Jasiak et al., 2021). Operational from 1938-2004, Con Mine (1938-2003), Negus Mine (1939-1952), and Giant Mine (1948-2004), were major economic drivers for the Yellowknife region, but like many industrial activities of the time, were subject to little environmental oversight (Hocking et al., 1978; Bullen & Robb, 2006). As a result, the combined atmospheric emissions from Giant Mine and Con Mine were estimated to have released 5 tonnes of toxic arsenic trioxide ($As_2O_3$) dust per day between 1949 and 1953, resulting in over 20,000 tonnes of $As_2O_3$ contamination in the region (Hocking et al., 1978; Palmer et al., 2025). Therefore, despite the fact that gold mining activities have not taken place in the region for almost two decades, much of the land and waterscape remain host to arsenic levels much higher than water safety guidelines (drinking water = 10 µg $L^{-1}$; WHO, 1993 / aquatic life = 5 µg $L^{-1}$; CCME, 2003). According to a 2015 survey of the area, the mean total arsenic concentration of the 98 lakes sampled was found to be 40.2 µg $L^{-1}$, generally within a range of 0.5 – 646 µg $L^{-1}$ (Palmer et al., 2015), although

concentrations as high as 2,070 μg $L^{-1}$ have been reported, which is 400x the guideline for the protection of aquatic life (Sivarajah et al., 2019).

### 1.6 Dissertation Goals & Objectives

The goal of this dissertation is to investigate the seasonal biogeochemical cycling of arsenic in lakes contaminated by legacy mining in the Yellowknife region, with emphasis on its interactions with plankton communities, and to ascertain whether certain times of the year might exhibit increased exposure risk. By integrating methods from aquatic biogeochemistry, community ecology, and ecotoxicology, the research aimed to more comprehensively characterize arsenic dynamics and interactions in real-world food webs across multiple seasons. As Yellowknife faces renewed mining interest (as does northern Canada more broadly), understanding the long-term ecological legacy of historical industrial pollution is essential for guiding current and planning future mines, while also evaluating remediation potential and protections for lake ecosystems impacted by legacy mining-related arsenic contamination.

This thesis is divided into three data chapters (Chapters 2 – 4) which have been written as manuscripts for publication in peer-reviewed journals. Each of the three data chapters is based on repeated water chemistry and plankton sampling across multiple seasons for five lakes in the Yellowknife region that spanned a gradient of arsenic contamination, as well as other gradients (e.g., depth, phosphorus, dissolved organic carbon) that are relevant to arsenic biogeochemistry and ecotoxicity. Chapter 2 aimed to characterize the seasonal biogeochemical cycling of total and inorganic (As(III), As(V)) arsenic and its potential interactions with exposed plankton (phytoplankton, rotifers, and zooplankton) communities. Chapter 3 focused on the spring thaw season specifically, which we defined as a short (7-10 days) transitional period between the end of April into early May in 2022 and 2023 when lake ice and snow first begin to melt. We

hypothesized that spring thaw would be a period of rapid and dynamic change for lake water arsenic concentration and form, as well as for primary productivity and plankton community composition. In addition to the water chemistry and plankton communities that were analyzed for Chapters 2 and 3, the concentration of total arsenic in bulk plankton samples representing two main size categories (small: ≥ 20 – 62 μm (mostly phytoplankton); large ≥ 63 μm (mostly zooplankton)) were also quantified. Chapter 4 investigated arsenic bioaccumulation in the two plankton categories, with emphasis on the potential drivers and mediators of arsenic uptake.

This dissertation therefore provides novel information related to how seasonal and ecological factors influence arsenic-plankton community dynamics, and highlights the importance of considering lake-specific factors and seasonal processes in assessments of ecotoxicological risk and the development of long-term monitoring and remediation strategies in northern mining-impacted regions.

# Chapter 2: Seasonal arsenic cycling and its potential impacts to plankton communities in subarctic lakes

Amanda J. Little, Michael J. Palmer, Marc Amyot, and Jennifer B. Korosi

## Author Contributions

AJL, MJP, and JBK conceived of research ideas and conducted fieldwork, MJP and JBK secured funding and were responsible for project administration and resource acquisition. AJL conducted all other analyses and led the writing of the manuscript. All authors contributed to the creation of the methodology, contributed in the editing of manuscript drafts.

## 2.1 Abstract

The concentration, speciation, and toxicity of arsenic in lakes is influenced by seasonally-mediated environmental factors like temperature, dissolved oxygen levels, and redox conditions; however, the majority of studies on arsenic ecotoxicity in lakes have historically focused on the open-water season. In this study, we sampled water and plankton across multiple seasons in five lakes in the Yellowknife region (Northwest Territories, Canada) that spanned a gradient of legacy arsenic contamination (1.1 – 455 μg $L^{-1}$). The study aim was to better characterize the seasonal biogeochemical cycling of total and inorganic arsenic (As(V), As(III)), and its potential impacts on exposed plankton communities (zooplankton, rotifers, phytoplankton). Concentrations of total arsenic and trivalent arsenic (As(III)) were highest during the ice-on season, especially in the most contaminated study lakes. Multivariate analysis and generalized additive models revealed that zooplankton and phytoplankton taxa and communities were correlated with inorganic arsenic variables across the five study lakes, but only when the ice-on season was included (i.e., there was no relationship with arsenic in the ice-free season). The rotifer community was not correlated with any arsenic variables. Cyanobacteria and cyclopoid copepods appeared to be the groups most tolerant of arsenic contamination, and their relative abundances increased during the ice-on period when arsenic concentrations were highest, while herbivorous zooplankton taxa were observed to do the opposite and therefore appeared to be more sensitive. These findings highlight the potential importance of the ice-on season for arsenic exposure to plankton in subarctic lakes, though further study is needed to better disentangle the effects of potentially confounding variables.

## 2.2 Introduction

Arsenic is an aquatic pollutant of concern due to its widespread distribution, high toxicity, and persistence in contaminated landscapes, and can be detrimental to both human and ecosystem health (Wang & Mulligan, 2006). Arsenic pollution is commonly associated with gold and silver mine tailings, but arsenic can also be volatized during the roasting process at mine sites, resulting in contamination of the broader surrounding environment (Smedley & Kinniburgh, 2002; Jasiak et al., 2021). Arsenic concentrations over 47,000 μg $L^{-1}$ have been reported in at least one mining impacted lake in Canada (Wang & Mulligan, 2006; Palmer et al., 2025), well in excess of water quality guidelines intended to protect aquatic life (e.g., Canadian Council of Ministers of the Environment guideline = 5 μg $L^{-1}$; CCME, 2001). Recent evidence has shown that terrestrial runoff from the landscape can be a persistent source of arsenic to aquatic ecosystems even in catchments where mining activities ended decades ago, delaying chemical and biological recovery (Palmer et al., 2024).

Typical ecotoxicity endpoints for arsenic in freshwater systems based on controlled lab conditions can range from 250 – 1,150 μg $L^{-1}$ for phytoplankton exposed to arsenate (As(V); 72-hr $IC_{50}$ *Monoraphdium arcuantum*; Levy et al., 2005; vs 72-hr $EC_{50}$ *Chlorella* sp. strain CE-35; Rahman et al., 2014) compared to 550 – 2,500 μg $L^{-1}$ for zooplankton exposed to arsenite (As(III); 48-hr $LC_{50}$ *Daphnia carinata;* He et al., 2009; vs 48-hr $LC_{50}$ *Daphnia pulex;* Shaw et al., 2007). Pronounced impacts of arsenic pollution on plankton assemblages have also been inferred from environmental reconstructions using lake sediment cores (i.e., paleolimnology). The loss of all Cladocera, a keystone group of zooplankton, as well as all planktonic diatoms (siliceous algae) was observed for a contaminated lake in Yellowknife coincident with a 1700% increase in sedimentary arsenic concentrations (> 30,000 μg $g^{-1}$ sediment concentration during

peak industrial activities Thienpont et al., 2016; > 2,000 μg $L^{-1}$ in lake water as of 2014; Sivarajah et al., 2019). Industrial arsenic contamination was also associated with a decrease in crustacean zooplankton and an increase in metal-tolerant algae in two contaminated lakes in China (sediment arsenic concentrations of 479 μg $g^{-1}$ and 949 μg $g^{-1}$; Chen et al. 2015). However, associations between arsenic concentration and bioindicators of ecosystem health are less clear when assessed across wider gradients of present-day arsenic contamination, even when arsenic concentrations well exceed water quality guidelines (e.g., Sivarajah et al., 2019; Little et al., 2020; Persuad et al., 2021). There are likely several reasons for this disconnect, including differences in the chemical form of arsenic measured and the temporal effects of sampling designs that tend to focus on a limited number of sampling events concentrated in the summer.

To date, the majority of studies on aquatic biota exposure to arsenic have examined total arsenic but not arsenic chemical speciation. The two most common forms of arsenic in freshwater systems are inorganic As(V) and As(III). As(V) is considered more toxic to phytoplankton and other simple aquatic organisms because it is a chemical analogue of inorganic phosphate ($PO_4^{3-}$), and can easily enter phytoplankton cells via $PO_4^{3-}$-transporters present in cell walls (Hellweger et al., 2003; Rahman et al., 2014). As(III) is thought to be more toxic to higher trophic organisms such as zooplankton and fish (Akter et al., 2005). Dissolved oxygen (DO) concentrations, the position of the redoxcline, and temperature are important controls on arsenic chemical speciation and total concentrations in lakes (Rodie et al., 1995). Under anoxic conditions, arsenic concentrations can increase in the water column due to efflux from the sediment (Arsic et al., 2018). Arsenic is also more likely to be present as As(III) under low redox conditions, while As(V) is more prevalent under high redox potential (Rodie et al., 1995). Both DO and redox conditions follow predictable, seasonal patterns, such as increasing during periods

of lake turnover for lakes that seasonally stratify and decreasing during instances of anoxia (late winter, late summer) (Senn et al., 2007; Barrett et al., 2019; Palmer et al., 2019; 2020).

Most aquatic sampling occurs during the summer, and often only includes one sampling event per lake. Winter has been overlooked in limnology more generally, largely due to difficulties associated with cold weather fieldwork logistics, but also because it was previously considered to be a period of biological dormancy (Block et al., 2019). Recent literature has challenged this assumption, showing that under-ice lake ecosystems are dynamic and can have a significant impact on the subsequent open-water season (Hampton et al., 2015; 2017). A bias in the scientific literature towards studies that include only total arsenic, from samples collected in summer, limits our full understanding of the ecological impacts of arsenic pollution in lakes. Late winter, specifically, may be a critical period for arsenic ecotoxicity in shallow lakes that experience seasonal ice cover, as this period is often characterized by higher total arsenic concentrations (Palmer et al., 2019; 2020) and vulnerable plankton life history stages (Little et al., 2026). Plankton are also sensitive to changes in temperature, light, nutrient concentrations, and DO availability, all of which experience major shifts during the winter period (Hampton et al., 2017; Boulianne et al., 2025). These may act cumulatively to affect arsenic toxicity to under-ice plankton communities in subarctic lakes.

The aim of this research was to address the knowledge gaps described above regarding the impacts of arsenic on plankton communities, with emphasis on seasonal effects in subarctic lakes that are ice-covered for more than 50% of the year. We explored covariation between inorganic arsenic (As(V), As(III)) cycling and plankton community dynamics (zooplankton, rotifers, and phytoplankton) across seasons over one year of sampling in five Yellowknife-area lakes (Northwest Territories, Canada) that spanned a gradient of arsenic contamination (1.1 – 455

μg $L^{-1}$) from historic gold mining operations (Palmer et al., 2025). Shallow Yellowknife lakes are known to experience large increases in total arsenic concentrations during winter, including one lake that experienced a four-fold increase from 172 to 846 μg $L^{-1}$ (Palmer et al., 2019; 2020). The increase in arsenic occurs due to the combined effects of arsenic remobilization from the sediment under low redox conditions and cryoconcentration, whereby solute ions are pushed out of lake ice crystals as they form and become concentrated in the first few meters of water under the ice (Palmer et al., 2019). Low redox conditions in late winter also increases the proportion of arsenic present as As(III). Therefore, since winter already represents a period of enhanced ecological stress, it is important to characterize arsenic dynamics and potential associations with plankton communities across seasons. Overall, this study generates novel insights into the ecological impacts of (and recovery from) legacy mining pollution in northern ecosystems.

## 2.3 Materials & Methods

### 2.3.1 Study Site Description

Yellowknife is located on the northern shores of Great Slave Lake in Northwest Territories, Canada. It is within Treaty 8 and Chief Drygeese Territory, which has been the traditional home of the Tłı̨cho and Wıılıìdeh Yellowknives Dene First Nations and Northwest Territory Métis Nation for over 7,000 years (O'Reilly, 2015). The region experiences a continental subarctic climate, with sub-zero temperatures beginning in October and lasting until late April, and small lakes tend to remain ice-covered for the majority of the year (190-243 days) (Benson et al., 2013). The mean annual air temperature is -4°C and mean annual precipitation is 293.3 mm (1991-2020 Climate Normal; ECCC, 2025). The region is underlain by discontinuous permafrost which is limited to areas with thick peat deposits or mineral soils (Ecosystem

Classification Group, 2009). The geology of the region is known for its high mineral potential and was the site of three major gold mines (Con, Negus, and Giant Mine) (Palmer et al., 2025; Hocking et al., 1978). Recent studies have found modern day arsenic concentrations as high as 2,070 μg $L^{-1}$ in lakes from the region (Sivarajah et al., 2019), which is over 400x greater than the CCME guideline for the protection of aquatic life (5 μg $L^{-1}$; CCME, 2001).

Five study lakes were selected in the region to represent a gradient of mining-related arsenic contamination (Figure 2.1). Four lakes are well within the zone of influence of local mining contamination, including Handle Lake, Frame Lake, Jackfish Lake, and Sammy's Lake (Houben et al., 2016; Jasiak et al., 2021) (Table S 2-1). Handle Lake is the closest of the five lakes to Giant Mine, which was the main source of historic atmospheric arsenic emissions in the region (Hocking et al., 1978). Frame Lake and Jackfish Lake are both located within the downtown Yellowknife area and are subject to multiple stressors related to industrial and urban development, in addition to arsenic contamination. Frame Lake has been impacted by organic matter pollution related to historical illegal sewage dumping in the lake and has a high sediment oxygen demand which causes anoxia during the ice-on period (Gavel et al., 2018). A diesel-powered generating station and solid waste disposal site at Jackfish Lake are sources of thermal and nutrient pollution, and the lake has experienced frequent Cyanobacteria (*Planktothrix* genus) blooms since 2013 (Sivarajah et al., 2021). Sammy's Lake is located just outside of the city limits adjacent to the Yellowknife Highway. Finally, Stuart Lake (a.k.a, "Small Lake;" Blais et al., 2025) was selected as a reference site because it is located the furthest away from Giant Mine (Table S 2-1) (Palmer et al., 2015).

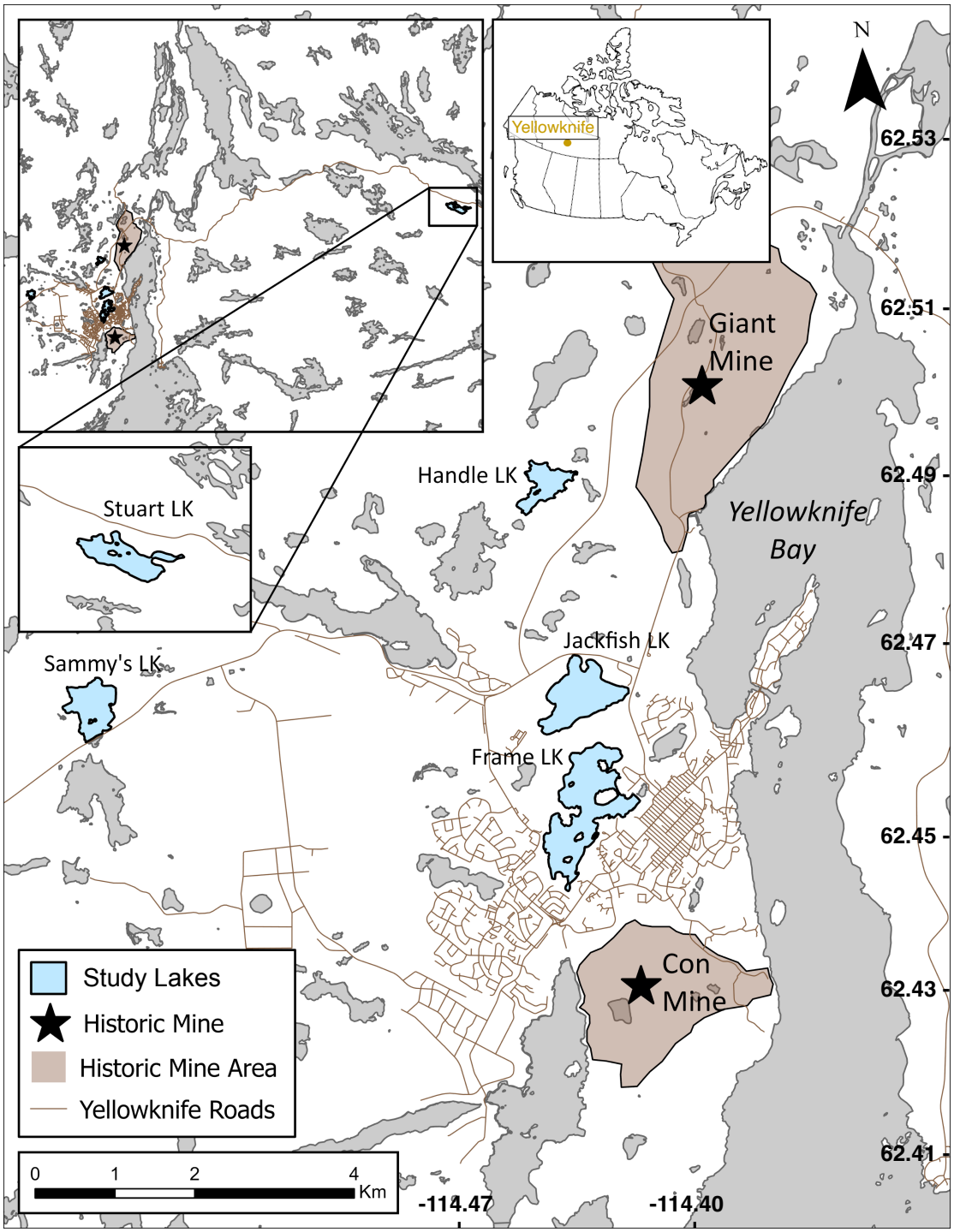


**Figure 2.1.** Map of the five study lakes in the Yellowknife region, including important historical mine sites. Map created by Seamus Daly.

### 2.3.2 Sample Collection

Lakes were sampled eight times between April 2022 and May 2023, always at the same location near the center of the lakes (Table S 2-1). A multi-parameter YSI probe (YSI EXOII, Yellow Springs Inc., Yellow Springs, Ohio) was used to measure vertical profiles of DO (mg $L^{-1}$), specific conductivity (ability of a solution to conduct electricity; μS $cm^{-1}$), oxidative-reduction potential (tendency of a solution to gain or lose electrons; ORP; mV), temperature (°C), and chlorophyll-a (μg $L^{-1}$) at 1 m depth intervals. Water samples for analysis of total and dissolved phosphorus, nitrogen, organic carbon, and a general suite of metal(loid)s, including total dissolved arsenic, As(III), and As(V), were collected at 1 m intervals using a peristaltic pump and Teflon™ line that was prerinsed with 5% hydrochloric acid (HCl) solution and ultrapure water (Palmer et al., 2020). Dissolved metal(loid)s, As(III), and As(V) were filtered in the field using a 0.45 μm polyethersulfone (PES) syringe tip filter. The As(III) and As(V) samples were filtered directly into 15 mL trace-metal free vials preloaded with 150 μL of 0.25 M ethylenediaminetetraacetic acid (ETDA). Once back in the lab, the arsenic speciation samples were preserved with an additional 25 μL of glacial acetic acid, while water samples for the general suite of metal(loid) were preserved to 1% (v/v) with nitric acid (Palmer et al., 2019). All samples were preserved within 4 hours of collection. Field blanks and duplicates for arsenic samples were collected as a quality assurance/quality control (QA/QC) measure, and all field blanks reported below the method detection limits (DL) for arsenic (DL = 0.2 μg $L^{-1}$; N = 19; Table S 2-2). Duplicate samples had relative percent differences ranging from 0.5-9.1% (mean = 3.4%, N = 7; Table S 2-3). Inorganic arsenic samples could not be sampled from Handle Lake in April 2022 due to equipment malfunction and no samples at all were collected from Stuart Lake in May 2023 due to unsafe ice conditions.

Rotifer and zooplankton samples were collected using vertical net tows with a Wisconsin zooplankton net (Wildco, Florida, USA; 63 μm mesh size, 0.127 m mouth diameter, 1 m net length) beginning 1 m above the lake bed, and were transferred into 50 mL vials preserved with ethanol to a final concentration of ~70%. Phytoplankton samples were collected as discrete samples using a 2.2 L Van Dorn (Wildco, Florida, USA), starting from 0.5 m below the surface of the water, and then again at 1 m and every metre interval afterwards until 1 m above the surface of the lake bed. Samples were homogenized and integrated in the field to match the vertical column sampling done for rotifer and zooplankton samples. Phytoplankton samples were subsampled into two 100 mL duplicates and preserved with 3% Lugol's solution. All water and plankton samples were stored cold and dark until analysis.

### 2.3.3 Lab Analyses

Water chemistry samples for nutrients (ammonia, nitrogen, phosphorus, and organic carbon) and the general suite of metal(loid)s were analyzed at the Canadian Association for Laboratory Accreditation (CALA) accredited government laboratory in Yellowknife, Northwest Territories (Taiga Environmental Laboratory). Total organic carbon and major anions were analyzed using high temperature combustion with a total carbon analyzer (standard method (SM) 5310) and ion chromatography (SM4110) (Greenberg et al., 1992). Total and dissolved metal(loid)s, as well as an additional round of phosphorus samples to avoid potential As(V) interference, were measured using inductively coupled plasma-mass spectrometry (ICP-MS) (Agilent 7900 Single Quadruple ICP-MS; Environmental Protection Agency (EPA) method 200.8) (Creed et al., 1994; Linge & Oldham, 2001). Samples for As(III) and As(V) were sent to the Université de Montréal and were analyzed using high-performance liquid chromatography

with ICP-QQQ (Agilent 8900 Triple Quadrupole ICP-MS). QA/QC protocols for arsenic speciation and all method detection limits can be found in the supplementary file (Table S 2-4; Table S 2-5).

Rotifer and zooplankton samples were homogenized and pipetted as 1 mL aliquots into a gridded Sedgewick-Rafter cell using a Hensen-Stemple pipette. A minimum of 100 individuals were counted per subsample for each plankton type, with a minimum of 3 subsamples per sample (300 individuals sample$^{-1}$). In samples with less than 300 adult individuals, all of the organisms were identified and counted. Both rotifers and zooplankton were identified to the lowest taxonomic level possible (species) using an OMAX V83 series inverted microscope. Due to structural similarities in multiple small rotifer species belonging to the genus *Keratella,* a catch-all category – *Keratella species complex* – was created and included the species: *Keratella cochlearis, Keratella crassa,* and *Keratella earlinae.* Similarly, the identification guides used for calanoid copepods were based on male individuals and could not identify females beyond their lack of a geniculate antenna and so they were categorized as "female calanoid copepods". Rotifer and zooplankton densities (individuals L$^{-1}$) were determined based off of the calculated volume of water sampled per tow and per aliquot.

The phytoplankton samples were allowed to settle for a minimum of 48 hours and then decanted to a volume of 20 mL to create a 5x concentration. Aliquots of 1 mL were pipetted into a gridded Sedgewick-Rafter cell and identified using three different magnifications (40x whole cell; 100-200x 1 transect; 400x 100 random fields of view) using the OMAX V83 series inverted microscope. A minimum of 300 natural units (1 natural grouping of algae (i.e., individual filament, colony, or isolated cell = 1 natural unit)) were counted per sample. Phytoplankton were identified to the genus level (reference guides listed in Table S 2-6). Cell densities and relative

abundance were calculated using cell counts, sample aliquot volume, and concentration factor (5x), and both were based on natural unit abundance (filament, colony, and individual cells) and not biomass, biovolume, or surface area.

### 2.3.4 Statistical Analyses

All data analyses were conducted using the statistical software RStudio (version 2024.12.0+467; R Core Team 2020). Relationships between plankton community composition, lakes, season, and environmental variables were visualized in 2D space using ordination techniques. Environmental variables were averaged across collected depth intevals for each sampling date and lake. They were run through a correlation matrix (package *corrplot*) (Wei & Simko, 2017), and removed if found to be highly correlated with other parameters ($r > 0.7$) (Figure S 2-1). The remaining variables were tested for normality using the Shapiro-Wilk test and $\log_{10}$-transformed if found to be non-normal. A 1% relative abundance threshold was applied to all plankton groups in order to improve the signal-to-noise ratio and reduce the influence of rare genera (Legendre & Legendre, 2012). The plankton relative abundance data were then transformed using the Hellinger transformation, and (dis)similarity was assessed using the Bray-Curtis dissimilarity metric (Legendre & Gallagher, 2001). A detrended correspondence analysis (DCA) was run on each plankton dataset to identify which ordination techniques were the most appropriate based on the length of the first axis (DCA1) (Lepš & Šmilauer, 2003).

Nonmetric multidimensional scaling (NMDS – unconstrained) and canonical correspondence analysis (CCA – constrained) were selected for all sampling periods and plankton types (package *vegan*; Oksanen et al., 2019). NMDS was used to visualize patterns of plankton taxa composition and lake characteristics (Figure S 2-2; Figure S 2-3; Figure S 2-4),

while CCA was used to specifically model how highlighted environmental variables influenced plankton species and composition (McCune & Grace, 2002). When selecting environmental parameters for inclusion in the CCA models, we prioritized arsenic (total arsenic, As(V), As(III)) and important seasonal (temperature, DO) variables since we were specifically interested in exploring how plankton communities were structured along arsenic and seasonality gradients (Symons et al., 2014; Fernández-Aláez et al., 2026). We then followed forward selection procedures (function *ordistep,* package *vegan*) (Oksanen et al., 2019) to identify any remaining influential parameters ($p < 0.05$) in order to avoid model overfitting (Mihalik et al., 2022). A list of the environmental variables included in each CCA can be found in Figure S 2-1 and Table S 2-7. Generalized additive models (GAMs) (package *mgcv*; Wood, 2025) were run on plankton relative abundance data to further explore potential correlations with arsenic variables specifically (Hastie & Tibshirani, 1987). The CCA models were therefore used to explore significant drivers among the entire water quality dataset, with an emphasis on arsenic and seasonal variables, while the GAMs were used to investigate arsenic-species specific relationships.

A t-test and Wilcoxon test were used to determine whether cyanobacterial relative abundance was statistically greater in the contaminated lakes compared to the reference lake; 95% confidence intervals were used in all analyses. All graphs were created using the *ggplot2* package (Wickham, 2016).

## 2.4 Results

### 2.4.1 Lake Characteristics and Environmental Variables

Lakes were categorized into different trophic statuses based on chlorophyll-a, phytoplankton density, and nutrient concentrations (Table 2.1), before being assessed for seasonal patterns in arsenic and plankton cycling. The two least contaminated lakes (Stuart, Sammy's) were determined to be oligotrophic, while the most contaminated lakes were found to be meso- to eutrophic (Frame, Handle, Jackfish) (Table 2.1). The seasons explored in this study – open-water and ice-on – were distinguished from one another by the presence or absence of lake ice cover. The open-water season (May to September) was characterized by conditions of warm water temperature and high DO, with intermittent (Frame, Sammy's) to strong thermal stratification (Stuart, Jackfish) observed to occur in the bottom layers of the deeper study lakes by June 2022 (Figure S 2-5). Handle Lake is the shallowest lake in this study and does not stratify (Figure S 2-5). During the ice-on season (November to April), both water temperature and DO levels were much lower, with the surface layer located immediately under the ice observed to be the coldest depth interval in each lake (Figure S 2-5). By mid-winter (February 2023), Frame Lake was observed to be fully anoxic (DO < 0.2 mg $L^{-1}$), as was the bottom layer of Handle Lake (Figure S 2-5).

**Table 2.1.** The minimum (MN), maximum (MX), and average (AV) values of environmental variables used to determine study lake trophic status and total dissolved arsenic. Method detection limits (DL) for each parameter are as follows: chlorophyll-a (0.1 μg $L^{-1}$), dissolved organic carbon (0.5 mg $L^{-1}$), dissolved phosphorus (10 μg $L^{-1}$), dissolved nitrogen (60 μg $L^{-1}$), and dissolved arsenic (0.2 μg $L^{-1}$). There was no method detection limit for phytoplankton density as these values were counted and calculated manually.

| Lake | Chlorophyll-a (μg $L^{-1}$) | | | Phytoplankton Density (x $10^7$ cells $L^{-1}$) | | | Dissolved Organic Carbon (mg $L^{-1}$) | | | Dissolved Phosphorus (μg $L^{-1}$) | | | Dissolved Nitrogen (μg $L^{-1}$) | | | N:P | Trophic Status* | Total Dissolved Arsenic (μg $L^{-1}$) | | |
|---|---|---|---|---|---|---|---|---|---|---|---|---|---|---|---|---|---|---|---|---|
| | MN | MX | AV | MN | MX | AV | MN | MX | AVG | MN | MX | AV | MN | MX | AV | AV | | MN | MX | AV |
| Handle | 0.3 | 3.6 | 1.8 | 3.0 | 51.7 | 18.3 | 23.7 | 36.9 | 30.2 | <DL | 12.0 | 10.3 | 1100 | 2960 | 2167 | 210 | M | 124 | 252 | 206 |
| Frame | 0.2 | 5.9 | 2.3 | 5.6 | 23.8 | 11.2 | 14.0 | 28.2 | 20.9 | <DL | 24.0 | 12.0 | 960 | 2870 | 1971 | 164 | M | 93.4 | 455 | 256 |
| Jackfish | <DL | 7.1 | 3.0 | 2.7 | 48.7 | 22.1 | 11.7 | 32.6 | 13.8 | <DL | 63.8 | 25.7 | 660 | 1570 | 1086 | 42.3 | E | 54.3 | 68.2 | 60.7 |
| Sammy's | <DL | 7.4 | 3.9 | 1.7 | 10.1 | 4.4 | 5.3 | 17.4 | 11.2 | <DL | <DL | <DL | 340 | 540 | 473 | 47.3 | O | 4.23 | 12.6 | 6.2 |
| Stuart | <DL | 6.8 | 3.4 | 0.2 | 8.1 | 3.7 | 14.7 | 17.6 | 16.2 | <DL | 11.8 | 10.7 | 510 | 510 | 581 | 54.3 | O | 1.06 | 1.92 | 1.34 |

*Trophic status of the five lakes was determined following the criteria established by Ryding and Forsberg (1980) and were classified as oligotrophic (O), mesotrophic (M), and eutrophic (E).

Total dissolved arsenic concentrations were generally higher during the ice-on season and lower during the open-water season, with the contaminated lakes (Frame, Handle) experiencing the largest differences in overall concentration (Figure S 2-6; Table S 2-8). Concentrations were typically highest closer to the SWI (Figure S 2-6). Maximum total dissolved arsenic concentrations in the ice-on season increased from 102 μg $L^{-1}$ to 455 μg $L^{-1}$ in Frame Lake and 188 μg $L^{-1}$ to 252 μg $L^{-1}$ in Handle Lake (Figure S 2-6; Table S 2-8). Sammy's Lake was the only study lake to deviate from this pattern and was observed to increase in arsenic concentration during the transition period between the ice-on and open-water seasons (Figure S 2-6). This was likely due to the fact that the catchment area surrounding Sammy's Lake is relatively high in arsenic compared to the lake itself, and therefore terrestrially-sourced meltwaters can be a significant source of arsenic to the lake (Little et al., 2026).

Following a similar pattern to total dissolved arsenic, As(III) tended to be higher in concentration under the ice towards the SWI (Figure S 2-6; Table S 2-8). The largest change in As(III) concentration was recorded in Handle Lake, which increased from a minimum of 0.08 μg $L^{-1}$ As(III) at the beginning of the season to a maximum of 117 μg $L^{-1}$ by the end of it (Figure S 2-6; Table S 2-8). The increase in As(III) was again found to be much higher in the two most contaminated lakes (Handle, Frame) compared to the other, less contaminated lakes. As(V) was typically higher during the open-water season and in the surface layers of the study lakes where DO levels were high and oxic conditions more stable (Figure S 2-6). Although concentrations were still lower compared to the ice-on season, all five study lakes showed an increase in total dissolved arsenic concentrations between June and September, which was likely the result of evapoconcentration and/or partial mixing events with the onset of cooling temperatures (Figure S 2-6).

### 2.4.2 Phytoplankton

Forty-five phytoplankton genera were identified across all sampling dates in the five study lakes, with 43 observed during ice-on and 41 during the open-water season (Table S 2-9). The most common form of phytoplankton was determined to be Cyanobacteria, with *Planktothrix/Oscillatoria*, *Microcystis*, and *Aphanocapsa* found to be the most dominant genera (Figure S 2-7; Figure S 2-8). Cyanobacteria reached maximum relative abundance during the ice-on period (February 2023), and the four arsenic-contaminated lakes were observed to have a statistically higher proportion of Cyanobacteria compared to the non-contaminated reference lake ($p = 0.02$; Stuart Lake) (Figure S 2-9). This test was run again without Jackfish Lake since this system is consistently and overwhelmingly dominated by the cyanobacteria genera *Planktothrix,* and the relationship was once again found to be significant ($p = 0.03$). When the full year of phytoplankton community data was explored using canonical correspondence analysis (CCA), total dissolved arsenic ($p = 0.03$), As(V) ($p < 0.01$), temperature ($p = 0.03$), and phosphorus ($p = 0.04$) were important explanatory variables (Figure 2.2a). Cyanobacteria genera such as *Synechococcus, Rhabdoderma,* and *Anabaenopsis* were observed to load the most strongly in the direction of total arsenic, while Chlorophyta genera, such as *Schizochlamys, Planctonema,* and *Palmella,* and Chrysophyta genera, like *Uroglena/Uroglenopsis* and *Fragilaria/Ulnaria,* loaded more strongly in the direction of As(V) (Figure 2.2a). When run on the ice-on data only, temperature ($p < 0.01$) and As(V) ($p < 0.01$) were found to be significant explanatory variables (Figure 2.2b). The open-water CCA determined that depth ($p = 0.01$) was the only significant driver of phytoplankton community composition (Figure 2.2c).


**Figure 2.2.** CCA plots of phytoplankton communities and statistically correlated environmental gradients for the: a) entire sampling period (April 2022 – May 2023), b) ice-on season (November – April), and c) open-water season (May – October).

Potential correlations between phytoplankton genera and the three arsenic variables were explored using a series of generalized additive models (GAMs), and many Cyanobacteria genera were found to be statistically correlated with both total dissolved arsenic and As(III) (Figure 2.3; Table S 2-10). The majority of these correlations were found to be either linearly positive or positive up until a certain threshold (usually ~350 µg $L^{-1}$) (Table S 2-10). A few non-Cyanobacteria genera were also found to have statistically relevant correlations with total

dissolved arsenic, but they tended to be either quite variable (e.g.,, the chlorophyte *Sphaerocystis*: $p < 0.01$; $R^2 = 0.19$) or negative (e.g.,, the chrysophyte *Fragilaria/Ulnaria*: $p = 0.02$; $R^2 = 0.10$, and cryptophyte *Cryptomonas*: $p = 0.02$; $R^2 = 0.10$) (Table S 2-10). Seasonality played an important role in potential arsenic toxicity to specific plankton groups, with Cyanobacteria found to have the majority of statistically significant correlations during the ice-on season periods, while the majority of correlations with chlorophytes occurred during the open-water season (Table S 2-10).

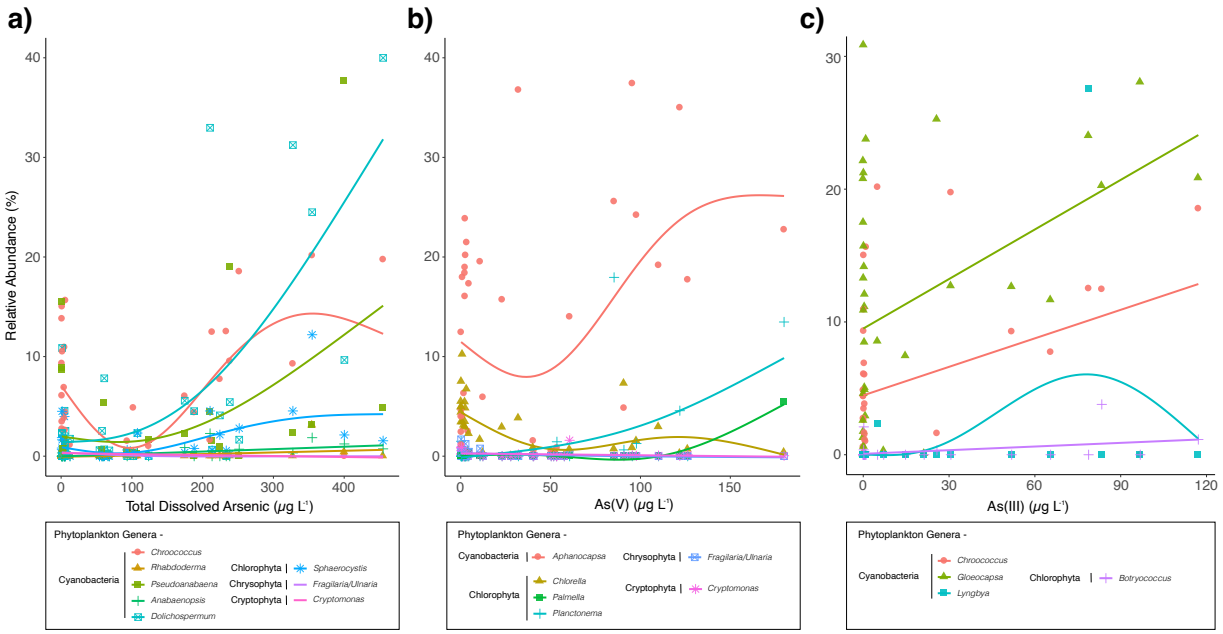


**Figure 2.3.** GAM plots of phytoplankton relative abundance data from across all sampling dates (April 2022 – May 2023) with statistically significant correlations between specific genera and: a) total dissolved arsenic, b) As(V), and c) As(III).

### 2.4.3 Rotifers

Twenty-one rotifer species were identified in the five study lakes, with all 21 occurring during the open-water season, but only 11 in the ice-on season (Table S 2-11). The three most common rotifer species were found to be *Kellicottia longispina*, *Keratella species complex* and

*Keratella hiemalis,* with *K. longispina* and *K. hiemalis* both observed to increase during the ice-on season (Figure S 2-10; Figure S 2-11). *K. longispina* was very abundant in the two most contaminated lakes (Frame, Handle) and made up 100% of the rotifer community under the ice in Handle Lake in April 2022, while *K. species complex* was observed to be more common during the open-water season in the three least contaminated lakes (maximum of 97.2% in Jackfish Lake in September 2022) (Figure S 2-10; Figure S 2-11). No arsenic variables were highlighted in any of the CCA models used to explore potential environmental variable influence on rotifer community composition (Figure S 2-12). While no environmental variables were selected for the full year data (Figure S 2-12a), aluminum ($p = 0.03$) was highlighted for the ice-on community data (Figure S 2-12b) and copper was found to be a significant community gradient for the open-water rotifer community (Figure S 2-12c).

Three rotifer species were found to be correlated with total dissolved arsenic across all sampling dates when explored with GAMs (Figure 2.4; Table S 2-12). *K. longispina* was found to be positively correlated with total dissolved arsenic ($p < 0.01$; $R^2 = 0.39$), while *K. species complex* ($p = 0.02$; $R^2 = 0.12$) and *Polyartha remata* ($p = 0.03$; $R^2 = 0.19$) were both negatively correlated with total dissolved arsenic (Figure 2.4; Table S 2-12). *K. longispina* was found to have consistently positive relationships with all three forms of arsenic across all three sampling periods, while *K. species complex* and *P. remata* both had exclusively negative relationships, mostly with total dissolved arsenic across all sampling dates (Table S 2-12). No clear seasonal trends could be established for any rotifer species (Table S 2-12).

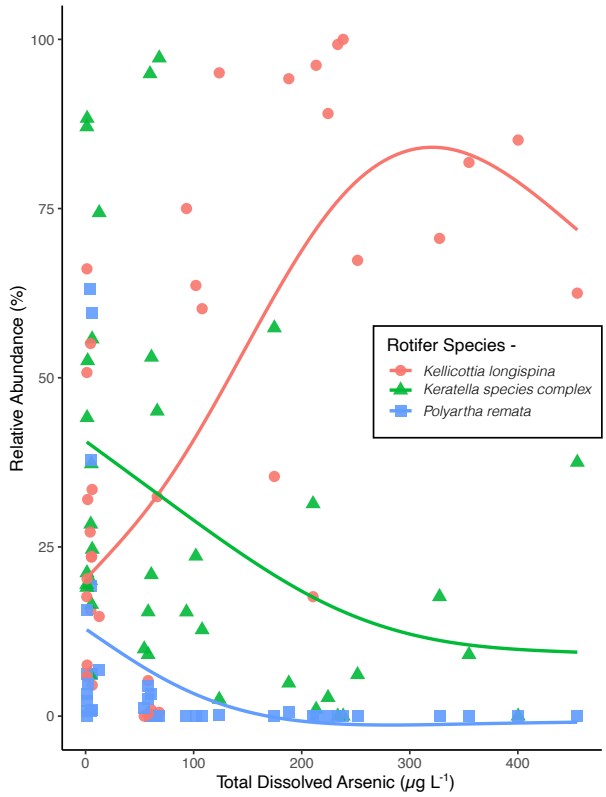


**Figure 2.4.** The correlations between total dissolved arsenic and the rotifer species *K. longispina, K. species complex*, and *P. remata* as assessed using GAMs across all sampling dates and study lakes.

### 2.4.4 Zooplankton

Thirty zooplankton species were identified across the five study lakes, with 22 species observed during ice-on and 29 during the open-water season (Table S 2-13). All species present during the ice-on period were also observed during the open-water season, with the exception of the calanoid copepod species *Eurytemora affinis* (Table S 2-13). The three most common zooplankton species were the cyclopoid copepod *Diacyclops thomasi,* and two Cladoceran species – *Daphnia longiremus* and *Bosmina longirostris* (Figure S 2-13; Figure S 2-14). *D. thomasi* was observed to be relatively common during every sampling date, but was particularly dominant during the ice-on season in all of the study lakes except the reference lake (Stuart) (Figure S 2-13; Figure S 2-14). In contrast, both of the Cladoceran species (*D. longiremus, B.*

*longirostris*) were found to be more common in the three least contaminated lakes and during the open-water season (Figure S 2-13; Figure S 2-14). The full year CCA model highlighted total dissolved arsenic ($p < 0.01$), As(III) ($p = 0.02$), temperature ($p < 0.01$), and dissolved nickel ($p = 0.04$) as being statistically significant drivers of zooplankton community composition (Figure 2.5a). Total dissolved arsenic and As(III) were found to load in the same direction, and although no zooplankton species were observed nearby, many Cladoceran and calanoid copepod species were found to load very strongly in the opposite direction (e.g., *Holopedium gibberum, D. longiremus, Daphnia middendorffiana* (Cladocera), *Leptodiaptomus sicilis* and *Limnocalanus macrurus* (calanoid copepods)) (Figure 2.5a). When the CCA was run on the ice-on community, total dissolved arsenic ($p = 0.03$) and As(III) ($p = 0.04$) were found to be significant, with Cladoceran species, such as *B. longirostris, Daphnia species,* and *D. mendotae,* observed to load in the opposite direction of total arsenic and As(III) (Figure 2.5b). No environmental variables were selected in the open-water CCA model.

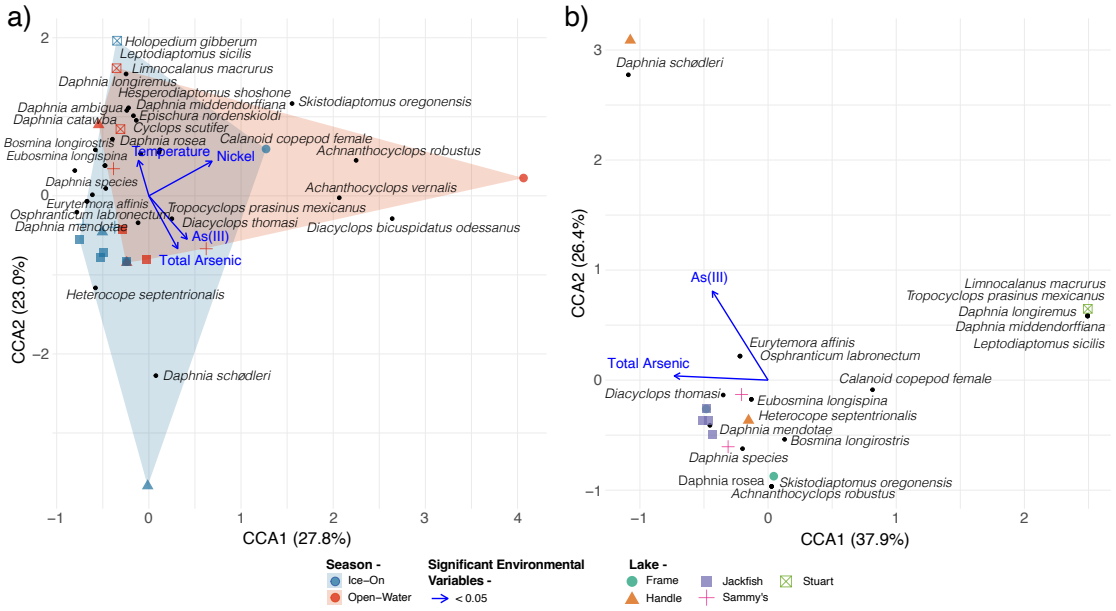


**Figure 2.5.** CCA plots of zooplankton communities and statistically correlated environmental gradients for the: a) entire sampling period (April 2022 – May 2023), and b) ice-on season (November – April). No environmental gradients were identified for the open-water season.

When assessed using GAMs, two cladoceran zooplankton species were found to have weak, negative relationships with total dissolved arsenic across all seasons – *B. longirostris* ($p = 0.03$; $R^2 = 0.11$) and *D. longiremus* ($p = 0.03$; $R^2 = 0.11$) (Figure 2.6; ). In general, cladoceran species appeared to be more sensitive to As(III) while calanoid copepods appeared to be more sensitive to As(V) (Table S 2-14). Seasonality also appeared to play an important role in driving these patterns, with cladoceran species, such as *D. middendorffiana* ($p < 0.05$; $R^2 = 0.18$), *Daphnia rosea* ($p = 0.03$; $R^2 = 0.22$), *Holopedium gibberum* ($p = 0.03$; $R^2 = 0.22$), and *Eubosmina longispina* ($p < 0.01$; $R^2 = 0.64$) all found to exhibit threshold-like relationships with As(III), usually between 0 and 120 μg $L^{-1}$ during the ice-on season (Table S 2-14). In contrast, calanoid copepod species, such as female calanoid copepods ($p = 0.04$; $R^2 = 0.18$), *Heterocope septentrionalis* ($p = 0.02$; $R^2 = 0.24$), *Skistodiaptomus oregonensis* ($p < 0.01$; $R^2 = 0.35$), and *Skistodiaptomus pallidus* ($p < 0.05$; $R^2 = 0.17$), were all found to be correlated with As(V), specifically during the open-water season (Table S 2-14).

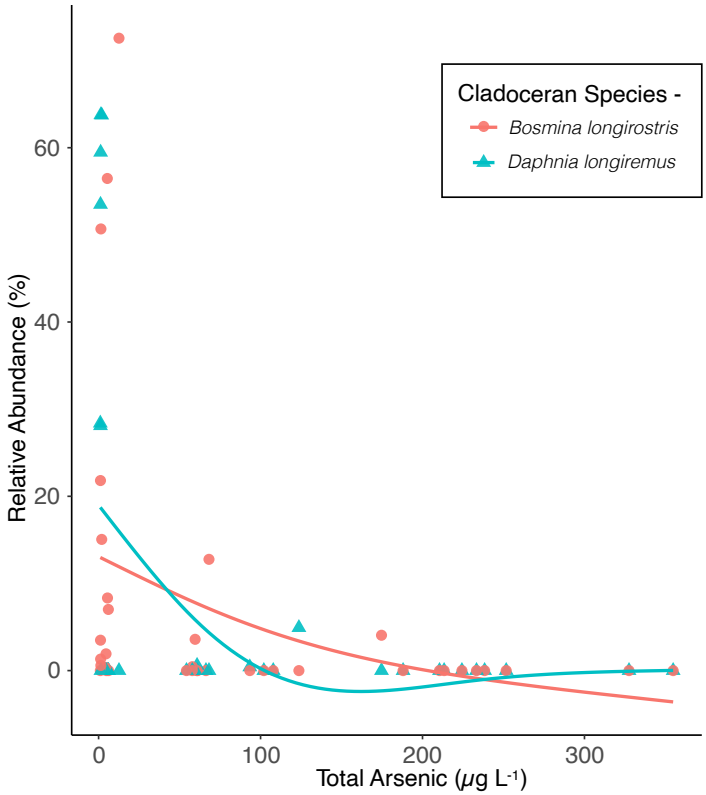


**Figure 2.6.** Negative correlations between total dissolved arsenic and zooplankton Cladocera species *B. longirostris* and *D. longiremus* as assessed using GAMs across all sampling dates and study lakes.

## 2.5 Discussion

The aim of this study was to investigate seasonal covariation in arsenic cycling and plankton communities in subarctic lakes across trophic and legacy mining contamination gradients (1.1 – 455 µg $L^{-1}$). We examined the concentrations of total and inorganic arsenic forms (As(V), As(III)) and the community dynamics of three groups of plankton (phytoplankton, rotifers, zooplankton) eight times over a single year (2022 – 2023) in five lakes from the Yellowknife, Northwest Territories region. Consistent with previous studies in the Yellowknife region (Palmer et al., 2019), winter was characterized by large increases in total arsenic and As(III) concentrations, particularly in the two most contaminated lakes. These under-ice arsenic dynamics were found to be important environmental gradients for the winter phytoplankton and

zooplankton communities, with each plankton group found to be correlated with the form of arsenic known to be more toxic to it (i.e., As(V) for phytoplankton, As(III) for zooplankton) (Akter et al., 2005). These large winter-time increases in arsenic concentration, particularly as the more toxic As(III), appear to be unique to contaminated subarctic systems, as studies based in temperate settings report decreasing arsenic concentrations over the winter period (Barrett et al., 2018; 2019). This difference is likely due to longer ice-cover duration in subarctic systems, which prolongs winter-time anoxia and the efflux of arsenic from the SWI (Palmer et al., 2019). Increases in arsenic concentration and form under the ice likely contribute to the ecological stress plankton experience during the winter, and it is therefore important to gain a better understanding of how subarctic plankton communities vary seasonally along with arsenic. In addition, the dynamic arsenic conditions captured through seasonal sampling in Yellowknife lakes allows us to explore species-specific relationships across wide arsenic gradients.

### 2.5.1 Phytoplankton

Phytoplankton were found to be associated with total dissolved arsenic and As(V) at both the individual (based on GAMs) and community (based on CCAs) levels. Phytoplankton are known to be more sensitive to As(V) than As(III) because it is a chemical analogue of phosphate ($PO_3^{4-}$), which allows it to enter phytoplankton through the phosphate transporters in their cell walls and disrupt important glycolytic and respiration pathways (Hughes, 2002; Hellweger et al., 2003). Our study results suggest that Chrysophytes, Cryptophytes, and Chlorophytes were the most sensitive to arsenic, with genera such as *Fragilaria/Ulnaria* and *Cryptomonas* negatively associated with total dissolved arsenic in both the CCAs and GAMs. Experimental studies of *Cryptomonas* and *Chlorella* have found that these taxa do not typically exhibit ecologically

relevant toxicity endpoints for arsenic unless phosphate levels are decreased (Planas & Healey, 1978; Levy et al., 2005). While no lab-based experiments have been run on *Fragilaria/Ulnaria,* these diatom taxa preserve well in lake sediments and potential sensitivity to arsenic can be inferred from paleolimnological studies. The impacts of arsenic on *Fragilaria/Ulnaria* based on previous paleolimnological research appear to be mixed, with one study from Yellowknife highlighting that *Fragilaria/Ulnaria* increased in relative abundance with increasing arsenic concentrations along a gradient of contamination (Sivarajah et al., 2019), while another study of two lakes from China ranging in concentration from 177 to 1,140 μg $L^{-1}$ found that *Fragilaria/Ulnaria* substantially decreased after inputs of industrial arsenic. Higher $PO_4^{3-}$:As(V) have been shown to decrease overall As(V) toxicity to phytoplankton due to increased competition for uptake via membrane-bound $PO_4^{3-}$-transporters (Levy et al., 2005). As a result, phytoplankton in eutrophic lakes may be at lower risk from As(V) exposure compared to oligotrophic systems. However, with the exception of Jackfish Lake, phosphorus levels were relatively low in our study lakes, which may explain why our results indicate that *Fragilaria/Ulnaria* and *Cryptomonas* were sensitive to arsenic compared to other studies.

Several phytoplankton genera exhibited positive associations with arsenic, especially the Cyanobacteria genera *Rhabdoderma*, *Anabaenopsis*, and *Pseudoanabaena*. Prior research has found that *Pseudoanabaena* in lakes impacted by gold mining were capable of the uptake and bio-transformation of arsenic into less toxic forms (Obuekwe et al., 2024), which may explain its positive association with the contaminant. Some Chlorophytes (e.g., *Planctonema*, *Palmella*) were also found to have positive associations with arsenic, typically in the form of As(V) and during the open-water season (0.2 – 180 μg $L^{-1}$). This is somewhat surprising, as many Chlorophyta species have been shown to be sensitive to As(V), including *Monoraphidium*

*arcuatum* (72-hr $IC_{50}$ = 250 µg $L^{-1}$; Levy et al., 2005) and *Scenedesmus obliquus* (14-d $EC_{50}$ = 48 µg L-1; Vocke et al., 1980).

### 2.5.2 Rotifers

Arsenic was not a significant driver of rotifer assemblages based on the CCAs, although three rotifer taxa had statistically significant correlations with arsenic. *K. longispina* exhibited positive relationships with all three arsenic variables, and across all seasons. *K. longispina* was the most common rotifer species in the five study lakes, and has been shown to increase under the ice in lakes from the Yellowknife region since the 1970s when arsenic emissions were still quite high (Moore, 1980). Therefore, *K. longispina* is likely very tolerant of arsenic, at least in the Yellowknife region. *K. species complex* and *P. remata* were both found to have negative relationships, mostly with total dissolved arsenic, suggesting that these taxa may be more sensitive to arsenic pollution. An $LC_{50}$ of 44.5 µg $L^{-1}$ has been calculated for the rotifer species *Brachionus calyciforus* with mining-related arsenic trioxide, with exposure found to result in higher rates of diapause, lower egg quality, and the accumulation of high arsenic levels in tissues across multiple generations (Aránguiz-Acuña & Serra, 2016). Arsenic trioxide was the main form of arsenic released by mines in the Yellowknife region, and while modern levels were not measured by this study, As(III) was found to range from 0.3 to 168 µg $L^{-1}$ across the study lakes.

### 2.5.3 Zooplankton

Zooplankton species belonging to the Cladocera and calanoid copepod families appeared to be relatively sensitive to arsenic, and specifically As(III), while cyclopoid copepods appeared to be more tolerant. In contrast to phytoplankton, As(III) is generally accepted as the more toxic

form of arsenic to higher trophic organisms like zooplankton due to its higher affinity for sulfhydryl groups which negatively impacts protein function (NRC, 1999; Akter et al., 2005). Both total dissolved arsenic and As(III) were found to be statistically significant drivers of zooplankton community composition across all sampling dates, but also during the ice-on season when concentrations of both were highest (arsenic was not a significant driver of zooplankton assemblage structure in the open-water season). The cladoceran species *B. longirostris* and *D. longiremus* were observed to be negatively correlated with total dissolved arsenic and As(III) based on the GAMs and CCAs. Other Cladoceran species, including *D. middendorffiana, D. rosea,* and *H. gibberum,* were observed to initially have positive correlations with As(III) until ~80 μg $L^{-1}$, after which their relative abundance decreased. Cladocera are common model organisms used in ecotoxicological trials, and many studies have reported ecologically relevant endpoints similar to the arsenic gradient established in this study (1.1 – 455 μg $L^{-1}$) (e.g., Biesinger & Christensen 1972; Spehar et al., 1980; Passino & Novak, 1984; He et al., 2008). Both *Bosmina* and *Daphnia* have previously been observed to decrease in lakes after inputs of industrially-sourced arsenic at concentrations similar to those in the lakes from this study (e.g., Thienpont et al., 2016 & Sivarajah et al., 2019: > 2,000 μg $L^{-1}$; Chen et al., 2015: 177 and 1,140 μg $L^{-1}$). Interestingly, Thienpont et al. (2016) found that *Daphnia* initially increased in a Yellowknife-area lake with the onset of arsenic pollution, then disappeared from the sediment record as arsenic concentrations increased. Calanoid copepod species, such as *L. sicilis*, *L. macrurus, Hesperodiaptomus shoshone, Epischura nordenskiøldi,* and female calanoid copepods, were also found to be sensitive to arsenic in this study, although many individual species appeared to be more influenced by As(V), specifically during the open-water season. A previous study looked at the indirect impacts of arsenic on the calanoid copepod species *E.*

*affinis*, and found that phytoplankton exposed to As(V) specifically resulted in a net negative effect on *E. affinis* via decreased nutrition (i.e., As(V)-contaminated phytoplankton) and compositional changes to the phytoplankton community which impacted food web dynamics (Sanders, 1986).

Cyclopoid copepods appeared to be tolerant of arsenic in our study lakes compared to other zooplankton groups. When assessed at the community scale based on the CCAs, species, such as *D. thomasi, Tropocyclops prasinus mexicanus, Achnanthocyclops robustus, Achnanthocyclops vernalis,* and *Diacyclops bicuspidatus odessanus* were associated with total dissolved arsenic and As(III) in ordination space. Only two cyclopoid copepod species were found to have statistically significant relationships with any arsenic variables (*A. robustus, T. prasinus mexicanus*). This appears to be supported by the literature as well, with most ecologically relevant toxicity endpoints found to be sublethal for cyclopoid copepods (CCME, 2001). A study of the cyclopoid copepod *Tigriopus japonicus* found that prolonged exposure to 50, 100, and 500 μg $L^{-1}$ of As(V) resulted in longer development time for future generations, lower overall fecundity, and an increase in overall toxicity for each subsequent generation, but not mortality (Liu & Zhang, 2023). The five lakes in this study reached maximum concentrations of 455 μg $L^{-1}$ for total arsenic, 180 μg $L^{-1}$ for As(V), and 117 μg $L^{-1}$ for As(III), and therefore likely did not have concentrations high enough to negatively impact cyclopoid copepods.

### 2.5.4 Under-Ice Ecology

Predatory cyclopoid copepods, such as the omnivorous *Cyclops scutifer,* tend to be more successful than herbivorous calanoid copepods, such as *Eudiaptomus graciloides*, during the winter as they can select for small, animal prey, such as rotifers and nauplii, which tend to be

more readily available and higher in lipid content compared to phytoplankton (Grosbois et al., 2017). Although common under-ice zooplankton species were observed across the five study lakes, the dominance of the community by the cyclopoid copepod *D. thomasi* (except for in the reference lake), suggests that *D. thomasi* may potentially be more tolerant of aquatic arsenic contamination compared to other zooplankton species. This is further supported by the absence of an increase in common, under-ice calanoid copepod species (*E. affinis*) which we observed to be more sensitive of arsenic in this study. Therefore, the dominance of the under-ice zooplankton community in the contaminated study lakes by *D. thomasi* may be a potential response to increasing arsenic concentration and toxicity during the ice-on season, although further study is needed to resolve potential confounding variables such as nutrients, DO, and other environmental variables that are influenced by prolonged ice cover. Cladocera tend to be less abundant and diverse under the ice compared to during the summer, and sometimes enter diapause or lay resting eggs in response to decreasing light, temperature, and food availability (Shchapov et al., 2021; Alekseev, 2025). While Cladoceran taxa were relatively scarce in the two most contaminated lakes (except for a brief period in the open-water season), they were abundant in the least contaminated lake and reference lake, with *D. longispina* observed to make up the largest proportion of the under-ice zooplankton community in Stuart Lake, even in late winter. Therefore, Cladocera appear to be relatively sensitive to lake water arsenic concentrations, increasing in abundance in contaminated lakes only when concentrations are relatively lower, such as in the summer. Copepods do not leave subfossil remains in lake sediments like the cladocerans do, but emerging developments in eDNA (Domaizon et al., 2017) may provide opportunities to test this hypothesis using paleolimnological data.

The under-ice phytoplankton community across our five study lakes differed substantially from other lake systems due to the dominance of Cyanobacteria. Most studies of under-ice phytoplankton communities typically report dominance by low light adapted and flagellated species, with the majority of reported under-ice blooms typically driven by diatoms (e.g., Vanderploeg et al., 1992; Twiss et al., 2012; Bashenkhaeva et al., 2015). The lakes in this study were found to be dominated by Cyanobacteria during every sampling date, and this dominance increased during the ice-on season. The genera *Chroococcus, Gloeocapsa, Pseudoanabaena, Planktothrix,* and *Dolichospermum* all increased during the ice-on period, particularly in the most contaminated lakes. *Gloeocapsa* (Phillips & Fawley, 2002), *Planktothrix, Pseudoanabaena* (Babanazarova et al., 2013), and *Dolichospermum* (Reinl et al., 2023) have been observed to be present under the ice in other phytoplankton community surveys, with the latter two genera also observed to be tolerant of arsenic in different studies (e.g., Patel et al., 2021; Obuekwe et al., 2024). While occasional under-ice cyanobacterial blooms have been reported, the overall dominance by the group appears to be unique to the lakes sampled in this study (Van Hove et al., 2008; Gabyshev et al., 2023; Reinl et al., 2023; Kers et al., 2024).

The dominance of Cyanobacteria in our arsenic-contaminated lakes was observed against a backdrop of increasing Cyanobacteria in freshwater systems globally, including subarctic lakes since 1945 (Taranu et al., 2015; Cederwall & Cott, 2025). However, some Cyanobacteria have been found to exhibit higher resistance to As(V) toxicity than other phytoplankton groups due to their *ars* (arsenic resistance) operon which aids in arsenic efflux and enzyme production (Maeda et al., 1988; 1993; Thiel, 1988; Miyashita et al., 2012; 2016). The authors of a 2013 study found that *Microcystis aeruginosa* is very tolerant of arsenic exposure, and they posited that *Microcystis* may dominate freshwater systems that have been contaminated with arsenic (Wang

et al. 2013). *Microcystis* was one of the dominant Cyanobacteria in all five of the study lakes, including the reference lake. It is therefore possible that the dominance of the phytoplankton communities in the five study lakes represents a form of pollution-induced community tolerance (PICT) (Blanck & Wängberg, 1988), although its dominance in the reference lake is evidence against this. In order to explore these ideas further, we recommend that future research efforts investigate changes in Cyanobacteria in response to regional arsenic contamination using paleolimnological approaches, such as the analysis of cyanobacterial pigments preserved in lake sediment cores via high-performance liquid chromatography (HPLC) or visible near-infrared reflectance spectroscopy (VNIRS) (Errat et al., 2026).

While winter appears to be a time of increased arsenic exposure risk in shallow, subarctic lakes, other confounding variables may also contribute to differences between under-ice and open-water plankton communities independent of (or cumulatively with) arsenic. It is therefore possible that the plankton highlighted in this study were responding to other environmental changes, such as decreasing temperature, light, and DO, and not necessarily arsenic in the winter. For example, zooplankton biomass has been shown to decrease substantially under anoxic conditions (Karpowicz et al., 2020). In contrast, nutrients are often reported to increase under lake ice due to sediment efflux and reduced plankton uptake, which could result in phytoplankton community shifts in the proportions of $N_2$-fixing Cyanobacteria during the winter (Gu, 2012), although N:P across the five study lakes were quite high (>29:1; Smith, 1983) (Table 2.1). However, many of the plankton taxa we observed to decrease in relative abundance during the winter in the contaminated lakes were also found to be more common in the least contaminated lakes, and vice versa. This was particularly evident for Cyanobacteria, which have been reported to be resistant to arsenic exposure (Miyashita et al., 2012; 2016) and were found to be most

dominant in the most contaminated lakes specifically during the winter at the same time when arsenic concentrations were highest in this study. Therefore, although confounding environmental variables, such as DO, temperature, and nutrients, may have also contributed to seasonal shifts in under-ice plankton communities in the five study lakes, arsenic concentrations increased concurrently and were specifically highlighted as a significant predictor of multiple plankton community structures (phytoplankton, zooplankton) in multivariate analysis (CCAs) and at the individual taxa level (GAMs).

## 2.6 Conclusions

The results of this study highlight the importance of multi-seasonal sampling in assessments of arsenic biogeochemical cycling, with particular emphasis on the increase in concentration and potential toxicity to exposed plankton communities in ice-dominated subarctic lakes during the winter season. We found that both zooplankton and phytoplankton communities were influenced by total dissolved arsenic across all sampling dates, and that As(III) was a significant driver for zooplankton while As(V) was a significant driver for phytoplankton. The zooplankton groups Cladocera and calanoid copepods appeared to be more sensitive to arsenic contamination (abundances were lower when arsenic was elevated), while cyclopoid copepods appeared to be more tolerant. This same pattern was observed during the ice-on season when the lakes were dominated by the potentially arsenic-resistant *D. thomasi.* Cyanobacteria dominated the phytoplankton community during all sampling dates but were significantly more abundant in the contaminated lakes. This is consistent with previous studies that have found that cyanobacteria are relatively tolerant of arsenic. We suggest future studies should explore changes in phytoplankton communities over time using sedimentary pigment analysis, to test whether

cyanobacteria increased after the onset of arsenic pollution, and therefore whether the present-day dominance of cyanobacteria in these lakes represents a form of pollution-induced community tolerance (PICT) (Blanck & Wängberg, 1988).

## 2.7 Supplementary Information

**Table S 2-1.** Location and physical characteristics of the five study lakes.

| Lake | Sampling Coordinates | Size ($km^2$) | Max Depth (m) | Distance to Giant Mine Roaster Stack (km) |
|---|---|---|---|---|
| Handle | 62.4916, -114.3959 | 0.2 | 3.8 | 2.5 |
| Frame | 62.4574, -114.3879 | 0.9 | 6.4 | 6.1 |
| Jackfish | 62.4659, -114.3924 | 0.5 | 8.2 | 4.0 |
| Sammy's | 62.4688, -114.5098 | 0.3 | 6.7 | 8.4 |
| Stuart | 62.5168, -113.8214 | 1.0 | 12.0 | 10.2 |

**Table S 2-2.** Field blank (FB) data from the five study lakes collected from 2022-2024 (N = 19). Measurements of total dissolved arsenic (Total As) below the method detection limit of 0.2 μg $L^{-1}$ are indicated by < DL.

| Sample Date | Sample ID | Total As (μg $L^{-1}$) |
|---|---|---|
| November 23, 2022 | FB1 | < DL |
| | FB2 | < DL |
| | Reagent Blank 1 | < DL |
| February 9, 2023 | FB1 | < DL |
| | FB2 | < DL |
| February 21, 2023 | FB1 | < DL |
| | FB4 | < DL |
| April 6, 2023 | FB1 | < DL |
| | FB2 | < DL |
| April 21, 2023 | FB1 | < DL |
| | FB2 | < DL |
| July 14, 2023 | FB1 | < DL |
| | FB2 | < DL |
| November 18, 2023 | FB1 | < DL |
| | FB2 | < DL |
| January 23, 2024 | FB1 | < DL |
| | FB2 | < DL |
| February 2, 2024 | FB1 | < DL |
| | FB2 | < DL |

**Table S 2-3.** Field replicate data from Handle and Jackfish Lakes collected in November 2020 and January 2021 using the same sampling methods as described in the paper (N = 4).

| Lake | Sample Date | Depth (m) | Total Arsenic ($\mu g\ L^{-1}$) | Relative Percent Difference (%) |
|---|---|---|---|---|
| Handle | November 16, 2020 | 1 | 203 | 0.49 |
| | | 1A | 204 | |
| Jackfish | January 1, 2021 | 4 | 70 | 0.57 |
| | | 4A | 70.4 | |

**Table S 2-4.** Optimization parameters for separation and determination of arsenic species using HPLC-ICP-MS.

| **ICP-MS-MS ( Agilent 8900 ICP-QQQ )** | |
|---|---|
| RF power | 1500 w |
| Plasma gas flow | 15 L $min^{-1}$ |
| Nebulizer (carrier) gas flow | 1.01 L $min^{-1}$ |
| Sampling depth | 8 mm |
| Peristaltic pump speed | 0.4 rps |
| Spray chamber temp | 2°C |
| Collision cell | He @ 5.0 mL $min^{-1}$ (dependent on instrument sensitivity) |
| Data acquisition mode | Time-resolved, m/z 75 for 75As+, and m/z 77 for 40Ar37Cl+ |
| **HPLC Conditions - Agilent 1260** | |
| Column | PRP-X100 Anion Exchange HPLC Column, 4.1 x 250 mm, 10 µm |
| Mobile phase composition | 20 mM (NH4)2HPO4,5mM (NH4H2PO4 ). pH 8.25,2% MeOH |
| Mobile phase flow rate | 1 mL $min^{-1}$ |
| Injection volume | 50 µL |
| Acquisition time | 12 min |

Samples were separated by HPLC-ICP-MS/MS (Agilent) and quantified using Agilent software (MassHunter 4.6).

**QA/QC Protocols:** Sequence accuracy was verified by inserting continuous calibration verification (OPR2) standards approximately every 10 samples. To ensure the quality of these measurements, a second source of PTC from Proficiency Testing Canada was used for As(V) quantification. Analyses with dosed additions were used in order to fortify samples to control the percentage recovery of all species as an analytical quality variables. Samples were measured in duplicate to verify the accuracy and reliability of analytical results.

**Table S 2-5.** Methods and detection limits (DL) for measured water chemistry variables. ICP-MS stands for inductively coupled plasma-mass spectrometry and ICP-QQQ refers to triple quadrupole ICP-MS.

| Variable | Methods | Units | Detection Limit or Range |
|---|---|---|---|
| As(V) | ICP-QQQ | $\mu g\ L^{-1}$ | 0.05 |
| As(III) | ICP-QQQ | $\mu g\ L^{-1}$ | 0.01 |
| Chlorophyll-a | YSI Multi-Meter Probe | $\mu g\ L^{-1}$ | 0.1 |
| Dissolved Oxygen (DO) | YSI Multi-Meter Probe | $mg\ L^{-1}$ | 0.05 |
| Oxidative-Reduction Potential (ORP) | YSI Multi-Meter Probe | mV | -1,000 – 1,000 |
| pH | YSI Multi-Meter Probe | NA | 0.0 – 14.0 |
| Specific Conductivity | YSI Multi-Meter Probe | $\mu S\ cm^{-1}$ | 0.055 |
| Temperature | YSI Multi-Meter Probe | °C | -40 – 400 |
| Ammonia | Ion Chromatography (SM4110) | $\mu g\ L^{-1}$ | 5 |
| Nitrogen (Total) | Ion Chromatography (SM4110) | $\mu g\ L^{-1}$ | 60 |
| Sulphate | Ion Chromatography (SM4110) | $\mu g\ L^{-1}$ | 1 |
| Organic Carbon (Dissolved) | Total Carbon Analyzer (SM 5310) | $mg\ L^{-1}$ | 0.5 |
| Aluminum (Dissolved) | ICP-MS (EPA 200.8) | $\mu g\ L^{-1}$ | 0.6 |
| Arsenic (Dissolved) | ICP-MS (EPA 200.8) | $\mu g\ L^{-1}$ | 0.2 |
| Copper (Dissolved) | ICP-MS (EPA 200.8) | $\mu g\ L^{-1}$ | 0.2 |
| Iron (Dissolved) | ICP-MS (EPA 200.8) | $\mu g\ L^{-1}$ | 5 |
| Nickel (Dissolved) | ICP-MS (EPA 200.8) | $\mu g\ L^{-1}$ | 0.1 |
| Phosphorus (Dissolved) | ICP-MS (EPA 200.8) | $\mu g\ L^{-1}$ | 10 |
| Selenium (Dissolved) | ICP-MS (EPA 200.8) | $\mu g\ L^{-1}$ | 0.3 |
| Zinc (Dissolved) | ICP-MS (EPA 200.8) | $\mu g\ L^{-1}$ | 0.4 |

**Table S 2-6.** Reference guides for zooplankton, rotifer, and phytoplankton identification.

| Plankton Type | Reference |
|---|---|
| **Zooplankton & Rotifers** | Haney, J. F., Aliberti, M. A., Allan, E., Allard, S., Bauer, D. J., Beagen, W., Bradt, S. R., Carlson, B., Carlson, S. C., Doan, U. M., Dufresne, J., Godkin, W. T., Greene, S., Kaplan, A., Maroni, E., Melillo, S., Murby, A. L., Smith (Nowak), J. L., Ortman, B., Quist, J. E., Reed, S., Rowin, T., Schmuck, M., Stemberger, R. S., & Travers, B. (2013). *An image-based key to the zooplankton of North America.* (Version 5). University of New Hampshire Center for Freshwater Biology: Durham, NH. Retrieved from http://cfb.unh.edu/cfbkey/html/ |
| **Zooplankton** | Balcer, M. D., Korda, N. L., & Dodson, S. I. (1982). *Zooplankton of the Great Lakes: a guide to the identification and ecology of the common crustacean species*. Madison, WI: University of Wisconsin Press. |
| **Phytoplankton** | Baker, A. L., Gretz, M., Coesel, P. F. M., Delwiche, C., Sarnoff, S., Silverside, A., St. Amand, A., Toh, R., & van Egmond, W. (2012). *An image based key to algae (PS Protista), Cyanobacteria, and other aquatic objects.* PhycoKey. Retrieved from https://cfb.unh.edu/phycokey/phycokey.htm<br>Graham, L. E., Graham, J. M., Wilcox, L. W., & Cook, M. E. (Eds). (2016). *Algae.* (3rd ed.). Madison, WI: LJLM Press.<br>Guiry, M. D., & Guiry, G. M. (2024). *AlgaeBase*. Galway, Ireland: National University of Ireland. Retrieved from http://www.algaebase.org<br>Krammer, K., & Lange-Bertalot, H. (1986). *Bacillariophyceae, Part 2, Volume 1: Naviculaceae. Freshwater Flora of Middle Europe*. New York, NY: Gustav Fischer Publisher.<br>Krammer, K., & Lange-Bertalot, H. (1988). *Bacillariophyceae, Part 2, Volume 2: Bacillariaceae, Epithemiaceae, Surirellaceae. Freshwater Flora of Middle Europe*. New York, NY: Gustav Fischer Publisher.<br>Krammer, K., & Lange-Bertalot, H. (1991a). *Bacillariophyceae, Part 2, Volume 3: Centrales, Fragilariaceae, Eunotiaceae. Freshwater Flora of Middle Europe*. Struttgart, Germany: Gustav Fischer Publisher.<br>Krammer, K., & Lange-Bertalot, H. (1991b). *Bacillariophyceae, Part 2, Volume 4: Achnanthaceae, Critical Supplement to Navicula (Lineolatae) and Gomphonema, Complete List of Literature for Volumes 1-4. Freshwater Flora of Middle Europe*. Stuttgart, Germany: Gustav Fischer Publisher.<br>PhycoTech. (2017). *PhycoTech image collection.* St. Joseph, MI: PhycoTech. Retrieved from: <https://phycotech.smugmug.com/2017-Image-Library/AlgaeOtherMicroscopicTaxa/Algae><br>Prescott, G. W. (1962). *Algae of the western great lakes area: with an illustrated key to the genera of desmids and freshwater diatoms*. Dubuque, IA: Wm. C. Brown Company Publishers.<br>Prescott, G. W. (1954). *How to know the fresh-water algae.* Dubuque, IA: Wm. C. Brown Company Publishers.<br>Rosen, B. H., & St. Amand, A. (2015). *Field and laboratory guide to freshwater cyanobacteria harmful algal blooms for Native American and Alaska Native Communities* (U.S. Geological Survey Open-File Report 2015–1164). http://dx.doi.org/10.3133/ofr20151164<br>Spaulding, S., & Edlund, M. (2024). *Diatoms of North America*. Retrieved from https://diatoms.org |

**Table S 2-7.** List of environmental variables included in each of the CCA models. Total arsenic (TAs), As(V), As(III), temperature, and DO were included in every model in order to specifically examine plankton community structure along these gradients. Variables indicated by (*) were chosen by the forward selection process (*ordistep*) in R. DO was not included in the open-water phytoplankton CCA since the model became overfitted when all variables were included. Preference was given to the forward selected variables.

| Plankton Type | CCA Dataset | Variables Included in Model |
|---|---|---|
| Phytoplankton | Full Year | TAs, As(V), As(III), DO, temperature*, P*, Ni*, Fe* |
| | Ice-On | TAs, As(V), As(III), DO, temperature*, Fe* |
| | Open-Water | TAs, As(V), As(III), temperature, depth*, Cu*, Zn* |
| Rotifers | Full Year | TAs, As(V), As(III), DO, temperature |
| | Ice-On | TAs, As(V), As(III), DO, temperature, Al*, P* |
| | Open-Water | TAs, As(V), As(III), DO, temperature, Cu* |
| Zooplankton | Full Year | TAs, As(V), As(III)*, DO, temperature*, Ni*, Zn* |
| | Ice-On | TAs, As(V), As(III)*, DO, temperature, depth*, Al* |
| | Open-Water | TAs, As(V), As(III), DO, temperature*, Ni*, Zn* |

**Table S 2-8.** Minimum, maximum, and average concentrations (□g L-1) of total dissolved arsenic (DAs), As(V), and As(III) during the early open-water (EO; May, June 2022, May 2023), late open-water (LO; September 2022), early ice-on (EI; November 2022), and late ice-on (LI; April 2022, February, April 2023) seasons in each of the five study lakes. Method detection limits were as follows: Total DAs (0.2 μg $L^{-1}$), As(V) (0.05 μg $L^{-1}$), and As(III) (0.01 μg $L^{-1}$).

| Lake | Total DAs | | | | As(V) | | | | As(III) | | | |
|---|---|---|---|---|---|---|---|---|---|---|---|---|
| Handle | EO | LO | EI | LI | EO | LO | EI | LI | EO | LO | EI | LI |
| Min. | 123.7 | | | 233.3 | 97.8 | | | 90.8 | 0.8 | | | 78.8 |
| Max. | 224.3 | | | 251.7 | 126.3 | | | 110.1 | 83.4 | | | 117.1 |
| Avg. | 187.1 | 174.7 | 188.0 | 241.1 | 115.3 | 179.9 | 85.3 | 100.4 | 49.9 | 0.5 | 0.08 | 98.0 |
| Frame | EO | LO | EI | LI | EO | LO | EI | LI | EO | LO | EI | LI |
| Min. | 107.8 | | | 354.8 | 12.3 | | | 1.0 | 14.8 | | | 5.0 |
| Max. | 327.5 | | | 455.0 | 60.6 | | | 4.0 | 51.9 | | | 96.8 |
| Avg. | 125.3 | 93.4 | 102.0 | 403.3 | 32.0 | 95.5 | 32.1 | 2.3 | 30.8 | 0.5 | 0.02 | 44.2 |
| Jackfish | EO | LO | EI | LI | EO | LO | EI | LI | EO | LO | EI | LI |
| Min. | 54.3 | | | 57.8 | 50.3 | | | 40.3 | 0.2 | | | 0.02 |
| Max. | 61.0 | | | 66.3 | 53.3 | | | 57.6 | 7.2 | | | 0.2 |
| Avg. | 58.7 | 68.2 | 59.6 | 60.7 | 51.8 | 40.6 | 27.8 | 50.5 | 2.6 | 21.3 | 0.04 | 0.1 |
| Sammy's | EO | LO | EI | LI | EO | LO | EI | LI | EO | LO | EI | LI |
| Min. | 4.6 | | | 4.2 | 2.4 | | | 2.3 | 0.4 | | | 0.03 |
| Max. | 6.1 | | | 5.5 | 4.5 | | | 3.3 | 1.0 | | | 0.3 |
| Avg. | 5.6 | 12.6 | 5.4 | 4.8 | 3.1 | 10.8 | 2.7 | 2.6 | 0.7 | 0.6 | 0.1 | 0.2 |
| Stuart | EO | LO | EI | LI | EO | LO | EI | LI | EO | LO | EI | LI |
| Min. | 1.1 | | | 1.3 | 1.1 | | | 0.3 | 0.1 | | | 0.03 |
| Max. | 1.2 | | | 1.9 | 1.2 | | | 1.0 | 0.2 | | | 0.2 |
| Avg. | 1.1 | 1.4 | 1.2 | 1.5 | 1.1 | 0.3 | 0.2 | 0.6 | 0.1 | 0.2 | NA | 0.1 |

**Table S 2-9.** List of the phytoplankton genera identified and counted across the five study lakes and which season they were present in. The open-water season was from May – October, and the ice-on season was from November – April. All samples collected from April 2022 – May 2023.

| Phytoplankton Genera | Open-Water | Ice-On |
|---|---|---|
| **Cyanobacteria –** | | |
| *Aphanocapsa* | X | X |
| *Apanothece* | X | X |
| *Chroococcus* | X | X |
| *Coelosphaerium* | - | X |
| *Cyanogranis* | X | X |
| *Gleocapsa* | X | X |
| *Eucapsis* | - | X |
| *Merisomopedia* | X | X |
| *Microcystis* | X | X |
| *Rhabdoderma* | X | X |
| *Romeria* | X | - |
| *Snowella* | X | X |
| *Synechococcus* | X | X |
| *Lyngbya* | - | X |
| *Planktothrix/Oscillatoria* | X | X |
| *Pseudoanabaena* | X | X |
| *Anabaenopsis* | X | X |
| *Dolichospermum* | X | X |
| *Cuspidothrix* | X | - |
| **Chlorophyta –** | | |
| *Clamydomonas* | X | X |
| *Platydorina* | X | X |
| *Botryococcus* | X | X |
| *Chlorella* | X | X |
| *Chlorococcum* | X | X |
| *Coelastrum* | X | X |
| *Crucigenia* | X | X |
| *Oocystis* | X | X |
| *Palmella* | X | X |
| *Schizochlamys* | X | X |
| *Sphaerocystis* | X | X |
| *Tetraspora* | X | X |
| *Microspora* | X | X |
| *Mougeotia* | X | X |
| *Geminella* | X | X |
| *Planctonema* | X | X |
| **Chrysophyta –** | | |
| *Uroglena/Uroglenopsis* | X | X |
| *Chrysococcus* | X | X |
| *Ochromonas* | X | X |
| *Dinobryon* | X | X |
| *Synura* | X | X |
| *Aulocosiera* | X | X |
| *Asterionella* | X | X |
| *Fragilaria/Ulnaria* | X | X |
| *Grammatophora* | - | X |
| **Cryptophyta –** | | |
| *Cryptomonas* | X | X |

**Table S 2-10.** Phytoplankton genera found to have statistically significant ($p < 0.05$) relationships with an arsenic variable (T = total dissolved arsenic, III = As(III), V = As(V)) according to individual GAMs. Seasons were denoted by A = all sampling dates, I = ice-on, and O = open-water, and brief descriptions of relationships were given (N = negative, P = positive).

| Phytoplankton Group | Genus | Season | As Variable | p-value / Adjusted $R^2$ | Relationship |
|---|---|---|---|---|---|
| Cyanobacteria | Chroococcus | A | T | 0.02 / 0.11 | P |
| | Chroococcus | A | III | 0.03 / 0.1 | Variable |
| | Chroococcus | I | T | 0.03 / 0.20 | P |
| | Rhabdoderma | A | T | 0.02 / 0.11 | Slight P |
| | Pseudoanabaena | A | T | 0.02 / 0.12 | P |
| | Pseudoanabaena | I | T | 0.03 / 0.19 | P |
| | Anabaenopsis | A | T | < 0.01 / 0.33 | P |
| | Anabaenopsis | I | T | < 0.01 / 0.52 | Threshold; 350 μg $L^{-1}$ |
| | Dolichospermum | A | T | < 0.01 /0.45 | P |
| | Dolichospermum | I | T | < 0.01 / 0.55 | P |
| | Dolichospermum | O | T | < 0.01 / 0.34 | P |
| | Gleocapsa | A | III | < 0.01 / 0.16 | P |
| | Gleocapsa | I | III | 0.02 / 0.25 | P |
| | Lyngbya | A | III | 0.04 / 0.09 | Threshold; 1 point only |
| | Aphanothece | I | T | 0.02 / 0.22 | Threshold; 350 μg $L^{-1}$ |
| | Synechococcus | I | III | 0.03 / 0.22 | Threshold; 1 point only |
| | Romeria | O | T | 0.01 / 0.28 | Slight P |
| | Chlorococcum | O | T | < 0.01 / 0.38 | Threshold; 100 – 200 μg $L^{-1}$ |
| | Aphanocapsa | A | V | 0.04 / 0.09 | P |
| Chlorophyta | Sphaerocystis | A | T | < 0.01 / 0.19 | Variable |
| | Sphaerocystis | O | T | < 0.01 / 0.35 | P |
| | Chlorella | A | V | < 0.01 / 0.19 | N |
| | Chlorella | O | V | < 0.01 / 0.34 | N |
| | Palmella | A | V | < 0.01 / 0.23 | P; 1 point only |
| | Palmella | O | V | < 0.01 / 0.31 | P; 1 point only |
| | Planctonema | A | V | < 0.01 / 0.25 | P |
| | Planctonema | O | V | < 0.01 / 0.47 | P |
| | Botrycoccus | A | III | 0.02 / 0.13 | Variable |
| | Botrycoccus | O | III | < 0.01 / 0.40 | T; 40 μg $L^{-1}$ |
| | Geminella | A | III | < 0.01 / 0.16 | T; 100 μg $L^{-1}$ |
| | Geminella | O | III | < 0.01 / 0.41 | P; 1 point only |
| | Schizochlamys | I | T | 0.02 / 0.24 | P; 1 point only |
| Chrysophyta | Fragilaria/Ulnaria | A | T | 0.02 / 0.10 | N |
| | Fragilaria/Ulnaria | A | V | 0.03 / 0.10 | N |
| Cryptophyta | Cryptomonas | A | T | 0.02 / 0.10 | N |
| | Cryptomonas | I | T | 0.03 / 0.20 | N |

**Table S 2-11.** List of the rotifer species identified and counted across the five study lakes and which season they were present in. The open-water season was from May – October, and the ice-on season was from November – April. All samples collected from April 2022 –May 2023.

| Rotifer Species | Open-Water | Ice-On |
|---|---|---|
| *Anuraeopsis fissa* | X | - |
| *Ascomorpha species* | X | X |
| *Asplanchna priodonta* | X | - |
| *Collotheca pelagica* | X | X |
| *Filinia terminalis* | X | X |
| *Gastropus stylifer* | X | X |
| *Hexartha mira* | X | - |
| *Kellicottia bostoniensis* | X | X |
| *Kellicottia longispina* | X | X |
| *Keratella hiemalis* | X | X |
| *Keratella quadrata* | X | X |
| *Keratella species complex* | X | X |
| *Lepadella acuminata* | X | - |
| *Lepadella patella* | X | - |
| *Monostyla closertocerca* | X | - |
| *Monostyla copies* | X | - |
| *Monostyla lunaris* | X | - |
| *Monostyla stenroosi* | X | - |
| *Polyartha dolichoptera* | X | - |
| *Polyartha remata* | X | X |
| *Pompholyx sulcata* | X | X |

**Table S 2-12.** Rotifer species found to have statistically significant ($p < 0.05$) relationships with an arsenic variable (T = total dissolved arsenic, III = As(III), V = As(V)) according to individual GAMs. Seasons were denoted by A = all sampling dates, I = ice, and O = open-water, and brief descriptions of relationships were given (N = negative, P = positive).

| Species | Season | As Variable | p-value / Adjusted $R^2$ | Relationship |
|---|---|---|---|---|
| *Kellicottia longispina* | A | T | < 0.01 / 0.39 | P |
| *Kellicottia longispina* | A | V | 0.01 / 0.14 | Mostly P |
| *Kellicottia longispina* | A | III | < 0.01 / 0.27 | Mostly P |
| *Kellicottia longispina* | I | T | < 0.01 / 0.49 | Threshold; 100 – 400 μg $L^{-1}$ |
| *Kellicottia longispina* | I | III | 0.01 / 0.25 | P |
| *Kellicottia longispina* | O | T | 0.02 / 0.26 | P |
| *Kellicottia longispina* | O | V | 0.03 / 0.20 | P |
| *Kellicottia longispina* | O | III | 0.02 / 0.26 | P |
| *Keratella species complex* | A | T | 0.02 / 0.12 | N |
| *Keratella species complex* | A | III | 0.02 / 0.11 | N |
| *Polyartha remata* | A | T | 0.03 / 0.10 | N |
| *Polyartha remata* | O | T | 0.04 / 0.19 | N |

**Table S 2-13.** List of the zooplankton species identified and counted across the five study lakes and which season they were present in. The open-water season was from May – October, and the ice-on season was from November – April. All samples collected from April 2022 – May 2023.

| Zooplankton Species | Open-Water | Ice-On |
|---|---|---|
| **Cladocera –** | | |
| *Bosmina longirostris* | X | X |
| *Ceriodaphnia rigaudi* | X | - |
| *Daphnia ambigua* | X | X |
| *Daphnia catawba* | X | - |
| *Daphnia longiremus* | X | X |
| *Daphnia mendotae* | X | X |
| *Daphnia middendorffiana* | X | X |
| *Daphnia rosea* | X | X |
| *Daphnia schødleri* | X | X |
| *Daphnia species* | X | X |
| *Diaphanosoma brachyurum* | X | - |
| *Eubosmina longispina* | X | X |
| *Holopedium gibberum* | X | X |
| *Alona species* | X | - |
| **Calanoids –** | | |
| *Epischura nordenskiøldi* | X | - |
| *Calanoid copepod female* | X | X |
| *Eurytemora affinis* | - | X |
| *Hesperodiaptomus shoshone* | X | - |
| *Heterocope septentrionalis* | X | X |
| *Leptodiaptomus sicilis* | X | X |
| *Limnolocalanus macrurus* | X | X |
| *Osphranticum labronectum* | X | X |
| *Skistodiaptomus oregonensis* | X | X |
| *Skistodiaptomus pallidus* | X | X |
| **Copepods –** | | |
| *Achnanthocyclops robustus* | X | X |
| *Achnanthocyclops vernalis* | X | - |
| *Cyclops scutifer* | X | X |
| *Diacyclops bicuspidatus odessanus* | X | - |
| *Diacyclops thomasi* | X | X |
| *Tropocyclops prasinus mexicanus* | X | X |

**Table S 2-14.** Zooplankton species found to have statistically significant ($p < 0.05$) relationships with an arsenic variable (T = total dissolved arsenic, III = As(III), V = As(V)) according to individual GAMs. Seasons were denoted by A = all sampling dates, I = ice-on, and O = open-water, and brief descriptions of relationships were given (N = negative, P = positive).

| Zooplankton Group | Species | Season | Arsenic Variable | p-value / Adjusted $R^2$ | Relationship |
|---|---|---|---|---|---|
| Cladocera | Bosmina longirostris | A | T | 0.03 / 0.11 | True N |
| | Daphnia longiremus | A | T | 0.03 / 0.11 | True N |
| | Daphnia longiremus | A | V | 0.03 / 0.11 | True N |
| | Daphnia middendorffiana | A | III | < 0.01 / 0.27 | Variable |
| | Daphnia middendorffiana | I | III | < 0.05 / 0.18 | Threshold; 0 – 120 μg $L^{-1}$ |
| | Daphnia rosea | A | III | < 0.01 / 0.37 | Variable |
| | Daphnia rosea | I | III | 0.03 / 0.22 | Threshold; 0 – 120 μg $L^{-1}$ |
| | Holopedium gibberum | A | III | < 0.01 / 0.34 | P; 1 point only |
| | Holopedium gibberum | I | III | 0.03 / 0.222 | Threshold; 0 –120 μg $L^{-1}$ |
| | Eubosmina longispina | I | III | < 0.01 / 0.64 | Variable |
| | Eubosmina longispina | I | V | 0.03 / 0.24 | P; 1 point only |
| | Daphnia species | O | V | 0.05 / 0.16 | P; 1 point only |
| | Alona species | O | V | < 0.01 / 0.31 | P; 1 point only |
| Calanoid | Female calanoid | A | V | 0.01 / 0.14 | Threshold; 100 – 200 μg $L^{-1}$ |
| | Female calanoid | O | V | 0.04 / 0.18 | Variable |
| | Heterocope septentrionalis | A | V | 0.03 / 0.10 | Threshold; 100 – 200 μg $L^{-1}$ |
| | Heterocope septentrionalis | I | V | 0.02 / 0.27 | P; 1 point only |
| | Heterocope septentrionalis | O | V | 0.02 / 0.24 | Slight P |
| | Epischura nordenskioldi | A | III | 0.01 / 0.14 | Variable |
| | Skistodiaptomus oregonensis | O | V | < 0.01 / 0.35 | Slight P |
| | Skistodiaptomus pallidus | O | V | < 0.05 / 0.17 | Variable |
| Copepods | Achnanthocyclops robustus | A | V | < 0.01 / 0.25 | P; 1 point only |
| | Tropocyclops prasinus mexicanus | I | III | < 0.05 / 0.18 | Threshold; 0 – 120 μg $L^{-1}$ |

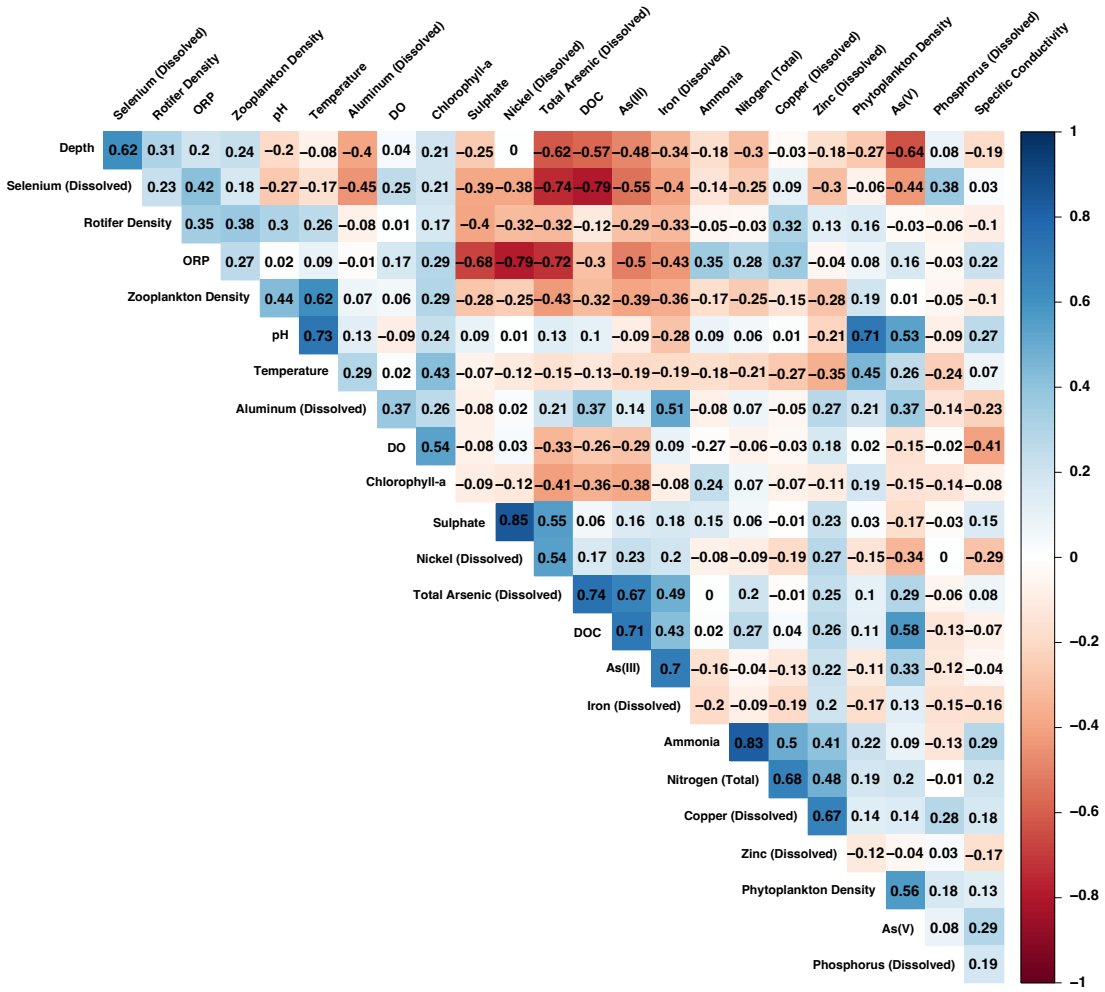


**Figure S 2-1.** Correlation matrix of all environmental variables in the original dataset created in R (package corrplot). Variables were removed if they were highly correlated ($r > 0.7$) with another important variable (i.e., arsenic). Variables included in the final model were: plankton densities, arsenic variables (total, As(III), As(V)) temperature, aluminum (Al), DO, chlorophyll-a, nickel (Ni), iron (Fe), total nitrogen (TN), copper (Cu), zinc (Zn), phosphorus (P), and specific conductivity.

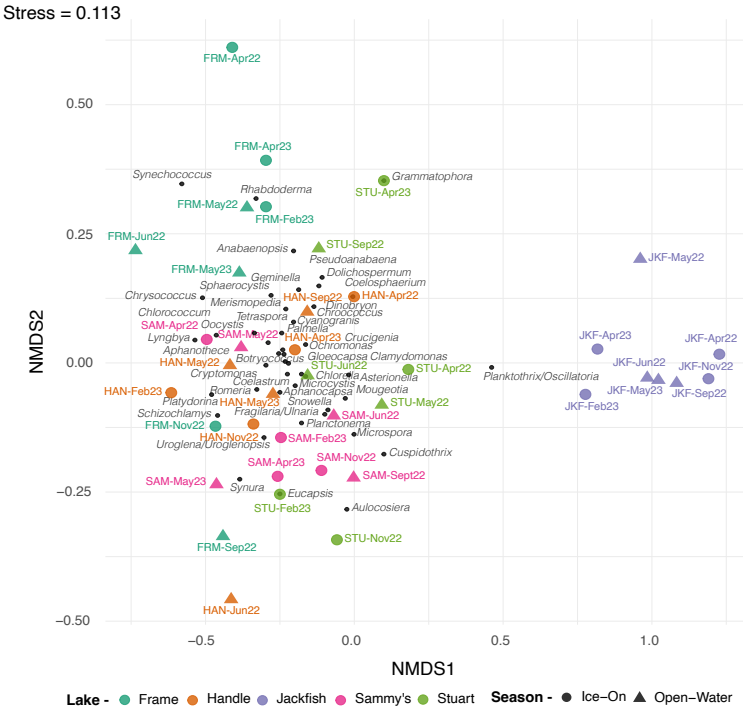


**Figure S 2-2.** NMDS plot for the full year phytoplankton dataset collected between April 2022 and May 2023.

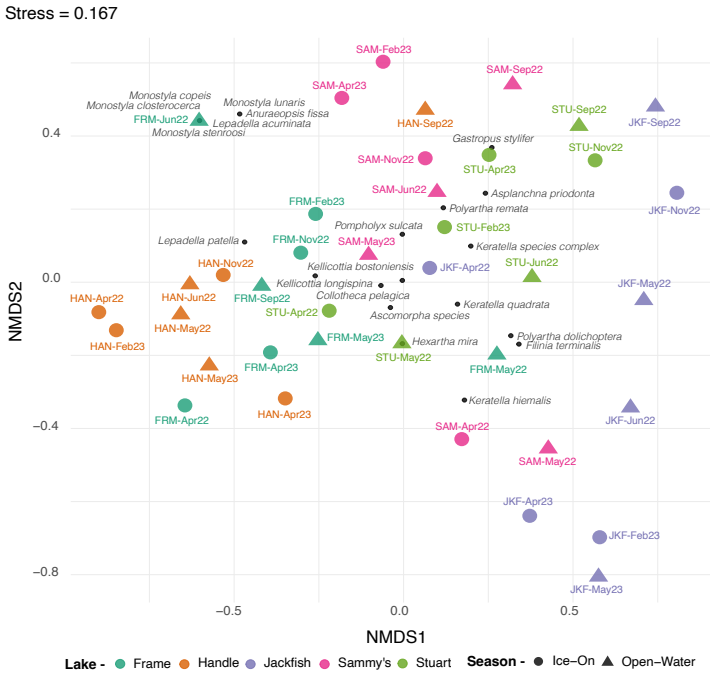


**Figure S 2-3.** NMDS plot for the full year rotifer dataset collected between April 2022 and May 2023.

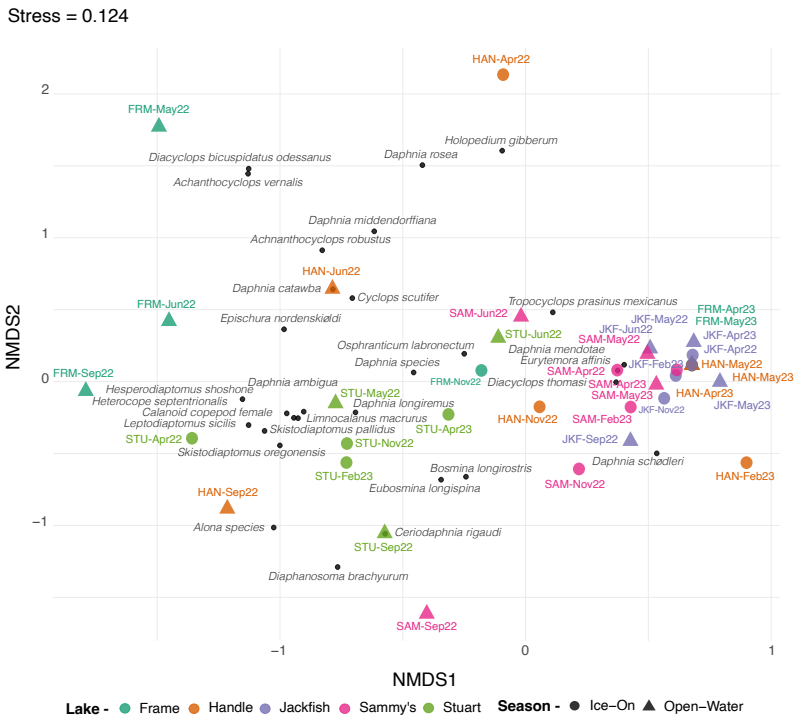


**Figure S 2-4.** NMDS plot for the full year zooplankton dataset collected between April 2022 and May 2023.

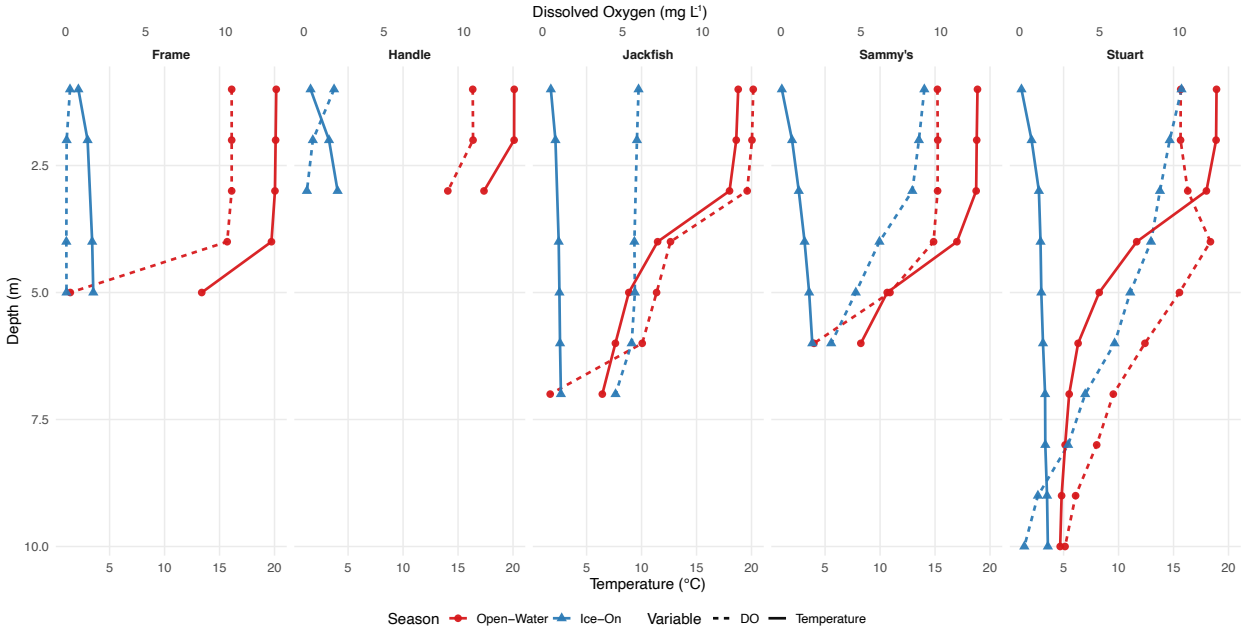


**Figure S 2-5.** Lake-depth profiles of the five study lakes showing the change in DO and temperature between the middle of the open-water season (June 2022) and ice-on season (February 2023).

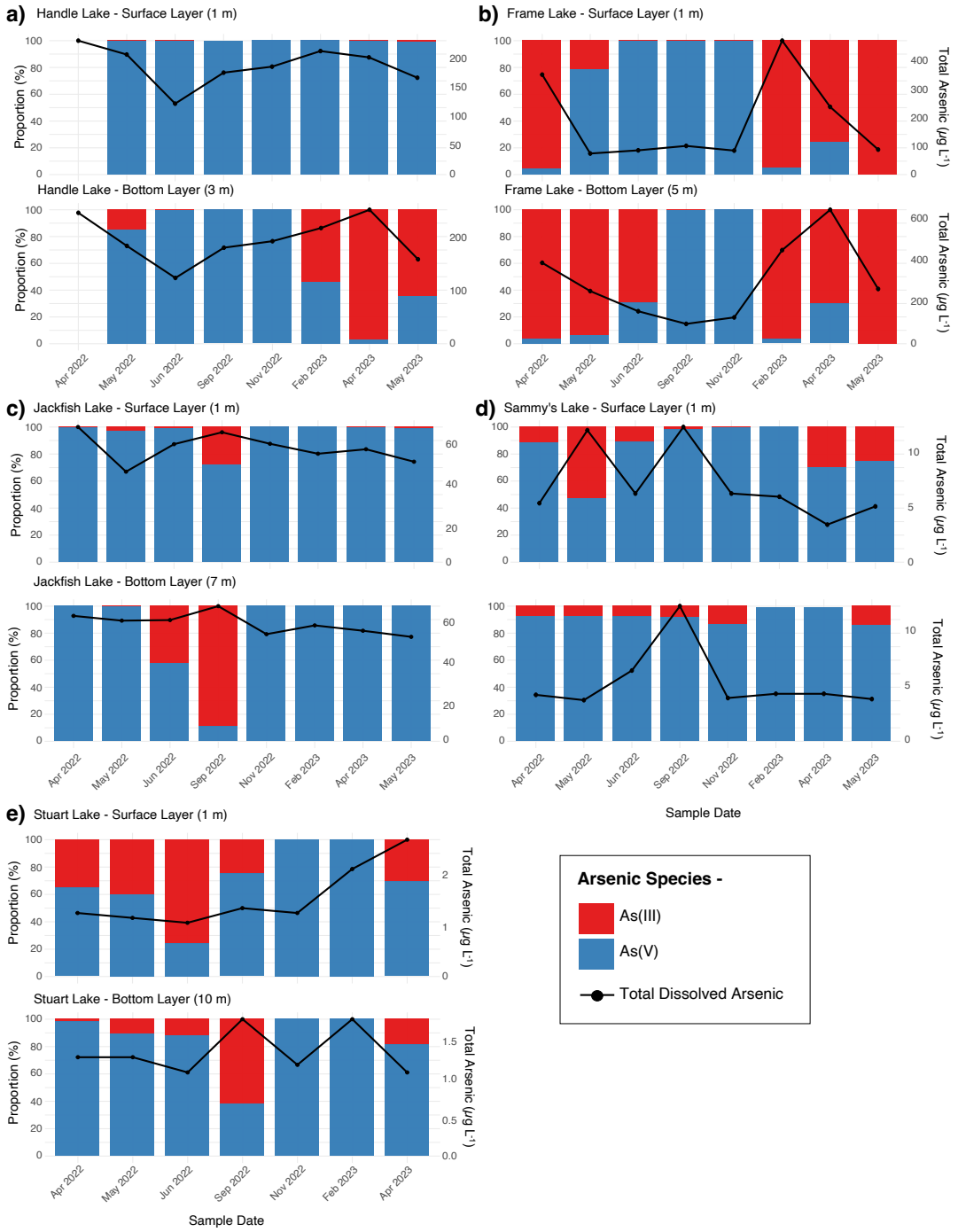


**Figure S 2-6.** Total dissolved arsenic concentrations and proportions of As(III) and As(V) in the top and bottom layers of the five study lakes across all sampling dates (April 2022 – May 2023). Inorganic arsenic samples were not collected from Handle Lake in April 2022 due to equipment malfunction, and no samples were collected from Stuart Lake in May 2023 due to unsafe lake ice conditions.

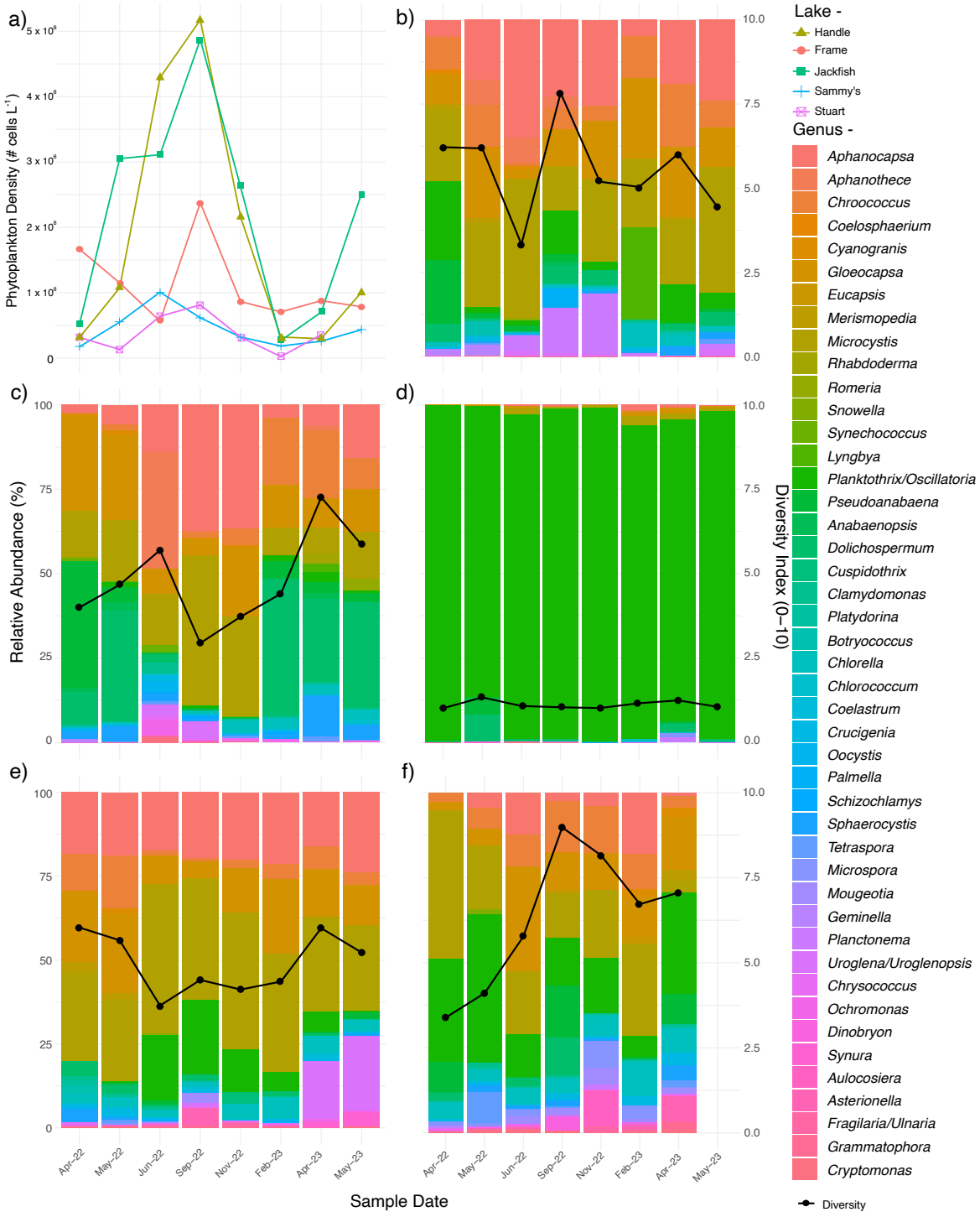


**Figure S 2-7.** a) Phytoplankton absolute density for the five study lakes, followed by phytoplankton relative abundances and diversity for b) Handle Lake, c) Frame Lake, d) Jackfish Lake, e) Sammy's Lake, and f) Stuart Lake. Phytoplankton ID samples were collected from April 2022 – May 2023 except for in Stuart Lake, which could only be sampled until April 2023. Diversity (Hill's N2) was calculated using the *vegan* package in RStudio (Oksanen et al., 2019).

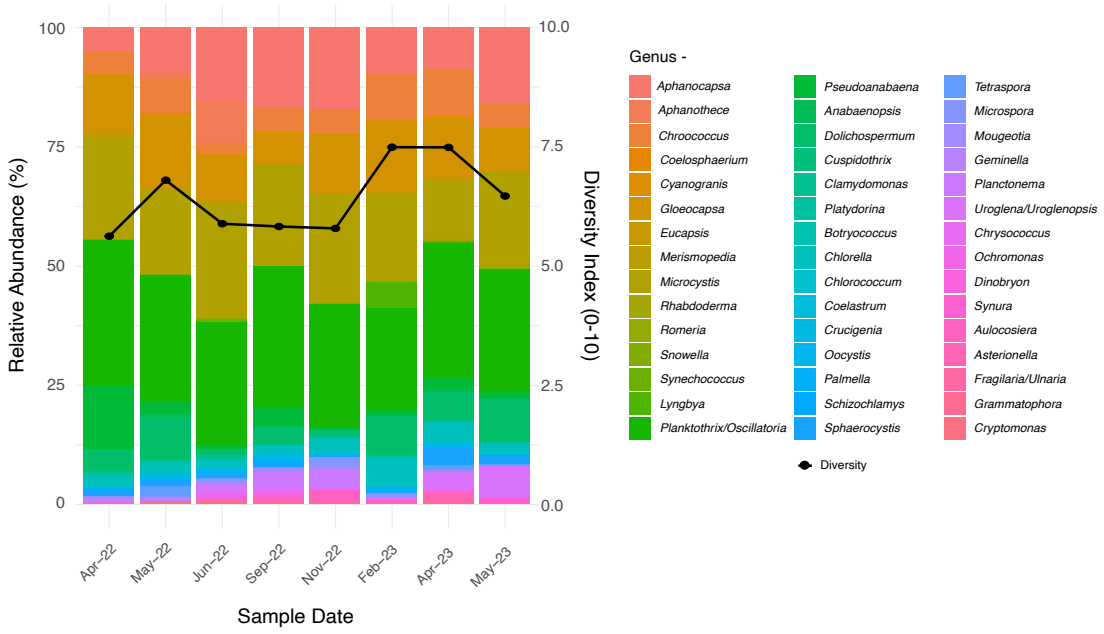


**Figure S 2-8.** Combined and averaged phytoplankton relative abundances and diversity values for all five study lakes except for May 2023 when Stuart Lake could not be sampled. Diversity (Hill's N2) was calculated using the vegan package in RStudio (Oksanen et al., 2019).

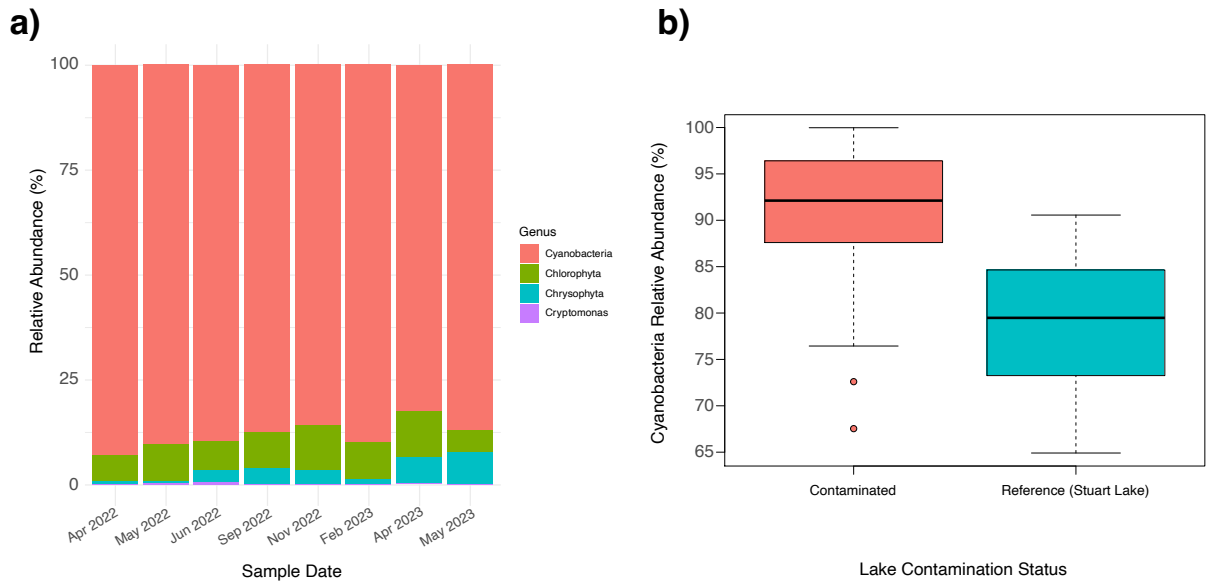


**Figure S 2-9.** a) The relative abundance of each major phytoplankton group during each sampling date averaged across the five study lakes, and b) the difference in cyanobacteria relative abundance in the four arsenic-contaminated lakes compared to the one reference lake.

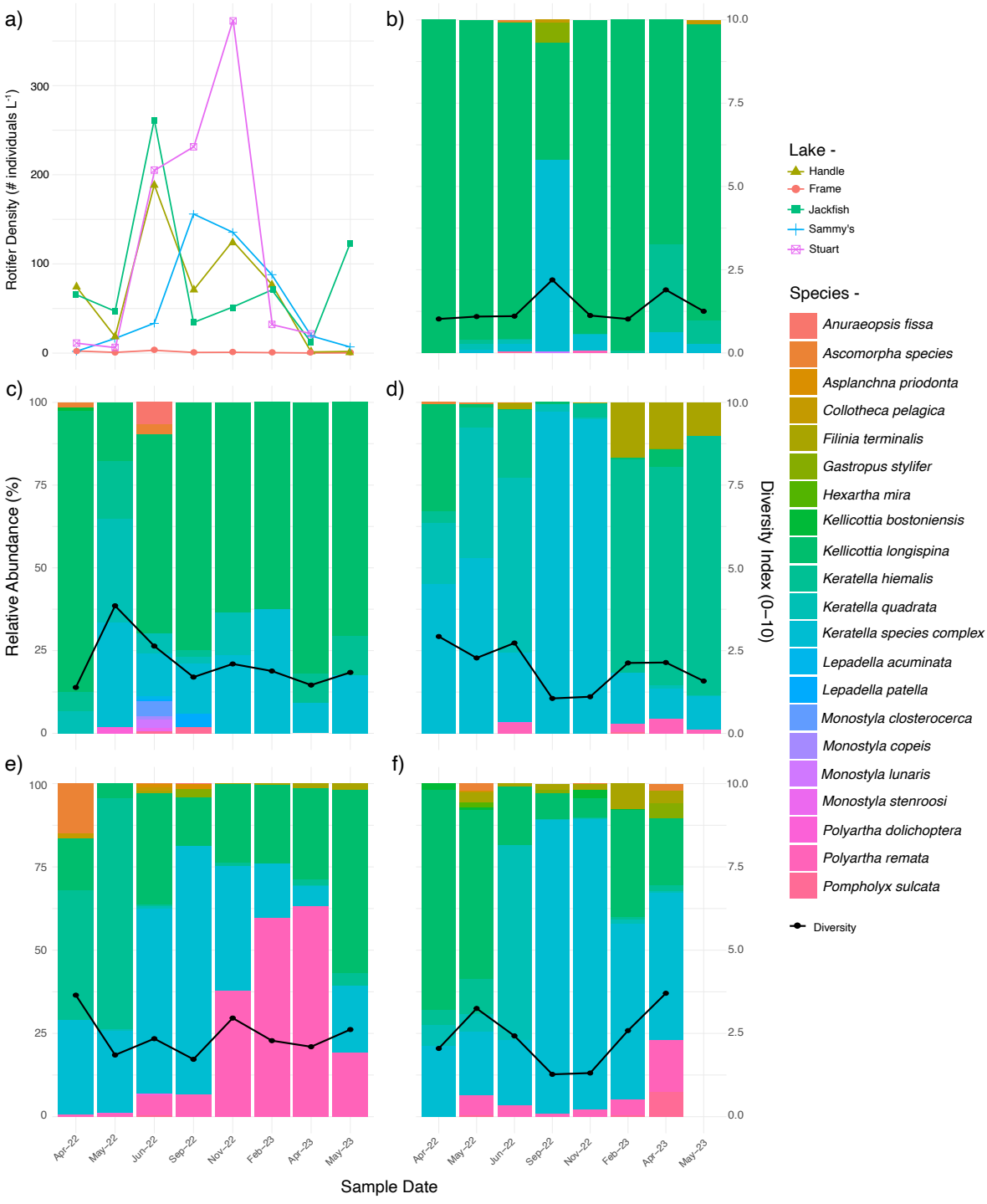


**Figure S 2-10.** a) Rotifer absolute density for the five study lakes, followed by rotifer relative abundances and diversity for: b) Handle Lake, c) Frame Lake, d) Jackfish Lake, e) Sammy's Lake, and f) Stuart Lake. Rotifer ID samples were collected from April 2022 – May 2023 except for in Stuart Lake, which could only be sampled until April 2023. Diversity (Hill's N2) was calculated using the vegan package in RStudio (Oksanen et al., 2019).

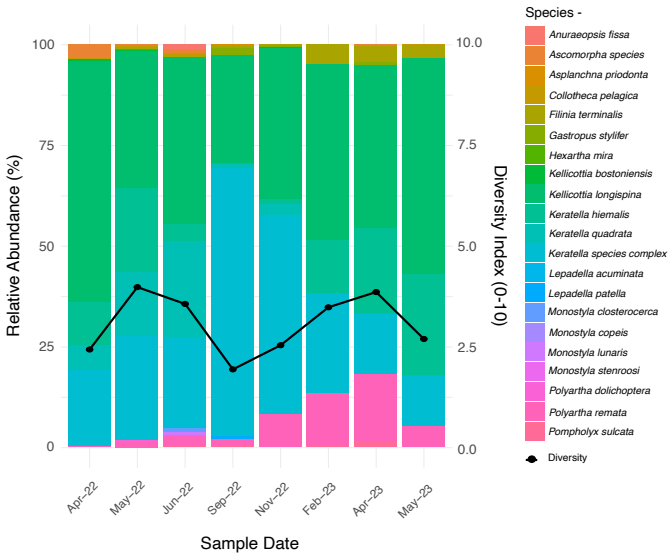


**Figure S 2-11.** Combined and averaged rotifer relative abundances and diversity values for all five study lakes except for May 2023 when Stuart Lake could not be sampled. Diversity (Hill's N2) was calculated using the *vegan* package in RStudio (Oksanen et al., 2019).

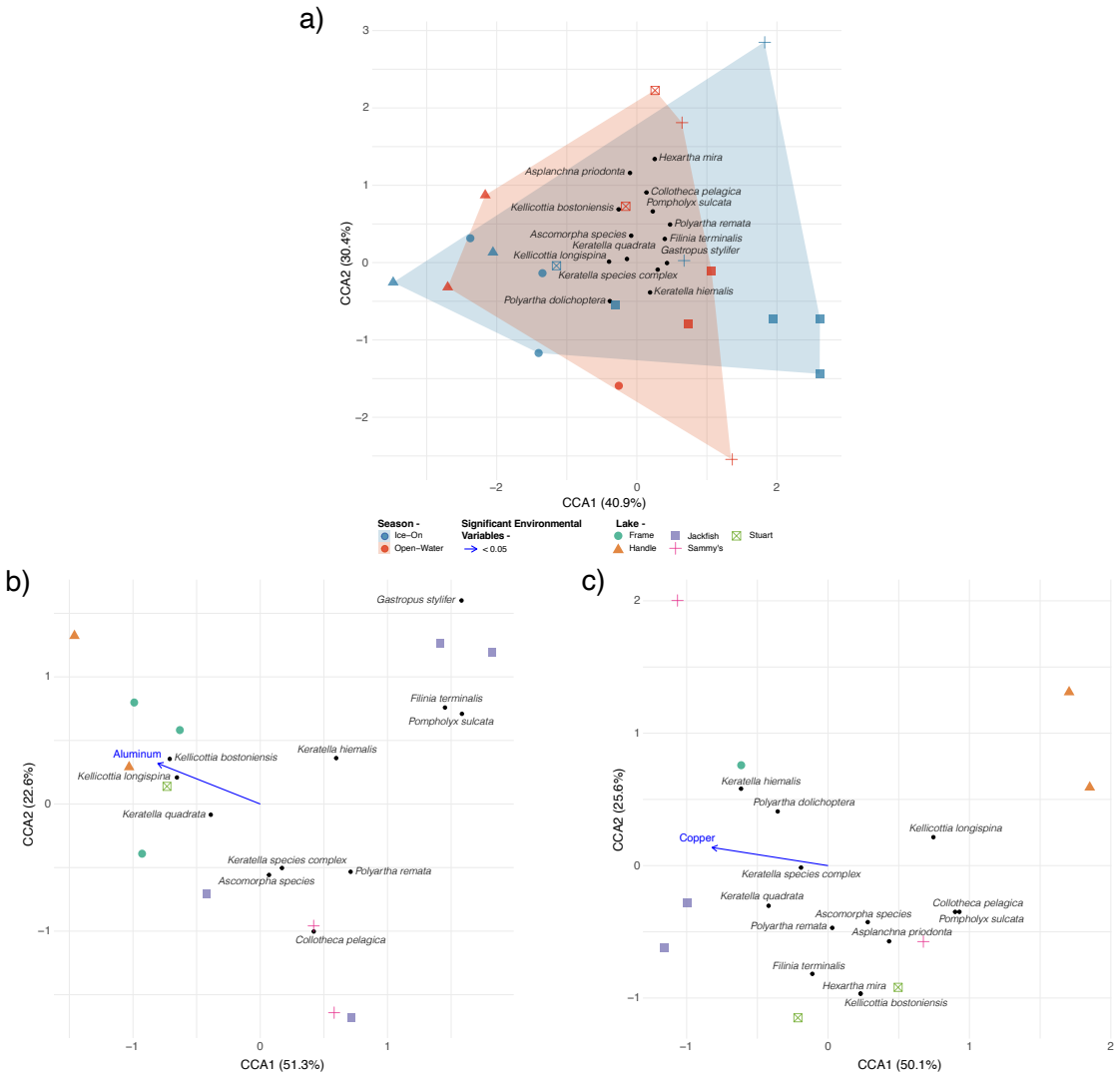


**Figure S 2-12.** CCA plots of rotifer communities and statistically correlated environmental gradients for the: a) entire sampling period (April 2022 – May 2023), b) ice-on season (November – April), and c) open-water season (May – October).

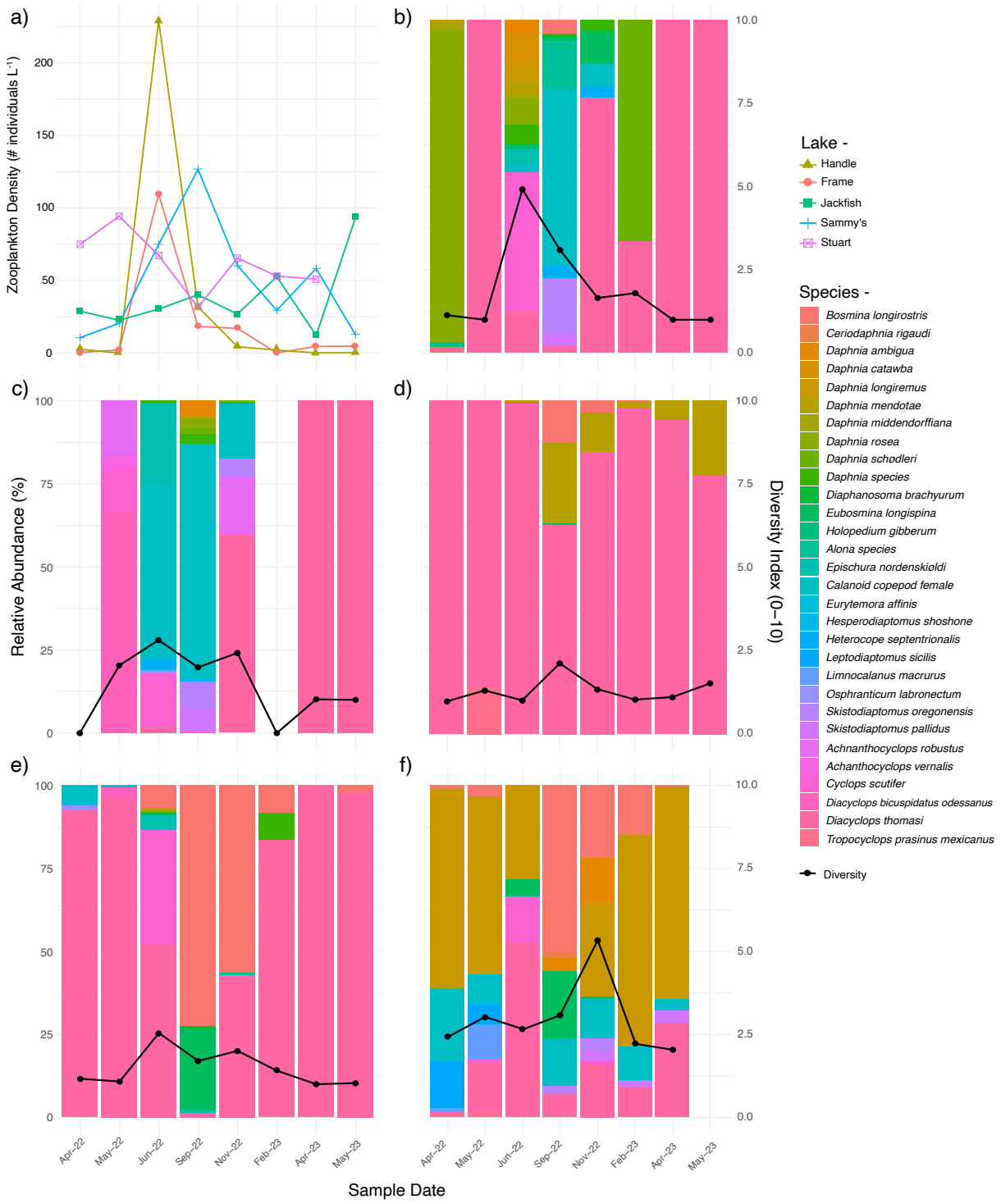


**Figure S 2-13.** a) Adult zooplankton absolute density for the five study lakes, followed by adult zooplankton relative abundances and diversity for: b) Handle Lake, c) Frame Lake, d) Jackfish Lake, e) Sammy's Lake, and f) Stuart Lake. Zooplankton ID samples were collected from April 2022 – May 2023 except for in Stuart Lake, which could only be sampled until April 2023. Diversity (Hill's N2) was calculated using the *vegan* package in RStudio (Oksanen et al., 2019).

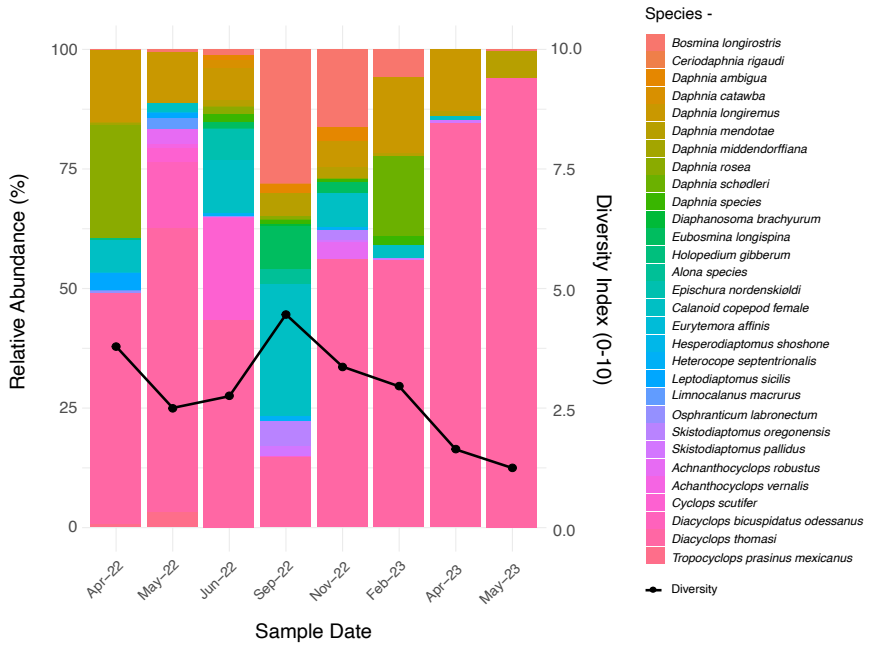


**Figure S 2-14.** Combined and averaged adult zooplankton relative abundances and diversity values for all five study lakes except for May 2023 when Stuart Lake could not be sampled. Diversity (Hill's N2) was calculated using the *vegan* package in RStudio (Oksanen et al., 2019).

# Chapter 3: Under-ice ecological and biogeochemical dynamics at the onset of spring thaw in four arsenic-contaminated subarctic lakes

Amanda J. Little, Michael J. Palmer, Marc Amyot, and Jennifer B. Korosi

Author Contributions

AJL, MJP, and JBK conceived of research ideas and conducted fieldwork, MJP and JBK secured funding and were responsible for project administration and resource acquisition. AJL conducted all other analyses and led the writing of the manuscript. All authors contributed to the creation of the methodology, contributed in the editing of manuscript drafts, and gave approval for submission to JGR: Biogeosciences for publication.

This chapter was published in JGR: Biogeosciences as: Little, AJ, Palmer, MJ, Amyot, M., Korosi, JB. 2026. Under-ice ecological and biogeochemical dynamics at the onset of spring thaw in four arsenic-contaminated subarctic lakes. JGR Biogeosciences. 131. e2025JG009231.

## 3.1 Abstract

Interactions between aquatic organisms and contaminants in under-ice lake environments are poorly characterized relative to ice-free seasons. Here, we compared under-ice arsenic biogeochemical processes and plankton community composition in four subarctic lakes spanning an arsenic contamination gradient. We focused on a short (7-10 days) late winter transitional period where lakes began to thaw but were still ice-covered; a potentially significant but understudied period of rapid biological and chemical change. We observed decreases in conductivity over the late winter transitional period, due to snowmelt influx. We also observed decreases in ice thickness and increases in photosynthetically active radiation, dissolved oxygen, and water temperatures, which corresponded with a proliferation of under-ice phytoplankton. The two study lakes with the highest under-ice arsenic concentrations experienced a dilution in the surface waters following the influx of snowmelt, while meltwater was likely a source of arsenic enrichment to the study lake with the lowest under-ice arsenic concentration. The introduction of oxygen into surface waters also shifted the arsenic pool to a higher relative fraction of arsenate compared to arsenite for lakes experiencing under-ice anoxia. The organic arsenic pool increased at spring thaw onset in 2022, as would be expected based on the increase in biological activity, a result not replicated in 2023. Arsenite was a statistically significant driver of late winter variation in phytoplankton assemblages, but not for zooplankton or rotifers. Overall, this study generates new insights into under-ice arsenic cycling and ecotoxicity in subarctic lakes, which remain ice-covered for much of year.

## 3.2 Introduction

Giant Mine, a gold mine that was operational in Yellowknife (Northwest Territories, Canada) from 1948 to 2004, sits atop 237,000 tonnes of buried toxic arsenic trioxide ($As_2O_3$) dust and has associated remediation costs estimated at $4.38 billion, making it one of Canada's most pressing environmental liabilities (Government of Canada, 2022). From 1948-1953, Giant, and other gold mines in the region, released an estimated 5 tonnes of atmospheric $As_2O_3$ emissions per day (Hocking, 1978; Palmer et al., 2025), resulting in a legacy of arsenic enrichment in soils and lake sediments upwards of 80 km away from the roaster stacks (Cheney et al., 2020; Jasiak et al., 2021). Much of the landscape remains contaminated with arsenic, despite the fact that gold mining activities ceased over two decades ago and arsenic emissions peaked over seventy years ago. Many lakes in the region exhibit arsenic levels significantly higher than the currently accepted guidelines for drinking water (10 $\mu g\ L^{-1}$) and the protection of aquatic life (5 $\mu g\ L^{-1}$) (World Health Organization [WHO], 1993; Canadian Council of Ministers of the Environment [CCME], 2001, respectively), with water from two lakes recently measured to be in excess of 600 $\mu g\ L^{-1}$ and 2,000 $\mu g\ L^{-1}$ (Palmer et al., 2015; Sivarajah et al., 2019). Yellowknife can therefore provide a useful case study for assessing the long-term impacts of arsenic on lake ecosystem health and function, particularly in a subarctic context.

Most investigations about the impacts of legacy arsenic contamination on the biota of Yellowknife lakes have been paleolimnological studies that reconstructed changes in aquatic assemblages by analyzing subfossil remains of ecological indicator taxa. Significant ecological impacts were observed in a sediment core collected from a highly contaminated lake within the Giant Mine lease boundaries, including the extirpation of Cladocera (a group of crustacean zooplankton) and planktonic diatoms (siliceous single-celled algae) following peak arsenic

emissions (Thienpont et al. 2016). In contrast, regional studies that examined changes in diatom and Cladocera assemblages across a gradient of arsenic contamination in the Yellowknife area noted only subtle changes over time, and arsenic did not appear to have a strong influence on assemblage structure (Persaud et al. 2019; Sivarajah et al. 2019). Paleolimnological studies integrate signals across seasons and years, and only provide data on aquatic taxonomic groups that leave identifiable remains in lake sediments. Similarly, paleolimnological studies report only total arsenic concentrations in sediments, and are unable to account for variation in arsenic speciation (e.g., arsenite (As(III)), arsenate (As(V)) that can influence its toxicity to aquatic biota (Akter et al., 2005). Paired investigations into ecological communities and arsenic biogeochemical cycling are therefore needed to better understand the ecological legacies of arsenic contamination in Yellowknife lakes.

The winter period may be especially relevant for studying arsenic ecotoxicological implications for aquatic biota in shallow Yellowknife lakes. This is because dissolved arsenic concentrations in water have been documented to be higher in winter when shallow (<4 m) lakes are ice-covered, with a higher proportion of arsenic occurring as the more toxic As(III) form (Palmer et al., 2019; 2020). This is due to a combination of solute exclusion during lake ice formation, and efflux of arsenic from the sediment as As(III) via reductive dissolution of metal-oxyhydroxides in response to declining redox conditions (Arsic et al., 2018). Winter has historically been an overlooked limnological sampling period due to issues associated with fieldwork logistics (i.e., equipment freezing, extreme cold temperatures, ice safety, etc.), and because it was previously thought to be a dormant time of year from a biological perspective (Block et al., 2019). However, recent studies challenge this assumption and suggest that under-

ice ecosystem dynamics also have a significant impact on subsequent open-water seasons (Hampton et al., 2015; 2017).

The late winter period immediately preceding ice-off has been highlighted as a potentially significant period of rapid biological and chemical change that may set the stage for spring open-water conditions (Cavaliere & Baulch, 2020). In particular, this transition period often encompasses the "spring bloom", when phytoplankton growth under the ice rapidly proliferates (Sommer et al., 2012; Twiss et al., 2012; Cavaliere & Baulch, 2020). The limnological changes that occur at the transition from late winter into spring thaw, including increased light penetration, snowmelt incursion, and increased primary productivity, also have the potential to impact arsenic cycling through altered photochemical reactions and changing redox conditions (Cullen & Reimer, 1989; Amyot et al., 2021). Furthermore, the production of organic arsenic species may also be enhanced during spring thaw conditions, as its production occurs via uptake and bio-transformation by aquatic biota (Hellweger et al., 2003) and therefore reflects biological activity in freshwater lakes (Caumette et al., 2012; 2014). The late winter transition period is often unsampled, even within winter limnological investigations, as this time of year presents unique safety challenges due to the deterioration of lake ice conditions.

The aim of this study was to assess and compare arsenic biogeochemical processes and plankton communities (phytoplankton, rotifers, and zooplankton) at the late winter to spring thaw transition period (referred to hereafter as spring thaw) in four Yellowknife-area lakes spanning a gradient of arsenic contamination (5.5 – 350 $\mu g\ L^{-1}$ in 2022). We hypothesized that spring thaw would be a dynamic period of change in lakewater arsenic concentrations and speciation, as well as primary productivity and plankton community composition. We also sought to answer the following research questions: (1) Is there variation in spring thaw dynamics

across two years of data collection (2022, 2023), and if so, does the variation reflect preceding winter conditions? (2) Is arsenic a significant predictor of plankton community composition? Overall, this study generates new insights into the influence of winter conditions on arsenic cycling and ecotoxicity in subarctic lakes, which is required to understand the potential interactions between future climate change and legacy mining pollution.

## 3.3 Materials and Methods

### 3.3.1 Study Lakes

The City of Yellowknife is located on the northern shores of Great Slave Lake on Treaty 8 and Chief Drygeese Territory in the Northwest Territories, Canada. It has been the traditional home of the Yellowknives Dene First Nation (YKDFN) for over 7,000 years (O'Reilly, 2015). The region experiences a continental subarctic climate, with an average annual air temperature of -4.0°C (1990-2020 Climate Normal; ECCC, 2025). Mean annual precipitation is 293.3 mm, with an average of 180.2 mm of rainfall and 155.0 cm of snowfall (ECCC, 2025). Temperatures in the region typically fall below 0°C in early October, and remain below freezing until late April. As a result, small lakes in the area typically remain ice-covered for at least half of the year, ranging from 190-243 days based on data from 1956-1994 (Benson et al., 2013). Four study lakes were selected due to their proximity to Giant Mine, road accessibility, and inclusion in a long-term monitoring program currently run by the Aurora Research Institute (ARI; SLACC: Subarctic Lakes in a Changing Climate) (Figure 3.1; Table S 3-1). All four study lakes are natural waterbodies that are underlain by granitoid or volcanic bedrock (Palmer et al., 2015; Cousens, 2000). Sammy's and Handle Lake are located to the west of the Yellowknife Greenstone Belt, while Frame and Jackfish Lake have formed directly on top of it (Palmer et al., 2015; Cousens, 2000).

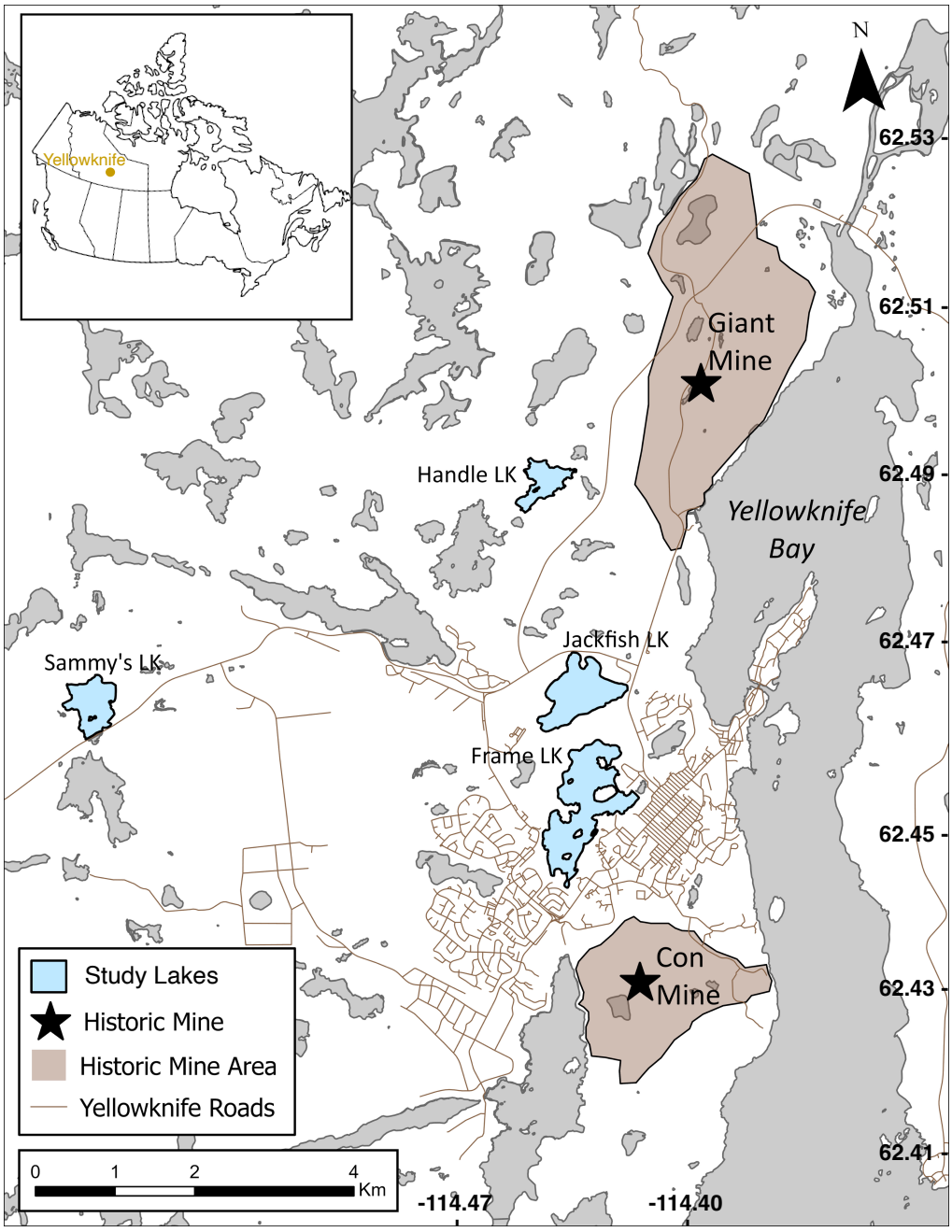


**Figure 3.1.** Map showing the locations of the four study lakes in relation to the historical gold mine property lease boundaries in the Yellowknife (Northwest Territories, Canada) region. Most arsenic emissions are associated with Giant Mine. Coordinates are in decimal degrees. Inset shows the location of Yellowknife within Canada. Map created by Seamus Daly.

### 3.3.2 Sample Collection

Each lake was sampled twice within a 7-10 day timeframe, including once prior to the beginning of the spring thaw period (late April), defined here as the onset of snow and ice melt, and once during the spring thaw period (early May) when snow and ice melt had begun but the lakes were still ice-covered and safe to walk on. We identified the sampling dates based on a combination of local long-range weather forecasts, ice safety reports, as well as visual inspection of snow depths and ice structure made by the research team. In 2022, 10 days passed between the two sampling dates, while in 2023, only 7 days passed before it was determined sampling should occur again due to the rapid rate at which the lake ice was beginning to melt (Table S 3-2).

In order to maintain the highest safety standards, all fieldwork team members wore life jackets or dry suits the entire time they were on lake ice. Safety holes were drilled through the ice at 10 m transects from the edge of the lake using an ice auger, and lake ice thickness was measured. Ice thickness and structure were tested more frequently using an ice pick, specifically to identify whether ice candling (when ice begins to structurally disintegrate forming long, thin vertical columns during melt) had occurred, particularly during the post-snowmelt sampling periods. A safety throw rope and first aid kit were brought on every sampling trip, as well as a canoe during the post-snowmelt trips in case team members needed to get off the ice quickly. Finally, multiple researchers in the area were made aware of when a sampling trip was occurring, and drove by every few hours to make sure the fieldwork team did not require additional support.

Sampling sites were located at the deepest part of each lake. Before drilling any sampling holes, snow and ice thickness were measured and recorded, and notes on meteorological data were recorded (Table S 3-2). Vertical water column profiles of temperature (°C), dissolved oxygen (DO; mg $L^{-1}$), oxidation-reduction potential (ORP; mV), specific conductivity (μS $cm^{-1}$),

and chlorophyll-a (μg $L^{-1}$) were measured using a multi-parameter YSI probe (YSI EXOII, Yellow Springs Inc., Yellow Springs, Ohio). Photosynthetically active radiation (PAR) was measured at 1 m intervals until approximately 0.5 m above lake bed using a LI-COR probe equipped with an underwater quantum cosine sensor (LI-192SA with cable, lowering frame, and LI-250A light meter) (LI-COR Biosciences, Lincoln, USA). Water samples were collected at 1 m intervals for water chemistry analyses using a peristaltic pump and Teflon™ line that was prerinsed with 5% HCl solution and ultrapure water (Table S 3-3) (Palmer et al., 2020).

Samples collected for dissolved metal(loid)s and arsenic speciation analyses were filtered in the field using a syringe and 0.45 μm polyethersulfone (PES) syringe tip filter. Water samples collected for total and dissolved metal(loid)s were preserved to 1% (v/v) with nitric acid. Arsenic speciation samples were collected in 14 mL vials preloaded with 150 μL of 0.25 M ETDA, and preserved with an additional 25 μL of glacial acetic acid within 4 hours of collection (Palmer et al., 2019). All water samples were kept cool and stored in the dark until analysis. Arsenic speciation samples could not be collected for Handle Lake during the pre-snowmelt period in 2022 due to equipment malfunction. Field blanks and duplicate samples were collected for arsenic speciation samples for QA/QC (Table S 3-4). All field blanks were below the method detection limit for arsenic (MDL = 0.2 μg $L^{-1}$; N = 19), and duplicate samples were calculated to have relative percent differences ranging from 0.5 – 9% (mean = 0.53%; N = 4) (Table S 3-5).

In 2023, we collected meltwater run-off (overland flow) from the surrounding catchment of the study lakes during the spring thaw period when it was deemed safe enough to do so. Locations of incoming meltwater run-off were identified visually, and safety was assessed based on the thickness and stability of the lake ice adjacent to the meltwater entry point. Meltwater runoff samples were collected by hand in a 14 mL vial, and preserved using the same methods

described above. We were able to collect meltwater run-off samples from all lakes except Frame Lake (Table S 3-6).

Water samples for phytoplankton analysis were collected using a 2.2 L vertical Van Dorn. Water samples were collected at 1 m depth intervals starting at 1 m below the ice until 1 m above the sediments (Table S 3-3). Samples were then homogenized and subsampled into two 100 mL duplicates to provide an integrated sample of the entire water column. Zooplankton samples were collected via vertical net tows using a Wisconsin zooplankton net (Wildco, Florida, USA; 63 μm mesh size, 0.127 m mouth diameter, 1 m length) beginning at 1 m above the lake bed. Zooplankton samples were preserved in the field to an approximate concentration of 70% ethanol, while phytoplankton samples were preserved back at the lab with 3% Lugol's solution. All samples were stored in a refrigerator until taxonomic identification and enumeration.

### 3.3.3 Lab Analyses

Bulk water samples for water chemistry were delivered to an accredited government laboratory (Taiga Laboratory, Yellowknife, NWT) the same day as collection. Samples were analyzed for major ions, dissolved organic carbon, and nitrogen (nitrate, nitrite, and ammonium), as well as total (unfiltered) and dissolved (filtered < 0.45 μm) concentrations of 25 metal(loids) (Palmer et al., 2019). Dissolved organic carbon and major ion concentrations were determined via high temperature combustion using a total carbon analyzer (SM5310) and ion chromatography (SM4110), respectively (Greenberg et al., 1992). Total and dissolved metal(loid) concentrations were measured using inductively coupled plasma mass spectrometry (ICP-MS) (Agilent 7900 Single Quadruple ICP-MS; EPA method 200.8) (Creed et al., 1994). Phosphorus was analyzed using ICP-MS in order to minimize potential interference from As(V) in the

samples (Linge & Oldham, 2001). Arsenic speciation samples were analyzed at the Université de Montréal via high-performance liquid chromatography with ICP-QQQ (Agilent 8900 Triple Quadrupole ICP-MS). For more information regarding the QA/QC protocols established for this method, please see the supplementary information section (Table S 3-7).

For phytoplankton taxonomic analysis, water samples (100 mL) were settled for a minimum of 48 hours, then decanted to a volume of 20 mL to create a 5x concentration. Next, 1 mL aliquots were pipetted into a gridded Sedgewick-Rafter cell and identified under a microscope at three different counting efforts (40x whole cell; 100-200x 1 transect; 400x 100 random fields of view) using an OMAX V83 series inverted microscope. A minimum of 300 natural units, defined as one natural grouping of algae (i.e., individual filament, colony, or isolated cell) were counted per sample. Phytoplankton were identified to the genus level using a variety of references (Guiry & Guiry, 2024; Spaulding & Edlund, 2024; PhycoTech, 2017; Graham et al., 2016; Baker et al., 2012; Rosen & Amand, 2015; Krammer & Lange-Bertalot, 1991a, 1991b, 1988, 1986; Prescott, 1962; 1954), and confirmed with international algal taxonomic experts (PhycoTech, Inc., St. Joseph's, Michigan, USA). Cell densities were calculated based on cell counts and volume of the sample aliquot. A 1% relative abundance threshold was applied to phytoplankton genera in order to improve the signal-to-noise ratio and reduce the influence of rare genera (Legendre & Legendre, 2012).

Aliquots of zooplankton samples (1 mL) were pipetted into a gridded Sedgewick-Rafter cell via a Hensen-Stemple pipette to reduce instances of clogging and potential exclusion of larger-bodied organisms. Rotifers and zooplankton were identified and counted together in each aliquot. A minimum of 100 individual rotifers and zooplankton were counted per subsample, with a minimum of 3 subsamples per sample. In samples with less than 300 adult individuals, all

of the organisms in the sample were identified and counted. Both rotifers and zooplankton were identified to the lowest taxonomic level possible (species) using an OMAX V83 series inverted microscope following the Haney et al. (2013) and Balcer et al. (1984) reference guides. Rotifer and zooplankton densities (individuals $L^{-1}$) were determined based off of the calculated volume of water sampled per tow and per aliquot.

### 3.3.4 Statistical Analyses

We explored changes in important environmental variables between the late winter and spring thaw periods and across the two sampling years using a combination of t-tests and Wilcoxon tests (Table S 3-8). We started by running paired t-tests on all environmental variables, and then checked the distributions of the residuals using Shapiro-Wilks tests. Where residuals were confirmed to be normally distributed, we also confirmed statistical power (Table S 3-8). Where residuals were found to be non-normal, the variables were re-run through non-parametric Wilcoxon tests. A 95% confidence interval was used in all tests. Relative abundances were calculated from the phytoplankton, rotifer, and zooplankton count data. Dissimilarity between plankton community assemblage between the two time periods (late winter, spring thaw) and years (2022, 2023) were assessed using the Bray-Curtis dissimilarity metric on relative abundance data (Legendre & Gallagher, 2001). Permutational multivariate analysis of variance (PERMANOVA) with 999 permutations (function *adonis2*) was used to test for significant differences between plankton community composition. Within-group homogeneity of variance was tested using the function *betadisper* (Oksanen et al., 2019) and was paired with similarity percentage analysis (SIMPER), in order to identify which plankton species and genera contributed the most to any significant dissimilarity between the various time periods.

Relationships between plankton community composition and environmental variables were assessed using redundancy analysis (RDA) based on the results of a de-trended correspondence analysis (DCA) (Lepš & Šmilauer, 2003). Environmental variables were tested for normality using the Shapiro-Wilk test, and then $\log_{10}$-transformed where appropriate (i.e., not normally distributed). A Hellinger transformation was applied to the plankton relative abundance data in order to reduce the influence of dominant taxa. A correlation matrix was run on the environmental data using the *corrplot* package, and variables found to be highly correlated ($r \geq 0.7$) were removed from the dataset (Wei & Simko, 2017). A forward selection process (function *ordistep*) was used to identify which environmental variables, if any, were significant drivers of plankton community composition. Models with the selected environmental variables were run against null models containing no variables and compared using the Akaike Information Criterion (AIC) framework (Burnham & Anderson, 2002).

All data analyses were conducted in the statistical computing environment RStudio, and all graphics were created using the *ggplot2* package (version 2024.12.0+467; R Core Team 2020; Wickham et al., 2016).

### 3.4 Results

The winter of 2023 was significantly warmer than the winter of 2022 ($p < 0.001$), with mean temperatures of -12.6°C (2023) and -16.2°C (2022) observed for the ice-on period (November-May) (Figure S 3-1). Lake ice thickness across the four study lakes ranged from 76-130 cm at the end of winter (late April, prior to the onset of thaw) in 2022, compared to 65-72 in 2023 (Table S 3-2). Ice thickness declined between the two sampling dates (pre-thaw in late April and thaw onset in early May) at an average rate of -1.93 cm/day in 2022 and -1.5 cm/day in

2023. The onset of thaw occurred ~7-10 days earlier in 2023 than in 2022 (Table S 3-2) and ice thickness was significantly greater in 2022 ($p = 0.004$).

The introduction of snowmelt into each lake during spring thaw was confirmed by recorded decreases in specific conductivity between the two sampling dates (Figure 3.2; Table S 3-9); however, evidence of diluted surface waters was apparent in the late winter sampling from 2023, which indicates that thaw might have already been occurring in these lakes and we missed the "pre-snowmelt" period. The onset of thaw happened much more rapidly in 2023 than it did in 2022. Increases in surface (1 m depth) temperatures were also recorded between the two sampling periods ($p = 0.02$; Table S 3-9). Photosynthetically active radiation (PAR) and chlorophyll-*a* also tended to increase (with some exceptions) between the pre- and post-snowmelt periods across both years (Figure S 3-2).

### 3.4.1 Lakewater Arsenic

Dissolved arsenic concentrations were higher during the pre-thaw period compared to the thaw onset period in Handle Lake and Frame Lake, as well as Jackfish Lake in 2022 (Figure 3.2). In contrast, Sammy's Lake exhibited increases in dissolved arsenic concentrations in the surface waters corresponding to an influx of snowmelt, as indicated by decreases in specific conductivity (Figure 3.2). Meltwater runoff into Sammy's Lake was enriched in arsenic relative to the lakewater (~45 $\mu g\ L^{-1}$ compared to ~3.5 $\mu g\ L^{-1}$ in the pre-thaw lake waters; Table S 3-6). Meltwater runoff arsenic concentrations for Jackfish Lake were slightly enriched relative to pre-thaw lakewater concentrations (~80 $\mu g\ L^{-1}$ compared to ~50-60 $\mu g\ L^{-1}$; Table S 3-6), while meltwater runoff arsenic concentrations into Handle Lake were diluted (~140 $\mu g\ L^{-1}$ compared to ~230 $\mu g\ L^{-1}$ in the lake water; Table S 3-6). No meltwater data was available for Frame Lake.

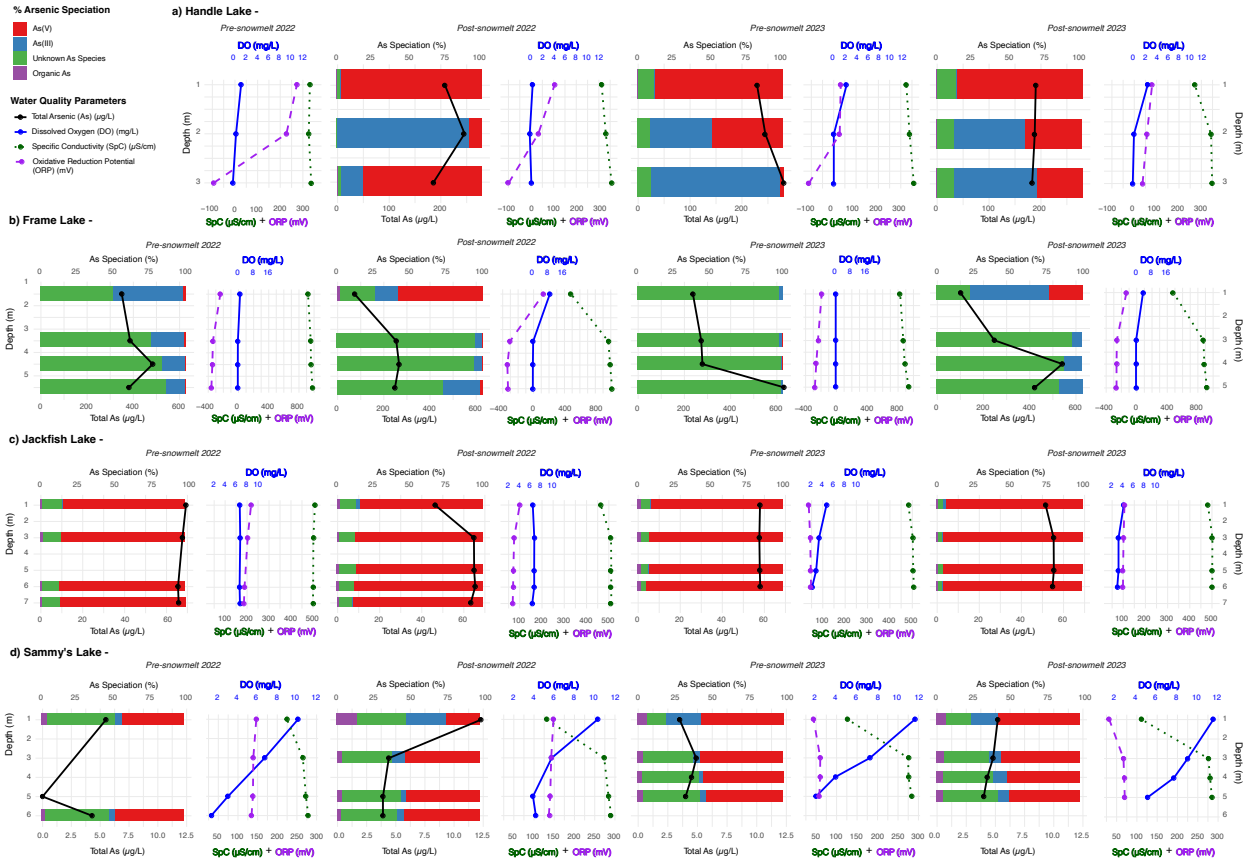


**Figure 3.2.** Lake-depth profiles of the four study lakes showing the change in total dissolved arsenic concentration, proportion of different arsenic species, DO, and specific conductivity between the pre- and post-snowmelt periods in both 2022 and 2023. Pre-snowmelt lake arsenic data could not be collected from Handle Lake in 2022.

Dissolved arsenic concentrations and As(III) exhibited a negative relationship with dissolved oxygen (DO) and oxidative-reductive potential (ORP), particularly in the two most contaminated lakes (Handle Lake and Frame Lake) (Figure 3.2; Figure S 3-3). Arsenic concentrations tended to be higher under low DO/ORP, with a higher proportion of inorganic arsenic present as As(III). Frame Lake and Handle Lake had the highest total dissolved arsenic and As(III) concentrations of the four study lakes, and both experienced under-ice anoxia, particularly in the bottom waters (Figure 3.2). The highest concentration of arsenic was reported

in the bottom layer of Frame Lake in 2023 (631 μg $L^{-1}$). An unknown arsenic species dominated the late under ice period in Frame Lake, which we speculate may be a thio-arsenic species given that Frame Lake water samples exhibited a strong sulphur smell, and sulfide concentrations have previously been reported in the lake at concentrations in excess of 200-300 μg $L^{-1}$ compared to ~20 μg $L^{-1}$ in Handle Lake (Table S 3-10). Thio-arsenicals have been found to dominate in similar sulfate reducing conditions in temperate arsenic-contaminated freshwater lakes (Hollibaugh et al., 2005; Kubachka et al., 2009). The influx of meltwater into Frame Lake (and Handle Lake in 2023) introduced DO into the surface waters, corresponding to increases in the proportion of arsenic present as As(V) (Figure 3.2). No arsenic speciation data was available for Handle Lake in 2022.

Jackfish Lake and Sammy's Lake were well oxygenated throughout the water column in the pre-thaw period, with no notable increases in oxygen at thaw onset (Figure 3.2). Total dissolved arsenic concentrations were lower in Jackfish and Sammy's relative to Frame and Handle, and had higher proportions of As(V) compared to As(III) but no notable changes in arsenic speciation between the pre-snowmelt and post-snowmelt onset sampling periods (Figure 2). An unknown arsenic species was also prevalent in Sammy's Lake (Figure 3.2). Organic arsenic made up a higher proportion of the total arsenic pool in Sammy's Lake, which had the lowest total arsenic concentrations (Figure 3.2). Arsenobetaine (AsB) was the most prevalent organic arsenic form measured in all of the lakes (Figure 3.2; Table 3.1). In 2022, organic arsenic increased in the surface waters between the pre-thaw and thaw onset sampling periods in Frame Lake and Sammy's Lake, with no change observed in Jackfish Lake and pre-thaw data unavailable for Handle Lake (Figure 3.2; Table 3.1). This trend was not observed in 2023, and organic arsenic concentrations were similar at pre-thaw and thaw onset in all lakes (Figure 3.2;

Table 3.1). Surface water AsB concentrations were notably lower in 2023 compared to 2022, but otherwise there were only minimal differences in dissolved arsenic and arsenic speciation between the two sampling years (Figure 3.2; Table 3.1).

**Table 3.1.** Arsenic concentrations in the surface (1 m) layer of the four study lakes during pre- and post-snowmelt of the 2022 and 2023 spring thaw periods. Method detection limits (DL) of 0.2, 0.05, 0.01, 0.02, 0.02, and 0.02 μg $L^{-1}$ for dissolved As, As(V), As(III), and the organic arsenic species monomethylarsonate (MMA), dimethylarsonate (DMA), and arsenobetaine (AsB), respectively. The unknown arsenic species was calculated by subtracting the known speciations of arsenic as measured via HPLC-ICP-QQQ from the dissolved arsenic value measured by ICP-MS.

| Lake | Period | Total Dissolved Arsenic (μg $L^{-1}$) | As(V) (μg $L^{-1}$) | As(III) (μg $L^{-1}$) | MMA (μg $L^{-1}$) | DMA (μg $L^{-1}$) | AsB (μg $L^{-1}$) | Unknown Arsenic Species (μg $L^{-1}$) |
|---|---|---|---|---|---|---|---|---|
| **2022** | | | | | | | | |
| Frame | Pre-snowmelt | 350.0 | 8.0 | 168.0 | < DL | < DL | < DL | 174.0 |
| | Post-snowmelt | 73.9 | 42.8 | 11.6 | 0.5 | 0.5 | 0.3 | 18.2 |
| Handle | Pre-snowmelt | 232.0 | - | - | - | - | - | - |
| | Post-snowmelt | 208.0 | 203.0 | 0.4 | < DL | < DL | 0.2 | 4.4 |
| Jackfish | Pre-snowmelt | 69.3 | 58.5 | 0.4 | 0.5 | 0.1 | 0.4 | 9.4 |
| | Post-snowmelt | 46.4 | 39.1 | 1.3 | 0.3 | 0.1 | 0.4 | 5.2 |
| Sammy's | Pre-snowmelt | 5.5 | 2.4 | 0.3 | < DL | < DL | 0.2 | 2.6 |
| | Post-snowmelt | 12.3 | 3.0 | 3.3 | 0.1 | 0.6 | 1.1 | 4.2 |
| **2023** | | | | | | | | |
| Frame | Pre-snowmelt | 237.0 | 1.6 | 5.0 | < DL | < DL | < DL | 230.4 |
| | Post-snowmelt | 101.0 | < DL | 16.8 | < DL | < DL | < DL | 84.2 |
| Handle | Pre-snowmelt | 229.0 | 201.5 | 1.4 | < DL | < DL | 0.2 | 25.9 |
| | Post-snowmelt | 208.0 | 203.0 | 0.4 | < DL | < DL | 0.2 | 4.4 |
| Jackfish | Pre-snowmelt | 57.9 | 52.5 | 0.3 | 1.0 | 0.1 | 0.5 | 3.5 |
| | Post-snowmelt | 51.5 | 48.4 | 0.7 | < DL | 0.1 | 0.4 | 1.9 |
| Sammy's | Pre-snowmelt | 3.5 | 2.0 | 0.8 | < DL | < DL | 0.2 | 0.5 |
| | Post-snowmelt | 5.2 | 3.0 | 1.0 | 0.1 | < DL | 0.3 | 0.8 |

### 3.4.2 Plankton Communities

#### *3.4.2.1 Zooplankton*

Across both years, 16 unique zooplankton species were observed, but all lakes and time periods were dominated (83-97%) by immature copepodites and nauplii (Figure 3.3a). *Diacyclops* taxa made up the highest proportion of adult zooplankton, while Cladocera and

calanoid copepod species made up a very small proportion (<2%) of the community (Figure 3.3a). The 2023 pre-snowmelt period had the highest proportion of adult zooplankton (17%) compared to other time periods. This was largely driven by the presence of the copepod species *Diacyclops bicuspidatus odessanus*, which made up 34% of the relative abundance of zooplankton in the community from Frame Lake. A SIMPER analysis identified that 86.2% of the dissimilarity in zooplankton communities between the pre- and post-snowmelt periods could be attributed to nauplii (44.4%) and immature copepodites (41.8%). A higher proportion of immature copepodites (61% and 58%) relative to nauplii individuals (22% and 36%) was documented in 2023 compared to 2022. However, there were no statistically significant differences in community structures between the pre- and post-snowmelt periods, and between 2022 and 2023, based on PERMANOVA. The absolute density of zooplankton across all lakes ranged from a minimum of 0.5 individuals $L^{-1}$ to a maximum of 171 individuals $L^{-1}$ and no notable changes occurred between the pre-snowmelt and post-snowmelt periods (Figure 3.4). Depth ($p = 0.001$) and rotifer density ($p = 0.009$) were selected by the RDA as being the most influential drivers of zooplankton assemblages across all sampling events (Figure 3.3b)., explaining 72% of the variation (adjusted $R^2$ of 0.67) (Table S 3-11).

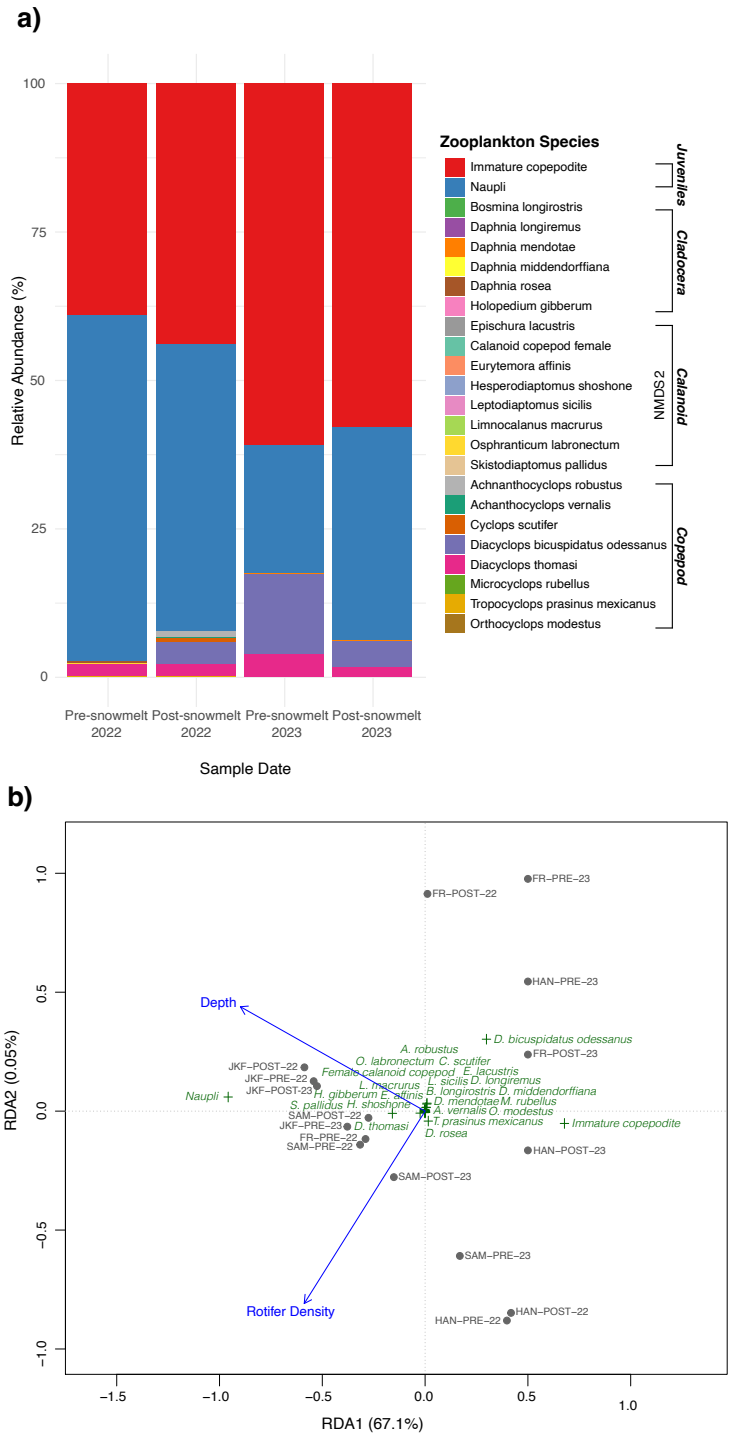


**Figure 3.3.** a) Combined relative abundance plot of zooplankton (including nauplii and immature copepodites) encountered across all lakes and sampling events; b) RDA ordination plot with explanatory environmental variables highlighted by forward selection for zooplankton community composition across all lakes and sampling events.

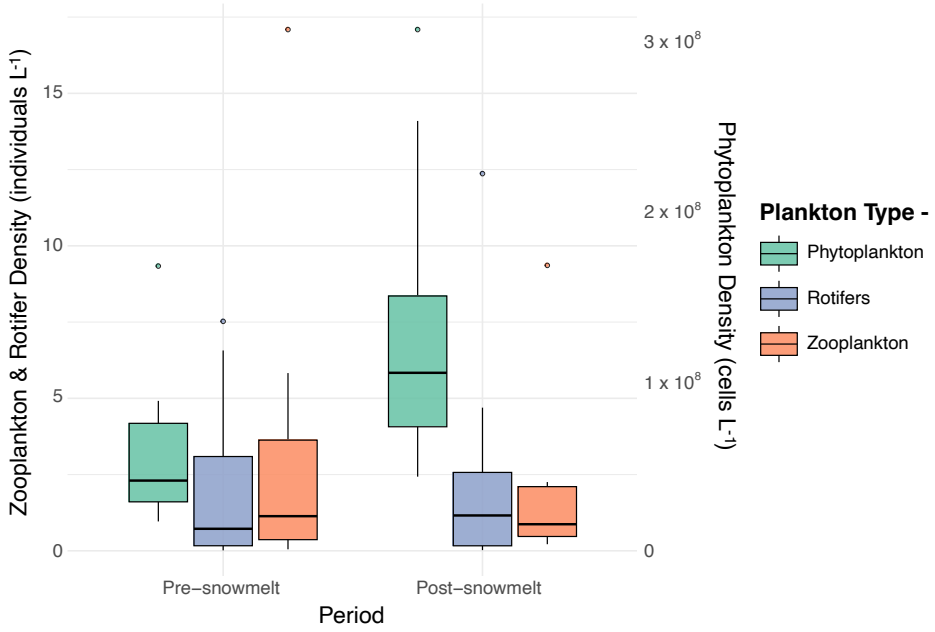


**Figure 3.4.** Mean plankton density during the pre-snowmelt and post-snowmelt periods across both study years and all four study lakes. More information related to plankton densities in each study lake from each sampling period can be found in Table S 3-12.

*3.4.2.2 Rotifers*

Seventeen unique species of rotifers were recorded across the four study lakes (Figure 3.5a). *Kellicotia longispina, Keratella hiemalis,* and *Keratella species complex* (a group consisting of small *Keratella* species, such as *Keratella crassa*, *Keratella earline*, and *Keratella cochlearis*) were the most dominant rotifer species across all time periods (Figure 3.5a). *Keratella quadrata* and *Polyartha remata* were also prevalent, and *P. remata* increased between the pre- and post-snowmelt periods in both years (Figure 3.5a). A SIMPER analysis identified that 76.1% of the dissimilarity between the pre- and post-snowmelt rotifer communities was due to the species *K. longispina* (37.0%), *K. hiemalis* (23.3%), and *K. species complex* (15.8%). The *K. species complex* decreased between the pre- and post-snowmelt periods in both years, but there were no consistent directional changes in *K. longispina* or *K. hiemalis* (Figure 3.5a). As

with the zooplankton assemblage, differences in rotifer assemblages across snowmelt period and study years were not statistically significant (Bray-Curtis dissimilarity matrix via PERMANOVA). Rotifer density did not change between the pre- and post-snowmelt periods (Figure 3.4). Depth ($p = 0.001$) was the only environmental variable selected by the RDA (Figure 3.5b), explaining only 30.2% of the variation (adjusted $R^2$ of 0.25) (Table S 3-11).

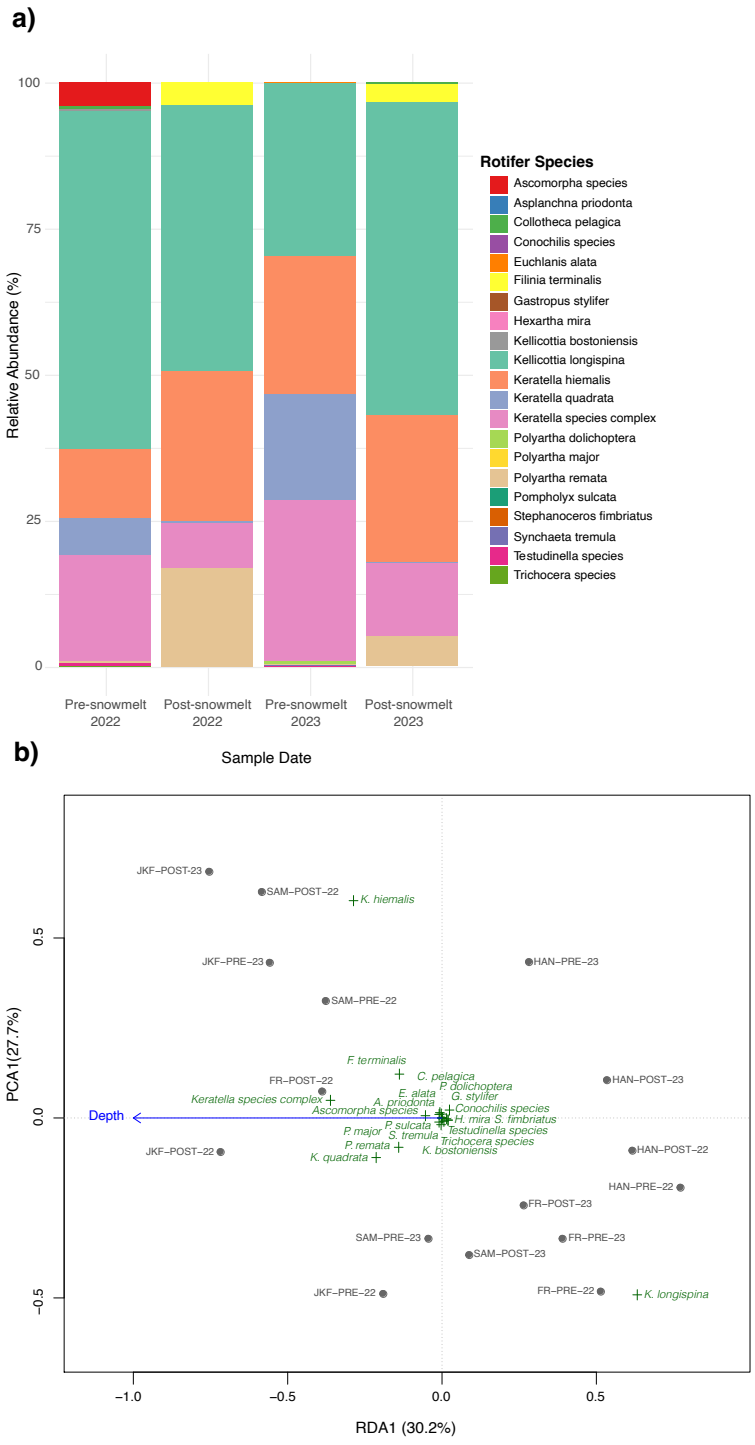


**Figure 3.5.** a) Combined relative abundance plot of rotifers across all lakes and sampling events; and b) RDA ordination plot with explanatory environmental variables highlighted by forward selection for rotifer community composition across all lakes and sampling events.

*3.4.2.3 Phytoplankton*

After the 1% threshold was applied, 36 distinct phytoplankton genera were observed, including 15 *Cyanobacteria* genera, 13 *Chlorophyta* genera, and 2 genera belonging to *Chrysophyta* (Figure 3.6a). Cyanobacteria dominated the phytoplankton community assemblage across all time periods (93-94% in 2022, and 86-87% in 2023). *Planktothrix/Oscillatoria* was the dominant genera in Jackfish Lake across all sampling periods, ranging in relative abundances from 86-99%. The cryptophyte genera *Uroglena/Uroglenopsis* was notably more abundant in 2023 compared to 2022, as well as *Aphanocapsa* (Figure 3.6a), while Cyanobacteria overall were lower in 2023 compared to 2022 (decreasing from 93-94% to 86-87%). *Aphanocapsa* also tended to increase between the pre- and post-snowmelt periods in both years (Figure 3.6a), although SIMPER analysis determined that 70.3% of community dissimilarity between pre- and post-snowmelt periods was due to *Planktothrix/Oscillatoria* (32.0%), *Microcystis* (11.1%), *Dolichospermum/Anabaena* (9.2%), *Gloeocapsa* (9.1%), and *Aphanocapsa* (8.9%). There was no significant difference in overall phytoplankton assemblages between the pre- and post-snowmelt periods, or between years, as analyzed by PERMANOVA, but phytoplankton cell densities did increase between the pre- and post-snowmelt sampling periods (Figure 3.4). As(III) ($p = 0.02$), PAR ($p = 0.001$), and rotifer density ($p = 0.09$) were selected by the RDA as being the most influential drivers of phytoplankton assemblages across all sampling events (Figure 3.6b), explaining 66.2% of the variation (adjusted $R^2$ of 0.58) (Table S 3-11). Clustering by lakes in ordination space is visible on the RDA biplot, particularly for Jackfish Lake and Frame Lake (Figure 3.6b), which was not as apparent for rotifers and zooplankton.

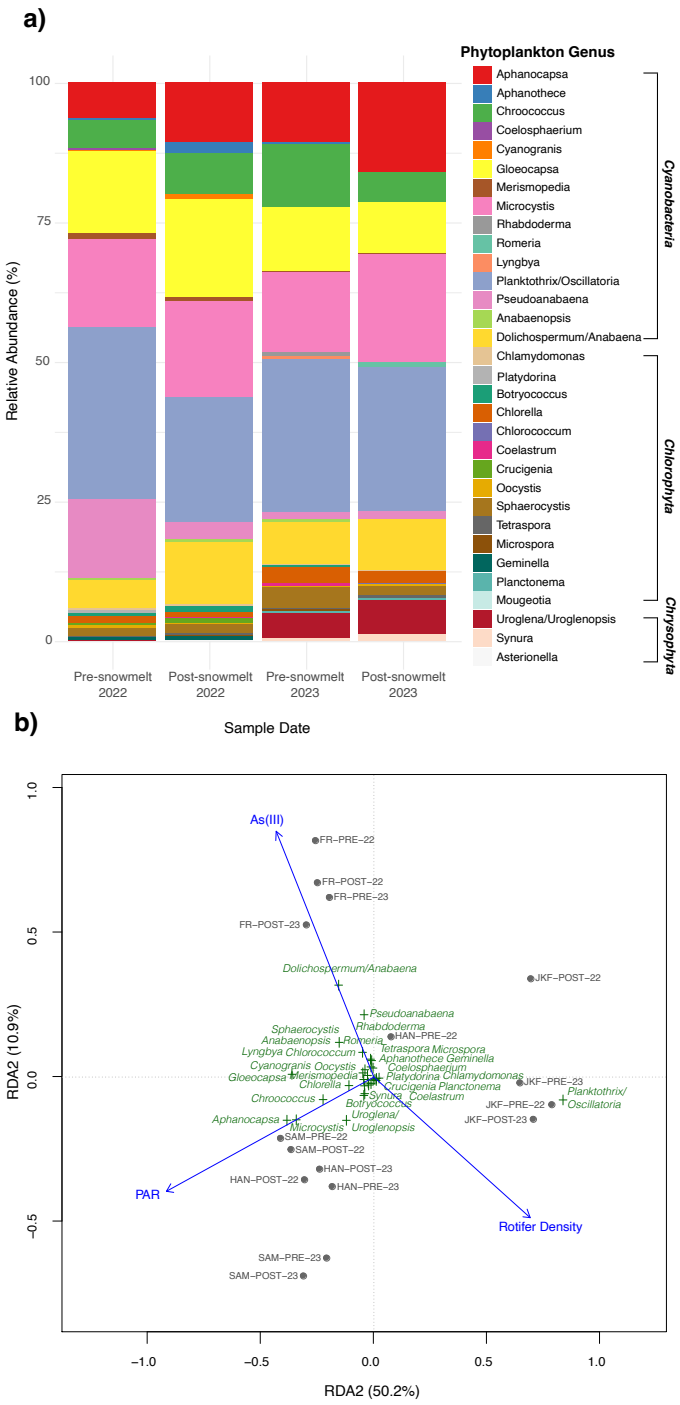


**Figure 3.6.** a) Combined relative abundance plot for phytoplankton genera, and b) RDA ordination plot with explanatory environmental variables highlighted by forward selection for phytoplankton community composition across all four lakes and study period.

## 3.5 Discussion

The aim of this study was to investigate the spring thaw transition as a potentially significant period of change in lake physicochemical and biological characteristics, and to consider its implications for the cycling and ecotoxicity of arsenic pollution in subarctic lakes. We examined arsenic concentrations and chemical speciation in combination with plankton communities (phytoplankton, rotifers, and zooplankton) in 2022 and 2023 at the late winter to spring thaw transition period (two sampling events separated by 7-10 days that capture the onset of thaw). Sampling was conducted in four Yellowknife-area lakes spanning a gradient of arsenic contamination. Decreases in surface water conductivity occurred between the two rounds of data collection, with the exception of Jackfish Lake and Sammy's Lake in 2023, where thaw appeared to have already begun during our "pre-snowmelt" sampling period (Figure 3.2; Table S 3-9). The onset (or continuation) of spring thaw corresponded to decreases in lake ice thickness and increases in PAR and surface water temperatures (Table S 3-9). We also documented an increase in phytoplankton density between our pre-snowmelt and post-snowmelt (i.e., onset of spring thaw) sampling points, in both years, adding further evidence to the prevalence and importance of spring blooms initiating under the ice in late winter (Figure 3.4) (Sommer et al. 2012; Twiss et al. 2012; Cavaliere & Baulch 2020).

### 3.5.1 Influence of spring thaw on arsenic biogeochemistry

Our results suggest that the impacts of meltwater influx on lakewater arsenic concentrations depends on antecedent concentrations, where lakes with high under-ice arsenic concentrations experience a dilution of arsenic with meltwater influx, while lakes with low arsenic experience arsenic enrichment from meltwater. The two lakes with the highest under-ice

dissolved arsenic concentrations (Handle Lake and Frame Lake) experienced an influx of meltwater which corresponded to decreases in dissolved arsenic concentrations in both 2022 and 2023 (Table 3.1). This dilution effect is typical of spring thaw, and has resulted in the dilution of other chemical and physical parameters (Bergmann & Welch, 1985; Welch & Bergmann, 1985). In contrast, dissolved arsenic concentrations increased with the onset of thaw in both sampling years in the least contaminated lake (Sammy's Lake). This was likely due to landscape runoff meltwater inputs which were enriched in arsenic compared to its surface waters (Table S 3-6). Snowmelt run-off from soils impacted by legacy arsenic emissions in the Yellowknife region has been documented to have exceptionally high concentrations of arsenic, in excess of 200 $\mu g\ L^{-1}$ in more heavily impacted catchments (Palmer et al., 2024). The contribution of arsenic from snowmelt runoff is the result of interactions with contaminated soils rather than contributions from the snowpack directly, since atmospheric emissions ended more than 20 years ago (Palmer et al. 2024).

Frame Lake and Handle Lake also experienced under-ice anoxia, and the influx of meltwater also introduced oxygen into these systems (Figure 3.2; Table S 3-9). As winter progresses, DO is consumed through sediment and water column oxygen demand, but is not replenished, as primary productivity is reduced and the ice cover prevents gas exchange with the atmosphere. Arsenic therefore builds up under the ice over the winter via cryoconcentration and sediment efflux (Palmer et al., 2019). The introduction of DO into Frame Lake and Handle Lake that occurred with meltwater influx predictably resulted in a decrease in As(III) and an increase in As(V), while overall dissolved arsenic concentrations decreased (Figure 3.2; Table 3.1). As(V) is more thermodynamically favourable under aerobic conditions and elevated temperatures, and the oxidation of As(III) into As(V) occurs quite rapidly under these conditions (Cullen & Reimer,

1989; Rodie et al., 1995). Arsenate (As(V)) is also more particle reactive than As(III), and it can be quickly removed from the water column by sorbing onto settling particles and depositing onto surface sediments, thus potentially contributing (along with meltwater dilution) to an overall decrease in total arsenic concentrations (De Vitre et al., 1991; Dixit & Hering, 2003). Oxygen wasn't depleted over the winter in Jackfish Lake or Sammy's Lake, and the influx of meltwater did not appreciably alter the redox conditions (Figure 3.2).

Arsenite (As(III)) can also be transformed into As(V) by microbial oxidation and photo-oxidation (Huang, 2014; Amyot et al., 2021). Using PAR as a proxy for ultra-violet (UV) radiation, the increases in PAR (and therefore potentially UV radiation) that we observed in the study lakes, which coincided with decreases in ice thickness, could also be contributing to the shift from As(III) to As(V) (Figure 3.2; Figure S 3-2) Sammy's Lake provides some support for the influence of PAR on arsenic speciation, as a slight increase in As(III) and decrease in As(V) was observed between the pre- and post-snowmelt sampling periods in 2022, which corresponded to a decrease in PAR but no change in DO. In 2023, when PAR increased, there were no notable changes in As(III) relative to As(V). In Jackfish Lake, most of the arsenic was present as As(V), with very little As(III), and no appreciable changes in arsenic speciation were observed.

Organic arsenic was detected under the ice during at least one sampling event for each lake, indicating sufficient levels of biological activity to mediate the transformation of inorganic arsenic into organic forms (Table 3.1). Arsenobetaine (AsB) was the form of organic arsenic detected most consistently. Arsenobetaine (AsB) is formed from the transformation and degradation of arsenic by higher trophic organisms, such as rotifers and zooplankton (Caumette

et al., 2011). The increase in phytoplankton density at the onset of thaw corresponded to an increase in organic arsenic in 2022 (except in Jackfish), but not in 2023.

### 3.5.2 Changes in plankton communities at spring thaw

There were no significant changes in zooplankton and rotifer density or species assemblage between the pre- and post-snowmelt sampling periods, and no chemical variables were selected by redundancy analysis as explaining a significant proportion of variation in species assemblage (Figure 3.3; Figure 3.5). Adult zooplankton made up a very small proportion of the under-ice zooplankton community, which was overwhelmingly dominated by juveniles (Figure 3.3a). Juvenile life stages of rotifers and zooplankton are more sensitive to contaminant exposure than adult forms, due to their less developed detoxification systems, higher metabolic rates, and limited energy reserves (Snell & Janssen, 1995; Connon et al., 2012). The implications of sensitive juvenile zooplankton life stages being exposed to high arsenic concentrations under the ice, and the potential carry-forward effects on open-water zooplankton communities, is beyond the scope of this study but would be an interesting avenue of future research.

Phytoplankton density increased under the ice at spring thaw in our study lakes, and *Aphanocapsa* tended to increase between the pre- and post-snowmelt periods in both years, but no significant differences in phytoplankton assemblages were detected based on PERMANOVA (Figure 3.4; Figure 3.6a). Redundancy analysis selected As(III) as a significant driver of variation in phytoplankton assemblages, with *Dolichospermum/Anabaena* associated with higher As(III) in the RDA biplot (Figure 3.6b). The association with As(III) was somewhat surprising, as As(V) is generally considered more toxic to phytoplankton due to it being an analogue of phosphate, which results in As(V) being readily uptaken through $PO_4^{3-}$-transporters (Caumette et

al., 2011; Rahman et al., 2014; Barrett et al., 2018). However, different sampling points (2022 and 2023, pre- and post-snowmelt) from individual lakes tended to cluster together in ordination space, and As(III) was associated with phytoplankton assemblages from Frame Lake (Figure 3.6b). Therefore, As(III) being identified as a significant driver may be an artifact of it being more prevalent in Frame Lake, while an as yet unidentified lake-specific factor may be the underlying driver of variation in phytoplankton. We note, however, that under-ice phytoplankton communities in our lakes were dominated by Cyanobacteria, which have been found to exhibit higher resistance to arsenic As(V) toxicity than other phytoplankton groups due to their *ars* (arsenic resistance) operon (Figure 3.6a) (Miyashita et al., 2012; 2016). A 2013 study found that *Microcystis aeruginosa* was specifically tolerant of arsenic exposure and was able to bio-transform inorganic arsenic into various organic forms (Wang et al., 2013). Future study is needed to understand the potential role that arsenic plays as a driver of phytoplankton in Yellowknife lakes, including additional seasons and control lakes unimpacted by legacy arsenic pollution. Similar to the discussion above on juvenile zooplankton, additional research would also be required to understand the implications of the under-ice spring bloom occurring while arsenic is (presumably) still concentrated in lake water under the ice, and present as As(V).

### 3.5.3 Comparison of a warmer and a colder winter

The winter of 2022 was significantly colder than 2023, and ice was thicker at the end of the winter season (Figure S 3-1; Table S 3-2). Yellowknife has been warming at 4x the global average (Rantanen et al., 2022), and warmer winters and shorter durations of lake ice-cover are projected in response to future climate warming (Basu et al., 2024). Thus, a comparison of our two years of data allows us to speculate on the potential implications of warming winters on

under-ice arsenic cycling and plankton ecology. We did not observe any notable differences in arsenic concentrations and speciation between 2022 and 2023 that would suggest a warmer winter had an influence on arsenic conditions at the end of the winter season (Table 3.1). However, we did observe some subtle differences in some plankton taxa between the two years, although overall plankton assemblages were not significantly different between years. In 2023 (the warmer of the two winters), the phytoplankton community had a greater proportion of chrysophytes, particularly *Uroglena/Urglenopsis,* while the rotifer community had slightly higher abundances of taxa known to be competitive under warming temperatures (*Keratella, Polyartha,* and *Filinia*) (Figure 3.5; Figure 3.6) (Devkota et al., 2025), and the zooplankton community contained a larger proportion of later-stage juveniles (immature copepodites versus nauplii) (Figure 3.3a).

## 3.6 Conclusions

Lakes with higher under-ice dissolved arsenic concentrations experienced a dilution of arsenic in the surface waters corresponding to the influx of meltwater runoff, while meltwater was likely a source of arsenic enrichment to Sammy's Lake, which had substantially lower under-ice arsenic concentrations. For the two lakes that became anoxic in late winter, the influx of meltwater also introduced DO into the surface waters, likely resulting in the conversion of As(III) into As(V). Organic arsenic increased at spring thaw in 2022, as would be predicted from an increase in biological activity, but not in 2023. Phytoplankton density increased with the onset of thaw, but no significant changes were observed for zooplankton and rotifer density, or assemblage composition of any of the three plankton groups, although *Aphanocapsa* tended to increase between the pre- and post-snowmelt periods in both years. Redundancy analysis

selected As(III) as a significant driver of variation in phytoplankton assemblages, but no chemical variables were selected for rotifers or zooplankton.

In this study, we focused on a short (7-10 day) but dynamic transitional period when lakes are beginning to thaw but are still ice-covered. Through the exploration of this period of rapid change in lake redox conditions, light penetration, and primary productivity (among other limnological factors), we can gain new insights into the controls on, and potential interactions between, arsenic cycling and plankton community dynamics. We recommend future research expand on the ideas introduced in this study to explore the interactions between plankton ecology and arsenic biogeochemical cycling across seasons, including both the open-water and ice-covered season. Notable questions of interest include the extent to which sensitive life or population stages (e.g., juvenile zooplankton; spring phytoplankton bloom) overlap with periods of enhanced exposure to arsenic.

## 3.7 Supplementary Information

**Table S 3-1.** Location and physical characteristics of the four study lakes.

| Lake | Sampling Location Coordinates | Surface Area ($km^2$) | Max Depth (m) | Distance to Giant Mine Roaster (km) |
|---|---|---|---|---|
| Handle | 62.4916, -114.3959 | 0.2 | 3.8 | 2.5 |
| Frame | 62.4574, -114.3879 | 0.9 | 6.4 | 6.1 |
| Jackfish | 62.4659, -114.3924 | 0.5 | 8.2 | 4.0 |
| Sammy's | 62.4688, -114.5098 | 0.3 | 6.7 | 8.4 |

**Table S 3-2.** Environmental and meteorological data from our spring thaw sampling dates at our four study lakes. Air temperature data was recorded during sampling from the Environment Canada mobile application.

| Lake | Year | Sample Period | Sampling Date | Snow Thickness (cm) | Ice Thickness (cm) | Air Temperature (°C) |
|---|---|---|---|---|---|---|
| Handle | 2022 | Pre-snowmelt | April 25 | - | 80 | - |
| | | Post-snowmelt | May 4 | - | 75 | -2 |
| | 2023 | Pre-snowmelt | April 22 | 0.5 | 72 | +4 |
| | | Post-snowmelt | April 29 | 0.0-0.5 | 55 | +7 |
| Frame | 2022 | Pre-snowmelt | April 28 | - | 130 | -2 |
| | | Post-snowmelt | May 10 | - | 75 | -1 |
| | 2023 | Pre-snowmelt | April 24 | 0.5-1.0 | 65 | +3 |
| | | Post-snowmelt | May 1 | 0.0-0.5 | 50 | +9 |
| Jackfish | 2022 | Pre-snowmelt | April 26 | - | 80 | - |
| | | Post-snowmelt | May 5 | - | 75 | +7 |
| | 2023 | Pre-snowmelt | April 21 | 2 | 65 | +2 |
| | | Post-snowmelt | April 28 | 0.0-0.5 | 62 | +7 |
| Sammy's | 2022 | Pre-snowmelt | April 29 | - | 76 | -4 |
| | | Post-snowmelt | May 10 | - | 57 | -4 |
| | 2023 | Pre-snowmelt | April 23 | 0.5-1.0 | 72 | +4 |
| | | Post-snowmelt | April 30 | 0.0-0.5 | 55 | +7 |

**Table S 3-3.** Collection size and depth of each sample type taken from our four study lakes. Plankton sampled collected for IDing purposes were integrated from the entire water column, starting from 1 m above the lake bed.

| Lake | Sample Type | Sample Size | Sampled Depths (m) |
|---|---|---|---|
| Handle | Bulk Water – Filtered | 1 L | 1, 2, 2.5 |
| | Bulk Water – Unfiltered | 1 L | |
| | Total Metals | 14 mL | |
| | Dissolved Metals | 14 mL | |
| | Arsenic Speciation | 14 mL | |
| | Phytoplankton ID | 100 mL | All – 1 m above lake bed |
| | Zooplankton ID | 50 mL | |
| Frame | Bulk Water – Filtered | 1 L | 1, 3, 4, 5 |
| | Bulk Water – Unfiltered | 1 L | |
| | Total Metals | 14 mL | |
| | Dissolved Metals | 14 mL | |
| | Arsenic Speciation | 14 mL | |
| | Phytoplankton ID | 100 mL | All – 1 m above lake bed |
| | Zooplankton ID | 50 mL | |
| Jackfish | Bulk Water – Filtered | 1 L | 1, 3, 5, 6, 7 |
| | Bulk Water – Unfiltered | 1 L | |
| | Total Metals | 14 mL | |
| | Dissolved Metals | 14 mL | |
| | Arsenic Speciation | 14 mL | |
| | Phytoplankton ID | 100 mL | |
| | Zooplankton ID | 50 mL | |
| Sammy's | Bulk Water – Filtered | 1 L | 1, 3, 4, 5, 6 |
| | Bulk Water – Unfiltered | 1 L | |
| | Total Metals | 14 mL | |
| | Dissolved Metals | 14 mL | |
| | Arsenic Speciation | 14 mL | |
| | Phytoplankton ID | 100 mL | All – 1 m above lake bed |
| | Zooplankton ID | 50 mL | |

**Table S 3-4.** Field blank (FB) data from the four study lakes collected from 2022-2024 (N = 19). Measurements of DAs below the method detection limit of 0.2 μg $L^{-1}$ are indicated by < MDL.

| Sample Date | Sample ID | Total As (μg $L^{-1}$) |
|---|---|---|
| November 23, 2022 | FB1 | < MDL |
| | FB2 | < MDL |
| | Reagent Blank 1 | < MDL |
| February 9, 2023 | FB1 | < MDL |
| | FB2 | < MDL |
| February 21, 2023 | FB1 | < MDL |
| | FB4 | < MDL |
| April 6, 2023 | FB1 | < MDL |
| | FB2 | < MDL |
| April 21, 2023 | FB1 | < MDL |
| | FB2 | < MDL |
| July 14, 2023 | FB1 | < MDL |
| | FB2 | < MDL |
| November 18, 2023 | FB1 | < MDL |
| | FB2 | < MDL |
| January 23, 2024 | FB1 | < MDL |
| | FB2 | < MDL |
| February 2, 2024 | FB1 | < MDL |
| | FB2 | < MDL |

**Table S 3-5.** Field replicate data from Handle and Jackfish Lakes collected in November 2020 and January 2021 using the same sampling methods as described in the paper (N = 4).

| Lake | Sample Date | Depth (m) | Dissolved As (μg $L^{-1}$) | Relative Percent Difference (%) |
|---|---|---|---|---|
| Handle | November 16, 2020 | 1 | 203 | 0.49 |
| | | 1A | 204 | |
| Jackfish | January 1, 2021 | 4 | 70 | 0.57 |
| | | 4A | 70.4 | |

**Table S 3-6.** Total dissolved arsenic (As) concentrations in terrestrial snowmelt water samples collected from runoff sites directly next to three of the study lakes. Meltwater samples were collected during the post-snowmelt 2023 season. Surface lake water total dissolved arsenic concentrations collected during the pre-snowmelt 2023 period included for easier comparison.

| Lake | Sample # | Terrestrial snowmelt water As (µg $L^{-1}$) | Lake water surface As (µg $L^{-1}$) |
|---|---|---|---|
| Handle | 1 | 143.0 | 229.0 |
| | 2 | 155.0 | |
| | 3 | 154.0 | |
| Jackfish | 1 | 80.1 | 57.9 |
| | 2 | 79.2 | |
| Sammy's | 1 | 45.3 | 3.5 |
| | 2 | 44.8 | |
| | 3 | 45.4 | |

**Table S 3-7.** Optimization parameters for separation and determination of arsenic species using HPLC-ICP-MS. Samples were separated by HPLC-ICP-MS/MS (Agilent) and quantified using Agilent software (MassHunter 4.6).

| **ICP-MS-MS ( Agilent 8900 ICP-QQQ )** | |
|---|---|
| RF power | 1500 w |
| Plasma gas flow | 15 L/min |
| Nebulizer (carrier) gas flow | 1.01 L/min |
| Sampling depth | 8 mm |
| Peristaltic pump speed | 0.4 rps |
| Spray chamber temp | 2°C |
| Collision cell | He @ 5.0 mL/min (dependent on instrument sensitivity) |
| Data acquisition mode | Time-resolved, m/z 75 for 75As+, and m/z 77 for 40Ar37Cl+ |
| **HPLC Conditions - Agilent 1260** | |
| Column | PRP-X100 Anion Exchange HPLC Column, 4.1 x 250 mm, 10 µm |
| Mobile phase composition | 20 mM (NH4)2HPO4,5mM (NH4H2PO4 ). pH 8.25,2% MeOH |
| Mobile phase flow rate | 1 mL/min |
| Injection volume | 50 µL |
| Acquisition time | 12 min |

**QA/QC Protocols:** Sequence accuracy was verified by inserting continuous calibration verification (OPR2) standards approximately every 10 samples. To ensure the quality of these measurements, a second source of PTC from Proficiency Testing Canada was used for As(V) quantification. Analyses with dosed additions were used in order to fortify samples to control the percentage recovery of all species as an analytical quality variables. Samples were measured in duplicate to verify the accuracy and reliability of analytical results.

**Table S 3-8.** Environmental variables analyzed via t-tests and Wilcoxon tests and their associated p-values and power test results (where applicable).

| Time Period Tested | Environmental Variable | Test Used | p-value | Significant (Y/N) | Power Test Result |
|---|---|---|---|---|---|
| **2022 vs. 2023** | Ice-On Mean Temperature | t-test | $1.30 \times 10^{-8}$ | Y | 76% |
| | Specific Conductivity | t-test | 0.035 | Y | 6% |
| | DO | t-test | 0.48 | N | |
| | Temperature | t-test | 0.24 | N | |
| | PAR | t-test | 0.52 | N | |
| | Ice Thickness | Wilcoxon | 0.0037 | Y | |
| | Total Dissolved Arsenic | t-test | 0.33 | N | |
| | As(III) | t-test | 0.19 | N | |
| | As(V) | t-test | 0.52 | N | |
| | Organic Arsenic | t-test | 0.30 | N | |
| | Phytoplankton density | t-test | 0.13 | N | |
| **Pre- vs Post-snowmelt** | Specific Conductivity | Wilcoxon | 0.33 | N | |
| | DO | t-test | 0.25 | N | |
| | Temperature | t-test | 0.049 | Y | 54% |
| | PAR | t-test | 0.18 | N | |
| | Ice Thickness | t-test | 0.047 | Y | 36% |
| | Total Dissolved Arsenic | t-test | 0.12 | N | |
| | As(III) | t-test | 0.95 | N | |
| | As(V) | t-test | 0.58 | N | |
| | Organic Arsenic | t-test | 0.62 | N | |
| | Phytoplankton density | t-test | 0.083 | N | |
| **Pre- vs Post snowmelt 2022** | Specific Conductivity | t-test | 0.22 | N | |
| | DO | Wilcoxon | 0.89 | N | |
| | Temperature | t-test | 0.092 | N | |
| | PAR | t-test | 0.48 | N | |
| | Ice Thickness | t-test | 0.22 | N | |
| | Total Dissolved Arsenic | Wilcoxon | 0.69 | N | |
| | As(III) | t-test | 0.77 | N | |
| | As(V) | Wilcoxon | 0.63 | N | |
| | Organic Arsenic | t-test | 0.22 | N | |
| | Phytoplankton density | t-test | 0.31 | N | |
| **Pre- vs Post snowmelt 2023** | Specific Conductivity | t-test | 0.20 | N | |
| | DO | t-test | 0.42 | N | |
| | Temperature | t-test | 0.093 | N | |
| | PAR | t-test | 0.22 | N | |
| | Ice Thickness | t-test | 0.069 | N | |
| | Total Dissolved Arsenic | t-test | 0.84 | N | |
| | As(III) | t-test | 0.71 | N | |
| | As(V) | Wilcoxon | 0.89 | N | |
| | Organic Arsenic | t-test | 0.29 | N | |
| | Phytoplankton density | t-test | 0.22 | N | |
| **Pre- 2022 vs. Pre-snowmelt 2023** | Specific Conductivity | t-test | 0.095 | N | |
| | DO | t-test | 0.75 | N | |
| | Temperature | t-test | 0.43 | N | |
| | PAR | Wilcoxon | 0.69 | N | |
| | Ice Thickness | Wilcoxon | 0.029 | Y | |
| | Total Dissolved Arsenic | Wilcoxon | 0.69 | N | |
| | As(III) | t-test | 0.16 | N | |
| | As(V) | t-test | 0.42 | N | |

| | | | | | |
|---|---|---|---|---|---|
| | Organic Arsenic | t-test | 0.41 | N | |
| | Phytoplankton density | t-test | 0.60 | N | |
| **Post- 2022 vs. Post-snowmelt 2023** | Specific Conductivity | t-test | 0.30 | N | 99% |
| | DO | t-test | 0.59 | N | |
| | Temperature | t-test | 0.36 | N | |
| | PAR | t-test | 0.78 | N | |
| | Ice Thickness | t-test | 0.036 | Y | |
| | Total Dissolved Arsenic | t-test | 0.87 | N | |
| | As(III) | t-test | 0.33 | N | |
| | As(V) | t-test | 0.42 | N | |
| | Organic Arsenic | t-test | 0.14 | N | |
| | Phytoplankton density | t-test | 0.090 | N | |

**Table S 3-9.** Surface water layer (top 1 m) physical and chemical parameters of the four study lakes during the pre- and post-snowmelt periods and across both study years (2022, 2023). Method detection limit (DL) of 10 µg $L^{-1}$ for dissolved phosphorus.

| Lake | Period | PAR (µmol $s^{-1}$) | Temperature (°C) | Dissolved Oxygen (mg $L^{-1}$) | Specific Conductivity (mS $cm^{-1}$) | Dissolved Phosphorus (µg $L^{-1}$) | Chlorophyll-a (µg $L^{-1}$) | ORP (mV) |
|---|---|---|---|---|---|---|---|---|
| **2022** | | | | | | | | |
| Frame | Pre-snowmelt | 10.8 | 2.8 | 1.1 | 920 | < DL | 0.4 | -241 |
| | Post-snowmelt | 138.3 | 3.2 | 8.4 | 485 | < DL | 0 | +127.1 |
| Handle | Pre-snowmelt | 7.3 | 1.7 | 1.4 | 331 | < DL | 1.95 | +273.4 |
| | Post-snowmelt | 44.4 | 3.1 | 0.6 | 312 | < DL | 0.4 | +227.4 |
| Jackfish | Pre-snowmelt | 0.5 | 0.5 | 6.7 | 509 | 16 | 1.43 | +218.1 |
| | Post-snowmelt | 3.3 | 2 | 6.4 | 464 | 234 | 16 | +100 |
| Sammy's | Pre-snowmelt | 83.4 | 1.5 | 10.0 | 225 | < DL | 12.58 | +5.5 |
| | Post-snowmelt | 35.5 | 5.4 | 10.1 | 131 | < DL | 0.11 | +12.3 |
| **2023** | | | | | | | | |
| Frame | Pre-snowmelt | 7.1 | 2.8 | 0.0 | 827 | < DL | 1.2 | -191.2 |
| | Post-snowmelt | 8.1 | 3.9 | 3.5 | 478 | < DL | 0.6 | -134.7 |
| Handle | Pre-snowmelt | 90.8 | 0.9 | 2.2 | 325 | < DL | 1.0 | +31.4 |
| | Post-snowmelt | 121.6 | 2.6 | 2.6 | 271 | < DL | 1.0 | +79.7 |
| Jackfish | Pre-snowmelt | 1.4 | 0.9 | 4.8 | 482 | 29 | 5.1 | +37.3 |
| | Post-snowmelt | 1.5 | 1.5 | 4.3 | 482 | 31 | 16.5 | +105.6 |
| Sammy's | Pre-snowmelt | 84.2 | 0.8 | 11.4 | 127 | < DL | 0.11 | +3.5 |
| | Post-snowmelt | 157.1 | 0.9 | 11.3 | 11 | < DL | 0.8 | +5.2 |

**Table S 3-10.** The oxidation reduction potential (ORP) and sulphide ($S^{2-}$) concentrations of Frame and Handle Lakes during the ice-on season from 2020-2022. Measurements of dissolved $S^{2-}$ exceeding the maximum DL (MDL) of 800 μg $L^{-1}$ are indicated by > MDL. N/A represents no measurements taken on the indicated sampling date. Data collected and provided via ARI. Oxidation reduction potential measurements were collected via YSI while $S^{2-}$ samples were collected using the peristaltic pump as described in the methods section of this study. Samples were analyzed by Taiga Laboratories (M. Palmer, ARI, unpublished data).

| Lake | Sample Date | Depth (m) | ORP (mV) | $S^{2-}$ (μg $L^{-1}$) |
|---|---|---|---|---|
| Handle | November 16, 2020 | 1 | 118.4 | 19 |
| | | 2 | 106.7 | 19 |
| | | 3 | 98.8 | 19 |
| | January 18, 2021 | 1 | 183 | 16 |
| | | 2 | 178 | 20 |
| | | 3 | 155 | 22 |
| | April 15, 2021 | 1 | 72.9 | 19 |
| | | 2 | 52 | 11 |
| | | 3 | -139 | 201 |
| Frame | January 20, 2021 | 1 | 33.4 | 308 |
| | | 2 | -302 | > MDL |
| | | 3 | -318 | > MDL |
| | | 4 | -315 | > MDL |
| | | 5 | -320 | N/A |
| | April 8, 2021 | 1 | -245.3 | N/A |
| | | 2 | -324.4 | N/A |
| | | 3 | -339.4 | 0.05 |
| | | 4 | -330.9 | 0.05 |
| | | 5 | -331.8 | 0.1 |
| | March 30, 2022 | 1 | -349 | > MDL |
| | | 2 | -352 | > MDL |
| | | 3 | -356 | > MDL |
| | | 4 | -366 | > MDL |
| | | 5 | -374 | > MDL |
| | December 14, 2022 | 1 | 174.4 | N/A |
| | | 2 | 57.5 | 237 |
| | | 3 | -28.6 | 18 |
| | | 4 | -127 | N/A |
| | | 5 | -69.6 | 21 |

**Table S 3-11.** The environmental variables selected by RDA with forward selection for each plankton type, the amount variance (%) explained by the selected variables, p-values, and $R^2$ values for each model. All samples collected between April 2022 and May 2023.

| | Selected Variables | % Variance Explained | p-values | Model $R^2$ | Model AIC (with variables) | Model AIC (null) |
|---|---|---|---|---|---|---|
| **Zooplankton** | | | | | | |
| | Depth;<br>Rotifer density | 71.2 | 0.001;<br>0.009 | 0.67 | -33.0 | -16.8 |
| **Rotifers** | | | | | | |
| | Depth | 30.2 | 0.002 | 0.25 | -19.1 | -15.3 |
| **Phytoplankton** | | | | | | |
| | As(III);<br>PAR;<br>Rotifer density | 66.2 | 0.02;<br>0.001;<br>0.09 | 0.58 | -24.8 | -13.4 |

**Table S 3-12.** Plankton density values for each of the four study lakes across all four sampling periods. Samples collected from April 2022 – May 2023. PR = pre-snowmelt, PO = post-snowmelt.

| | Zooplankton Density (individuals $L^{-1}$) | | | | Rotifers Density (individuals $L^{-1}$) | | | | Phytoplankton Density (x $10^7$ cells $L^{-1}$) | | | |
|---|---|---|---|---|---|---|---|---|---|---|---|---|
| **Lake** | **PR22** | **PO22** | **PR23** | **PO23** | **PR22** | **PO22** | **PR23** | **PO23** | **PR22** | **PO22** | **PR23** | **PO23** |
| **Handle** | 179.9 | 5.5 | 0.7 | 5.0 | 75.2 | 18.6 | 1.3 | 1.9 | 3.1 | 10.8 | 3.0 | 10.1 |
| **Frame** | 0.5 | 2.4 | 4.7 | 4.8 | 2.4 | 0.9 | 0.2 | 0.2 | 16.7 | 11.5 | 8.8 | 7.8 |
| **Jackfish** | 29.0 | 22.6 | 12.2 | 93.6 | 65.7 | 46.9 | 12.0 | 123.7 | 5.1 | 30.5 | 7.0 | 25.2 |
| **Sammy's** | 10.8 | 21.5 | 61.5 | 14.4 | 1.8 | 16.4 | 19.3 | 6.8 | 1.7 | 5.5 | 2.6 | 4.3 |

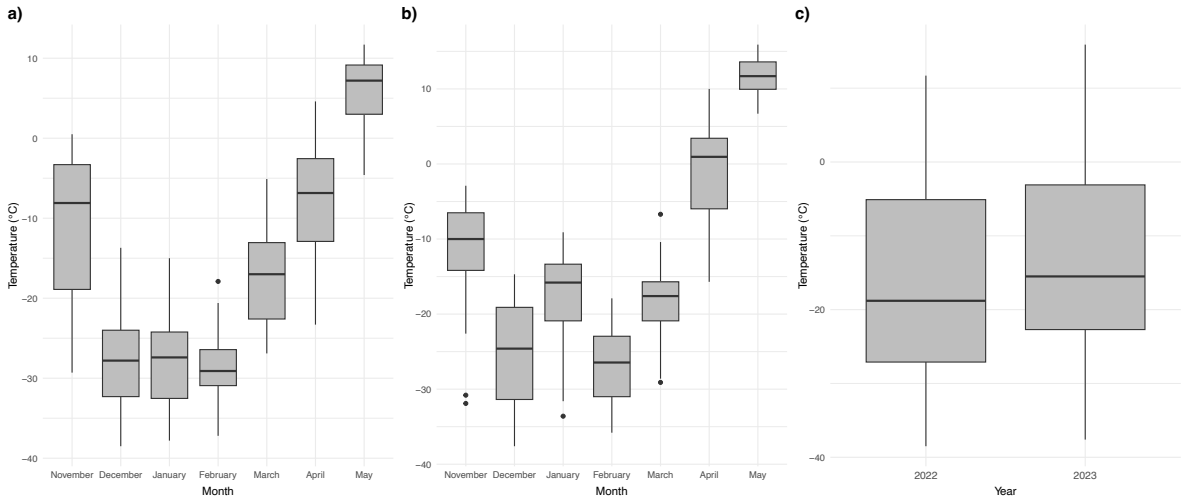


**Figure S 3-1.** Mean daily air temperatures of: a) 2022 ice-on months, b) 2023 ice-on months, and c) average 2022 versus 2023 ice-on periods. Air temperature data collected by and retrieved from ECCC (2025).

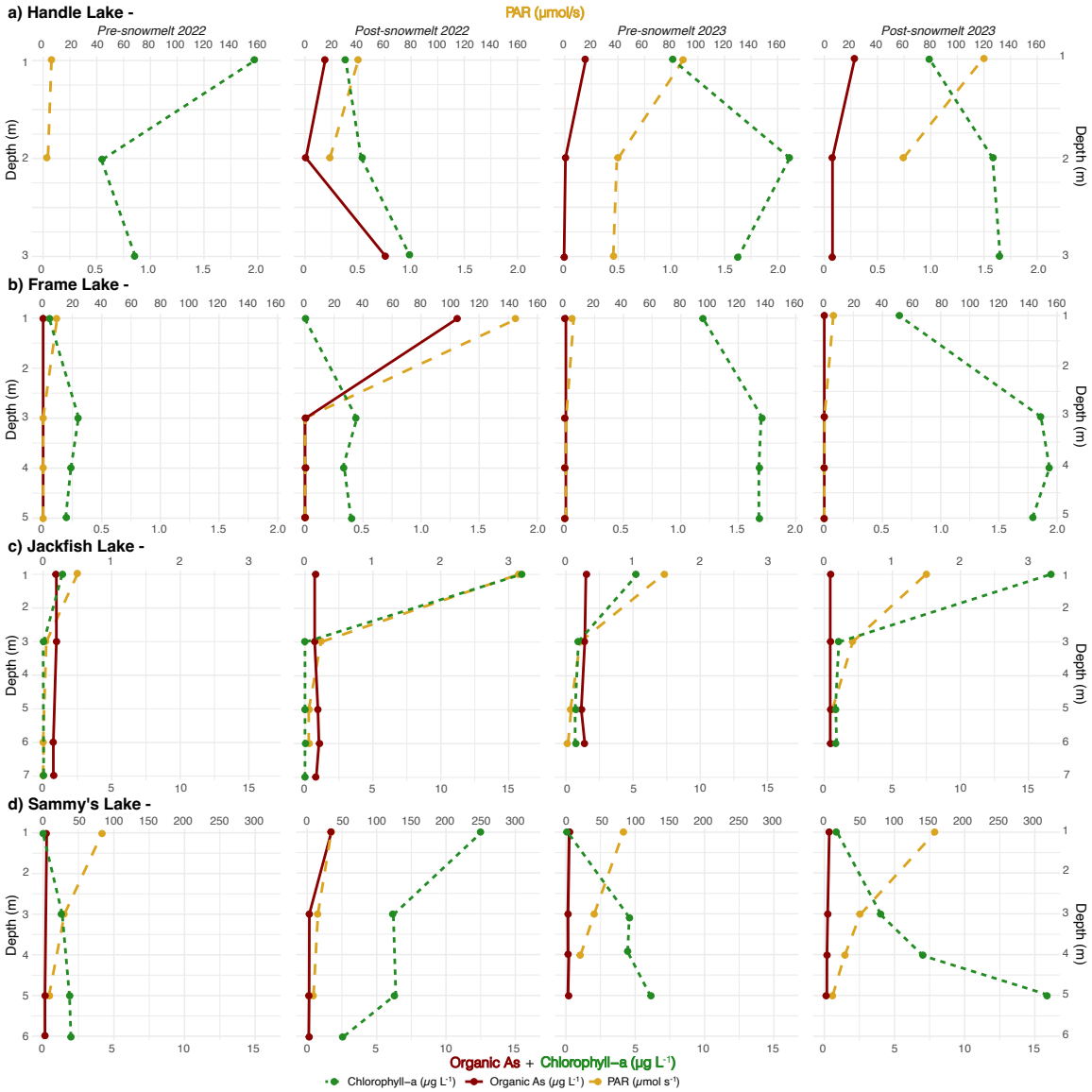


**Figure S 3-2.** Lake-depth profiles of the four study lakes showing the change in chlorophyll-a, total organic arsenic, and PAR between the pre- and post-snowmelt periods during spring thaw in both 2022 and 2023.

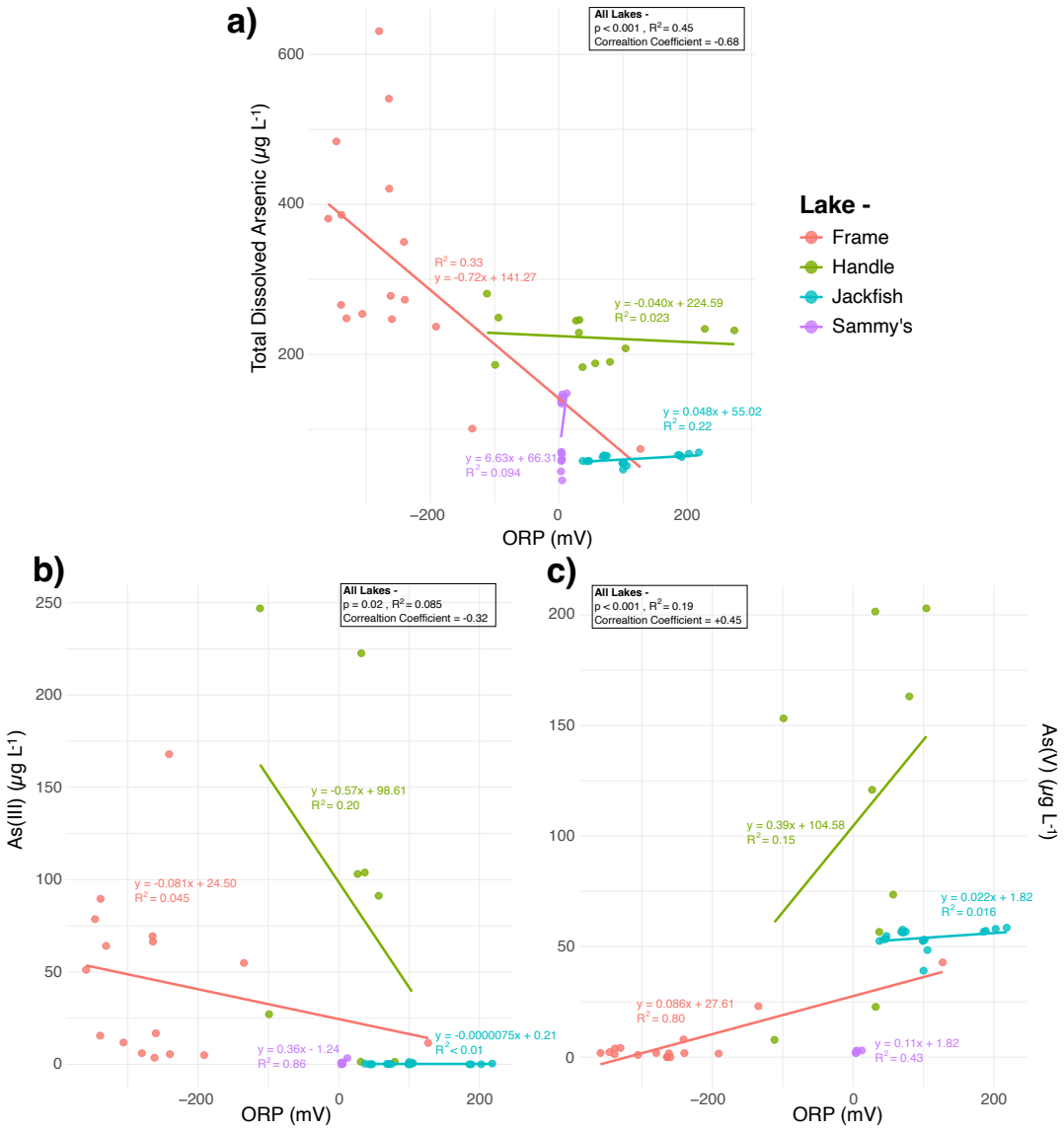


**Figure S 3-3.** ORP measurements in each study lake compared to: a) total dissolved arsenic, b) As(III), and c) As(V) concentrations. Lines of best fit were calculated for each lake via linear regression.

# Chapter 4: Drivers of arsenic bioaccumulation in plankton from subarctic lakes impacted by legacy mining contamination

Amanda J. Little, John Chételat, Michael J. Palmer, Marc Amyot, and Jennifer B. Korosi

Author Contributions

AJL, MJP, and JBK conceived of research ideas and conducted fieldwork, MJP and JBK secured funding and were responsible for project administration and resource acquisition. AJL conducted all other analyses and led the writing of the manuscript. All authors contributed to the creation of the methodology, contributed in the editing of manuscript drafts.

## 4.1 Abstract

The aim of this study was to investigate the drivers of arsenic bioaccumulation in plankton from five subarctic lakes that spanned a gradient of arsenic contamination (Yellowknife, Northwest Territories, Canada). Water chemistry, plankton community composition, and arsenic concentrations in bulk plankton samples from two size categories (small: ≥ 20 – 62 μm; predominantly phytoplankton, large: ≥ 63 μm; predominantly zooplankton) were collected and analyzed over two years (2022-2024), in both summer and winter. Results showed that lake water arsenic concentration was only a moderate predictor of arsenic bioaccumulation in plankton, and the highest plankton arsenic concentrations were consistently reported in Sammy's Lake, which had the second-lowest water arsenic concentrations among the five lakes. Arsenic concentrations in both phytoplankton and zooplankton from Sammy's Lake were also notably elevated in autumn compared to summer, suggesting that autumn lake turnover may be a critical period for arsenic bioavailability in this lake. Statistical analyses indicated that dissolved organic carbon and arsenate concentrations influenced arsenic bioaccumulation in phytoplankton. Arsenic bioaccumulation in zooplankton was more strongly associated with the amount of arsenic in phytoplankton than in water, indicating dietary exposure was an important exposure pathway. Overall, study findings indicate that the relationship between water arsenic concentrations and arsenic bioaccumulation in plankton can be complex and strongly modified by interacting environmental factors.

## 4.2 Introduction

Arsenic contamination of aquatic ecosystems is an environmental issue of global concern due to its widespread distribution, high toxicity, and persistence in contaminated landscapes (Wang & Mulligan, 2006). Mining is the largest anthropogenic source of arsenic to the environment, with global atmospheric emissions currently estimated to exceed 25,000 tonnes per year (Barral-Fraga et al., 2020; Faria et al., 2023). Gold and silver mines in particular been found to result in excessive amounts of arsenic pollution into the environment, often through the migration of contaminated mine tailings or from the volatilization of arsenic during the roasting process (Kwong et al., 2006; Jasiak et al., 2021). Lakes and rivers in regions impacted by mining have documented arsenic levels as high as 47,000 $\mu g\ L^{-1}$ during peak industrial activities (Wang & Mulligan, 2006; Palmer et al., 2025). Even after the cessation of mining activities, contaminated catchments have been found to be a persistent source of arsenic to aquatic ecosystems via terrestrial runoff, often delaying ecological recovery in lakes (Palmer et al., 2024).

Arsenic exists in many different chemical forms, but the two most common in freshwater environments are arsenate (As(V)) and arsenite (As(III)). As(V) is more stable and dominant under oxic conditions, and is generally accepted as being more toxic to lower trophic microorganisms like bacteria and phytoplankton (Rodie et al., 1995; Rahman et al., 2014). This is because As(V) is a chemical analogue of phosphate ($PO_4^{3-}$), a macronutrient, which allows it to easily enter the cells of microorganisms via the $PO_4^{3-}$-transporters in their cell walls, resulting in oxidative stress and cell division inhibition (Hellweger et al., 2003; Wang et al., 2015). As(III) tends to be more prevalent and stable under low redox potential, conditions that are often prevalent in lakes during the ice-on season or in the bottom waters during periods of thermal

stratification (Rodie et al., 1995; Palmer et al., 2019). As(III) is considered to be more toxic to higher trophic aquatic organisms like zooplankton and fish (Rodie et al., 1995; Akter et al., 2005). The major mode of toxicity for As(III) is through the inhibition of oxidative damage enzymatic scavenger production (e.g., glutathione), which are critical for the formation of metal-binding phytochelatins and without which results in cell death (Rahmen et al., 2014; Wang et al., 2015). According to the United States Environmental Protection Agency (US EPA), the highest concentrations of total arsenic that can be found in freshwater without causing any deleterious effects to exposed organisms are 340 $\mu g\ L^{-1}$ (acute; 1 hour) and 150 $\mu g\ L^{-1}$ (chronic; several days) (US EPA, 2014). As a precaution, the Canadian Council of Ministers of the Environment (CCME) has set a guideline of 5 $\mu g\ L^{-1}$ for the protection of aquatic life (CCME, 2001). However, the total concentration of arsenic in freshwaters may not accurately reflect the portion that is bioavailable.

Previous studies have observed that lake water arsenic concentration tends to be highly correlated with arsenic bioaccumulation in aquatic organisms (Jia et al., 2018; Lepage et al., 2024; Blais et al., 2025). While only a few studies have included plankton in their investigation, microorganisms have consistently been reported to have the highest amount of arsenic bioaccumulation, with decreasing concentrations observed as trophic level increases (i.e., bio-diminution) (Chen & Folt, 2000; Caumette et al., 2011; 2014; Barret et al., 2018; 2019; Hull et al., 2023; Blais et al., 2025). The bioaccumulation of arsenic in plankton has been found to have significant negative impacts on higher trophic organisms, often increasing the overall ecotoxicological risk beyond simple exposure from surrounding lake water (Sanders, 1986; Barrett et al., 2018; Hull et al., 2023). For example, one study found that the freshwater zooplankton calanoid copepod species *Eurytemora affinis* was relatively unimpacted by arsenic

exposure in water until it was fed As(V)-contaminated phytoplankton (Sanders, 1986). Another study found that planktivorous fish (diet consisting mainly of plankton) had higher concentrations of arsenic compared to the other fish species in the study, as well as compared with any other metal they were exposed to (Chen & Folt, 2000). Plankton are therefore vital in the transfer of arsenic through freshwater food webs.

Since arsenic is a redox-sensitive element, and As(V) is a chemical analogue of $PO_4^{3-}$, there exists a high potential for environmental factors to interfere with the overall uptake and transfer of arsenic by freshwater plankton. Although research has been limited, lake depth and thermal stratification dynamics have been shown to impact plankton arsenic bioaccumulation, with studies from temperate lakes reporting that shallow, weakly stratified lakes typically host plankton with higher overall arsenic levels due to the higher bioavailability of arsenic in more oxic waters (Barrett et al., 2018; 2019). Higher levels of $PO_4^{3-}$ have also been observed to result in lower As(V) uptake by phytoplankton, thereby decreasing the overall toxicity of arsenic (Levy et al., 2005). Iron (Fe) and dissolved organic carbon/matter (DOC/M) concentrations can also control the mobility and overall concentration of arsenic in lake water through binding to arsenic via sorption and coprecipitation processes (Rodie et al., 1995; Pothier et al., 2020). DOM can also interfere with the photooxidation of As(III) into As(V), further reducing its bioavailability to microorganisms (Pothier et al., 2020).

The objective of this study was to build on our understanding of the environmental mediators of arsenic uptake and bioaccumulation at the base of freshwater food webs, with a focus on subarctic lakes. Specifically, we explored the potential moderating influence of lake water chemistry and plankton community composition on the relationship between water arsenic concentrations and bioaccumulation in plankton in five lakes in the Yellowknife region

(Northwest Territories, Canada) that span a gradient of legacy mining-related arsenic contamination. We sampled lakes across multiple seasons from 2022 to 2024, including the ice-on and open-water periods, as Yellowknife-area lakes are known to exhibit substantial seasonal variation in arsenic speciation and concentration (Palmer et al., 2019; 2020). The overall study aim is to improve assessments of ecotoxicological risk from arsenic in mining-impacted subarctic lakes.

## 4.3 Materials and Methods

### 4.3.1 Study Lakes

The City of Yellowknife (Northwest Territories, Canada) is located on the northern arm of Great Slave Lake on Treaty 8 and Chief Drygeese Territory, and has been the traditional home of the Yellowknives Dene First Nation (YKDFN) for the past 7,000 years (O'Reilly, 2015). Yellowknife experiences a continental subarctic climate, with below freezing temperatures starting in early October lasting through to late April. As a result, many small lakes in the area remain ice-covered for the majority of the year (190-243 days) (Benson et al., 2013). The region is underlain by the Yellowknife Greenstone Belt, which is known for its high mineral potential and was the site of three major gold mines operational from 1938 to 2004 (Con, Negus, and Giant Mine) (Hocking et al., 1978). During this time, approximately 20,000 tonnes of arsenic was aerially deposited across the landscape, resulting in the enrichment of soils and lake sediments upwards of 80 km away (Jasiak et al., 2021; Palmer et al., 2025). Previous studies have reported modern arsenic concentrations upwards of 2,000 $\mu g\ L^{-1}$ in lakes adjacent to the largest historical polluter – Giant Mine (Palmer et al., 2015; Sivarajah et al., 2019).

Five study lakes were selected to represent spatial environmental gradients related to arsenic contamination and potential drivers of arsenic uptake by plankton in the Yellowknife region. Study lakes were chosen based off of their proximity to Giant Mine and inclusion in a long-term monitoring program run by the Aurora Research Institute (ARI; SLACC: Subarctic Lakes in a Changing Climate) (Figure 4.1; Table S 4-1). The order from most to least contaminated is: Handle Lake, Frame Lake, Jackfish Lake, Sammy's Lake, and Stuart Lake (Table S 4-1). In addition to having the highest concentration of total arsenic, Handle Lake is the most shallow and experiences large seasonal increases in arsenic concentration and form (Figure 4.1; Table S 4-1) (Palmer et al., 2019). The second and third most contaminated lakes (Frame Lake and Jackfish Lake) are both eutrophic due to additional stressors related to nutrient pollution from urban inputs (Figure 4.1; Table S 4-1) (Gavel et al., 2018; Sivarajah et al., 2021). Frame Lake experiences high sediment oxygen demand related to eutrophication which causes anoxia starting in early winter and contributes to large seasonal fluxes in arsenic and other redox-sensitive elements, such as Fe and sulphur (Gavel et al., 2018; Harbinson et al., 2023). Jackfish Lake is home to a diesel-powered generating station and is downhill from a solid waste disposal facility which has led to a unique combination of thermal and nutrient pollution, which supports high phytoplankton density dominated by the Cyanobacteria genus *Planktothrix* (Figure 4.1; Table S 4-1) (Sivarajah et al., 2021; Little et al., 2026). Sammy's Lake has much lower total arsenic and DOC concentrations compared to the other contaminated lakes (Figure 4.1; Table S 4-1). The final lake (Stuart Lake; referred to as "Small Lake" in Blais et al., 2025) was selected as a reference site since it is over 10 km away from the historical Giant Mine site (Figure 4.1; Table S 4-1 (Palmer et al., 2015).

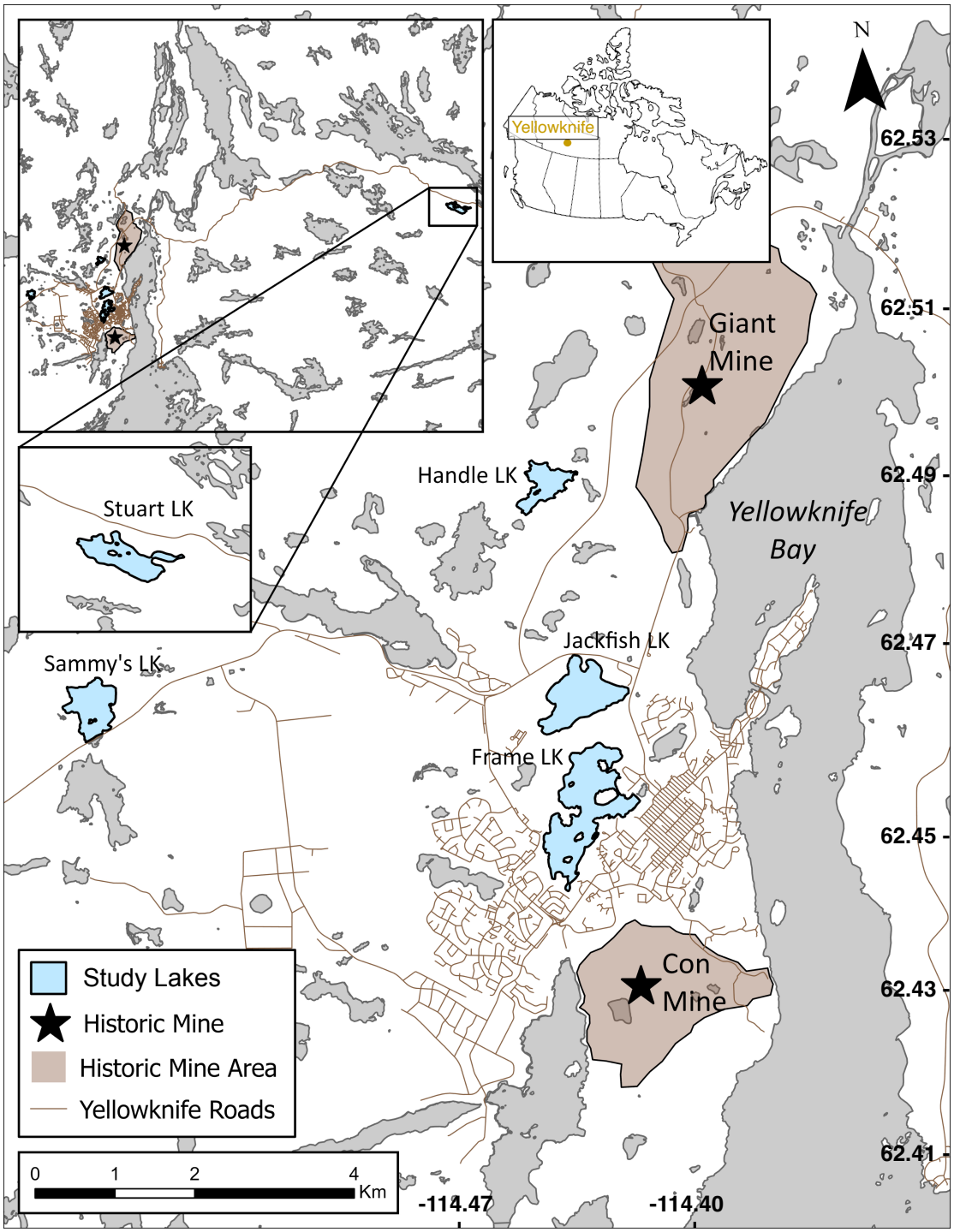


**Figure 4.1.** Site map of the five study lakes and historical mine site boundaries from the Yellowknife, Northwest Territories, Canada region. Map created by Seamus Daly.

### 4.3.2 Field Sample Collection

The five study lakes were sampled in early (November) and late (March-April) winter, early spring (May), early summer (June), and autumn (September/October) from April 2022 until May 2023, with additional samples collected from three of the five lakes (Handle, Frame, and Sammy's) in June, October, and November of 2023 and March and June of 2024 (Table S 4-2). Sampling was consistently conducted at the same location near the centre of each lake. All equipment was rinsed and soaked in lake water for at least 2 minutes prior to sample collection. Water column profiles of dissolved oxygen (DO) (mg $L^{-1}$), specific conductivity (ability of a solution to conduct electricity; µS $cm^{-1}$), oxidative-reduction potential (tendency of a solution to gain or lose electrons; ORP; mV), temperature (°C), and chlorophyll-a (µg $L^{-1}$) were collected using a multi-parameter YSI probe (YSI EXOII, Yellow Springs Inc., Yellow Springs, Ohio). All measurements were recorded at 1-metre intervals from 0.5 m below lake surface to approximately 1 m above the lake bottom. Water samples were collected at 1-metre intervals for the analysis of total and dissolved phosphorus, dissolved organic carbon, total and dissolved metal(loid)s, and different forms of arsenic (speciation) using a peristaltic pump and Teflon™ line that was prerinsed with 5% HCl solution and ultrapure water (Palmer et al. 2020) or with a pre-rinsed 2.2 L Van Dorn (Wildco, Florida, USA).

Samples collected for dissolved metal(loids)s and arsenic speciation were filtered through a 0.45 µm polyethersulfone (PES) syringe tip filter in the field. Arsenic speciation samples were filtered into 15 mL trace-metal free vials preloaded with 150 µL of 0.25 M ETDA and preserved with an additional 25 µL of glacial acetic acid within 4 hours of collection (Palmer et al., 2019). Total and dissolved metal(loid)s were preserved to 1% (v/v) with nitric acid. Field blanks and

replicate samples were taken for arsenic samples as QA/QC measures (Table S 4-3; Table S 4-4). All water samples were stored in the cold and dark until analyzed.

Water samples were collected for plankton quantification and taxonomic identification as depth-integrated samples using a 2.2 L Van Dorn. Water was collected at 1-m depth intervals starting at 0.5 m from the surface of the lake until 1 m above the lake bed. All samples were homogenized via physical stirring, split into 100 mL duplicate subsamples, and preserved with 3% Lugol's solution. Zooplankton samples were collected for quantification and taxonomic identification via vertical net tows using a Wisconsin zooplankton net (Wildco, Florida, USA; 63 μm mesh size, 0.127 m mouth diameter, 1 m net length), and stored in 50 mL vials preserved with 100% ethanol to a final concentration of ~70%. Phytoplankton and zooplankton samples were stored cold and dark until analysis.

Plankton biomass collected during the first year of sampling when lake ice was present (April – May and November 2022; April – May 2023) were pumped up from the first few meters of water immediately under the lake ice and collected with a phytoplankton net (Dynamic Aqua Supply, British Columbia, Canada; 20 μm mesh size, 0.5 m mouth diameter, 1.5 m net length). In total, 400 L of lake water was pumped and filtered in the field for plankton biomass samples. However, issues related to low small plankton biomass persisted and this method was dropped after May 2023, and replaced with vertical tows (2 sets of 10 tows) of large plankton only using a 63 μm Wisconsin zooplankton net (Wildco, Florida, USA; 63 μm mesh size, 0.127 m mouth diameter, 1 m net length), which were collected through a hole drilled in the ice. During the open-water season, plankton were collected via horizontal tows using the phytoplankton net, which was towed behind an inflatable zodiac motorboat. Replicate samples were collected during each sampling effort.

Bulk plankton samples for arsenic bioaccumulation analysis were separated (same day) into two size classes (small: ≥ 20 – 62 μm; and large: ≥ 63 μm) by filtering through a 63 μm mesh-aperture plastic sieve. Once separated, samples were rinsed with deionized water and concentrated via centrifuging for 10 minutes (4,300 rpm), after which they were transferred to 50 mL falcon tubes. The samples were stored dark and frozen at -80°C until they could be freeze-dried and analyzed. We were unable to separate the two size classes in Jackfish Lake due to high abundances of filamentous *Planktothrix* taxa, and instead have only one size class (≥ 20 μm) which we refer to hereafter as combined plankton. The small size class was assumed to be predominantly made up of phytoplankton, while the large class was assumed to be predominantly zooplankton. However, large colonies of the *Cyanobacteria* genera *Microcystis* and *Aphanocapsa* were observed under the microscope during the identification of some zooplankton samples (large size class), and juvenile zooplankton life stages and rotifers smaller than 63 μm were occasionally reported during phytoplankton identification (small size class).

### 4.3.3 Lab Analyses

All water chemistry analyses except for arsenic speciation were performed at Taiga Laboratory in Yellowknife. Organic carbon and major anions (total and dissolved) were analyzed using high temperature combustion with a total carbon analyzer (standard method (SM) 5310) and ion chromatography (SM4110) (Greenberg et al., 1992). Total (unfiltered) and dissolved (filtered < 0.45 μm) metal(loid) concentrations were measured using inductively coupled plasma mass spectrometry (ICP-MS) (Agilent 7900 Single Quadruple ICP-MS; EPA method 200.8) (Creed et al., 1994). Phosphorus was analyzed using ICP-MS instead of the standard spectrophotometer due to potential interference from As(V) in the samples (Linge & Oldham,

2001). Analyses for arsenic speciation (As(III), As(V)) in lake water were conducted at the Université de Montréal via high-performance liquid chromatography with ICP-QQQ (Agilent 8900 Triple Quadrupole ICP-MS). QA/QC protocols included analysis of spikes and calibration verifications using certified reference materials (Table S 4-5; Table S 4-6). Method detection limits can be found in the supplementary information file (Table S 4-7).

Freeze-dried plankton biomass samples (minimum dried weight 0.002 g) was analyzed for total arsenic at the Université de Montréal. The plankton samples were processed using high-performance liquid chromatography (HPLC)-ICP-MS/tandem ICP-MS (MS), with anion exchange columns, following the protocols outlined in Caumette et al. (2011), Caumette et al. (2014), and Moreda-Piñeiro et al. (2011) and in the QA/QC section of the supplementary information file (Table S 4-5). Certified reference materials (CRM) were used to confirm and verify total arsenic concentrations in both lake water and plankton samples (Table S 4-6; Table S 4-8).

Rotifer and zooplankton taxonomic samples were homogenized and pipetted as 1 mL aliquots into a gridded Sedgewick-Rafter cell using a Hansen-Stemple pipette. Where possible, a minimum of 300 adult individuals were counted. In situations where this minimum could not be met, all of the adult individuals were identified and counted. Rotifers and zooplankton were identified to the species level where applicable using an OMAX V83 series inverted microscope, and final densities (individuals $L^{-1}$) were calculated based off the volume of water towed during collection, total subsample aliquot size, and final individual count.

Phytoplankton taxonomic samples were settled for a minimum of 48 hours and then decanted to a volume of 20 mL to create a 5x concentration. Aliquots of 1 mL were pipetted into a gridded Sedgewick-Rafter cell and identified using three different magnifications (40x 1 whole

cell; 100-200x 1 transect; 400x 100 random fields of view) using the OMAX V83 series inverted microscope. A minimum of 300 natural units (1 natural grouping of algae (i.e., individual filament, colony, or isolated cell = 1 natural unit) were counted per sample. Phytoplankton were identified to the genus level (reference guides for all plankton listed in Table S 4-9). Cell densities were calculated using cell counts, sample aliquot volume, and concentration factor (5x).

### 4.3.4 Statistical Analyses

All data analyses were run in the statistical computing environment RStudio (version 2024.12.0+467; R Core Team 2020) with confidence intervals set at 95% for all tests. Water chemistry data was averaged across all collected interval depths in order to represent the full water column. Prior to modelling, multicollinearity was assessed using variance inflation factors (VIFs) and variables found to be highly collinear were removed (Dormann et al., 2013). We used regression tree models (package *rpart*; Therneau & Atkinson, 2025) to determine the most influential environmental drivers of plankton arsenic bioaccumulation within the three size categories across the five study lakes (Elith et al., 2008). A Principle Components Analysis (PCA) was used to visualize the spread of environmental variables across the lakes (package *vegan*; Oksanen et al., 2019) (Legendre & Legendre, 2012). Linear Regressions (LR) and Generalized Additive Models (GAM) (package *mgcv*; Wood, 2025) were performed in order to assess the correlation strength between potential environmental variables of interest identified from the regression tree models and arsenic bioaccumulation in plankton. Correlations were considered to be strong if they were greater than 0.70 (i.e., $R^2 > 0.70$), moderate if they were between 0.3 and 0.7, and weak if they were below 0.3 (Cohen, 1988). Replicate plankton data were averaged prior to analysis in order to avoid issues related to replication and non-

independence (Allen et al., 2011; Smith & Lester, 2010; Hurlbert, 1984). Total plankton arsenic concentrations were $\log_{10}$ transformed in every model to maintain consistency. All environmental variables that were found to be predictors of arsenic bioaccumulation in plankton were put into a final Multiple Linear Regression (MLR) model, where variables were removed until only significant variables remained. Using the Akaike Information Criterion (AIC) framework, the final models were compared to models containing all of the environmental variables in order to determine which best fit the data (Burnham & Anderson, 2002). All final graphs were created using the *ggplot2* package (Wickham, 2016).

## 4.4 Results

### 4.4.1 QA/QC

Field blanks for lake water samples were all reported below the method detection limits (DL) for total arsenic (DL = 0.2 μg $L^{-1}$; N = 19; Table S 4-3). Duplicate samples were found to have calculated relative percent differences ranging from 0.5-9.1% (mean = 3.4%, N = 7; Table S 4-4). Control samples ORP-2 (Ongoing Precision and Recovery) and PTC (Proficiency Testing Canada) were used to verify total arsenic and speciation in lake water and consistently recorded between 90 – 120% recovery (Table S 4-6).

The majority of field blanks for plankton arsenic bioaccumulation samples reported either below DL (0.002 μg $g^{-1}$) or just slightly above it (Table S 4-8). Overall blank concentrations were still very low so the impacted samples were retained for inclusion in this study but were screened for further potential QA/QC issues related to minimum dried biomass (0.002 g) and how well the replicate and multi-year data matched (Table S 4-10; Table S 4-11). Certified reference materials DORM-4/5 (fish protein) and TORT-3 (lobster hepatopancreas) were used to

verify plankton arsenic bioaccumulation samples, and percent recovery consistently fell between 90 and 110% (Table S 4-8).

### 4.4.2 Plankton Arsenic Bioaccumulation and Seasonal Cycling

Handle Lake was the most arsenic-contaminated among the five study lakes (average lake water concentration = 208.4 μg $L^{-1}$), followed by Frame Lake (average lake water concentration = 205.7 μg $L^{-1}$) and Jackfish Lake (average lake water concentration = 61.6 μg $L^{-1}$), yet the highest concentrations of arsenic in plankton were consistently reported in Sammy's Lake (average lake water concentration = 8.0 μg $L^{-1}$) (Figure 4.2). This was the case for both the small and large plankton categories, with maximum arsenic bioaccumulation concentration found to be 1,834.5 μg $g^{-1}$ in small plankton compared to 765.0 μg $g^{-1}$ in large plankton (both from Sammy's Lake). From highest to lowest, the maximum arsenic bioaccumulation concentration in small plankton in each lake was: 1,834.5 μg $g^{-1}$ in Sammy's Lake, 1,167.2 μg $g^{-1}$ in Handle Lake, 494.0 μg $g^{-1}$ in Frame Lake, and 34.1 μg $g^{-1}$ in the reference lake (Stuart Lake) (Figure 4.2a). Maximum arsenic bioaccumulation concentration in large plankton (from highest to lowest) in each lake was: 765.0 μg $g^{-1}$ in Sammy's Lake, 487.9 μg $g^{-1}$ in Frame Lake, 193.8 μg $g^{-1}$ in Handle Lake, and 11.7 μg $g^{-1}$ in Stuart Lake (Figure 4.2b). Sammy's Lake documented notably elevated arsenic concentrations in both small and large plankton in autumn compared to June in 2022 and 2023 (Figure 4.2a-b).We were unable to separate Jackfish Lake biomass samples into two size categories, but the combined (≥ 20 μm) plankton samples from Jackfish Lake (average lake water concentration = 61.6 μg $L^{-1}$) were found typically lower than 50 μg $g^{-1}$ (Figure 4.2c).

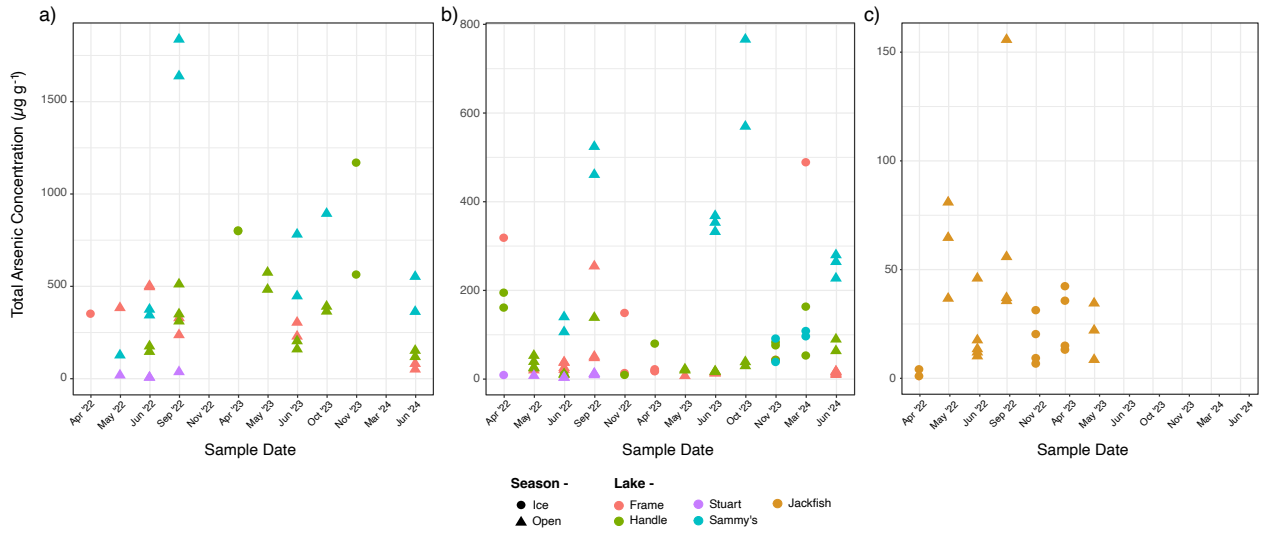


**Figure 4.2.** Measurements of arsenic bioaccumulation in plankton (µg $g^{-1}$) from the five study lakes across multiple sampling events from April 2022 to June 2024, including under-ice (circles) and open-water (triangles) sampling: a) small plankton (≥ 20 – 62 µm), b) large plankton (≥ 63 µm), and c) combined plankton (≥ 20 µm; Jackfish Lake only). Samples collected from April 2022 – June 2024.

### 4.4.3 Lake Water Arsenic as a Driver of Plankton Arsenic Bioaccumulation

When assessed using LRs and GAMs, total arsenic concentration in lake water was found to be a statistically significant driver for arsenic bioaccumulation in both small ($p = 0.01$; $R^2 = 0.27$; positive) and large ($p < 0.01$; $R^2 = 0.52$; non-linear) plankton size classes (Figure 4.3a-b), but not for the combined plankton in Jackfish Lake. When the statistical tests were re-run without data from Sammy's Lake, the strength of the relationships improved, with small plankton found to have an updated correlation strength ($R^2$) of 0.77 ($p < 0.001$; positive), while the direction of the correlation with large plankton became linear and more clearly positive ($R^2 = 0.48$; $p < 0.001$) (Figure 4.3c-d). When assessed using an AIC framework, the LR without the data from Sammy's Lake was found to be the stronger model (with Sammy's Lake – AIC = 53.8 versus without Sammy's Lake – AIC = 33.7) (Table S 4-12).

Small and large plankton were both found to be positively correlated with As(V) (small – $p < 0.01$; $R^2 = 0.40$; large – $p < 0.001$; $R^2 = 0.50$) (Figure 4.3c-d). When statistical tests were re-run without the data from Sammy's Lake, the correlation strength with small plankton arsenic bioaccumulation increased ($p < 0.001$; $R^2 = 0.75$; positive), but decreased for the large plankton category ($p = 0.03$; $R^2 = 0.33$; non-linear, positive) (Figure 4.3c-d). Neither small nor large plankton arsenic bioaccumulation was found to be correlated with As(III), regardless of whether the data from Sammy's Lake was included. Combined plankton were not found to be statistically correlated with As(V) or As(III) lake water concentrations.

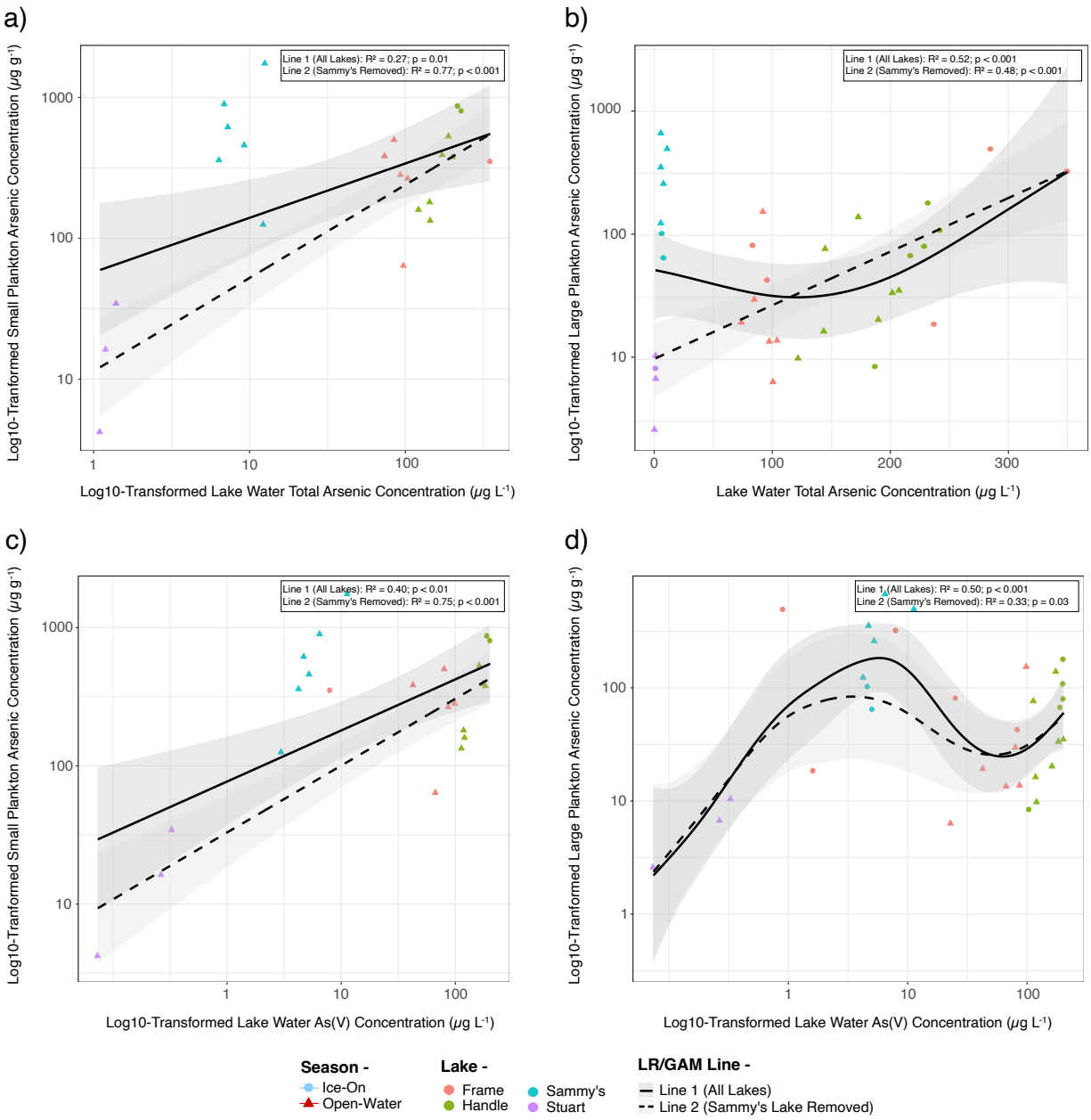


**Figure 4.3.** The results of statistically significant LR and GAM models highlighting the relationships between: (a) lake water total arsenic and plankton arsenic bioaccumulation for small plankton (≥ 20 – 62 μm); b) lake water total arsenic and plankton arsenic bioaccumulation for large plankton (≥ 63 μm); c) lake water As(V) and plankton arsenic bioaccumulation for small plankton; and d) lake water As(V) and plankton arsenic bioaccumulation for large plankton. All four plots compare the difference between the correlations with (solid line) and without (dashed line) the data from Sammy's Lake.

### 4.4.4 Other Potential Drivers of Plankton Arsenic Uptake

A PCA was run on the water chemistry data in order to examine variation in limnological variables among the five study lakes and to visualize potential key environmental gradients. The first two axes of the PCA were found to explain approximately 38.8% of the total variance in the dataset, with clear clustering of samples by lake (Figure 4.4). All environmental gradients except for phosphorus and DO were found to be statistically significant (Figure 4.4). The first axis (PCA1) was most strongly aligned with total arsenic, As(V), and DOC (Figure 4.4). PCA2 was more representative of chlorophyll-a, ORP, As(III), sulphate, and Fe (Figure 4.4). Handle Lake, Stuart Lake, and Sammy's Lake were separated primarily along PCA1, with Handle Lake associated with higher total arsenic, As(V), and DOC, and Sammy's and Stuart Lakes associated with lower total arsenic, As(V), and DOC. Frame Lake was associated with PCA2, with higher As(III), sulphate, and Fe, and lower ORP (Figure 4.4).

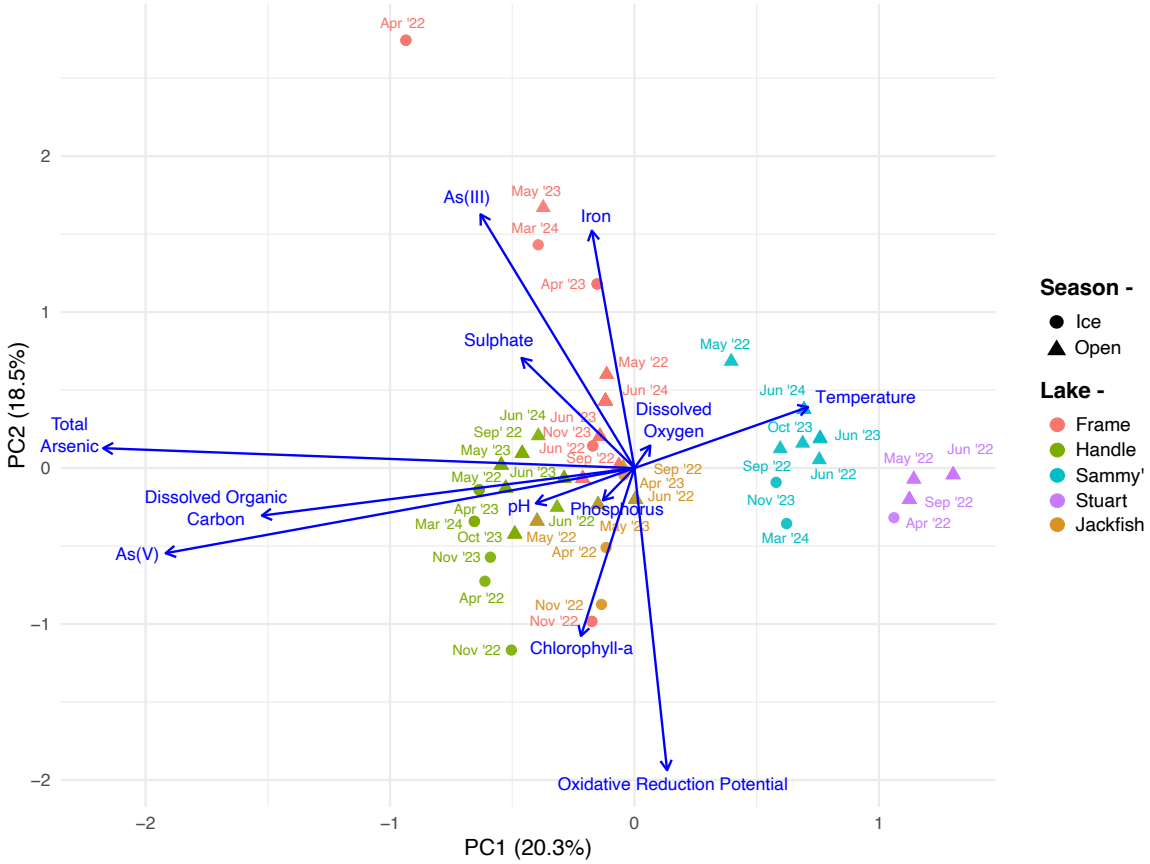


**Figure 4.4.** A PCA highlighting environmental gradients across the five study lakes.

### *4.4.4.1 Small Plankton*

The regression tree model run on the small plankton (≥ 20 – 62 µm) data identified DOC, temperature, and As(V) as the strongest predictor variables for arsenic bioaccumulation (Figure S 4-1a). The first split in the tree occurred at a DOC threshold of 11.3 mg $L^{-1}$, with DOC > 11.3 mg $L^{-1}$ associated with lower total arsenic bioaccumulation compared to DOC < 11.3 mg $L^{-1}$ (Figure S 4-1a). For DOC > 11.3 mg $L^{-1}$, a second split was identified at temperatures greater than or equal to 2.7°C, with higher temperatures associated with lower plankton arsenic concentrations (Figure S 4-1a). The last unique environmental variable identified by the regression tree was As(V) with a split occurring at concentrations less than 3.6 µg $L^{-1}$, with concentrations above 3.6

μg $L^{-1}$ associated with higher total arsenic bioaccumulation in small plankton (Figure S 4-1a). Sammy's recorded the lowest DOC concentrations and the highest arsenic bioaccumulation values and was likely a strong driver of the relationship as identified by the regression tree.

DOC and As(V) were found to be statistically important for arsenic bioaccumulation based on LRs and GAMs (see Section 4.4.3, above, for As(V) results), but temperature was not. When assessed using the data from all four study lakes (Handle, Frame, Sammy's, Stuart), the correlation with DOC was found to be non-linear and moderately weak ($p = 0.01$; $R^2 = 0.43$), but overall indicative of a positive relationship (Figure 4.5a). Unlike with the arsenic variables, the correlation was not improved after the data from Sammy's Lake was removed ($p = 0.04$; $R^2 = 0.38$; non-linear but positive) (Figure 4.5a). No variables associated with lake trophic status, including phosphorus, chlorophyll-a, and plankton density (phytoplankton, rotifers, and zooplankton) were found to be statistically correlated with small plankton arsenic bioaccumulation based on LRs and GAMs.

All of the above identified environmental predictors of arsenic bioaccumulation in small plankton were put into a final MLR model, but no significant model could be generated. When the data from Sammy's Lake was removed, a significant model was generated using total arsenic, As(V), and DOC ($p < 0.001$; $R^2 = 0.77$). Using an AIC framework, this model outperformed both the original model using data from all four study lakes, as well as the model run without data from Sammy's Lake but with all of the identified predictors of small plankton arsenic concentration included (Table S 4-12).

Arsenic bioaccumulation was significantly higher in Handle Lake during the ice-on season compared to the open-water season ($p = 0.03$; $R^2 = 0.56$), but there was no significant

difference detected for Frame Lake (Figure 4.5). Ice-on data for the small plankton category was not available for Sammy's Lake and Stuart Lake.

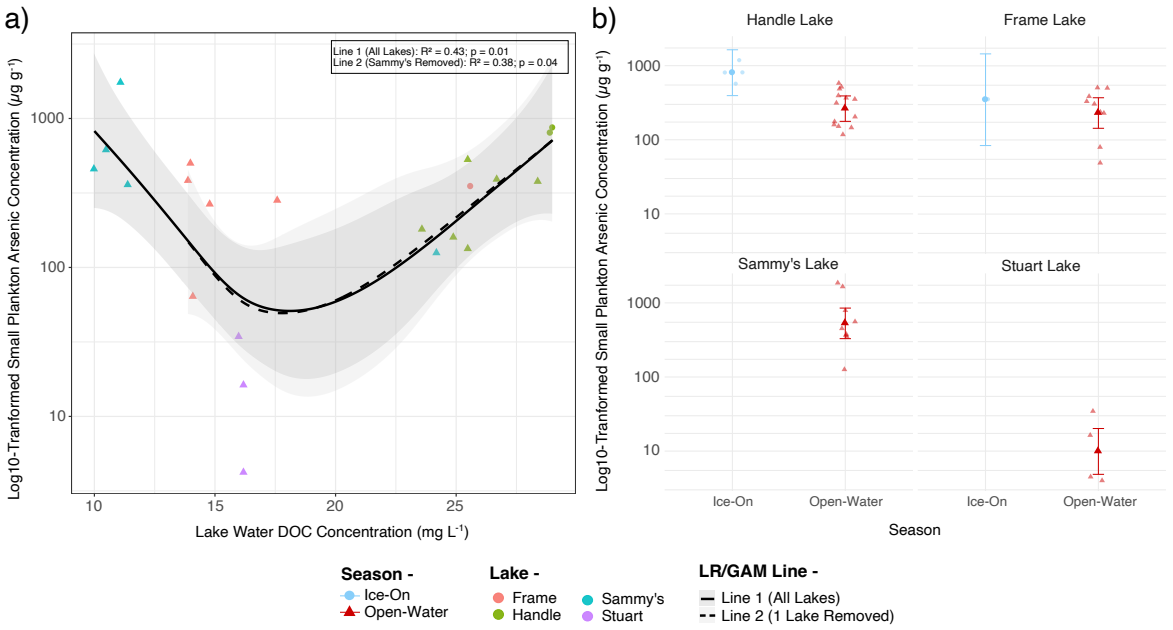


**Figure 4.5.** Environmental variables found to have a statistically significant relationship with small plankton arsenic concentration: a) DOC and b) season*. *Ice-on data was only available for small plankton samples collected from Handle Lake and Frame Lake due to issues related to low biomass.

### *4.4.4.2 Large Plankton*

The regression tree identified DOC, Fe, As(III), and sulphate as important drivers of large plankton arsenic bioaccumulation (Figure S 4-1b). Similar to the small plankton, the first split occurred at DOC concentrations greater than or equal to 11.25 mg $L^{-1}$, with higher bioaccumulation associated with lower DOC (Figure S 4-1b). Where lakes had DOC <11.25 mg $L^{-1}$, the regression tree identified a secondary split for As(III) 0.05 µg $L^{-1}$, with lower concentrations of As(III) associated with lower arsenic bioaccumulation (Figure S 4-1b). Where lakes had DOC >11.25 mg $L^{-1}$, Fe was identified as another key variable, with higher

concentrations of Fe (> 47.0 μg $L^{-1}$) associated with higher arsenic bioaccumulation (Figure S 4-1b). The final split in the regression tree occurred for sulphate at 74.0 μg $L^{-1}$, with higher concentrations of sulphate resulting in higher arsenic bioaccumulation (Figure S 4-1b).

When further analyzed via LRs and GAMs, DOC was found to be only moderately but positively correlated with large plankton arsenic bioaccumulation ($p = 0.01$; $R^2 = 0.33$), and removal of the data from Sammy's Lake did not strengthen this correlation ($p = 0.01$; $R^2 = 0.22$; positive) (Figure 4.6b). The relationship between Fe and large plankton bioaccumulation was only significant, albeit weakly correlated, when the data from Sammy's Lake was removed ($p = 0.04$; $R^2 = 0.13$) (Figure 4.6c). Sulphate was determined to have a strong but non-linear influence on large plankton arsenic ($p < 0.001$; $R^2 = 0.70$) that appeared to be mainly driven by the samples from Frame Lake. When separated out, sulphate was found to be positively associated with bioaccumulation in large plankton in both Frame Lake by itself ($p = 0.01$; $R^2 = 0.70$), as well as the three other study lakes (Handle Lake, Sammy's Lake, and Stuart Lake) with Frame Lake removed ($p < 0.001$; $R^2 = 0.68$; (Figure 4.6d).

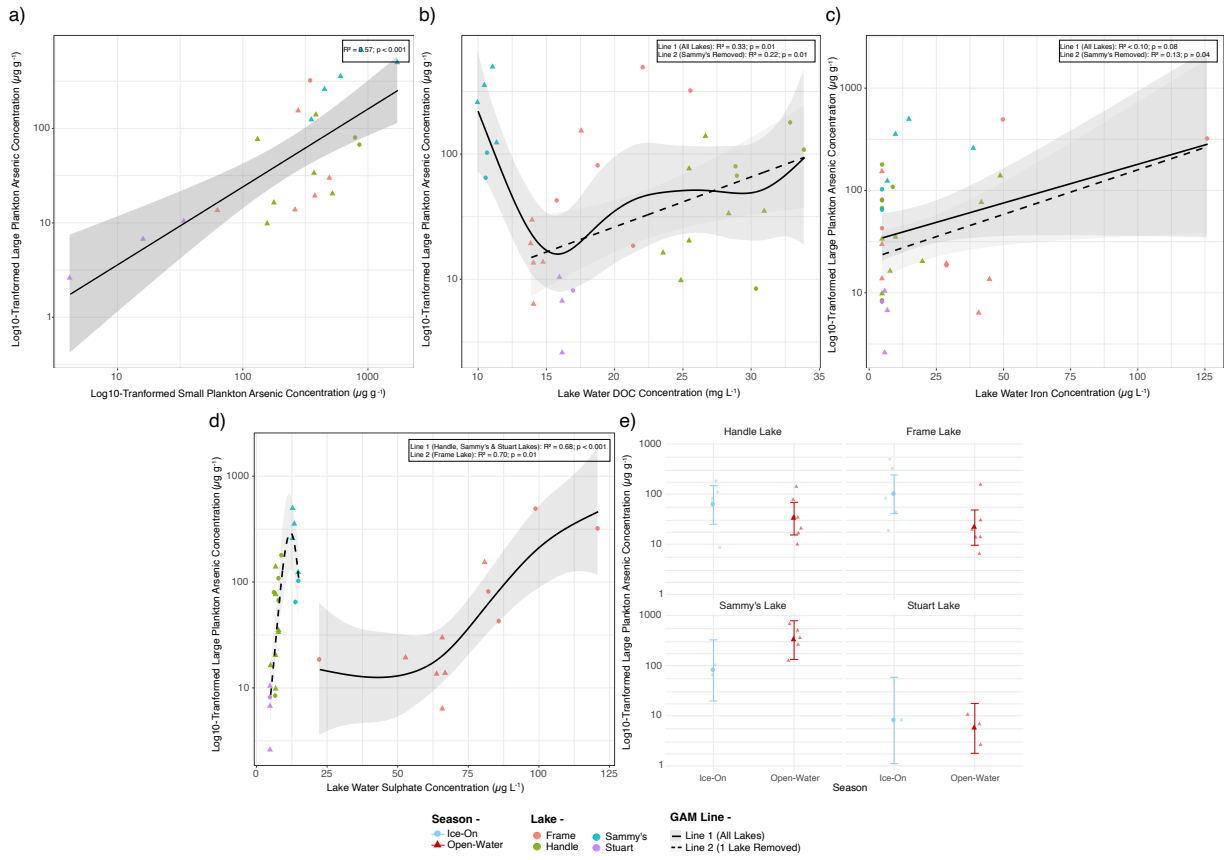


**Figure 4.6.** Environmental variables found to have a statistically significant relationship with large plankton arsenic concentration: a) small plankton arsenic concentration, b) DOC, c) iron, d) sulfate, and e) season.

No variables related to trophic status (nutrients, plankton density, chlorophyll-a) were found to be correlated with arsenic concentrations in large plankton, but arsenic bioaccumulation in large plankton was significantly, positively associated with bioaccumulation in small plankton ($p < 0.001$; $R^2 = 0.57$) (Figure 4.6a). The final MLR model determined that total arsenic, Fe, and small plankton arsenic concentration were the three most important environmental variables for predicting large plankton arsenic bioaccumulation in the study lakes from Yellowknife ($R^2 = 0.72$; p-value < 0.001) (Table S 4-12). The final model was compared to other models in an AIC framework and was found to be best supported by the data (Table S 4-12).

Arsenic concentrations in large plankton were found to be significantly higher during the ice-on season compared to open-water season for Frame Lake ($p = 0.02$), while it was significantly higher in the open-water season for Sammy's Lake ($p < 0.01$). Large plankton arsenic concentrations in Handle Lake and Stuart Lake were not found to be statistically different in the ice-on versus open-water season (Figure 4.6e).

#### *4.4.4.3 Combined Plankton*

The regression tree identified As(III), As(V), and total dissolved phosphorus as potential drivers of arsenic bioaccumulation in the combined plankton category from Jackfish Lake (Figure S 4-1c). The first split occurred at concentrations of As(III) above 0.99 μg $L^{-1}$, with higher levels of arsenic bioaccumulation above 0.99 μg $L^{-1}$ As(III) (Figure S 4-1c). For samples where As(III) was less than 0.99 μg $L^{-1}$ , a second split occurred at an As(V) threshold of 57.5 μg $L^{-1}$, with concentrations above this threshold resulting in lower total arsenic bioaccumulation (Figure S 4-1c). The final variable and split occurred at a concentration of 20.0 μg $L^{-1}$ of phosphorus, with arsenic bioaccumulation higher when phosphorus concentrations were higher Figure S 4-1c). When explored further with LRs and GAMs, no correlations were established between arsenic bioaccumulation and any of these three variables. Similar, no statistical relationships were reported for variables related to trophic status (nutrients, phytoplankton density, chlorophyll-a). There was also no significant difference in arsenic bioaccumulation between the open-water and ice-free season. As no environmental variables were found to be significant drivers of arsenic bioaccumulation in the combined plankton from Jackfish Lake, no final MLR model was created.

## 4.5 Discussion

In this study, we found that water arsenic concentration was only a moderate predictor of arsenic bioaccumulation in plankton, and we consistently reported the highest plankton arsenic concentrations in one of our low-arsenic study lakes (Sammy's Lake). This contrasts with previous studies that documented strong relationships between lake arsenic status and arsenic bioaccumulation in aquatic organisms (Jia et al., 2018; Lepage et al., 2024; Blais et al., 2025). When the data from Sammy's Lake was removed, water arsenic concentration was a stronger predictor of arsenic bioaccumulation in small plankton in the pooled data from Frame Lake, Handle Lake, and Stuart Lake ($R^2 = 0.77$ compared to $R^2 = 0.27$ for total arsenic; $R^2 = 0.75$ compared to $R^2 = 40$ for As(V)). As a comparison, a previous study of four temperate lakes documented a significant relationship ($R^2 = 0.5$) between phytoplankton arsenic concentrations and arsenic concentrations in oxic waters (likely predominantly As(V)), although the arsenic gradient was smaller than our study, with a maximum arsenic concentration of only of 56 μg $L^{-1}$ (Barrett et al., 2018).

Sammy's Lake exhibited the lowest DOC values of all five study lakes, with a mean DOC of 12.6 mg $L^{-1}$ compared to 19.4 mg $L^{-1}$ for the other lakes (Figure S 4-2). DOC was the first variable selected by the regression tree at a threshold of 11.3 mg $L^{-1}$ where low DOC was associated with higher arsenic bioaccumulation in both small plankton and large plankton. DOC was also a significant predictor variable in the final MLR model for small plankton. The relationship between DOC (and dissolved organic matter; DOM) and arsenic in freshwater systems can be complicated, and DOC has been shown to increase arsenic bioavailability under certain conditions, and decrease it under others (Pothier et al., 2020). Humic-rich DOM has a high affinity for arsenic, and studies have found that it decreased the overall bioavailability of

arsenic through coating of cell surfaces, preventing arsenic from entering the cell (Ren et al., 2017; Wang et al., 2020). Another study found that DOM can also form complexes with arsenic that cannot cross the cell membrane due to electrostatic and steric repulsion (Zhang et al., 2022). Our study results, particularly for Sammy's Lake, support the finding that arsenic is more bioavailable in lakes with low DOC.

DOC was not selected as a significant predictor in the MLR model for arsenic bioaccumulation in large plankton (> 63 μm, predominantly zooplankton), and instead arsenic bioaccumulation in small plankton was selected in combination with total arsenic in water and water Fe concentrations. This suggests that exposure through diet is more important for arsenic bioaccumulation in large plankton compared to water As(V) concentrations for bioaccumulation in small plankton. This has been observed in other studies, which have found that arsenic concentrations in contaminated sediment and phytoplankton were more clearly correlated with zooplankton arsenic bioaccumulation than surrounding lake water concentrations (e.g., Barrett et al., 2018; Hull et al., 2023). Arsenic concentrations in our large plankton samples were also lower than arsenic concentrations in the small plankton, consistent with the known bio-diminution tendencies of arsenic (Chen & Folt, 2000; Caumette et al., 2011; 2014; Barret et al., 2018; 2019; Hull et al., 2023; Blais et al., 2025).

Fe and sulphate were also found to have an influence on arsenic bioaccumulation in large plankton in our study, but not the small or combined plankton categories. This may be because these two chemicals are typically higher in concentration towards the sediment-water interface (SWI) especially during periods of thermal stratification and anoxia, and therefore are more accessible to motile, free-swimming plankton such as rotifers and zooplankton, which can cross the density barrier created between the epi- and hypolimnion (i.e., thermocline) more readily

than phytoplankton (Cantin et al., 2011). Both Fe and sulphate have been established as important controllers of arsenic mobility and toxicity in lake water, with Fe often forming As(V)-Fe-oxyhydroxides and surface complexes at the SWI under oxic conditions (Rodie et al., 1995). During periods of anoxia, oxyhydroxides are reduced, and the As(V) that was originally bound is released back into the water column, typically as As(III) (Rodie et al., 1995). Anoxia also results in the release of sulphate which further contributes to the reduction and release of arsenic bound to oxyhydroxides, before being re-sequestered as thio-arsenicals or arsenic-sulfide complexes (Oremland & Stolz, 2003; Kubachka et al., 2009). The relationships between large plankton arsenic bioaccumulation and Fe and sulphate were most prominent in Frame Lake, which undergoes dramatic periods of anoxia during the ice-on season due to high sediment and biological oxygen demand and lake-ice cover (Dirszowsky & Wilson, 2016). Frame Lake also had much higher levels of sulphate compared to the other study lakes (Figure S 4-2).

Plankton bioaccumulation data from Jackfish Lake had to be examined separately from the other four study lakes because we were unable to separate small and large size classes due to the high abundance of the filamentous Cyanobacteria genus *Planktothrix.* No statistically significant relationships were documented for plankton bioaccumulation in Jackfish Lake and any of the environmental variables explored in this study, including lake water arsenic. However, Jackfish Lake plankton arsenic concentrations more comparable to the reference lake (Stuart Lake) than the other lakes, despite have the third highest lake water arsenic values. Jackfish Lake is the most eutrophic of the five study lakes (Figure S 4-2), and higher levels of $PO_4^{3-}$ can limit As(V) uptake by phytoplankton compared to in oligotrophic systems (Levy et al., 2005; Hasegawa et al., 2010). Therefore, our findings for Jackfish Lake in comparison to the other four lakes lends some support to the contention that $PO_4^{3-}$ is an important modulating factor for

influencing the relationship between lake water arsenic and arsenic bioaccumulation (and ultimately bioavailability), although we did not document any statistically significant relationships between phosphorus and other trophic factors in our study.

Lastly, our dataset allowed us to examine potential seasonal patterns in arsenic bioaccumulation in plankton from subarctic lakes. Plankton from Handle Lake (small plankton) and Frame Lake (large plankton) exhibited statistically higher arsenic concentrations during the ice-on season, when arsenic concentrations in water are similarly higher due to under-ice anoxia and solute exclusion during lake-ice formation (Palmer et al., 2019; 2020). This is different from what has been reported in temperate lakes, where arsenic concentrations in water and plankton have been reported to be higher during the summer season (e.g., Barrett et al., 2018). Sammy's Lake behaved more similarly to the temperate lakes reported on in Barrett et al. (2018), with higher plankton arsenic concentrations during the open-water season as opposed to during ice-on, corresponding to higher arsenic concentrations in summer (Figure S 4-3). We also noted an interesting seasonal trend for Sammy's Lake, where arsenic bioaccumulation in both large and small plankton was highest in the samples collected in autumn in both sampling years, demonstrating a significant increase from the June samples. We postulate that this could be related to lake turnover that occurs in the fall, as Sammy's Lake exhibits thermal stratification in late summer that could concentration arsenic in the hypolimnion, which could then be mixed throughout the lake at fall turnover similar to what has been documented for phosphorus (Ghane & Boegman, 2025). Future research could focus on sampling at a higher temporal resolution during this critical transition period.

Overall, the results of this study emphasize that lake water arsenic concentrations may not be a good predictor of bioavailability and bioaccumulation in aquatic organisms, and that low

DOC in particular enhances arsenic bioaccumulation risk in plankton. Our results also highlight the complex ways in which bioaccumulation potential can change with the seasons, in ways that are lake specific. This represents a fruitful area for future research, but one that is challenged by difficulties with collecting sufficient plankton biomass under the ice in winter, especially in cold subarctic lakes.

## 4.6 Supplementary Information

**Table S 4-1.** Sampling coordinate locations, physical characteristics, average total arsenic concentration, and justification for inclusion in study design for the five study lakes.

| Lake | Sampling Coordinates | Size ($km^2$) | Max Depth (m) | Distance to Giant Mine Roaster Stack (km) | Average Total Arsenic Concentration ($\mu g\ L^{-1}$) | Justification for Inclusion in Study |
|---|---|---|---|---|---|---|
| Handle | 62.4916, -114.3959 | 0.2 | 3.8 | 2.5 | 208.4 | High [As], shallow, large seasonal fluxes in [As] |
| Frame | 62.4574, -114.3879 | 0.9 | 6.4 | 6.1 | 205.7 | High [As], large seasonal fluxes in [As], eutrophic |
| Jackfish | 62.4659, -114.3924 | 0.5 | 8.2 | 4.0 | 61.6 | Moderate [As], eutrophic, open year-round |
| Sammy's | 62.4688, -114.5098 | 0.3 | 6.7 | 8.4 | 8.0 | Low [As], low [DOC] |
| Stuart | 62.5168, -113.8214 | 1.0 | 12.0 | 10.2 | 1.3 | Reference (low [As]) |

**Table S 4-2.** Sampling dates for arsenic analysis in lake water and bulk plankton, and plankton for identification purposes. Samples collected indicated with an "X". No sample collected indicated with a "/".

| | Apr '22 | May '22 | Jun '22 | Jul '22 | Aug '22 | Sep '22 | Nov '22 | Jan '23 | Feb '23 | Mar '23 | Apr '23 | May '23 | Jun '23 | Jul '23 | Sep '23 | Oct '23 | Nov '23 | Dec '23 | Jan '24 | Feb '24 | Mar '24 | Apr '24 | Jun '24 |
|---|---|---|---|---|---|---|---|---|---|---|---|---|---|---|---|---|---|---|---|---|---|---|---|
| **Lake Water –** | | | | | | | | | | | | | | | | | | | | | | | |
| Handle | / | X | X | X | X | X | X | X | / | X | X | X | X | X | X | X | X | X | X | / | X | X | X |
| Frame | X | X | X | X | X | X | X | X | / | X | X | X | X | X | X | X | X | X | X | / | X | X | X |
| Jackfish | X | X | X | X | X | X | X | X | X | / | X | X | X | X | X | / | / | X | X | / | X | X | / |
| Sammy's | X | X | X | X | X | X | X | X | X | / | X | X | X | X | X | X | X | X | / | X | X | X | / |
| Stuart | X | X | X | X | X | X | X | / | X | / | X | / | / | / | / | / | / | / | / | / | / | / | / |
| **Plankton ID –** | | | | | | | | | | | | | | | | | | | | | | | |
| Handle | X | X | X | / | / | X | X | / | / | / | X | X | / | / | / | / | / | / | / | / | / | / | / |
| Frame | X | X | X | / | / | X | X | / | / | / | X | X | / | / | / | / | / | / | / | / | / | / | / |
| Jackfish | X | X | X | / | / | X | X | / | / | / | X | X | / | / | / | / | / | / | / | / | / | / | / |
| Sammy's | X | X | X | / | / | X | X | / | / | / | X | X | / | / | / | / | / | / | / | / | / | / | / |
| Stuart | X | X | X | / | / | X | X | / | / | / | X | / | / | / | / | / | / | / | / | / | / | / | / |
| **Small Plankton –** | | | | | | | | | | | | | | | | | | | | | | | |
| Handle | X | X | X | / | / | X | X | / | / | / | X | X | X | / | / | X | X | / | / | / | X | / | X |
| Frame | X | X | X | / | / | X | X | / | / | / | X | X | X | / | / | X | X | / | / | / | X | / | X |
| Sammy's | X | X | X | / | / | X | X | / | / | / | X | X | X | / | / | X | X | / | / | / | X | / | X |
| Stuart | X | X | X | / | / | X | X | / | / | / | X | / | / | / | / | / | / | / | / | / | / | / | / |
| **Large Plankton –** | | | | | | | | | | | | | | | | | | | | | | | |
| Handle | X | X | X | / | / | X | X | / | / | / | X | X | X | / | / | X | X | / | / | / | X | / | X |
| Frame | X | X | X | / | / | X | X | / | / | / | X | X | X | / | / | X | X | / | / | / | X | / | X |
| Sammy's | X | X | X | / | / | X | X | / | / | / | X | X | X | / | / | X | X | / | / | / | X | / | X |
| Stuart | X | X | X | / | / | X | X | / | / | / | X | / | / | / | / | / | / | / | / | / | / | / | / |
| **Combined Plankton –** | | | | | | | | | | | | | | | | | | | | | | | |
| Jackfish | X | X | X | / | / | X | X | / | / | / | X | X | / | / | / | / | / | / | / | / | / | / | / |

**Table S 4-3.** Field blank (FB) data from the four study lakes collected from 2022-2024 (N = 19). Measurements of dissolved arsenic below the method detection limit of 0.2 μg $L^{-1}$ are indicated by < DL.

| Sample Date | Sample ID | Total As (μg $L^{-1}$) |
|---|---|---|
| November 23, 2022 | FB1 | < DL |
| | FB2 | < DL |
| | Reagent Blank 1 | < DL |
| February 9, 2023 | FB1 | < DL |
| | FB2 | < DL |
| February 21, 2023 | FB1 | < DL |
| | FB4 | < DL |
| April 6, 2023 | FB1 | < DL |
| | FB2 | < DL |
| April 21, 2023 | FB1 | < DL |
| | FB2 | < DL |
| July 14, 2023 | FB1 | < DL |
| | FB2 | < DL |
| November 18, 2023 | FB1 | < DL |
| | FB2 | < DL |
| January 23, 2024 | FB1 | < DL |
| | FB2 | < DL |
| February 2, 2024 | FB1 | < DL |
| | FB2 | < DL |

**Table S 4-4.** Field replicate data from Handle and Jackfish Lakes collected in November 2020 and January 2021 using the same sampling methods as described in the paper (N = 4).

| Lake | Sample Date | Depth (m) | Dissolved Arsenic (μg $L^{-1}$) | Relative Percent Difference (%) |
|---|---|---|---|---|
| Handle | November 16, 2020 | 1 | 203 | 0.49 |
| | | 1A | 204 | |
| Jackfish | January 1, 2021 | 4 | 70 | 0.57 |
| | | 4A | 70.4 | |

**Table S 4-5.** Optimization parameters for separation and determination of arsenic species using HPLC-ICP-MS. Samples were separated by HPLC-ICP-MS/MS (Agilent) and quantified using Agilent software (MassHunter 4.6).

| **ICP-MS-MS ( Agilent 8900 ICP-QQQ )** | |
|---|---|
| RF power | 1500 w |
| Plasma gas flow | 15 L $min^{-1}$ |
| Nebulizer (carrier) gas flow | 1.01 L $min^{-1}$ |
| Sampling depth | 8 mm |
| Peristaltic pump speed | 0.4 rps |
| Spray chamber temp | 2°C |
| Collision cell | He @ 5.0 mL $min^{-1}$ (dependent on instrument sensitivity) |
| Data acquisition mode | Time-resolved, m/z 75 for 75As+, and m/z 77 for 40Ar37Cl+ |
| **HPLC Conditions - Agilent 1260** | |
| Column | PRP-X100 Anion Exchange HPLC Column, 4.1 x 250 mm, 10 µm |
| Mobile phase composition | 20 mM (NH4)2HPO4,5mM (NH4H2PO4 ). pH 8.25,2% MeOH |
| Mobile phase flow rate | 1 mL $min^{-1}$ |
| Injection volume | 50 µL |
| Acquisition time | 12 min |

**QA/QC Protocols:** Sequence accuracy was verified by inserting continuous calibration verification (OPR2) standards approximately every 10 samples. To ensure the quality of these measurements, a second source of PTC from Proficiency Testing Canada was used for As(V) quantification. Analyses with dosed additions were used in order to fortify samples to control the percentage recovery of all species as an analytical quality variables. Samples were measured in duplicate to verify the accuracy and reliability of analytical results.

Plankton Biomass Samples –

Data were quantified using Agilent software (MassHunter 4.6). Pure water and aqueous methanol (MeOH; $H_2O$, 50% v/v) were added to 0.1 g of sample. Samples were then placed in a shaker at 100 rpm for 6 hours and centrifuged at 3500 rpm for 20 minutes. The collected supernatant was filtered through an REM lipid cartridge with a vacuum pump in order to remove any lipids present, and the remaining water-soluble species in the aqueous phase was then injected by HPLC-ICP-MS/MS. An enzymatic extracted was performed on some of the later batches in order to improve species solubilization efficiency by denaturing the peptic and lipid bonds for As(III) and As(V). Next, 50 mg of sample was weighed and 20 mg of pepsin was added along with 5 mL of 0.1 M HCl. The solution was mixed via vortexing before being placed on a shaker at 150 rpm (at 37°C) and left overnight. The next day, the solution was sonicated in an ultrasonic bath for 30 minutes, before being centrifuged at 4000 rpm for 20 minutes (Moreda-Piñeiro et al., 2011). The supernatant was filtered to remove lipids and then injected by HPLC-ICP-MS/MS. Blank and certified material recovery data can be found below in QA/QC Table S5.

**Table S 4-6.** Matrix spike and certified material recovery data (% or □g g-1) for each batch of lake water arsenic speciation samples collected from April 2022 to June 2024. As(III) = arsenite, As(V) = arsenate, and ND refers to "no data". Certified reference material acronyms: TORT-3 = lobster hepatopancreas, DORM-4 = dogfish tissue. Control sample acronyms: OPR-2 = ongoing precision and recovery, and PTC = Proficiency Testing Canada. *PTC-1-2025 was fortified with the standard As(III) (second source).

| Sample Date Range | QA/QC Material | Sample # | As(III) (%; μg $g^{-1}$) | As(V) (%; μg $g^{-1}$) |
|---|---|---|---|---|
| Apr – May '22 | PTC-4-2021 | 1 | ND | 104% |
| | | 2 | ND | 101% |
| | | 3 | ND | 103% |
| | TORT-3 | 1 | 0.240 | 0.171 |
| | DORM-4 | 1 | ND | 0.041 |
| | | 2 | ND | 0.043 |
| | ORP-2 | 1 | 115% | 97% |
| | | 2 | 105% | 103% |
| | | 3 | 105% | 115% |
| Jun – Jul '22 | PTC-2022 | 1 | ND | 107% |
| | | 2 | ND | 110% |
| | | 3 | ND | 107% |
| | DORM-4 | 1 | ND | 0.056 |
| | | 2 | ND | 0.056 |
| | | 3 | ND | 0.048 |
| | ORP-2 | 1 | 107% | 104% |
| | | 2 | 108% | 108% |
| | | 3 | 104% | 112% |
| | | 4 | 102% | 105% |
| | Stuart Lake Jun '22 Matrix Spike | 1 | 101% | 99% |
| | | 2 | 107% | 110% |
| Aug – Sep '22 | PTC-2022 | 1 | ND | 107% |
| | | 2 | ND | 107% |
| | | 3 | ND | 99% |
| | DORM-4 | 1 | ND | 0.04 |
| | | 2 | ND | 0.04 |
| | | 3 | ND | 0.04 |
| | ORP-2 | 1 | 100% | 110% |
| | | 2 | 106% | 93% |
| | | 3 | 106% | 106% |
| | | 4 | 106% | 106% |
| | Small Lake Aug '22 Matrix Spike (1 m) | 1 | 107% | 92% |
| | Small Lake Sep '22 Matrix Spike (1 m) | 1 | 107% | 106% |
| Nov '22 – Mar '23 | PTC-2022 | 1 | ND | 102% |
| | | 2 | ND | 94% |
| | | 3 | ND | 98% |
| | | 4 | ND | 101% |
| | DORM-4 | 1 | ND | 0.10 |
| | | 2 | ND | 0.12 |
| | | 3 | ND | 0.11 |
| | | 4 | ND | 0.12 |
| | ORP-2 | 1 | 96% | 93% |
| | | 2 | 100% | 101% |
| | | 3 | 103% | 102% |
| | | 4 | 100% | 104% |
| | Small Lake Feb '23 Matrix Spike (3 m) | 1 | 96% | 103% |
| | Small Lake Feb '23 Matrix Spike (10 m) | 1 | 105% | 101% |
| Apr – Jun '23 | PTC-2022 | 1 | ND | 100% |
| | | 2 | ND | 95% |
| | | 3 | ND | 97% |
| | DORM-4 | 1 | ND | 0.10 |
| | | 2 | ND | 0.11 |
| | | 3 | ND | 0.11 |
| | ORP-2 | 1 | 98% | 100% |
| | | 2 | 106% | 109% |
| | | 3 | 114% | 108% |
| | | 4 | 97% | 116% |

| | | | | |
|---|---|---|---|---|
| Jul ’22 – Feb ‘24 | PTC-2022 | 1 | ND | 100% |
| | | 2 | ND | 104% |
| | | 3 | ND | 109% |
| | | 4 | ND | 105% |
| | ORP-2 | 1 | 112% | 100% |
| | | 2 | 107% | 104% |
| | | 3 | 106% | 109% |
| | | 4 | 98% | 105% |
| | Sammy’s Lake Matrix Spike (1 m) | 1 | 93% | 115% |
| | Sammy’s Lake Matrix Spike (3 m) | 1 | 91% | 106% |
| | Sammy’s Lake Matrix Spike (4 m) | 1 | 93% | 111% |
| | Sammy’s Lake Matrix Spike (5 m) | 1 | 93% | 108% |
| Mar – Apr ‘24 | PTC-2024 | 1 | ND | 102% |
| | | 2 | ND | 96% |
| | | 3 | ND | 102% |
| | | 4 | ND | 96% |
| | ORP-2 | 1 | 97% | 101% |
| | | 2 | 112% | 113% |
| | | 3 | 105% | 104% |
| | Sammy’s Lake Mar ’24 Matrix Spike (1 m) | 1 | 107% | 92% |
| | Sammy’s Lake Apr ’24 Matrix Spike (1 m) | 1 | 112% | 95% |
| Jun ‘24 | PTC-1-2025* | 1 | 109% | 100% |
| | | 2 | 101% | 112% |
| | | 3 | 102% | 95% |
| | | 4 | 107% | 110% |
| | | 5 | 111% | 104% |
| | | 6 | 110% | 92% |
| | | 7 | 102% | 100% |
| | ORP-2 | 1 | 104% | 110% |
| | | 2 | 105% | 113% |
| | | 3 | 101% | 105% |
| | | 4 | 110% | 105% |
| | | 5 | 100% | 107% |
| | | 6 | 108% | 116% |
| | | 7 | 106% | 111% |
| | | 8 | 99% | 103% |
| | | 9 | 97% | 99% |
| | ATR Pore Water 2 Matrix Spike | 1 | 97% | 101% |
| | SCCB Lower Creek Matrix Spike | 1 | 112% | 94% |
| | SCCU Lower Matrix Spike | 1 | 107% | 101% |

**Table S 4-7.** Methods and detection limits (DL) for measured water chemistry variables. ICP-MS stands for inductively coupled plasma-mass spectrometry and ICP-QQQ refers to triple quadrupole ICP-MS.

| Variable | Methods | Units | Detection Limit or Range |
|---|---|---|---|
| As(V) | ICP-QQQ | $\mu g\ L^{-1}$ | 0.05 |
| As(III) | ICP-QQQ | $\mu g\ L^{-1}$ | 0.01 |
| Chlorophyll-a | YSI Multi-Meter Probe | $\mu g\ L^{-1}$ | 0.1 |
| Dissolved Oxygen (DO) | YSI Multi-Meter Probe | $mg\ L^{-1}$ | 0.05 |
| Oxidative-Reduction Potential (ORP) | YSI Multi-Meter Probe | mV | -1,000 – 1,000 |
| pH | YSI Multi-Meter Probe | NA | 0.0 – 14.0 |
| Specific Conductivity | YSI Multi-Meter Probe | $\mu S\ cm^{-1}$ | 0.055 |
| Temperature | YSI Multi-Meter Probe | °C | -40 – 400 |
| Sulphate | Ion Chromatography (SM4110) | $\mu g\ L^{-1}$ | 1 |
| Organic Carbon (Dissolved) | Total Carbon Analyzer (SM 5310) | $mg\ L^{-1}$ | 0.5 |
| Arsenic (Dissolved) | ICP-MS (EPA 200.8) | $\mu g\ L^{-1}$ | 0.2 |
| Iron (Dissolved) | ICP-MS (EPA 200.8) | $\mu g\ L^{-1}$ | 5 |
| Phosphorus (Dissolved) | ICP-MS (EPA 200.8) | $\mu g\ L^{-1}$ | 10 |

**Table S 4-8.** Blank and certified material recovery data for each batch of plankton total arsenic bioaccumulation samples collected from April 2022 to June 2024. ND refers to "no data". Certified reference material acronyms: TORT-3 = lobster hepatopancreas, DORM-4/5 = dogfish tissue. The method detection limit for total arsenic in plankton was 0.002 $\mu g\ g^{-1}$.

| | Blanks ($\mu g\ g^{-1}$) | | | | | DORM-4/5 (%) | | | | | | | TORT-3 (%) | | | | | |
|---|---|---|---|---|---|---|---|---|---|---|---|---|---|---|---|---|---|---|
| **Sample Dates** | **1** | **2** | **3** | **4** | **5** | **1** | **2** | **3** | **4** | **5** | **6** | **7** | **1** | **2** | **3** | **4** | **5** | **6** |
| Apr '22 – Sep '22 | 0.0016 | 0.0014 | 0.0068 | 0.0158 | 0.0079 | 100 | 106 | 97 | 97 | 95 | 94 | 95 | 95 | 95 | 95 | 105 | 104 | 95 |
| Nov '22 – Jun '23 | ND | 0.0051 | 0.0016 | 0.0005 | | 96 | 103 | 104 | | | | | 99 | 100 | 101 | | | |
| Oct '23 – Mar '24 | 0.00061 | 0.00255 | 0.00094 | | | 94 | 94 | 96 | | | | | 102 | 103 | 106 | | | |
| Jun '24 | 0.0014 | 0.0276 | 0.0084 | | | | | | | | | | 102 | 106 | 103 | | | |

**Table S 4-9.** Reference guides for zooplankton and phytoplankton identification.

| Plankton Type | Reference |
|---|---|
| **Zooplankton & Rotifers** | Balcer, M. D., Korda, N. L., & Dodson, S. I. (1982). *Zooplankton of the Great Lakes: a guide to the identification and ecology of the common crustacean species*. Madison, WI: University of Wisconsin Press.<br>Haney, J. F., Aliberti, M. A., Allan, E., Allard, S., Bauer, D. J., Beagen, W., Bradt, S. R., Carlson, B., Carlson, S. C., Doan, U. M., Dufresne, J., Godkin, W. T., Greene, S., Kaplan, A., Maroni, E., Melillo, S., Murby, A. L., Smith (Nowak), J. L., Ortman, B., Quist, J. E., Reed, S., Rowin, T., Schmuck, M., Stemberger, R. S., & Travers, B. (2013). *An image-based key to the zooplankton of North America.* (Version 5). University of New Hampshire Center for Freshwater Biology: Durham, NH. Retrieved from http://cfb.unh.edu/cfbkey/html/ |
| **Phytoplankton** | Baker, A. L., Gretz, M., Coesel, P. F. M., Delwiche, C., Sarnoff, S., Silverside, A., St. Amand, A., Toh, R., & van Egmond, W. (2012). *An image based key to algae (PS Protista), Cyanobacteria, and other aquatic objects.* PhycoKey. Retrieved from https://cfb.unh.edu/phycokey/phycokey.htm<br>Graham, L. E., Graham, J. M., Wilcox, L. W., & Cook, M. E. (Eds). (2016). *Algae.* (3rd ed.). Madison, WI: LJLM Press.<br>Guiry, M. D., & Guiry, G. M. (2024). *AlgaeBase*. Galway, Ireland: National University of Ireland. Retrieved from http://www.algaebase.org<br>Krammer, K., & Lange-Bertalot, H. (1986). *Bacillariophyceae, Part 2, Volume 1: Naviculaceae. Freshwater Flora of Middle Europe*. New York, NY: Gustav Fischer Publisher.<br>Krammer, K., & Lange-Bertalot, H. (1988). *Bacillariophyceae, Part 2, Volume 2: Bacillariaceae, Epithemiaceae, Surirellaceae. Freshwater Flora of Middle Europe*. New York, NY: Gustav Fischer Publisher.<br>Krammer, K., & Lange-Bertalot, H. (1991a). *Bacillariophyceae, Part 2, Volume 3: Centrales, Fragilariaceae, Eunotiaceae. Freshwater Flora of Middle Europe*. Struttgart, Germany: Gustav Fischer Publisher.<br>Krammer, K., & Lange-Bertalot, H. (1991b). *Bacillariophyceae, Part 2, Volume 4: Achnanthaceae, Critical Supplement to Navicula (Lineolatae) and Gomphonema, Complete List of Literature for Volumes 1-4. Freshwater Flora of Middle Europe*. Stuttgart, Germany: Gustav Fischer Publisher.<br>PhycoTech. (2017). *PhycoTech image collection.* St. Joseph, MI: PhycoTech. Retrieved from: <https://phycotech.smugmug.com/2017-Image-Library/AlgaeOtherMicroscopicTaxa/Algae><br>Prescott, G. W. (1962). *Algae of the western great lakes area: with an illustrated key to the genera of desmids and freshwater diatoms*. Dubuque, IA: Wm. C. Brown Company Publishers.<br>Prescott, G. W. (1954). *How to know the fresh-water algae.* Dubuque, IA: Wm. C. Brown Company Publishers.<br>Rosen, B. H., & St. Amand, A. (2015). *Field and laboratory guide to freshwater cyanobacteria harmful algal blooms for Native American and Alaska Native Communities* (U.S. Geological Survey Open-File Report 2015–1164). http://dx.doi.org/10.3133/ofr20151164<br>Spaulding, S., & Edlund, M. (2024). *Diatoms of North America*. Retrieved from https://diatoms.org |

**Table S 4-10.** Plankton arsenic bioaccumulation sample duplicate data. Y = Yes to a duplicate available for a specific sample, while N = No. / = no sample available for that date. Samples found to be lacking a duplicate or thought to have potential QA/QC concerns are flagged with an asterisk (*). More information on all flagged samples is found below in Table S 4-11.

| Lake | Plankton Category | Apr '22 | May '22 | Jun '22 | Sep '22 | Nov '22 | Apr '23 | May '23 | Jun '23 | Oct '23 | Nov '23 | Mar '24 | Jun '24 |
|---|---|---|---|---|---|---|---|---|---|---|---|---|---|
| Handle | Small | / | / | Y | Y | / | Y* | Y* | Y | Y | Y* | / | Y |
| | Large | Y | Y | Y | N* | N* | N* | Y | Y | Y | Y | Y | Y |
| Frame | Small | N* | N* | Y | Y | / | / | / | Y | Y | / | / | Y |
| | Large | N* | N* | Y | Y | Y | Y | N* | Y | Y | Y | N* | Y |
| Sammy's | Small | / | N* | Y | Y | / | / | / | Y | N* | / | / | Y |
| | Large | / | / | Y | Y | / | / | / | Y | Y | Y | Y | Y |
| Stuart | Small | / | N* | Y | N* | / | / | / | / | / | / | / | / |
| | Large | N* | N* | Y | Y | / | / | / | / | / | / | / | / |
| Jackfish | Combined | Y* | Y | Y | Y | Y | Y | Y | / | / | / | / | / |

**Table S 4-11.** Plankton arsenic bioaccumulation samples flagged for potential QA/QC issues with a statement about why they were found to be acceptable.

| Lake | Plankton Category | Sample Date | Duplicate Available (Y/N) | Comment on Potential Quality Issue(s) |
|---|---|---|---|---|
| Handle | Small | Apr '23 | Y | Minimum mass requirement not met for one sample, but duplicate values are very close to one another (S1 - 796.5 μg $g^{-1}$ / S2 - 800.0 μg $g^{-1}$) |
| | | May '23 | Y | Minimum mass requirement not met for either sample, but sample concentrations follow expected seasonal pattern of being lower than late winter values but higher than summer values (S1 – 480.2 μg $g^{-1}$ / S2 – 572.5 μg $g^{-1}$) |
| | | Nov '23 | Y | Minimum mass requirement not met for either sample, but sample concentrations follow expected seasonal pattern of being higher than summer values (S1 – 561.2 μg $g^{-1}$ / S2 – 1,167.2 μg $g^{-1}$) |
| | Large | Sep '22 | N | No duplicate sample available, but sample concentration follows expected seasonal pattern of being higher than summer values; same pattern observed the following year (137.6 μg $g^{-1}$) |
| | | Nov '22 | N | Did not meet minimum mass requirement and no duplicate sample available, but sample concentration follows expected seasonal pattern of being lower than fall values; same pattern observed the following year although the value is lower in 2022 compared to 2023 (8.3 μg $g^{-1}$) |
| | | Apr '23 | N | No duplicate sample available, but sample concentration follows expected seasonal pattern of being higher than summer values (78.9 μg $g^{-1}$) |
| Frame | Small | Apr '22 | N | No duplicate sample available, but sample concentration is similar to concentration of following sample from May '22; low winter biomass due to anoxia and within acceptable concentration range (349.3 μg $g^{-1}$) |
| | | May '22 | N | No duplicate sample available, but sample concentration is similar to concentration of previous sample from Apr '22; low winter biomass due to anoxia; follows unique trend in Frame Lake which sees the surface layer increase in total arsenic slightly from spring thaw to early summer; also within acceptable concentration range (381.0 μg $g^{-1}$) |
| | Large | Apr '22 | N | No duplicate sample available and value much higher than following year, however the winter of 2022 was significantly colder than 2023 with a longer ice-on duration and other samples from the late winter/early spring thaw transition period were also much lower; sample also follows expected seasonal pattern of being higher than summer values (2022 – 317.7 μg $g^{-1}$ / 2023 – 16.6 – 21.1 μg $g^{-1}$) |
| | | May '23 | N | No duplicate sample available but also follows unique trend in Frame Lake which sees the surface layer increase in total arsenic slightly from spring thaw to early summer; also within acceptable concentration range (6.3 μg $g^{-1}$) |
| | | Mar '24 | N | Did not meet minimum mass requirement and no duplicate sample available, however concentration follows expected trend of being high in the winter and especially in Frame Lake under more anoxic conditions (487.9 μg $g^{-1}$) |
| Sammy's | Small | May '22 | N | No duplicate but sample concentrations follows expected seasonal pattern of being lower in the spring thaw period compared to summer values(124.5 μg $g^{-1}$) |

| | | | | |
|---|---|---|---|---|
| | | Oct ‘23 | N | No duplicate but sample concentration follows expected seasonal pattern of being higher than summer values (891.3 μg $g^{-1}$) |
| Stuart | Small | May ‘22 | N | No duplicate but sample concentrations follows expected seasonal pattern of being lower than late winter values but higher than summer values (16.1 μg $g^{-1}$) |
| | | Sep ‘22 | N | No duplicate but sample concentrations follows expected seasonal pattern of being higher at this time of year (34.1 μg $g^{-1}$) |
| | Large | Apr ‘22 | N | No duplicate but sample concentrations follows expected seasonal pattern of being higher than summer values (8.1 μg $g^{-1}$) |
| | | May ‘22 | N | No duplicate but sample concentrations follows expected seasonal pattern of being lower than late winter values but higher than summer values (6.7 μg $g^{-1}$) |
| Jackfish | Combined | Apr ‘22 | Y | Triplicate samples were available for this sampling date, but one was significantly lower and behaved differently than the others so it was removed (Removed Sample Total As: 0.4 μg $g^{-1}$ vs S1 – 1.8 μg $g^{-1}$ & S2 – 1.7 μg $g^{-1}$). |

**Table S 4-12.** Results of the final models run for each plankton category based off of the environmental drivers found to be significant predictors of arsenic bioaccumulation. Models were compared in an AIC framework and found to have smaller values than their null model counterparts. *Value after Sammy's Lake was removed (AIC beforehand = 44.3).

| Plankton Type | Variables Included | p-value | $R^2$ Value | Final AIC Value | Null Model AIC Value |
|---|---|---|---|---|---|
| Small | -Total Arsenic<br>-As(V)<br>-DOC | < 0.001 | 0.77 | 12.8* | 40.8 |
| Large | -Total Arsenic<br>-Iron<br>-Small Plankton Arsenic Concentration | < 0.001 | 0.72 | 19.5 | 21.7 |

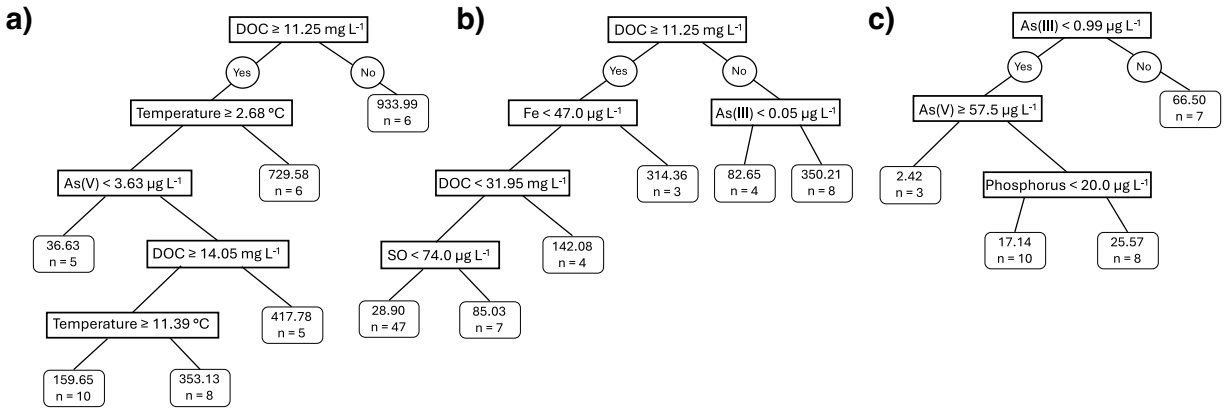


**Figure S 4-1.** Results of regression tree analyses identifying which environmental variables best explain total arsenic concentrations in each of the three plankton size categories: a) small plankton, b) large plankton, and c) combined plankton (Jackfish Lake only).

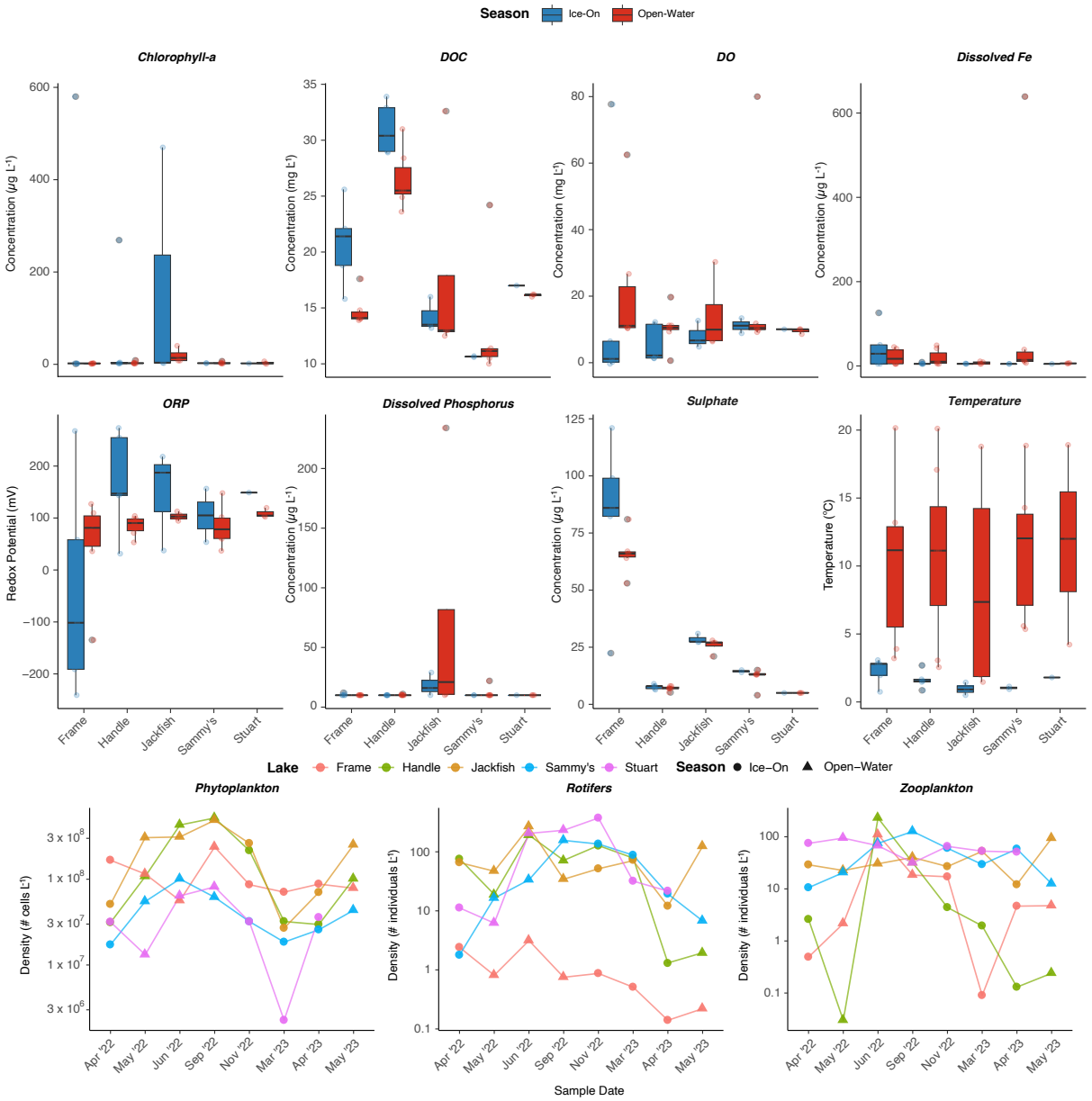


**Figure S 4-2.** Boxplots indicating the range of important environmental variables in the five study lakes with emphasis on the differences in concentration during the ice-on and open-water season and scatterplots indicating plankton density.

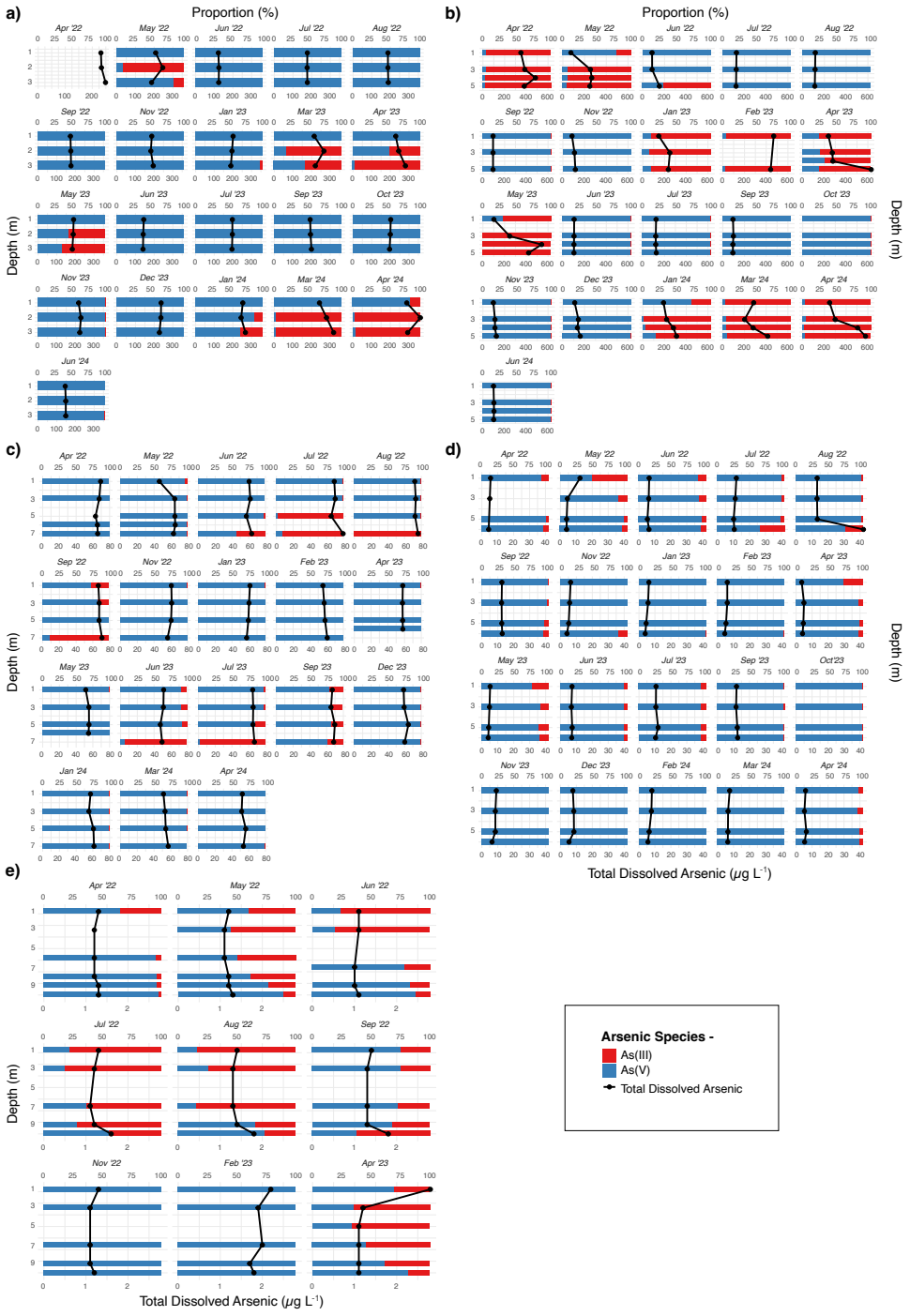


**Figure S 4-3.** The seasonal cycling of total dissolved arsenic (black line) and its two major inorganic forms – As(V) (blue) and As(III) (red) in the five study lakes: a) Handle, b) Frame, c) Jackfish, d) Sammy's, and e) Stuart. Samples were collected from April 2022 - June 2024. In certain situations samples could not be taken, such as: April 2022 from Handle Lake (equipment malfunction) and May 2023 from Stuart Lake (unsafe ice conditions).

# Chapter 5: Conclusions & Future Directions

## 5.1 Conclusions

The overall goal of this dissertation research was to investigate the biogeochemical cycling of arsenic, and its paired ecological implications, in lakes contaminated by legacy mining activities in the Yellowknife (Northwest Territories, Canada) region. I was particularly interested in exploring seasonal patterns in arsenic concentration, form, and bioavailability, as well as its linkages with plankton community dynamics in five lakes that span gradients in arsenic and other key limnological variables. Two key, novel findings emerged from this research: (1) Most studies on arsenic in lakes are based on summer sampling, but the winter and seasonal transitional periods may be more relevant for arsenic bioavailability and ecotoxicity; and (2) Total arsenic concentrations in lake water did not strongly correlate with arsenic bioaccumulation in plankton, which suggests that other lake-specific factors (particularly dissolved organic carbon (DOC)) influenced the overall bioavailability of arsenic across the five study lakes. This dissertation provides new data on associations between arsenic and individual zooplankton and phytoplankton taxa, including data on specific arsenic species (e.g., As(V), As(III)) that are not routinely measured in arsenic toxicity studies. When considered collectively, the results from Chapters 2, 3, and 4 highlight the importance of sampling across seasons, particularly in subarctic lakes which remain ice-covered for the majority of the year.

The results from Chapter 2 showed that the ice-on season was characterized by higher inorganic arsenic concentrations (particularly As(III)) compared to the open-water season in the two most heavily contaminated lakes. Multivariate analysis and generalized additive models highlighted that phytoplankton and zooplankton communities were structured along arsenic gradients when under-ice sampling is included, with phytoplankton associated with As(V) and

zooplankton associated with As(III). Cyanobacteria and cyclopoid copepods (specifically *Diacyclops thomasi*) were observed to be more prominent in the highly contaminated lakes compared to the reference and less contaminated lakes, and were both observed to have higher relative abundances during the ice-on season when arsenic concentrations were highest. This suggests that these taxa are more tolerant of arsenic, while the herbivorous crustacean zooplankton taxa *Bosmina* and *Daphnia* were more sensitive. Winter is already a period of increased stress on plankton communities independent of arsenic, since light, food (for zooplankton), and dissolved oxygen (DO) can all become limiting with the onset of lake ice cover and water temperatures are colder. This leads to natural, seasonal shifts in plankton community structure (e.g., low-light adapted, motile phytoplankton (Henshaw & Laybourn-Parry, 2002), zooplankton capable of overwintering (Grosbois et al., 2017)) outside of, or interacting with, potential influence from arsenic toxicity. While this chapter attempted to qualitatively tease out the influence of seasonal plankton succession through the use of a reference lake and comparison with the scientific literature, additional inquiry is needed to better untangle the potential effects of arsenic on winter plankton communities (described in more detail below in Section 5.2).

Chapter 3 focused exclusively on the spring thaw transition as a short but dynamic period of ecosystem change that has important implications for both arsenic biogeochemical cycling and under-ice plankton ecology. Spring thaw was characterized by inputs of oxygenated snow and ice meltwater into the surface layers of the study lakes. This diluted total arsenic concentrations in the most contaminated lakes but was a source of arsenic contamination to the least contaminated lakes (i.e., arsenic concentrations under-ice increased with snowmelt inputs). Notably, this chapter documented proliferation of phytoplankton density under the ice corresponding to the

onset of spring thaw, which occurred as total arsenic conditions and As(III) were elevated. A high proportion of juvenile zooplankton were also recorded during this time, which is a life stage likely to be more vulnerable to arsenic exposure. Although transient, the arsenic-plankton interactions during spring thaw may set the stage for open-water plankton community dynamics. This chapter also provided novel data on organic arsenic, the less toxic forms of arsenic produced by aquatic microorganisms, which was observed to increase alongside phytoplankton density in one of the two sampling years (2022).

Chapter 4 examined arsenic concentrations in bulk plankton tissues to investigate seasonal and inter-lake differences in arsenic bioavailability. Lake water arsenic and As(V) concentrations were found to be only moderate predictors of total arsenic bioaccumulation in plankton across the five study lakes. Arsenic bioaccumulation in plankton was consistently highest in Sammy's Lake, despite it being one of the least contaminated of the five study lakes. Statistical analyses indicated that DOC may be an important variable for influencing arsenic bioavailability, and Sammy's Lake exhibited the lowest DOC values among the five lakes. Within Sammy's Lake, plankton arsenic concentrations were highest during autumn based on two years of data collection, the only lake to clearly exhibit this pattern. While the reasons for this seasonal pattern are unclear (partial lake mixing events or evapoconcentration dynamics are posed as potential explanatory mechanisms), this finding underscores the need for sampling efforts at higher temporal resolution during periods of rapid, biogeochemical and ecological change. Chapter 3 focused on the spring thaw as a potentially important period of rapid limnological change, and the results from Chapter 4 suggests that the fall lake turnover period should also be explored.

## 5.2 Future Directions

Chapter 2 documented that Cyanobacteria were much more dominant in the five Yellowknife-area study lakes than what has been reported in other studies from the region (Moore et al., 1980; Cederwall & Cott, 2025). Cyanobacteria have been reported to be more resistant to arsenic than other plankton groups (Miyashita et al., 2016), but the study methodology used in Chapter 2 was not designed to test a causal linkage between arsenic concentrations and Cyanobacteria abundance. Future research specific to the Yellowknife region could explore associations between Cyanobacteria and arsenic across broader spatial and temporal scales to better resolve potential correlations between Cyanobacteria and arsenic as a foundation for additional mechanistic studies. Long-term records are unavailable for plankton in the Yellowknife region, but a paleolimnological approach could be used to indirectly infer or reconstruct phytoplankton (and Cyanobacteria) dynamics over time (Erratt et al. 2026). For example, algal pigment signatures are preserved in lake sediments and can be analyzed via high performance liquid chromatography (HPLC) or visible near-infrared reflectance spectroscopy (VNIRS) (Errat et al., 2026). Such an analysis could reveal if pigments derived from Cyanobacteria increased (either in absolute concentration or relative abundance) after the onset of arsenic pollution, which could represent a form of pollution-induced community tolerance ((PICT); Blanck et al., 1988) to arsenic. If there is no temporal association between Cyanobacteria and arsenic pollution, the higher abundance of Cyanobacteria in these lakes could instead represent a form of natural resilience to arsenic pollution if Cyanobacteria are indeed more resistant to arsenic. In either case, the association between Cyanobacteria and arsenic implicated in Chapter 2 is worth exploring further to better understand the legacy ecological impacts of and recovery from mining pollution.

While paleolimnological techniques can help identify ecological responses to contaminants through time, the plankton communities preserved in lake sediments tend to be skewed towards summer communities due to higher plankton densities during this time of the year, and therefore are less applicable for assessing environmental changes associated with seasonal (particularly winter) dynamics (Smol, 2008). This thesis focused on five lakes, with repeated sampling across seasons over two years, to better understand seasonal dynamics. A complementary approach would be to increase the number of study lakes to span broader spatial and limnological gradients, but with fewer sampling events. Our research team collected water samples for phytoplankton, rotifers, zooplankton, and water chemistry (including total, inorganic, and organic arsenic variables) from 50 lakes across the Yellowknife region in July 2022. The 50 lakes were chosen to span gradients that are important for arsenic ecotoxicity, including arsenic concentrations, lake depth, trophic status, and DOC. This is a rich dataset that can be used to further characterize plankton-arsenic associations and test hypotheses about species tolerances and plankton communities of arsenic contaminated lakes derived from the findings of Chapter 2. These same lakes could also be re-sampled in winter, to capture ecological and biogeochemical conditions under-ice as a snapshot comparison to the open-water season.

A third recommendation for potential future research that arose from the dissertation findings is to investigate (using a higher temporal-resolution sampling effort) the transitional period from late summer into early fall , which is when potential lake turnover (or smaller partial mixing) events occur as the surface waters of lakes begin to cool. Arsenic has been found to be released from the sediment-water interface (SWI) during periods of thermal stratification and anoxic conditions (Barrett et al., 2018; 2019). This remobilized arsenic can build up in the hypolimnion over the summer, until it is mixed into the rest of the water column during fall

turnover (Barrett et al., 2018; 2019). This is one potential explanatory mechanism for the increase in plankton arsenic bioaccumulation observed in autumn in Sammy's Lake in two different years of study. This observation, however, is only based on a comparison of early summer and early fall, with the intervening summer period not captured in the sampling design. Higher resolution sampling over the summer months, including capturing the period before, during, and after fall lake turnover, would allow for a better understanding of the influence of thermal mixing regimes on arsenic cycling and plankton uptake dynamics (i.e., bioavailability). This is especially relevant as climate change is expected to alter lake thermal stratification dynamics (Woolway et al., 2022).

Overall, this dissertation highlights the new insights that can be derived from studies that integrate metal(loid) biogeochemistry and plankton ecology while incorporating seasonal dynamics. The focus here was on subarctic Yellowknife-lakes that are ice-covered for approximately half the year. The approach used in this dissertation could be applied in arsenic-contaminated lakes from other climatic zones in future study, collectively building a knowledge foundation that can be synthesized to examine the influence of climate and seasons on arsenic cycling and ecotoxicity in freshwater systems more broadly. A more nuanced understanding of ecological patterns and processes in legacy metal(loid)-contaminated systems can lead to better processes for environmental assessments at proposed mine sites, ensuring that the lessons from the past support more sustainable development in future.

# References


Akter, K. F., Owens, G., Davey, D. E., & Naidu, R. (2005). Arsenic speciation and toxicity in biological systems. *Reviews of Environmental Contamination and Toxicology, 184,* 97–149.

Alekseev, V. (2025). Diapause in Cladocera: Mechanisms of induction, termination and seasonal information accumulation. *Journal of Plankton Research, 47*(6), fbaf056. https://doi.org/10.1093/plankt/fbaf056

Allen, M. R., VanDyke, J. N., & Cáceres, C. (2011). Metacommunity assembly and sorting in newly formed lake communities. *Ecology, 92*(2), 269-275. https://doi.org/10.1890/10-0522.1

Amyot, M., Bélanger, D., Simon, D. F., Chételat, J., Palmer, M., & Ariya, P. (2021). Photooxidation of arsenic in pristine and mine-impacted Canadian subarctic freshwater systems. *Journal of Hazardous Materials Advances, 2*, 100006. https://doi.org/10.1016/j.hazadv.2021.100006

Aránguiz-Acuña, A., & Serra, M. (2016). Diapuase as escape strategy to exposure to toxicants: response of Brachionus calyciforus to arsenic. *Ecotoxicology, 25*(4), 708-719. https://doi.org/10.1007/s10646-016-1629-7

Arsic, M., Teasdale, P. R., Welsh, D. T., Johnston, S. G., Burton, E. D., Hockmann, K., & Bennett, W. W. (2018). Diffusive gradients in thin films (DGT) reveals antimony and arsenic mobility differs in a contaminated wetland sediment during an oxic-anoxic transition. *Environmental Science & Technology, 52*, 1118–1127. https://doi.org/10.1021/acs.est.7b03882

Astles, B. C., Chételat, J., Palmer, M. J., & Vermaire, J. C. (2022). Experimental investigation of short-term warming on arsenic flux from contaminated sediments of two well-oxygenated subarctic lakes. *PLoS ONE, 17*(12), e0279412. https://doi.org/10.1371/journal.pone.0279412

Babanazarova, O., Sidelev, S., & Schischeleva, S. (2013). The structure of winter phytoplankton in Lake Nero, Russia, a hypertrophic lake dominated by Planktothrix-like Cyanobacteria. *Aquatic Biosystems, 9*(18). https://doi.org/10.1186/2046-9063-9-18

Baker, A. L., Gretz, M., Coesel, P. F. M., Delwiche, C., Sarnoff, S., Silverside, A., St. Amand, A., Toh, R., & van Egmond, W. (2012). *An image based key to algae (PS Protista), Cyanobacteria, and other aquatic objects.* PhycoKey. https://cfb.unh.edu/phycokey/phycokey.htm

Balcer, M. D., Korda, N. L., & Dodson, S. I. (1982). *Zooplankton of the Great Lakes: a guide to the identification and ecology of the common crustacean species*. University of Wisconsin Press.

Barral-Fraga, L., Barral, M. T., MacNeill, K. L., Martiña-Prieto, D., Morin, S., Rodríguez-Castro, M. C., Tuulaikhuu, B.-A., & Guasch, H. (2020). Biotic and abiotic factors influencing arsenic biogeochemistry and toxicity in fluvial ecosystems: A review. *International Journal of Environmental Research and Public Health, 17,* 2331. https://doi.org/10.3390/ijerph17072331

Barrett, P. M., Hull, E. A., Burkart, K., Hargrave, O., McLean, J., Taylor, V. F., Jackson, B. P., Gawel, J. E., & Neumann, R. B. (2019). Contrasting arsenic cycling in strongly and weakly stratified contaminated lakes: Evidence for temperature control on sediment-water arsenic fluxes. *Limnology and Oceanography, 64*(3), 1333-1346. https://doi.org/10.1002/lno.11119

Barrett, P. M., Hull, E. A., King, C. E., Burkart, K., Ott, K. A., Ryan, J. N., Gawel, J. E., & Neumann, R. B. (2018). Increased exposure of plankton to arsenic in contaminated weakly-stratified lakes. *Science of the Total Environment, 625*, 1606-1614. https://doi.org/10.1016/j.scitotenv.2017.12.336

Basu, A., Culpepper, J., Blagrave, K., & Sharma, S. (2024). Phenological shifts in lake ice cover across the Northern Hemisphere: A glimpse into the past, present, and the future of lake ice phenology. *Water Resources Research*, *60*(9), https://doi.org/10.1029/2023WR036392

Battuello, M., Mussat Sartor, R., Brizio, P., Nurra, N., Pessani, D., Abete, M. C., & Squadrone, S. (2017). The influence of feeding strategies on trace element bioaccumulation in copepods (*Calanoida*). *Ecological Indicators, 74,* 311-320. https://doi.org/10.1016/j.ecolind.2016.11.041

Belzile, C., Vincent, W. F., Gibson, J. A., & Hove, P. V. (2001). Bio-optical characteristics of the snow, ice, and water column of a perennially ice-covered lake in the High Arctic. *Canadian Journal of Fisheries and Aquatic Sciences, 58*, 2405–2418. https://doi.org/10.1139/cjfas-58-12-2405

Benson, B., Magnuson, J., & Sharma, S. (2013). Global Lake and River Ice Phenology Database, (Version 1) [Dataset]. National Snow and Ice Data Center (NSIDC). https://doi.org/10.7265/N5W66HP8

Bergmann, M. A., & Welch, H. E. (1985). Spring meltwater mixing in small arctic lakes. *Canadian Journal of Fisheries and Aquatic Sciences, 42*, 1789–1798. https://doi.org/10.1139/f85-224

Biesinger, K. E., & Christensen. G. M. (1972). Effects of various metals on survival, reproduction, and metabolism of Daphnia magna. *Canadian Journal of Fisheries and Aquatic Sciences, 29*, 125.

Blais, J. M., Yumvihoze, E., & Chan, H. M. (2025). Foodweb dynamics affect arsenic speciation and bioaccumulation in lakes affected by gold mines. *Environmental Pollution, 372,* 125999. https://doi.org/10.1016/j.envpol.2025.125999

Blanck, H., Wängberg, S.-Å., & Molander, S. (1988). Pollution-induced community tolerance – A new ecotoxicological tool. In J. Cairns Jr. & J. R. Pratt (Eds.), *Functional testing of aquatic biota for estimating hazards of chemicals* (ASTM STP 988, pp. 219-230). American Society for Testing and Materials.

Block, B. D., Denfield, B. A., Stockwell, J. D., Flaim, G., Grossart, H.-P. F., Knoll, L. B., Maier, D. B., North, R. L., Rautio, M., Rusak, J. A., Sadro, S., Weyhenmeyer, G. A., Bramburger, A. J., Branstrator, D. K., Salonen, K., & Hampton, S. E. (2019). The unique methodological challenges of winter limnology. *Limnology and Oceanography: Methods, 17*, 42-57. https://doi.org/10.1002/loem3.10295

Branstrator, D. K., Salonen, K., & Hampton, S. E. (2019). The unique methodological challenges of winter limnology. *Limnology and Oceanography: Methods, 17*(1), 42-57. https://doi.org/10.1002/lom3.10295

Bouvet, C., Beauregard, P. B., & Guéguen, C. (2025). Low-temperature biodegradation of freshwater dissolved organic matter during winter-to-spring transition. *Frontiers in Environmental Science, 12,* 1524626. https://doi.org/10.3389/fenvs.2024.1524626

Bullen, W., & Robb, M. (2006). Economic contribution of gold mining in the Yellowknife Mining District. In C. D. Anglin, H. Falck, D. F. Wright & Ambrose, E. .J. (Eds.), *Gold in the Yellowknife Greenstone Belt, Northwest Territories: Results of the EXTECH III multidisciplinary research project*. (Geological Association of Canada Special Publication No. 3, pp. 38-39). Mineral Deposits Division. Geological Association of Canada.

Burnham, K. P., & Anderson, D. R. (2002). Model selection and multimodel inference: a practical information-theoretic approach. (2nd ed). Springer.

Canadian Council of Ministers of the Environment [CCME]. (2003). *Canadian water quality guidelines for the protection of aquatic life: Summary table.* In: *Canadian environmental quality guidelines.* (1999).

Cantin, A., Beisner, B. E., Gunn, J. M., Prairie, Y. T., & Winter, J. G. (2011). Effects of thermocline deepening on lake plankton communities. *Canadian Journal of Fisheries and Aquatic Sciences, 68*(2), 260-276. https://doi.org/10.1139/F10-138

Caumette, G., Koch, I., Estrada, E., & Reimer, K. J. (2011). Arsenic speciation in plankton organisms from contaminated lakes: Transformations at the base of the freshwater food chain. *Environmental Science & Technology, 45,* 9917-9923. https://doi.org/10.1021/es2025092

Caumette, G., Koch, I., House, K., & Reimer, K. J. (2014). Arsenic cycling in freshwater phytoplankton and zooplankton cultures. *Environmental Chemistry.* https://doi.org/10.1071/EN14039

Caumette, G., Koch, I., Moriarty, M., & Reimer, K. J. (2012a). Arsenic distribution and speciation in Daphnia pulex. *Science of the Total Environment, 432*, 243–250. https://doi.org/10.1016/j.scitotenv.2012.05.050

Caumette, G., Koch, I., & Reimer, K. J. (2012b). Arsenobetaine formation in plankton: a review of studies at the base of the aquatic food chain. *Journal of Environmental Monitoring, 14*, 2841-2853. https://doi.org/10.1039/c2em30572k

Cavaliere, E., & Baulch, H. M. (2021). Winter in two phases: Long-term study of a shallow reservoir in winter. *Limnology and Oceanography*, *66*(4), 1335-1352. https://doi.org/10.1002/lno.11687

Cederwall, J., & Cott, P. A. (2025). Rapidly increasing cyanobacteria blooms in the subarctic Great Slave Lake: observations from Indigenous, local, and scientific knowledge. *Scientific Reports, 15*, 24492. https://doi.org/10.1038/s41598-025-07432-5

Chang, K.-H., Doi, H., Nishibe, Y., & Nakano, S.-i. (2010). Feeding habits of omnivorous Asplanchna: comparison of diet composition among Asplanchna herricki, A. priodonta, and A. girodi in pond ecosystems. *Journal of Limnology, 69*(2), 209-216. https://doi.org/jlimnol.2010.209

Chen, C. Y., & Folt, C. L. (2000). Bioaccumulation and diminution of arsenic and lead in a freshwater food web. *Environmental Science and Technology, 34*, 3878 – 3884. https://doi.org/10.1021/es991070c

Chen, G., Shi, H., Tao, J., Chen, L., Liu, Y., Lei, G., Liu, X., & Smol, J. P. (2015). Industrial arsenic contamination causes catastrophic changes in freshwater ecosystems. *Scientific Reports*, *5*, 17419. https://doi.org/10.1038/srep17419

Chen, Y., Wang, Z., Luo, Z., Zhao, Y., & Yu, J. (2022). Decreasing arsenic accumulation but promoting arsenate biotransformation in *Microcystis aeruginosa* regulated by nano-$Fe_2O_3$. *Environmental Science and Pollution Research, 29,* 62423-62431. https://doi.org/10.1007/s11356-022-20042-2

Cheney, C. L., Eccles, K. M., Kimpe, L. E., Thienpont, J. R., Korosi, J. B., Blais, J. M. (2020). Determining the effects of past gold mining using a sediment palaeotoxicity model. *Science of the Total Environment, 718*: 137308. https://doi.org/10.1016/j.scitotenv.2020.137308

Cohen, J. (1988). *Statistical power analysis for the behavioral sciences.* (2nd Ed.). Lawrence Erlbaum Associates.

Creed, J. T., Brockhoff, C. A., & Martin, T. D. (1994). *Method 200.8, revision 5.4: Determination of trace elements in waters and wastes by inductively coupled plasma – mass spectrometry*. United Statues Environmental Protection Agency.

Crognale, S., Zecchin, S., Amalfitano, S., Fazi, S., Casentini, B., Corsini, A., Cavalca, L., & Rossetti, S. (2017). Phylogenetic structure and metabolic properties of microbial communities in arsenic-rich waters of geothermal origin. *Frontiers in Microbiology, 8,* 2468. https://doi.org/10.3389/fmicb.2017.02468

Connon, R. E., Geist, J., & Werner, I. (2012). Effect-based tools for monitoring and predicting the ecotoxicological effects of chemicals in the aquatic environment. *Sensors, 12*, 12741-12771. https://doi.org/10.3390/s120912741

Cousens, B. L. (2000). Geochemistry of the Archean Kam Group, Yellowknife Greenstone Belt, Slave Province, Canada. *The Journal of Geology, 108*: 181-197.

Couture, R. M., Gobeil, C., & Tessier, A. (2010). Arsenic, iron and sulfur co-diagenesis in lake sediments. *Geochimica et Cosmochimica Acta, 74*(4), 1238-1255.

Cullen, W. R., & Reimer, K. J. (1989). Arsenic speciation in the environment. *Chemical Reviews. 89*(4), 713-764.

De Vitre, R., N. Belzile, & Tessier, A. (1991). Speciation and adsorption of arsenic on diagenetic iron oxyhydroxides. *Limnology and Oceanography, 36*, 1480–1485. https://doi.org/10.4319/lo.1991.36.7.1480

Devkota, N., Salis, R. K., & Hansson, L.-A. (2025). Warming of shallow temperate lakes: consequences for rotifer community composition and population dynamics. *Hydrobiologia, 852,* 971-985. https://doi.org/10.1007/s10750-024-05744-7

Dirszowsky, R. W., & Wilson, K. M. (2016). Biogeochemical evidence of eutrophication and metal contamination of Frame Lake, City of Yellowknife, Northwest Territories, Canada. *Environmental Earth Sciences, 75,* 76. https://doi.org/10.1007/s12665-015-4852-2

Dixit, S., & Hering, J. G. (2003). Comparison of arsenic(V) and arsenic(III) sorption onto iron oxide minerals: Implications for arsenic mobility. *Environmental Science and Technology, 37*, 4182–4189. https://doi.org/10.1021/es030309t

Domaizon, I., Winegardner, A., Capo, E., Gauthier, J., & Gregory-Eaves, I. (2017). DNA-based methods in paleolimnology: new opportunities for investigating long-term dynamics of lacustrine biodiversity. *Journal of Paleolimnology, 58,* 1-21. https://doi.org/10.1007/s10933-017-9958-y

Dormann, C. F., Elith, J., Bacher, S., Buchmann, C., Carl, G., Carré, G., Marquéz, J. R. G., Gruber, B., Lafourcade, B., Leitão, P. J., Münkemüller, T., McClean, C., Osborne, P. E., Reineking, B., Schröder, B., Skidmore, A. K., Zurell, D., & Lautenbach, S. (2013). Collinearity: a review of methods to deal with it and a simulation study evaluating their performance. *Ecography, 36*(1), 27-46. https://doi.org/10.1111/j.1600-0587.2012.07348.x

Ecosystem Classification Group. (2009). *Ecological regions of the Northwest Territories*. Department of Environment and Natural Resources. Government of the Northwest Territories.

Edmonds, J. S., Shibata, Y., Francesconi, K. A., Rippingale, R. J., & Morita, M. (1998). Arsenic transformations in short marine food chains studied by HPLC-ICP-MS. *Applied Organometallic Chemistry, 11*(4), 281-287. https://doi.org/10.1002/(SICI)1099-0739(199704)11:4<281::AID-AOC581>3.0.CO;2-S

Elith, J., Leathwick, J. R., & Hastie, T. (2008). A working guide to boosted regression trees. *Journal of Animal Ecology, 77*(4), 802-813. https://doi.org/10.1111/j.1365-2656.2008.01390.x

Environment and Climate Change Canada [ECCC]. (2025). *Canadian Climate Normals 1991-2020 Data*. Government of Canada. https://climate.weather.gc.ca/climate_normals/results_1991_2020_e.html?searchType=stnProv&lstProvince=&txtCentralLatMin=0&txtCentralLatSec=0&txtCentralLongMin=0&txtCentralLongSec=0&stnID=419000000&dispBack=0

Environmental Protection Agency [EPA]. (1984). *Ambient water quality criteria for arsenic* (Rep. 440/5-84-033). United States Environmental Protection Agency.

Errat, K. J., Creed, I. F., Blais, J. M., Favot, E. J., Gushulak, C. A. C., Korosi, J. B., McMullin, D. R., Rego, L. W., Simmatis, B., Sivarajah, B., Vinebrooke, R. D., Wood, S. A., & Smol, J. P. (2026). Paleolimnology uncovers environmental drivers of cyanobacterial blooms, species shifts and toxin emergence. *Harmful Algae, 154,* 103089. https://doi.org/10.1016/j.hal.2026.103089

Faria, M. C. d. S., Hott, R. d. C., Santos, M. J. d., Santos, M. S., Andrade, T. G., Bomfeti, C. A., Rocha, B. A., Barbosa, F., Jr., & Rodrigues, J. L. (2023). Arsenic in mining areas: Environmental contamination routes. *International Journal of Environmental Research and Public Health, 20*, 4291. https://doi.org/10.3390/ijerph20054291

Fernández-Aláez, C., Fernández-Aláez, M., López-Vázquez, M., & García-Girón, J. (2026). Local environmental and spatial processes, not land use, shape the taxonomic and functional structure of pond zooplankton communities. *Aquatic Sciences, 88*(44). https://doi.org/10.1007/s00027-026-01275-6

Francesconi, K. A., & Edmonds, J. S. (1998). Arsenic species in marine samples. *Croatica Chemica Acta, 71*(2), 343-359.

Gabyshev, V. A., Sidelev, S. I., Chernova, E. N., Vilnet, A. A., Davydov, D. A., Barinova, S., Gabysheva, O. I., Zhakovskaya, Z. A., & Voronov, I. V. (2023). Year-round presence of microcystins and toxin-producing *Microcystis* in the water column and ice cover of a eutrophic lake located in the continuous permafrost zone (Yakutia, Russia). *Toxins (Basel), 15*(7), 467. https://doi.org/10.3390/toxins15070467

Gavel, M. J., Patterson, R. T., Nasser, N. A., Galloway, J. M., Hanna, B. W., Cott, P. A., Roe, H. M., & Falck, H. (2018). What killed Frame Lake? A precautionary tale for urban planners. *PeerJ,* 4850. https://doi.org/10.7717/peerj.4850

Ghane, A., & Boegman, L. (2025). Vertical mixing, light penetration and phosphorus cycling regulate seasonal algae blooms in an ice-covered dimictic lake. *Journal of Geophysical Research: Biogeosciences*, *130*(1), e2024JG008258. https://doi.org/10.1029/2024JG008258

Government of Canada. (2022). *What's happening at Giant Mine? September to December 2022*. Crown-Indigenous Relations and Northern Affairs Canada. https://www.rcaanc-cirnac.gc.ca/eng/1671719019334/1671719068612

Graham, L. E., Graham, J. M., Wilcox, L. W., & Cook, M. E. (Eds). (2016). *Algae.* (3rd ed.). LJLM Press.

Greenberg, A. E., Clesceri, L. S., & Eaton, A. D. (Eds.). (1992). *Standard methods for the examination of water and wastewater.* (18th ed.). American Public Health Association.

Grosbois, G., Mariash, H., Schneider, T., & Rautio, M. (2017). Under-ice availability of phytoplankton lipids is key to freshwater zooplankton winter survival. *Scientific Reports, 7,* 11543. https://doi.org/10.1038/s41598-017-10956-0

Gu, B. (2012). Stable isotopes as indicators for seasonally dominant nitrogen cycling processes in a subarctic lake. *International Review of Hydrobiology, 97*(3), 233-243. https://doi.org/10.1002/iroh.201111466

Guiry, M. D., & Guiry, G. M. (2024). *AlgaeBase*. National University of Ireland. http://www.algaebase.org

Hampton, S. E., Galloway, A. W. E., Powers, S. M., Ozersky, T., Woo, K. H., Batt, R. D., Labou, S. G., O'Reilly, C. M., Sharma, S., Lottig, N. R., Stanley, E. H., North, R. L., Stockwell, J. D., Adrian, R., Weyhenmeyer, G. A., Arvola, L., Baulch, H. M., Bertani, I., Bowman Jr., L. L., Carey, C. C., Catalan, J., Colom-Montero, W., Domine, L. M., Felip, M., Granados, I., Gries, C., Grossart, H.-P., Haberman, J., Haldna, M., Hayden, B., Higgins, S. N., Jolley, J. C., Kahilainen, K. K., Kaup, E., Kehoe, M. J., MacIntyre, S., Mackay, A. W., Mariash, H. L., McKay, R. M., Nixdorf, B., Nõges, P., Nõges, T., Palmer, M., Pierson, D. C., Post, D. M., Pruett, M. J., Rautio, M., Read, J. S., Roberts, S. L., Rücker, J., Sadro, S., Silow, E. A., Smith, D. E., Sterner, R. W., Swann, G. E. A, Timofeyev, M. A., Toro, M., Twiss, M. R., Vogt, R. J., Watson, S. B., Whiteford, E. J., & Xenopoulos, M. A. (2017). Ecology under lake ice. *Ecology Letters, 20*(1), 98-111. https://doi.org/10.1111/ele.12699

Hampton, S. E., Moore, M. V., Ozersky, T., Stanley, E. H., Polashenski, C. M., & Galloway, A. W. E. (2015). Heating up a cold subject: prospects for under-ice plankton research in lakes. *Journal of Plankton Research, 37*(2), 277-284. https://doi.org/10.1093/plankt/fbv002

Haney, J. F., Aliberti, M. A., Allan, E., Allard, S., Bauer, D. J., Beagen, W., Bradt, S. R., Carlson, B., Carlson, S. C., Doan, U. M., Dufresne, J., Godkin, W. T., Greene, S., Kaplan, A., Maroni, E., Melillo, S., Murby, A. L., Smith (Nowak), J. L., Ortman, B., Quist, J. E., Reed, S., Rowin, T., Schmuck, M., Stemberger, R. S., & Travers, B. (2013). *An image-based key to the zooplankton of North America.* (Version 5). University of New Hampshire Center for Freshwater Biology. http://cfb.unh.edu/cfbkey/html/

Hasegawa, H., Akhyar, O., Omori, Y., Kato, Y., Kosugi, C., Miki, O., Mashio, A. S., & Papry, R. I. (2022). Role of Fe plaque on arsenic biotransformation by marine macroalgae. *Science of the Total Environment, 802,* 149776. https://doi.org/10.1016/j.scitotenv.2021.149776

Hasegawa, H., Papry, R.. I., Ikeda, E., Omori, Y., Mashio, A. S., Maki, T., & Rahman, M. A. (2019). Freshwater phytoplankton: biotransformation of inorganic arsenic to methylarsenic and organoarsenic. *Scientific Reports, 9,* 12074. https://doi.org/10.1038/s41598-019-48477-7

Hasegawa, H., Rahman, M. A., Kitahara, K., Itaya, Y., Maki, T., & Ueda, K. (2010). Seasonal changes of arsenic speciation in lake waters in relation to eutrophication. *Science of the Total Environment, 408*, 1684-1690. https://doi.org/10.1016/j.scitotenv.2009.11062

Hasegawa, H., Rahman, M. A., Matsuda, T., Kitahara, T., Maki, T., & Ueda, K. (2009). Effect of eutrophication on the distribution of arsenic species in eutrophic and mesotrophic lakes. *Science of the Total Environment, 407*(4), 1418-1425. https://doi.org/10.1016/j.scitotenv.2008.10.024

Hastie, T., & Tibshirani, R. (1987). Generalized additive models: some applications. *Journal of the American Statistical Association, 82*(398), 371-386.

Hazuková, V., Burpee, B. T., McFarlane-Wilson, I., & Saros, J. E. (2021). Under ice and early summer phytoplankton dynamics in two arctic lakes with differing DOC. *Journal of Geophysical Research: Biogeosciences, 126,* e2020JG005972. https://doi.org/10.1029/2020JG005972

He, W., Megharaj, M. & Naidu, R. (2009). Toxicity of tri- and penta-valent arsenic, alone and in combination, to the cladoceran *Daphnia carinata*: the influence of microbial transformation in natural waters. *Environmental Geochemistry and Health, 31,* 133-141. https://doi.org/10.1007/s10653-008-9239-9

Hébert, M.-P., Beisner, B. E., Rautio, M., & Fussmann, G. F. (2021). Warming winters in lakes: later ice onset promotes consumer overwintering and shapes springtime planktonic foodwebs. *Proceedings of the National Academy of Sciences, 118*(48), e2114840118. https://doi.org/10.1073/pnas.2114840118

Hellweger, F. L., Farley, K. J., Lall, U., & Di Toro, D. M. (2003). Greedy algae reduce arsenate. *Limnology and Oceanography, 48*, 2275–2288. https://doi.org/10.4319/Lo.2003.48.6.2275

Henshaw, T., & Laybourn-Parry, J. (2002). The annual patterns of photosynthesis in two large, freshwater, ultra-oligotrophic Antarctic lakes. *Polar Biology, 25*, 744–752.

Hirano, S., Kobayashi, Y., Cui, X., Kanno, S., Hayakawa, T., & Shraim, A. (2004). The accumulation and toxicity of methylated arsenicals in endothelial cells: important roles of thiol compounds. *Toxicology and Applied Pharmacology, 198*, 458–467.

Hocking, D., Kuchar, P., Plambeck, J. A., & Smith, R. A. (1978). The impact of gold smelter emissions on vegetation and soils of a sub-Arctic forest-tundra transition ecosystem. *Journal of the Air Pollution Control Association, 28*, 133-137.

Hollibaugh, J. T., Carini, S., Gürleyük, H., Jellison, R., Joye, S. B., LeCleir, G., Meile, C., Vasquez, L., & Wallschläger, D. (2005). Arsenic speciation in Mono Lake, California: response to seasonal stratification and anoxia. *Geochimica et Cosmochimica Acta, 69*(8), 1925-1937. https://doi.org/10.1016/j.gca.2004.10.011

Houben, A. J., D'Onofrio, R., Kokelj, S. V., & Blais, J. M. (2016). Factors affecting elevated arsenic and methyl mercury concentrations in small shield lakes surrounding gold mines near the Yellowknife, NT, (Canada) region. *PLoS ONE, 11*(4), e0150960. https://doi.org/10.1371/journal.pone.0150960

Huang, J.-H. (2014). Impact of microorganisms on arsenic biogeochemistry: a review. *Water, Air, & Soil Pollution, 225*, 1848. https://doi.org/10.1007/s11270-013-1848-y

Hughes, M. F. (2002). Arsenic toxicity and potential mechanisms of action. *Toxicology Letters, 133*, 1–16.

Hull, E. A., Stiling, R. R., Barajas, M., Neumann, R. B., Olden, J. D., & Gawel, J. E. (2023). Littoral sediment arsenic concentrations predict arsenic trophic transfer and human health risk in contaminated lakes. *PLoS ONE, 18*(10), e0293214. https://doi.org/10.1371/journal.pone.0293214

Hupfer, M., & Lewandowski, J. (2008). Oxygen controls the phosphorus release from lake sediments a long-lasting paradigm in limnology. *International Review of Hydrobiology, 93*, 415e432. https://doi.org/10.1002/iroh.200711054

Hurlbert, S. H. (1984). Pseudoreplication and the design of ecological field experiments. *Ecological Monographs, 54*(2), 187-211.

Hrycik, A. R., McFarland, S., Morales-Williams, A., & Stockwell, J. D. (2022). Winter severity shapes spring plankton succession in a small, eutrophic lake. *Hydrobiologia, 849,* 2127-2144. https://doi.org/10.1007/s10750-022-04854-4

Jackson, T. A., & Bistricki, T. (1995). Selective scavenging of copper, zinc, lead, and arsenic by iron and manganese oxyhydroxide coatings in plankton in lakes polluted with mine and smelter wastes: Results of energy dispersive X-ray micro-analysis. *Journal of Geochemical Exploration, 52,* 97-125.

Jasiak, I., Wilklund, J. A., Leclerc, E., Telford, J. V., Couture, R. M., Venkiteswaran, J. J., Hall, R. I., & Wolfe, B. B. (2021). Evaluating spatiotemporal patterns of arsenic, antimony, and lead deposition from legacy gold mine emissions using lake sediment records. *Applied Geochemistry, 134*, 105053. https://doi.org/10.1016/j.apgeochem.2021.105053

Jia, Y., Wang, L., Li, S., Cao, J., & Yang, Z. (2018). Species-specific bioaccumulation and correlated health risk of arsenic compounds in freshwater fish from a typical mine-impacted river. *Science of the Total Environment, 625,* 600-607. https://doi.org/10.1016/j.scitotenv.2017.12.328

Johnson, D. L., & Pilson, M. E. Q. (1975). The oxidation of arsenite in seawater. *Environmental Letters, 8*(2), 157-171. https://doi.org/10.1080/00139307509437429

Karpowicz, M., Ejsmont-Karabin, J., Kozłowska, Feniova, I., & Dzialowski, A. R. (2020). Zooplankton community responses to oxygen stress. *Water,* 12*(3),* 706. https://doi.org/10.3390/w12030706

Katz, S. L., Izmest'eva, L. R., Hampton, S. E., Ozerksy, T., Shchapov, K., Moore, M. V., Shimaraeva, S. V., & Silow, E. A. (2022). The "Melosira years" of Lake Baikal: Winter environmental conditions at ice onset predict under-ice algal blooms in spring. *Limnology and Oceanography,* 60*(6),* 1950-1964. https://doi.org/10.1002/lno.10143

Kers, E., Leu, E., Amundsen, P.-A., Primicerio, R., Kainz, M., & Poste, A. E. (2024). Under ice plankton and lipid dynamics in a subarctic lake. *Journal of Plankton Research, 46,* 323-337. https://doi.org/10.1093/plankt/fbae018

Korte, N. E., & Fernando, Q. (1991). A review of arsenic (III) in groundwater. *Critical Reviews in Environmental Control,* 21*(1),* 1-39. https://doi.org/10.1080/10643389109388408

Krammer, K., & Lange-Bertalot, H. (1986). *Bacillariophyceae, Part 2, Volume 1: Naviculaceae. Freshwater Flora of Middle Europe*. Gustav Fischer Publisher.

Krammer, K., & Lange-Bertalot, H. (1988). *Bacillariophyceae, Part 2, Volume 2: Bacillariaceae, Epithemiaceae, Surirellaceae. Freshwater Flora of Middle Europe*. Gustav Fischer Publisher.

Krammer, K., & Lange-Bertalot, H. (1991a). *Bacillariophyceae, Part 2, Volume 3: Centrales, Fragilariaceae, Eunotiaceae. Freshwater Flora of Middle Europe*. Gustav Fischer Publisher.

Krammer, K., & Lange-Bertalot, H. (1991b). *Bacillariophyceae, Part 2, Volume 4: Achnanthaceae, Critical Supplement to Navicula (Lineolatae) and Gomphonema, Complete List of Literature for Volumes 1-4. Freshwater Flora of Middle Europe*. Gustav Fischer Publisher.

Korosi, J. B., Little, A. J., Palmer, M. J., & Amyot, M. (2026). *Under-ice water chemistry and plankton community data collected at the onset of spring thaw in four arsenic-contaminated subarctic lakes in 2022 and 2023.* Borealis. https://doi.org/10.5683/SP3/33378A

Kubachka, K. M., Kohan, M. C., Herbin-Davis, K., Creed, J. T., & Thomas, D. J. (2009). Exploring the in vitro formation of trimethylarsine sulfide from dimethylthioarsinic acid in anaerobic microflora of mouse cecum using HPLC-ICP-MS and HPLC-ESI-MS. *Toxicology and Applied Pharmacology, 239*(2), 137-143. https://doi.org/10.1016/j.taap.2008.12.008

Kwong, Y., T., J., Beauchemin, S., Hossain, M., F., & Gould, W., D. (2007). Transformation and mobilization of arsenic in the historic Cobalt mining camp, Ontario, Canada. *Journal of Geochemical Exploration, 92*(2-3), 133-150. https://doi.org/10.1016/j.gexplo.2006.08.002

Lepage, A. T., Lescord, G. L., Lock, A., Johnston, T. A., Gandhi, J., & Gunn, J. M. (2024). Biodilution of organic species of arsenic in freshwater food webs. *Environmental Toxicology and Chemistry, 43*(4), 833-846. https://doi.org/10.1002/etc.5817

Legendre, P., & Gallagher, E. D. (2001). Ecologically meaningful transformations for ordination of species data. *Oecologia, 129,* 271–280. https://doi.org/10.1007/s004420100716

Legendre, P., & Legendre, L. (2012). *Numerical ecology.* (3rd ed.). Elsevier.

Lepš, J., & Šmilauer, P. (2003). *Multivariate analysis of ecological data using CANOCO.* Cambridge University Press.

Levy, J. L., Stauber, J. L., Adams, M. S., Maher, W. A., Kirby, J. K., & Jolley, D. F. (2005). Toxicity, biotransformation, and mode of action of arsenic in two freshwater microalgae (*Chlorella* sp. and *Monoraphidium arcuatum*). *Environmental Toxicology and Chemistry, 24*, 2630–2639. https://doi.org/10.1897/04-580R.1

Liao, C.-M., Jau, S.-F., Chen, W.-Y., Lin, C.-M., Jou, L.-J., Liu, C.-W., Liao, V. H.-C., & Chang, F.-J. (2008). Acute toxicity and bioaccumulation of arsenic in freshwater clam *Corbicula fluminea. Environmental Toxicity, 23*(6), 702-711. https://doi.org/10.1002/tox.20376

Linge, K. L., & Oldham, C. E. (2001). Interference from arsenate when determining phosphate by the malachite green spectrophotometric method. *Analytica Chimica Acta, 450*(1-2), 247-252. https://doi.org/10.1016/S0003-2670(01)01388-5

Little, A. J., Sivarajah, B., Frendo, C., Sprague, D. D., Smol, J. P. & Vermaire, J. C. (2020). The impacts of century-old, arsenic-rich mine tailings on multi-trophic level biological assemblages in lakes from Cobalt (Ontario, Canada). *Science of the Total Environment, 709,* 136212. https://doi.org/10.1016/j.scitotenv.2019.136212

Little, A. J., Palmer, M. J., Amyot, M., & Korosi, J. B. (2026). Under-ice ecological and biogeochemical dynamics at the onset of spring thaw in four arsenic-contaminated subarctic lakes. *Journal of Geophysical: Biogeosciences, 131,* e2025JGR009231. https://doi.org/10.1029/2025JG009231

Liu, T. & Zhang, L. (2023). Multigenerational effects of arsenate on development and reproduction in marine copepod *Tigripus japonicus*. *Chemosphere, 342,* 140158. https://doi.org/10.1016/j.chemosphere.2023.140158

Macháček, J., & Seda, J. (2013). Over-wintering Daphnia: Uncoupling the effects of temperature and food on offspring size and filtering screen morphology in D. galeata. *Journal of Plankton Research, 35*(5), 1069–1079.

McCune, B., & Grace, J. B. (2002). Analysis of Ecological Communities. MjM Software Design.

Mihalik, A., Chapman, J., Adams, R. A., Winter, N. R., Ferreira, F. S., Shawe-Taylor, J., & Mourão-Miranda. (2022). Canonical correlation analysis and partial least squares for identifying brain-behaviour associations: A tutorial and a comparative study. *Biological Psychiatry: Cognitive Neuroscience and Neuroimaging, 7,* 1055-1067. https://doi.org/10.1016/j.bpsc.2022.07.012

Miyashita, S., Fujiwara, S., Tsuzuki, M., & Kaise, T. (2012). Cyanobacteria produce arsenosugars. Environmental Chemistry, *9*(5), 474-484. https://doi.org/10.1071/EN12061

Miyashita, S.-I., Murota, C., Kondo, K., Fujiwara, S., & Tsuzuki, M. (2016). Arsenic metabolism in cyanobacteria. *Environmental Chemistry, 13,* 577-589. http://doi.org/10.1071/EN15071

Moore, J. W. (1980). Seasonal cycles of zooplankton and related phytoplankton development in three shallow, mesotrophic lakes in northern Canada. *Internationale Revue der gesamten Hydrobiologie und Hydrographie, 65*(3), 357-378.

National Research Council [NRC]. (1999). *Arsenic in drinking water*. National Academy Press.

Nikolaidis, N. P., Dobbsb, G. M., Chenc, J., & Lackovicc, J. A. (2004). Arsenic mobility in contaminated lake sediments. *Journal of Environmental Pollution, 129*(3), 479-487.

O'Reilly, K. (2015). Liability, Legacy, and Perpetual Care: Government Ownership and Management of the Giant Mine, 1999–2015. In Keeling, A. & Sandlos, J. (Eds.), *Mining and communities in Northern Canada: History, politics, and memory.* University of Calgary Press.

Obuekwe, I., Vaz, M. G. M. V., Veloso, R., Mello, J. V., & Ogugbue, C. J. (2024). Impact of arsenate on the growth and metabolism of cyanobacterial strains isolated from gold-mining areas. *Discover Applied Sciences, 6*(292). https://doi.org/10.1007/s42452-024-05966-3

Office of the Auditor General of Canada [OAGC]. (2024). *Contaminated sites in the north. Report 1. Independent Auditor's Report.* Reports of the Commissioner of the Environment and Sustainable Development to the Parliament of Canada. https://www.canada.ca/content/dam/oag-bvg/2021-2024-reports/documents/parl_cesd_202404_01_e.pdf

Oksanen, J., Guillaume, F. B., Friendly, M., Kindt, R., Legendre, P., McGlinn, D., Minchin, P. R., O'Hara, R. B., Simpson, G. L., Solymos, P., Stevens, M. H. H., Szoecs, E., & Wagner. H. (2019). *vegan: Community ecology package.* (R package version 2.5-6). [Computer software]. https://CRAN.R-project.org/package=vegan

Oremland, R. S., & Stolz, J. F. (2003). The ecology of arsenic. *Science, 300:* 939-944.

Paktunc, D. (2013). Mobilization of arsenic from mine tailings through reductive dissolution of goethite influence by organic cover. *Applied Geochemistry, 36,* 49-56. https://doi.org/10.1016/j.apgeochem.2013.05.012

Palmer, M. J., Chételat, J., Jamieson, H. E., McClelland, C., & Daly, S. (2025). Archived government correspondence reveals extreme arsenic pollution of local waterbodies from gold mining at Yellowknife, NT prior to environmental regulation. *FACETS, 10*, 1-15. https://doi.org/10.1139/facets-2024-0349

Palmer, M. J., Chételat, J., Jamieson, H. E., Richardson, M., & Amyot, M. (2020). Hydrologic control on winter dissolved oxygen mediates arsenic cycling in a small subarctic lake. *Limnology and Oceanography, 66*(S1), S30-S46. https://doi.org/10.1002/lno.11556

Palmer, M. J., Chételat, J., Richardson, M., Jamieson, H. E., & Galloway, J. M. (2019). Seasonal variation of arsenic and antimony in surface waters of small subarctic lakes impacted by legacy mining pollution near Yellowknife, NT, Canada. *Science of the Total Environment, 684*, 326-339. https://doi.org/10.1016/j.scitotenv.2019.05.258

Palmer, M. J., Galloway, J. M., Jamieson, H. E., Patterson, R. T., Falck, H., & Kokelj, S. V. (2015). *The concentration of arsenic in lake waters of the Yellowknife area*. Northwest Territories Geological Survey. (NWT Open File 2015-06).

Palmer, M. J., Richardson, M., Chételat, J., Spence, C., Connon, R., & Jamieson, H. E. (2024). Watershed hydrology mediates the recovery of an arsenic impacted subarctic landscape. *Environmental Pollution, 358*, 124480. https://doi.org/10.1016/j.envpol.2024.124480

Passino, D. R. M., & Novak, A. J. (1984). Toxicity of arsenate and DDT to the cladoceran *Bosmina longirostris*. *Bulletin of Environmental Contamination and Toxicology, 33*, 325-329.

Patel, A., Tiwari, S., & Prasad, S. M. (2021). Arsenate and arsenite-induced inhibition and recovery in two diazotrophic cyanobacteria *Nostoc muscorum* and *Anabaenea sp*.: study on time-dependent toxicity regulation. *Environmental Science and Pollution Research, 28(37),* 51088-51104. https://doi.org/10.1007/s11356-021-13800-1

Persaud, A. A., Cheney, C. L., Sivarajah, B., Blais, J. M., Smol, J. P. & Korosi, J. B. (2019). Regional changes in Cladocera (Branchiopoda, Crustacea) assemblages in subarctic (Yellowknife, Northwest Territories, Canada) lakes impacted by historic gold mining activities. *Hydrobiologia, 848*, 6. https://doi.org/10.1007/s10750-021-04534-9

Phillips, D. J. H. (1990). Arsenic in aquatic organisms: a review, emphasizing chemical speciation. *Aquatic Toxicology, 16*, 151-186.

Phillips, K. A., & Fawley, M. W. (2002). Winter phytoplankton community structure in three shallow temperate lakes during ice cover. *Hydrobiologia, 470,* 97-113.

PhycoTech. (2017). *PhycoTech image collection.* PhycoTech. https://phycotech.smugmug.com/2017-Image-Library/AlgaeOtherMicroscopicTaxa/Algae

Planas, D., & Healey, F. P. (1978). Effects of arsenate on growth and phosphorus metabolism of phytoplankton. *Journal of Phycology, 14*, 337-341.

Popowich, A., Zhang, Q., & Le, X. C. (2016). Arsenobetaine: the ongoing mystery. *National Science Review, 3,* 451-458. https://doi.org/10.1093/nsr/nww061

Pothier, M. P., Hinz, A. J., & Poulain, A. J. (2018). Insights into arsenite and arsenate uptake pathways using a whole cell biosensor. *Frontiers in Microbiology, 9,* 2310. https://doi.org/10.3389/fmicb.2018.02310

Pothier, M. P., Lenoble, V., Garnier, C., Misson, B., Rentmeister, C., & Poulain, A. J. (2020). Dissolved organic matter controls of arsenic bioavailability to bacteria. *Science of the Total Environment*, *716*, 137118. https://doi.org/10.1016/j.scitotenv.2020.137118

Prescott, G. W. (1962). *Algae of the western great lakes area: with an illustrated key to the genera of desmids and freshwater diatoms*. Wm. C. Brown Company Publishers.

Prescott, G. W. (1954). *How to know the fresh-water algae.* Wm. C. Brown Company Publishers.

R Core Team. (2020). R: a language and environment for statistical computing (Version 2024.12.0+467). [Software]. R. https://www.R-project.org/

Rahman, M. A., Hogan, B., Duncan, E., Doyle, C., Krassoi, R., Rahman, M. M., Naidu, R., Lim, R. P., Maher, W., & Hassler, C. (2014). Toxicity of arsenic species to three freshwater organisms and biotransformation of inorganic arsenic by freshwater phytoplankton (*Chlorella* sp. CE-35). *Ecotoxicology and Environmental Safety, 106,* 126-135. https://doi.org/10.1016/j.ecoenv.2014.03.004

Rahman, M. A., Hasegawa, H., & Lim, R. P. (2012). Bioaccumulation, biotransformation and trophic transfer of arsenic in the aquatic food chain. *Environmental Research, 116,* 118-135. https://doi.org/10.1016/j.envres.2012.03.014

Rahman, M. A., & Hassler, C. (2014). Is arsenic biotransformation a detoxification mechanisms for microorganisms? *Aquatic Toxicology, 146,* 212-219. https://doi.org/10.1016/j.aquatox.2013.11.009

Rantanen, M., Karpechko, A. Y., Lipponen, A., Nordling, K., Hyvärinen, O., Ruosteenoja, K., Vihma, T., & Laaksonen, A. (2022). The Arctic warmed nearly four times faster than the globe since 1979. *Communications: Earth and Environment, 3*(168). https://doi.org/10.1038/s43247-022-00498-3

Reinl, K. L., Harris, T. D., North, R. L., Almela, P., Berger, S. A., Bizic, M., Burnet, S. H., Grossart, H.-P., Ibelings, B. W., Jakobsson, E., Knoll, L. B., Lafrancois, B. M., McElarney, Y., Morales-Williams, A. M., Obertegger, U., Ogashawara, I., Paule-Mercado, M. C., Peierls, B. L., Rusak, J. A., Sarkar, S., Sharma, S., Trout-Haney, J. V., Urrutia-Cordero, P., Venkiteswaran, J. J., Wain, D. J., Warner, K., Weyhenmeyer, G. A., & Yokota, K. (2023). Blooms also like it cold. *Limnology and Oceanography Letters, 8,* 546-564. https://doi.org/10.1002/lol2.10316

Ren, J., Fan, W., Wang, X., Ma, Q., Li, X., Xu, Z., & Wei, C. (2017). Influences of size-fractionated humic acids on arsenite and arsenate complexation and toxicity to *Daphnia magna*. *Water Research, 108,* 68-77. https://doi.org/10.1016/j.watres.2016.10.052

Rodie, A., Gerits, J. J. P., & Azcue, J. M. (1995). Biogeochemical pathways of arsenic in lakes. *Environmental Reviews*, *3*(3–4), 304–317. https://doi.org/10.1139/a95-016

Rosen, B. H., & St. Amand, A. (2015). *Field and laboratory guide to freshwater cyanobacteria harmful algal blooms for Native American and Alaska Native Communities.* U.S. Geological Survey. (Open-File Report 2015–1164). http://dx.doi.org/10.3133/ofr20151164

Ryding, S. O., & Forsberg, C. (1980). Short-term load-response relationships in shallow, polluted lakes. In: Barica, J., & Mur, L. R. (Eds.), *Hypereutrophic ecosystems* (Developments in Hydrobiology, Vol 2). Springer.

Sanders, J. G. (1986). Direct and indirect effects of arsenic on the survival and fecundity of estuarine zooplankton. *Canadian Journal of Fisheries and Aquatic Sciences, 43,* 694-699.

Sandlos, J., Keeling, A. (2012). *Giant Mine: historical summary.* https://reviewboard.ca/upload/project_document/EA0809-001_Giant_Mine__History_Summary.PDF

Santer, B., & Lampert, W. (1995). Summer Diapause in Cyclopoid Copepods: Adaptive Response to a Food Bottleneck? *Journal of Animal Ecology, 64*(5), 600–613. https://doi.org/10.2307/5803

Senn, D. B., Gawel, J. E., Jay, J. A., Hemond, H. F., & Durant, J. L. (2007). Long-term fate of a pulse arsenic input to a eutrophic lake. *Environmental Science & Technology, 41,* 3062-3068. https://doi.org/10.1021/es062444m

Shaw, J. R., Glaholt, S. P., Greenberg, N. S., Sierra-Alvarez, R., & Folt, C. L. (2007). Acute toxicity of arsenic to *Daphnia pulex*: influence of organic functional groups and oxidation state. *Environmental Toxicology and Chemistry, 26*(7), 1532-1537.

Shchapov, K., Wilburn, P., Bramburger, A. J., Olmanson, L., Crawford, C. J., Litchman, E., & Ozersky, T. (2021). Taxonomic and functional differences between winter and summer crustacean zooplankton communities in lakes across a trophic gradient. *Journal of Plankton Research, 43*(5), fbab050. https://doi.org/10.1093/plankt/fbab050

Shibata, Y., Sekiguchi, M., Otsuki, A., & Morita, M. (1996). Arsenic compounds in zoo- and phyto-plankton of marine origin. *Applied Organometallic Chemistry, 10*(9), 713-719. https://doi.org/10.1002/(SICI)1099-0739(199611)10:9<713::AID-AOC536>3.0.CO;2-U

Sivarajah, B., Korosi, J. B., Blais, J. M., & Smol, J. P. (2019). Multiple environmental variables influence diatom assemblages across an arsenic gradient in 33 subarctic lakes near abandoned gold mines. *Hydrobiologia, 841*(1), 133-151. https://doi.org/10.1007/s10750-019-04014-1

Sivarajah, B., Simmatis, B., Favot, E. J., Palmer, M. J., & Smol, J. P. (2021). Eutrophication and climate changes lead to unprecedented cyanobacterial blooms in a Canadian sub-Arctic landscape. *Harmful Algae, 105,* 102036. https://doi.org/10.1016/j.hal.2021.102036

Smedley, P. L., & Kinniburgh, D. G. (2002). A review of the source, behaviour and distribution of arsenic in natural waters. *Applied Geochemistry, 17*, 517-568.

Smith, V. H. (1983). Low nitrogen to phosphorus ratios favor dominance by blue-green algae in lake phytoplankton. *Science,* 221(4611), 669-671. https://doi.org/10.1126/science.221.4611.669

Smith, K. F., & Lester, P. J. (2010). Cyanobacterial blooms appear to be driven by top-down rather than bottom-up effects in the Lower Karori Reservoir (Wellington, New Zealand). *New Zealand Journal of Marine and Freshwater Research, 40*(1), 53-63. https://doi.org/10.1080/00288330.2006.9517403

Smol, J. P. (2008). *Pollution of lakes and rivers. A paleoenvironmental perspective.* (2nd ed.). Blackwell Publishing.

Snell, T. W., & Janssen, C. R. (1995). Rotifers in ecotoxicology: a review. *Hydrobiologia*, *313,* 231-247.

Sommer, U., Adrian, R., De Senerpont Domis, L., Elser, J. J., Gaedke, U., Ibelings, B., Jeppesen, E., Lürling, M., Molinero, J. C., Mooij, W. M., van Donk, E., & Winder, M. (2012). Beyond the Plankton Ecology Group (PEG) model: mechanisms driving plankton succession. *Annual Review of Ecology, Evolution, and Systematics, 43,* 429-448. https://doi.org/10.1146/annurev-ecolsys-110411-160251

Sommer, U., Gliwicz, Z. M., Lampert, W., & Duncan, A. (1986). The PEG*-model of seasonal succession of planktonic events in fresh waters. *Archiv für Hydrobiologie, 106*(4), 433-471. https://doi.org/10.1127/archiv-hydrobiol/106/1986/433

Spaulding, S., & Edlund, M. (2024). *Diatoms of North America*. https://diatoms.org

Spehar, R. L., J. T. Fiandt, R. L. Anderson, & DeFoe, D. L. (1980). Comparative toxicity of arsenic compounds and their accumulation in invertebrates and fish. *Archives of Environmental Contamination and Toxicology, 9,* 53-63.

Sposito, G. (1984). *The surface chemistry of soils.* Oxford University Press.

Stumm, W. (1992). *Chemistry of the solid-water interface: processes at the mineral-water and particle-water interface in natural systems.* John Wiley & Sons.

Symons, C. C., Pedruski, M. T., Arnott, S. E., & Sweetman, J. N. (2014). Spatial, environmental, and biotic determinants of zooplankton community composition in subarctic lakes and ponds in Wapusk National Park, Canada. *Arctic, Antarctic, and Alpine Research, 46*(1), 159-190. https://doi.org/10.1657/1938-4246-46.1.159

Taranu, Z. E., Gregory-Eaves, I., Leavitt, P. R., Bunting, L., Buchaca, T., Catalan, J., Domaizon, I., Guilizzoni, P., Lami, A., McGowan, S., Moorhouse, H., Morabito, G., Pick, F. R., Stevenson, M. A., Thompson, P. L., & Vinebrooke, R. D. (2015). Acceleration of cyanobacterial dominance in north temperate-subarctic lakes during the Anthropocene. *Ecology Letters, 18*, 375-384. https://doi.org/10.1111/ele.12420

Taylor, W. D., Carey, J. H., Lean, D. R. S., & McQueen, D. J. (1991). Organochlorine concentrations in the plankton of lakes in southern Ontario and their relationship to plankton biomass. *Canadian Journal of Fisheries and Aquatic Sciences, 48,* 1960-1966. https://doi.org/10.1139/f91-233

Therneau, T., & Atkinson, B. (2025). *rpart: recursive partitioning and regression trees* (Version4.1-25) [Software]. R. https://github.com/bethatkinson/rpart

Thienpont, J. R., Korosi, J. B., Hargan, K. E., Williams, T., Eickmeyer, D. C., Kimpe, L. E., Palmer, M. J., Smol, J. P., & Blais, J. M. (2016). Multi-trophic level response to extreme metal contamination from gold mining in a subarctic lake. *Proceedings of the Royal Society, B, 283,* 20161125. https://doi.org/10.1098/rspb.2016.1125

Twiss, M .R., McKay, R. M. L., Bourbonniere, R. A., Bullerjahn, G. S., Carrick, H. J., Smith, R. E. H., Smith, J. G., Winter, N. A., D'souza, Furey, P. C., Lashaway, A. R., Saxton, M. A., & Wilhelm, S. W. (2012). Diatoms abound in ice-covered Lake Erie: investigation of offshore winter limnology in Lake Erie over the period 2007 to 2010. *Journal of Great Lakes Research, 38*(1), 18-30. https://doi.org/10.1016/j.jglr.2011.12.008

U.S. E.P.A. (2014). *National recommended water quality criteria: Aquatic life criteria.* US EPA.

Van Hove, P., Vincent, W. F., Galand, P. E., & Wilmotte, A. (2008). Abundance and diversity of picocyanobacterial in High Arctic lakes and fjords. *Algological Studies, 126,* 209-227. https://doi.org/10.1127/1864-1318/2008/0126-0209

Vanderploeg, H. A., Bolsenga, S. J., Fahnenstiel, G. L., Liebig, J. R., & Gardner, W. S. (1992). Plankton ecology in an ice-covered bay of Lake Michigan: utilization of a winter phytoplankton bloom by reproducing copepods. *Hydrobiologia, 243–244*(1), 175–183. https://doi.org/10.1007/BF00007033

Vocke, R. W., Sears, K. L., O'Toole, J. J., & Wildman, R. B. (1980). Growth responses of selected freshwater algae to trace elements and scrubber ash slurry generated by coal-fired power plants. *Water Research, 14*(2), 141-150. https://doi.org/10.1016/0043-1354(80)90230-4

Wagemann, R., Snow, N. B., Rosenberg, D. M., & Lutz, A. (1978). Arsenic in sediments, water and aquatic biota from lakes in the vicinity of Yellowknife, Northwest Territories, Canada. *Archives of Environmental Contamination and Toxicology, 7*, 169-191.

Wang, S., & Mulligan, C. N. (2006). Occurrence of arsenic contamination in Canada: sources, behavior and distribution. *Science of the Total Environment*, *366*(2–3), 701–721. https://doi.org/10.1016/j.scitotenv.2005.09.005

Wang, W., He, Z., Lv, J., Liu, X., Xie, S., & Feng, J. (2025). Cyanobacteria as dominant mediator of altitudinal gradient effects on phytoplankton community diversity in freshwater ecosystems: evidences from the freshwater lakes along the Hu Line. *Water Research X, 26,* 100281. https://doi.org/10.1016/j.wroa.2024.100281

Wang, X. Y., Liu, L. P., Wang, X. R., Ren, J. Q., Jia, A., & Fan, W. H. (2020). Influence of humic acid on arsenic bioaccumulation and biotransformation to zebrafish: A comparative study between As(III) and As(V) exposure. *Environmental Pollution, 256,* 113459. https://doi.org/10.1016/j.envpol.2019.113459

Wang, Y., Wang, S., Xu, P., Liu, C., Liu, M., Wang, Y., Wang, C., Zhang, C., & Ge, Y. (2015). Review of arsenic speciation, toxicity and metabolism in microalgae. *Reviews in Environmental Science and (Bio)Technology, 14,* 427-451. http://doi.org/10.1007/s11157-015-9371-9

Wei, T., & Simko, V. (2017). *corrplot: Visualization of a correlation matrix* (R package version 0.84). [Computer software]. https://github.com/taiyun/corrplot

Welch, H. E., & Bergmann, M. (1985). Water Circulation in Small Arctic Lakes in Winter. *Canadian Journal of Fisheries and Aquatic Sciences, 42*, 506–520. https://doi.org/10.1139/f85-068

Wickham, H., Chang, W., Henry, L., Pedersen, T. L., Takahashi, K., Wilke, C., Woo, K., Yutani, H., Dunnington, D., & van den Brand, T. (2016). *ggplot2: elegant graphics for data analysis* (Version 3.5.2). [Software]. R. https://ggplot2.tidyverse.org

Williams, L., Schoof, R. A., Yager, J. W., & Goodrich-Mahoney, J. W. (2006). Arsenic bioaccumulation in freshwater fishes. *Human and Ecological Risk Assessment: An International Journal, 12*(5), 904-923. https://doi.org/10.1080/10807030600826821

Wood, S. N. (2011). Fast stable restricted maximum likelihood estimation of semiparametric generalized linear models. *Journal of the Royal Statistical Society (B), 73*(1), 3-36. https://doi.org/10.1111/j.1467-9868.2010.00749.x.

Wood, S. N. (2025). *mgcv: Mixed GAM computation vehicle with automatic smoothness estimation.* (R package version 1.9-4). [Computer software]. https://CRAN.R-project.org/package=mgcv

Woolway, R. I., Sharma, S., & Smol, J. P. (2022). Lakes in hot water: The impacts of a changing climate on aquatic ecosystems. *BioScience, 72*(11), 1050-1061. https://doi.org/10.1093/biosci/biac052

World Health Organization [WHO]. (1993). *Guidelines for drinking-water.* World Health Organization.

Zhang, F., Li, Xue, Duan, L., Zhang, H., Gu, W., Yang, X., Li, J., He, S., Yu, J., & Ren, M. (2021). Effect of different DOM components on arsenate complexation in natural water. *Environmental Pollution, 270,* 116221. https://doi.org/10.1016/j.envpol.2020.116221

Zhang, W., Miao, A.-J., Wang, N.-X., Li, C., Sha, J., Jia, J., Alessi, D. S., Yan, B., & Ok, Y. S. (2022). Arsenic bioaccumulation and biotransformation in aquatic organisms. *Environment International, 163,* 107221. https://doi.org/10.1016/j.envint.2022.107221